

From Pyrene to Large Polycyclic Aromatic Hydrocarbons

Dissertation zur Erlangung des Grades
“Doktor der Naturwissenschaften”
am Fachbereich Chemie, Pharmazie und Geowissenschaften
der Johannes Gutenberg-Universität Mainz

Yulia Fogel
geboren in Moscow
Mainz, 2007

Dekan:

1. Berichterstatter:

2. Berichterstatter:

Tag der mündlichen Prüfung:

Herr Prof. Dr. K. Müllen,

unter dessen Anleitung ich die vorliegende Arbeit am Max-Planck Institut für Polymerforschung in Mainz in der Zeit von Februar 2003 bis Mai 2006 angefertigt habe, danke ich für seine wissenschaftliche und persönliche Unterstützung sowie seine ständig Diskussionsbereitschaft.

Dedicated to my family and all my friends

Index of Abbreviations

2D-WAXS	two-dimensional wide-angle X-ray scattering
AFM	atomic force microscopy
bd	doublet broad (NMR)
bipy	bipyridyl
bs	broad singlet (NMR)
cal.	calculated
d	doublet (NMR)
DBU	1,8-Diazabicyclo[5,4,0]undec-7-en
DCM	dichloromethane
DCTB	trans-2-[3-(4- <i>tert</i> -butylphenyl)-2-methyl-2-propenyldiene] malononitrile
DMF	N,N-dimethylformamide
DSC	differential scanning calorimetry
FD	field desorption
FET	field-effect transistor
FVP	flash vacuum pyrolysis
GPC	gel permeation chromatography
h	hour
HBC	hexa-peri-hexabenzocoronene
HOMO	highest occupied molecular orbital
HR-TEM	high-resolution transmission electron microscopy
J	coupling constant / Hz
LC	liquid crystal
LED	light emitting diode
LUMO	lowest unoccupied molecular orbital
m	multipllett (NMR)
M ⁺	molecular ion
MALDI-TOF	matrix-assisted laser desorption/ionization time-of-flight
Me	methyl

min	minute
MS	mass spectrometry
NMR	nuclear magnetic resonance
PAH	polycyclic aromatic hydrocarbon
PE	petroleum ether, low boiling
Ph	phenyl
PL	photoluminescence
PLE	photoluminescence excitation
POM	polarization optical microscopy
ppm	parts per million
s	singlet (NMR)
SEM	scanning electron microscopy
t	triplet (NMR)
tBu	<i>tert</i> -butyl
TBO	tetrabenzo[bc,ef,hi,uv]ovalene
TEM	transmission electron microscopy
THF	tetrahydrofuran
TGA	thermo-gravimetry analysis
TLC	thin layer chromatography
UV/vis	UV-visible absorption spectroscopy

Table of Content

FROM PYRENE TO LARGE POLYCYCLIC AROMATIC HYDROCARBONS	1
1 INTRODUCTION	2
1.1 Polycyclic Aromatic Hydrocarbons	2
1.2 Synthesis of PAH	4
1.2.1 Diels-Alder Cycloaddition	4
1.2.2 Friedel-Crafts-type Reactions	5
1.2.3 Extrusion of Heteroatoms	6
1.2.4 Photocyclization	7
1.2.5 Flash Vacuum Pyrolysis (Thermolysis)	7
1.2.6 Scholl-Cyclodehydrogenation	8
1.3 Supramolecular Organization	9
1.4 Extended PAHs	11
1.5 Metal-PAH complexes	12
1.6 Motivation and Objectives	13
1.7 References	15
2 FROM PYRENE TOWARDS GRAPHITE RIBBONS	20
2.1 Synthesis of Graphite Ribbons	20
2.2 Synthesis of Polyphenylene Ribbons	22
2.3 Synthesis of Ladder Polymers	29
2.4 Transmission Electron Microscopy of Ribbons	32
2.5 Cyclodehydrogenation of Ribbons	34
2.6 UV/Vis-Spectroscopy of Graphite Molecules	39
2.7 Summary	43
2.8 References	44
3 FROM PYRENE TO POLYCYCLIC AROMATIC HYDROCARBONS CONTAINING NITROGEN	48
3.1 Clar rule and Peripheries	48
3.2 Synthesis of the Building Block 3-13	50

3.3	Synthesis of Extended PAHs	55
3.4	Spectroscopic and Electrochemical Properties	59
3.5	Reductive protonation and alkylation of 3-20	67
3.5.1	Reduction of 3-20 by using $\text{Co}(\text{Cp})_2$	69
3.5.2	Reduction of 3-20 by using SnCl_2	69
3.5.3	Reduction of 3-20 by using PhLi	71
3.6	Summary	72
3.7	References.....	73
4	FROM PYRENE TO THE LARGEST PHTHALOCYANINES.....	79
4.1	Synthesis and physical properties of phthalocyanines.....	79
4.1.1	Synthesis	80
4.1.2	Synthesis of metal-ion-containing Pcs (MPc).....	81
4.1.3	The crystal structure of phthalocyanines	82
4.1.4	Spectroscopic properties	83
4.1.5	Discotic and columnar mesophases of Pcs	84
4.1.6	Conductivity of Pcs.....	84
4.2	Synthesis of extended Pcs.....	86
4.3	Characterization of extended Pc	90
4.4	Introduction of n-dodecyl chains	92
4.4.1	Synthesis	92
4.4.2	Characterization of second extended Pc	101
4.4.3	DSC and TGA.....	102
4.4.4	2D-WAXS.....	103
4.5	Summary	104
4.6	References.....	104
5	FROM PYRENE TOWARDS PHENANTHROLINE LIGANDS FOR METAL COMPLEXATION.....	109
5.1	Ruthenium (II) Complexes	109
5.2	Synthesis of Phenanthroline Ligands.....	114
5.3	Synthesis of Ru-complexes using ligands 5-17 and 5-18	121

5.4	Synthesis of a Copper (II) complex	124
5.5	Synthesis of a Pt(II)-complex	125
5.6	Spectroscopic properties	127
5.7	Summary	131
5.8	References.....	132
6	CONCLUSIONS AND OUTLOOK.....	137
7	EXPERIMENTAL SECTION.....	142
7.1	General Methods.....	142
7.2	Synthesis	143
7.2.1	2,7-Di- <i>tert</i> -butylpyrene-4,5,9,10-tetraone (1-32)	143
7.2.2	2,7-Di- <i>tert</i> -butyl-4,5:9,10-bis(2,5-di- <i>p</i> -dodecyl-phenylcyclopenta)- [<i>e,l</i>]pyrene-5,11-dione (2-7).....	144
7.2.3	2,7-Di- <i>tert</i> -butyl-4,5-(2,5-di- <i>p</i> -dodecylphenyl-2',3',4',5'-tetrakis(4'- dodecylphenyl)-[1',1'';2'',3]terphenyl-dibenzo[<i>l</i>])-9,10-cyclopenta[<i>e</i>]pyrene-10-one (2-12)	145
7.2.4	2,7-Di- <i>tert</i> -butyl-4,5:9,10-bis(2,5-di- <i>p</i> -dodecylphenyl-2',3',4',5'- tetrakis(<i>p</i> -dodecylphenyl)-[1',1'';2'',3]terphenyl)dibenzo[<i>e,l</i>]pyrene (2-13).....	146
7.2.5	2,7-Di- <i>tert</i> -butyl-4,5:9,10-(2,5-di- <i>p</i> -dodecylphenyl-2',3',4',5'-tetrakis(<i>p</i> - dodecylphenyl)-[1',1'';2'',3]terphenyl-2''-ethynyl-3-biphenyl)dibenzo[<i>e,l</i>]pyrene (2- 14)	147
7.2.6	1,2'-Bis(2,7-di- <i>tert</i> -butyl-4,5:9,10-bis(2,5-di- <i>p</i> -dodecylphenyl)-2',3',4',5'- tetrakis(<i>p</i> -dodecylphenyl)-[1',1'';2'',3]terphenyl)dibenzo[<i>e,l</i>]pyreno)biphenyl (2-15) 148	
7.2.7	2,7-Di- <i>tert</i> -butyl-4,5-(2,5-di- <i>p</i> -dodecylphenylbenzene-2',7'-di- <i>tert</i> -butyl- 4',5':9',10'-(2',5'-di- <i>p</i> -dodecylphenyl-2'',3'',4'',5''-tetrakis(<i>p</i> -dodecylphenyl)- [1'',1''';2''',3']terphenyl-3'-biphenyl)dibenzo[<i>e,l</i>]pyreno)-9,10- cyclopenta[<i>e</i>]pyrene-10-one (2-16).....	150
7.2.8	2,7-Di- <i>tert</i> -butyl-4,5:9,10-bis(2,5-di- <i>p</i> -dodecylphenyl-2',7'-di- <i>tert</i> -butyl- 4',5':9',10'-(2',5'-di- <i>p</i> -dodecylphenyl-2'',3'',4'',5''-tetrakis(<i>p</i> -dodecylphenyl)- [1'',1''';2''',3']terphenyl-3'-biphenyl)dibenzo[<i>e,l</i>]pyreno)dibenzo[<i>e,l</i>]pyrene (2-17) 151	

7.2.9	2,7-Di- <i>tert</i> -butyl-4,5:9,10-(2,5-di- <i>p</i> -dodecylphenyl-2',7'-di- <i>tert</i> -butyl-4',5':9',10'-(2',5'-di- <i>p</i> -dodecylphenyl-2'',3'',4'',5''-tetrakis(<i>p</i> -dodecylphenyl)-[1'',1''';2''',3]terphenyl-3-biphenyl)dibenzo[<i>e,l</i>]pyreno-2''''-ethinyl-3-biphenyl)dibenzo[<i>e,l</i>]pyrene (2-18)	152
7.2.10	1,2'-Bis(bis(2'',7''-di- <i>tert</i> -butyl-4'',5''':9'',10''-bis(2'',5''-di- <i>p</i> -dodecylphenyl)-2''',3''',4''',5''')-tetrakis(<i>p</i> -dodecylphenyl)-[1''',1'''';2''''',3''']terphenyldibenzo[<i>e,l</i>]pyreno))biphenyl (2-19)	154
7.2.11	2,7-Di- <i>tert</i> -butyl-4,5:9,10-bis(2,5-di- <i>p</i> -dodecylphenyl-bis(2',7'-di- <i>tert</i> -butyl-4',5':9',10'-(2',5'-di- <i>p</i> -dodecylphenyl-2'',3'',4'',5''-tetrakis(<i>p</i> -dodecylphenyl)-[1'',1''';2''',3']terphenyl-3'-biphenyl)dibenzo[<i>e,l</i>]pyreno))dibenzo[<i>e,l</i>]pyrene (2-21)	155
7.2.12	2,7-Di- <i>tert</i> -butyl-4,5:9,10-bis(3,4-dihexyl-2,5-di- <i>p</i> -dodecylphenyl)dibenzo[<i>e,l</i>]pyrene (2-26).....	156
7.2.13	3,4,10,11-Tetra-hexyl-7,14-di- <i>t</i> -butyl-tetra-dodecyltetrabenzo[<i>a,g,e,r</i>]ovalene (2-27).....	157
7.2.14	2,7-Di- <i>tert</i> -butylpyrene-4,5-dione (3-7)	158
7.2.15	2,7-Di- <i>tert</i> -butyl-4,5-bis-(4- <i>tetr</i> -butyl-phenyl)-cyclopenta[<i>e</i>]pyren-5-one (3-9)	159
7.2.16	2,7-Di- <i>tert</i> -butyl-4,5,6,7-tetrakis-(4- <i>tert</i> -butyl-phenyl)-benzo[<i>e</i>]pyrene (3-11)	160
7.2.17	1,6-Di- <i>tert</i> -butyl-8,11,14,17-tetra(<i>t</i> -butyl)tetrabenzo[<i>bc,ef,hi,uv</i>]ovalene (3-12)	161
7.2.18	1,6-Di- <i>tert</i> -butyl-8,11,14,17-tetra(<i>t</i> -butyl)tetrabenzo[<i>bc,ef,hi,uv</i>]ovalene-3,4-dione (3-13)	162
7.2.19	1,6-Di- <i>tert</i> -butyl-8,11,14,17-tetra(<i>t</i> -butyl)tetrabenzo[<i>jk,mn,pq,st</i>]benzo[1,2- <i>a</i>]pyrazine[2,3- <i>d</i>]ovalene (3-18)	163
7.2.20	Bis(1,6-di- <i>tert</i> -butyl-8,11,14,17-tetra(<i>t</i> -butyl)tetrabenzo[<i>jk,mn,pq,st</i>]benzo[1,2- <i>a</i>]pyrazine[2,3- <i>d</i>]ovaleno)-[5,6:5',6'- <i>b,b'</i>]-5,5'-biphenyl (3-19).....	164

7.2.21	Bis(1,6-di- <i>tert</i> -butyl-8,11,14,17-tetra(<i>t</i> -butyl)tetrabenzo[<i>bc,ef,hi,uv</i>]ovaleno)-[3,4:3',4'- <i>b,i</i>]-1,4,6,9-tetraazaanthracene (3-20)	165
7.2.22	1,6-Di- <i>tert</i> -butyl-8,11,14,17-tetra(<i>t</i> -butyl)tetrabenzo[<i>jk,mn,pq,st</i>]anthraquinone[1,2- <i>a</i>]pyrazine[2,3- <i>d</i>]ovalene (3-21)	166
7.2.23	1,6-Di- <i>tert</i> -butyl-8,11,14,17-tetra(<i>t</i> -butyl)tetrabenzo[<i>jk,mn,pq,st</i>]-4,5-dicyanobenzo[1,2- <i>a</i>]pyrazine[2,3- <i>d</i>]ovalene (4-9)	167
7.2.24	1,6-Di- <i>tert</i> -butyl-8,11,14,17-tetra(<i>t</i> -butyl)tetrabenzo[<i>jk,mn,pq,st</i>]benzo[1,2- <i>a</i>]pyrazine[2,3- <i>d</i>]ovalenocyanine (4-10)	169
7.2.25	2,7-Di- <i>tert</i> -butyl-4,5-bis-(4-dodecyl-phenyl)-cyclopenta[<i>e</i>]pyren-5-one (4-12)	170
7.2.26	2,7-Di- <i>tert</i> -butyl-4,5,6,7-tetrakis-(4-dodecyl-phenyl)-benzo[<i>e</i>]pyrene (4-14)	171
7.2.27	1,6-Di- <i>tert</i> -butyl-8,11,14,17-tetra- <i>n</i> -dodecyl-tetrabenzo[<i>bc,ef,hi,uv</i>]ovalene (4-15)	172
7.2.28	1,6-Di- <i>tert</i> -butyl-8,11,14,17-tetra- <i>n</i> -dodecyl-tetrabenzo[<i>bc,ef,hi,uv</i>]ovalene-3,4-dione (4-16)	173
7.2.29	1,6-Di- <i>tert</i> -butyl-8,11,14,17-tetra- <i>n</i> -dodecyl-tetrabenzo[<i>jk,mn,pq,st</i>]-4,5-dicyanobenzo[1,2- <i>a</i>]pyrazine[2,3- <i>d</i>]ovalene (4-17)	174
7.2.30	1,6-Di- <i>tert</i> -butyl-8,11,14,17-tetra- <i>n</i> -dodecyl-tetrabenzo[<i>jk,mn,pq,st</i>]benzo[1,2- <i>a</i>]pyrazine[2,3- <i>d</i>]ovalenocyanine (4-18)	175
7.2.31	Phendioxime 5-15	176
7.2.32	5,6-Diamino-1,10-phenanthroline (5-16)	176
7.2.33	2,7-Di- <i>tert</i> -butyl-1,10-phenanthro[5,6- <i>e</i>]pyrazine[2,3- <i>e</i>]pyrene (5-17)	177
7.2.34	1,6-Di- <i>tert</i> -butyl-8,11,14,17-tetra(<i>t</i> -butyl)tetrabenzo[<i>jk,mn,pq,st</i>]-1,10-phenanthro[5,6- <i>e</i>]pyrazine[2,3- <i>d</i>]ovalene (5-18)	178
7.2.35	2,7-Di- <i>tert</i> -butyl-bis(1,10-phenanthro[5,6- <i>e</i>]pyrazine[2,3- <i>e,l</i>]pyrene (5-19)	179
7.2.36	Ruthenium (II) complex 5-20	180
7.2.37	Ruthenium (II) complex 5-22	181
7.3	References	182

1 Introduction

1.1 Polycyclic Aromatic Hydrocarbons

For the past forty years inorganic silicon and gallium arsenide semiconductors, silicon dioxide insulators, and metals such as aluminum and copper have been the backbone of the semiconductor industry.^{1, 2} Lately, however, there has been a constantly growing research effort in “organic” electronics, aiming at improvement of conducting and photovoltaic properties of organic and hybrid materials through novel synthesis and controlled self-assembly.^{3, 4}

As result of these efforts, several types of organic materials were identified as suitable for electronic devices, in particular conjugated polymers and oligomers, discotic liquid crystals, organic-inorganic composites. The development in the field has been marked in 2000 by the Nobel Prize in chemistry given to HEEGER, MACDIARMID, and SHIRAKAWA for the discovery of conductive polymers.^{5, 6}

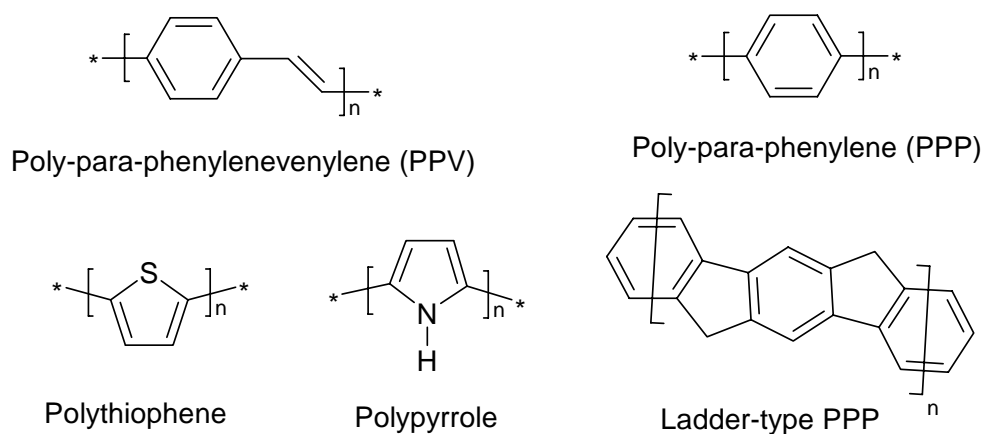


Figure 1-1. Examples of conjugated polymers

Conjugated polymers are organic macromolecules which have alternating single and double carbon-carbon (sometimes carbon-nitrogen) bonds. All conjugated polymers have a sigma-bonded backbone of overlapping sp^2 hybrid orbitals. The remaining out-of-plane p_z orbitals on the carbon (or nitrogen) atoms overlap with neighboring p_z orbitals to give π -bonds. The electrons that constitute the π -bonds are either delocalized over the entire molecule (good molecular ordering, band-like conduction) or partially localized

(disordered systems, hopping type of conduction). In both cases this makes conjugated polymers behave as one-dimensional conductors. Several representative examples of conjugate polymers are shown in Figure 1-1.

Another type of materials which is actively developed for use in organic electronics is based on extended polycyclic aromatic hydrocarbons (PAH). PAHs represent one of the most intensively investigated classes of compounds.⁷⁻⁹ Their discovery in coal tar in the middle of the 19th century helped to initiate rapid development of industrial organic chemistry, especially in the field of dyes. Since then PAHs have attracted interest of organic chemists, photo-physicists, and even astronomers, by helping them to identify the full extent of the dust structures in the universe.^{10, 11} Typical compounds are shown in Figure 1-2.

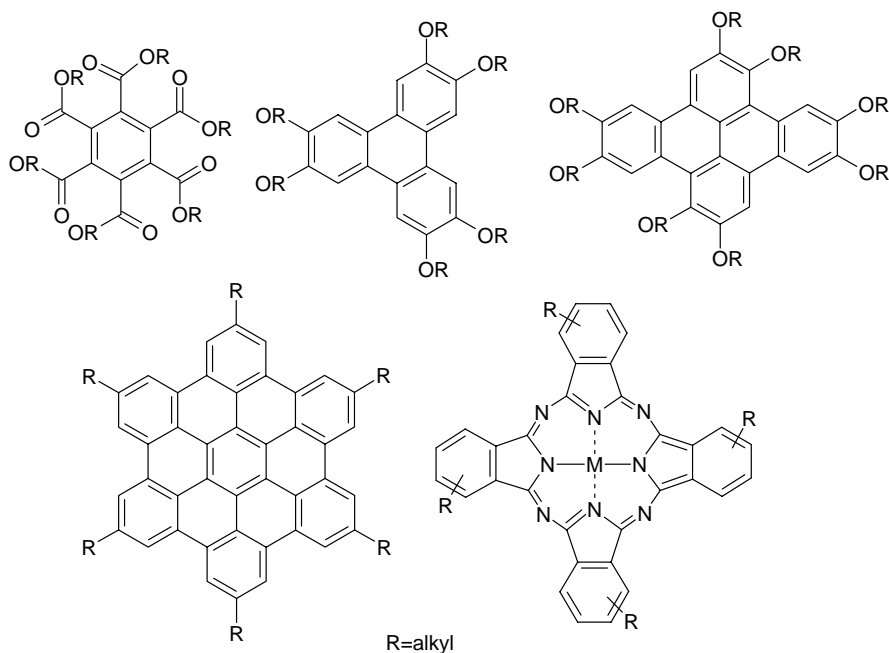


Figure 1-2. Typical examples of polycyclic aromatic hydrocarbons

Benzene is the simplest of aromatic compounds that consists of six sp^2 -hybridized carbon atoms, forming a uniform hexagon, similar to graphite. PAHs, since they are assembled from benzene rings in a periodic fashion, possess extraordinary and often unique electronic properties,¹²⁻¹⁶ which sparked an immediate interest of both basic research and industry.

1.2 Synthesis of PAH

Major sources of PAHs are crude oil, coal and oil shale.¹⁷⁻¹⁹ First fundamental contributions in the area of direct synthesis and characterization of PAHs were made by the pioneering work of SCHOLL²⁰⁻²², CLAR²³⁻²⁸ and ZANDER.^{7, 27-29} Classical synthetic methods tended to involve relatively vigorous reaction conditions that are high temperatures and pressures. The trend in recent years is towards the development of much milder methods, with better regioselectivity and higher yields. Widely used methods are:

1.2.1 Diels-Alder Cycloaddition

DIELS-ALDER cycloaddition (inter- or intra-molecular) is one of the most versatile methods for the construction of PAH systems. One of the examples of intermolecular cycloaddition is shown in Figure 1-3. The reaction of 1-vinylnaphthalene **1-1** with 1,4-benzoquinone **1-2** (both employed as dienophiles) affords a cycloadduct that is converted directly to chrysene-1,4-dione **1-3** by dehydrogenation with excess of benzoquinone. Chrysene-1,4-dione **1-3** is reduced to chrysene **1-4** by treatment with lithium aluminumhydride³⁰.

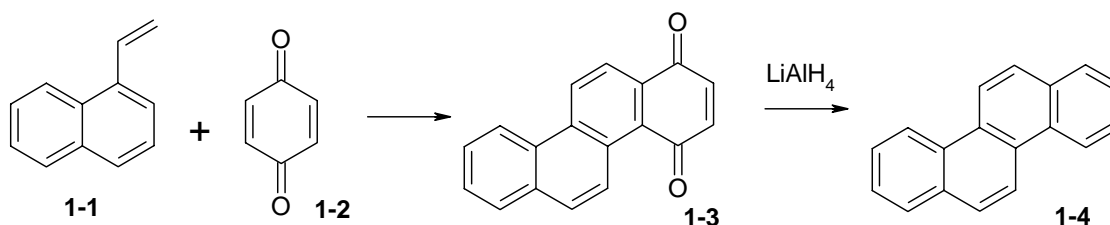


Figure 1-3. Example of the use of Diels-Alder cycloaddition for the construction of PAHs

MÜLLER³¹ utilized an intramolecular DIELS-ALDER reaction to construct a suitable precursor for a 60 carbon containing rhombus-shaped PAH (Figure 1-4). In the phenylenevinylene-precursor **1-5**, which is, on its own, the product of seven reaction steps, both dieno- and dienophilic components are arranged in a way that the intramolecular cycloaddition reaction at 135 °C yields **1-6**. After subsequent oxidation with 2,3-dichloro-4,5-dicyanonquinone (DDQ), the precursor could be planarized to the desired molecule **1-7**.

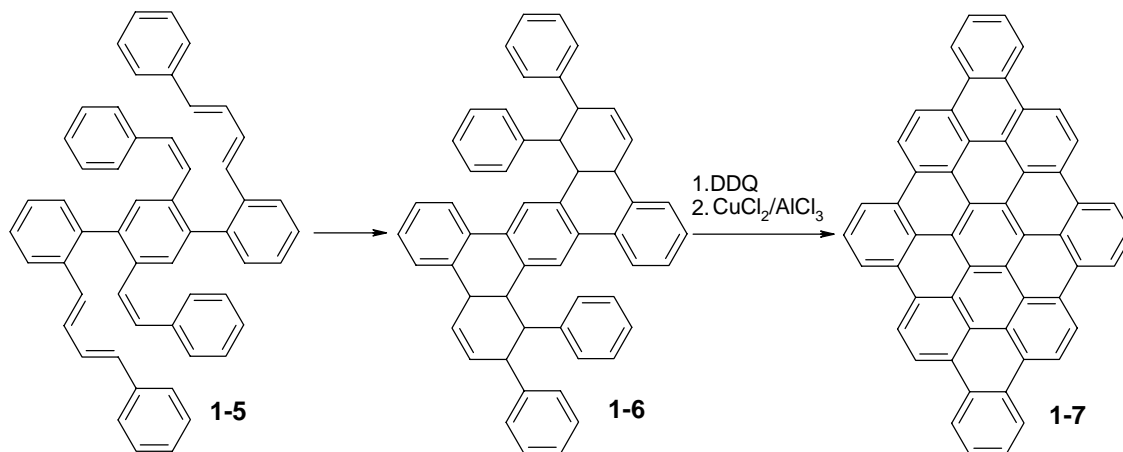


Figure 1-4. Synthesis of the rhombus-shaped PAH

1.2.2 Friedel-Crafts-type Reactions

The classic HAWORTH synthesis is FRIEDEL-CRAFTS condensation of succinic anhydride **1-9** with a polyarene (for example, naphthalene **1-8**) (Figure 1-5) towards a keto-acid intermediate **1-10**. The following reduction of the keto group and acid-catalyzed cyclization of the resulting carboxylic acid yields a ketone **1-12**, which can be aromatized to the corresponding PAH **1-13**³².

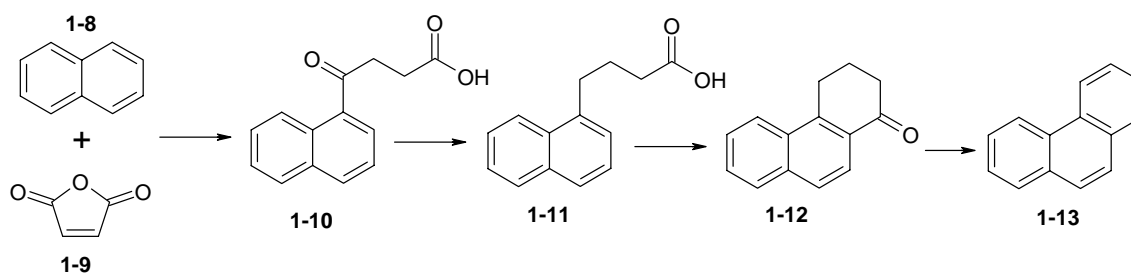


Figure 1-5. Example of the Harworth synthesis

Larger polycyclic ring systems can be synthesized by modifying the HARWORTH synthesis by using aromatic anhydrides, such as phthalic anhydride, thereby allowing fusion of two or more benzenoid rings to an existing aromatic system.

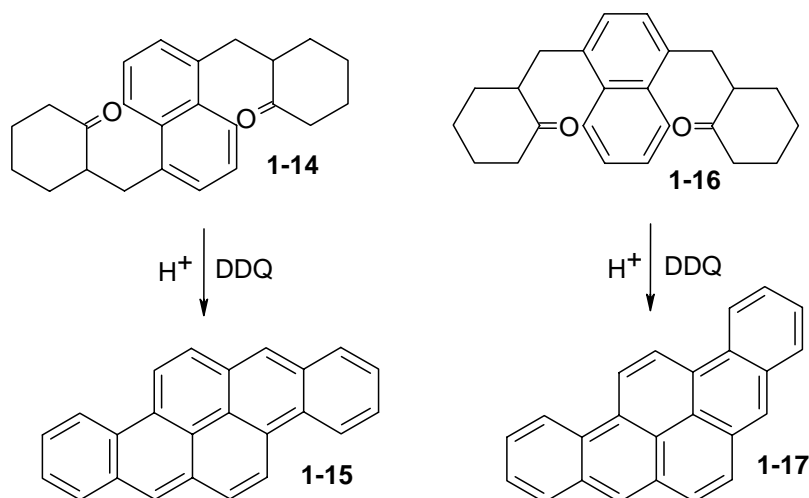


Figure 1-6. Acid-catalyzed cyclodehydration of diketones towards PAHs

In addition, different ketones and aldehydes can serve as precursors for the synthesis of PAHs.³³ For example, acid-catalyzed cyclodehydration of the diketone **1-14** and **1-16** provides a convenient synthetic access to dibenzoscrysene **1-15** and benzo[*rs*]pentaphene **1-17**, respectively (Figure 1-6). It is worth to mention that both reactions occur strictly regiospecifically without formation of side-products.

1.2.3 Extrusion of Heteroatoms

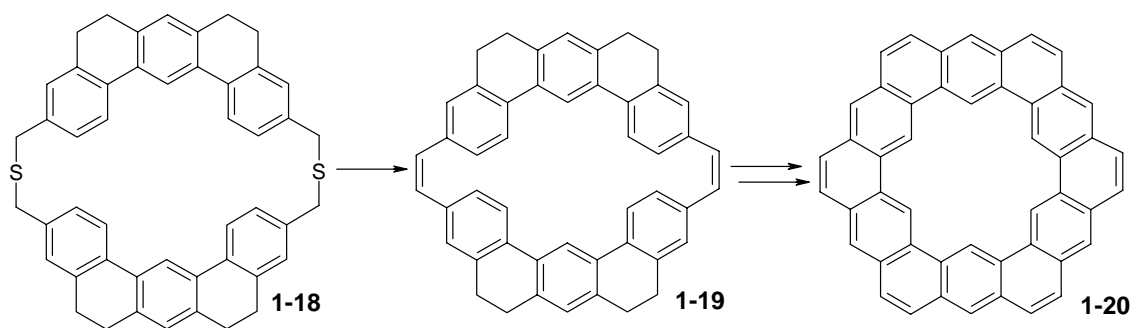


Figure 1-7. Synthesis of kekulene according to Diederich and Staab

One of the representative examples of this method is synthesis of kekulene **1-20**, which involves extrusion of sulfur. It was first reported by DIEDERICH and STAAB³⁴⁻³⁶. The key step for the multistep synthesis is the extrusion of the dithiaphanes **1-18** to form the carbocyclic system **1-19**, which is then converted to kekulene (Figure 1-7).

1.2.4 Photocyclization

Photochemical methods first gained popularity for the synthesis of helicenes.³⁷ Recently, the method has also been used for the synthesis of different PAHs, for example the conversion of stilbenes to phenanthrenes by irradiation with UV light in the presence of an oxidant, such as iodine or iron(III) chloride.³⁸ These reactions allowed to obtain cyclohexadienenes from 1,3,5-hexatrienes; the oxidant served to dehydrogenate the unstable primary dihydroaromatic products. A typical example of photocyclization of 2-(3,5-di-*tert*-butylstyryl)benzo[*c*]phenanthrene **1-21** to 1,3-di-*tert*-butylhexahelicene **1-22** is shown in Figure 1-8.

XIAO *et al.*³⁹ reported a novel approach towards a hexa-*cata*-hexabenzocoronone derivative **1-23**, where the decisive step is accomplished by the photocyclization of an adequate precursor molecule **1-24** (Figure 1-8).

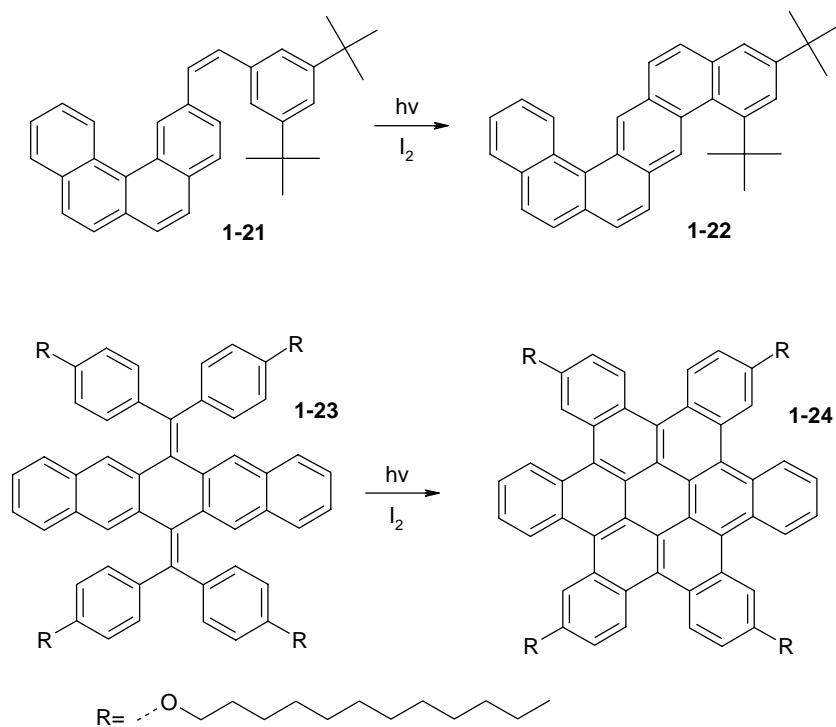


Figure 1-8. Photochemical cyclization as an approach to obtain PAH

1.2.5 Flash Vacuum Pyrolysis (Thermolysis)

Flash vacuum pyrolysis (FVP) is a high temperature gas-phase pyrolysis with short contact time in the hot zone. It results in electrocyclization with loss or migration of

hydrogen (or hydrogen halide). For example, FVP is the last key step in the synthesis of corannulene **1-29**.

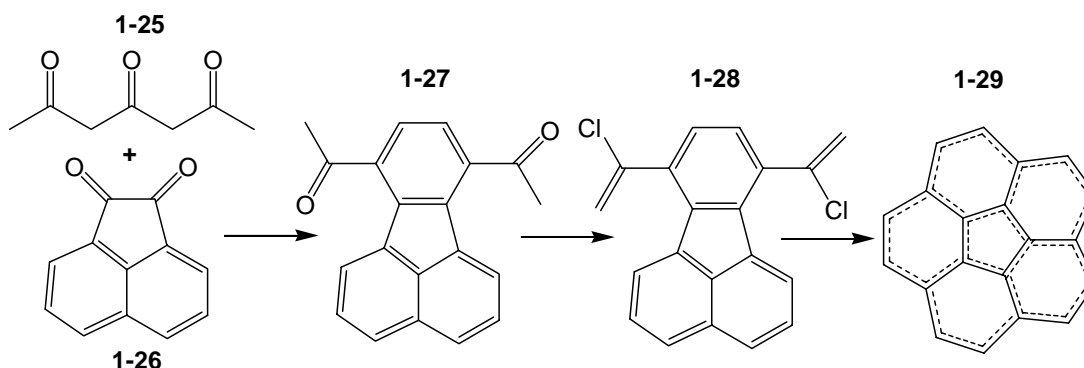


Figure 1-9. Synthetic route towards corannulene using FVP

The synthesis was started with commercially available materials via a route involving the synthesis of 7,10-(bis(1-chlorovinyl))fluoranthene **1-28** obtained from 7,10-diacetylfluoranthene **1-27** by reaction with phosphorous pentachloride^{40, 41} (Figure 1-9). Recently, the FVP has been used to synthesize fullerene.⁴²

1.2.6 Scholl-Cyclodehydrogenation

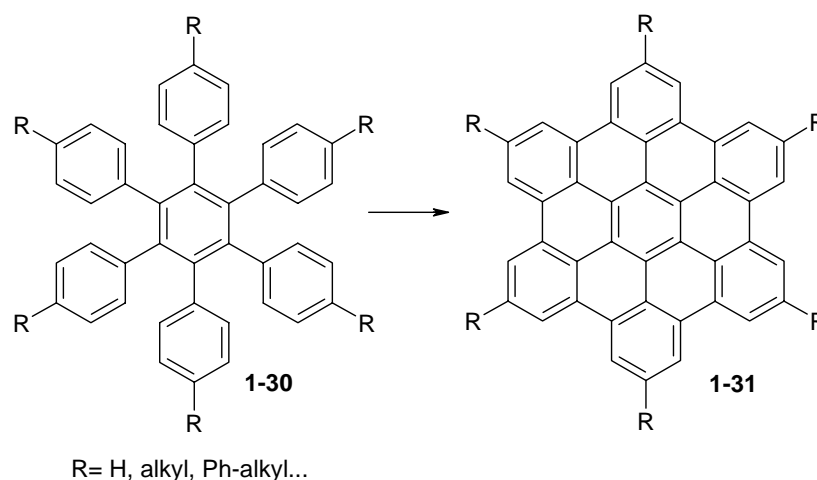


Figure 1-10. Cyclodehydrogenation of hexa-phenylbenzene towards HBC

Coupling of two aromatic molecules in the presence of a Lewis acid is called the SCHOLL reaction. This reaction is one of the principal methods for PAHs synthesis. This method

has been improved and hereafter applied to the synthesis of a wide range of different oligophenylenes, which serve as precursors for extended PAHs.⁴³⁻⁴⁵

A typical example is the reaction of substituted hexa-phenylbenzenes **1-30** with iron(III) chloride which gives, in one step, a fully planarized HBC derivative **1-31**, on a multi-gram scale (Figure 1-10). Following the synthesis optimization by HERWIG,⁴⁶ SCHOLL cyclodehydrogenation was used to obtain a large variety of differently substituted HBC derivatives, each with its own outstanding material properties.⁴⁷

One of the latest developments in the field is the synthesis of an extended, processable PAH, which contains 72 carbon atoms in the aromatic core⁴⁸ (Figure 1-11). Starting from the pyrenetetraone **1-32**, a suitable precursor for the SCHOLL planarization was built using the DIELS-ALDER reaction. The treatment with iron(III) chloride yielded the fully fused PAH **1-34**. Introduced *tert*-butyl groups cause a distortion of the aromatic core, which is crucial for the solubility of the compound, due to the lack of its self-aggregation.

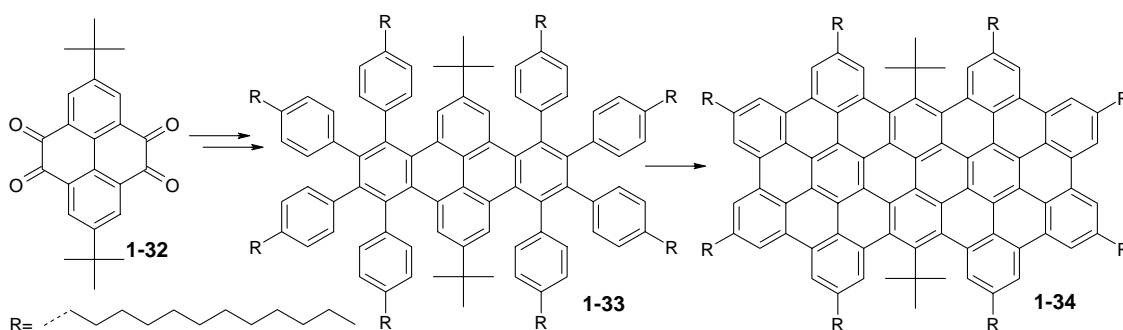


Figure 1-11. Synthesis of a non-planar 72 carbon-containing PAH

1.3 Supramolecular Organization

A vast number of PAHs and their derivatives self-assemble into supramolecular structures. Self-assembly, or supramolecular organization, is the autonomous ordering of components into patterns or structures, and are common throughout nature and technology.⁴⁹ In many materials, supramolecular structures appear from spontaneous association because of non-covalent interactions between their building blocks (e.g. molecules). Two main driving forces guide self-organization of supramolecular architecture: hydrogen bonding^{50, 51} and VAN DER WAALS forces due to π - π molecular

orbital overlaps. The molecular self-assembly and therefore the physical properties of the aggregates are extremely sensitive to the structure of a single molecule.

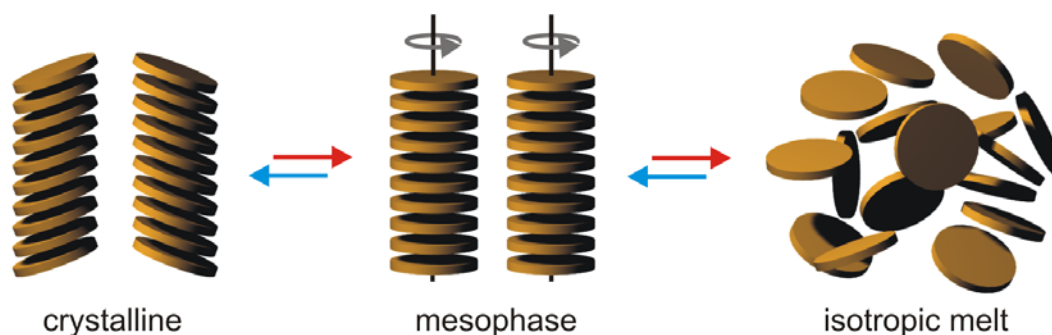


Figure 1-12. The long range organization with respect to the orientation of the molecules is disturbed

Liquid crystalline (LC) phases are typical systems which self-assemble on a microscopic scale. They possess unusual material characteristics, by combining properties of a crystalline solid (optical and electric anisotropy) with those of a liquid (inability to support shear, viscosity).⁵²

Two types of liquid crystals are known: lyotropic and thermotropic. Lyotropic phases are formed by dissolving amphiphilic compounds in suitable solvents; thermotropic phases can be found during heating of a solid or cooling of an isotropic liquid. Liquid crystallinity is due to shape anisotropy of the constituent molecules, which align along a particular direction (orientational order) but are still spatially disordered, see Figure 1-2. Most of LCs are made of rod- or disc-like shaped molecules.

While thermotropic liquid crystallinity was originally discovered for rod-like molecules, disc-shaped molecules such as hexa-substituted benzenes can also form such mesophases. Discotic mesogens can exhibit a nematic phase (N_D , Figure 1-13) in which the molecular discs are aligned (on average) parallel to each other, but their centers of mass are spatially disordered. They can also form various columnar mesophases, with different arrangement of molecules in a column and columns on a lattice, see Figure 1-13.

Mesophases can be distinguished between each other by using a polarizing optical microscope in combination with a hot stage to control the sample temperature.^{53, 54} Transition temperatures and changes in enthalpy (ΔH_t) are measured with differential scanning calorimetry (DSC).⁵⁵ X-ray diffraction allows structure determination from the

diffraction patterns, due to periodicities and symmetries of columnar mesophases.^{56, 57} Nuclear magnetic resonance (NMR) can be used to estimate the order parameter of the mesophases.⁵⁸

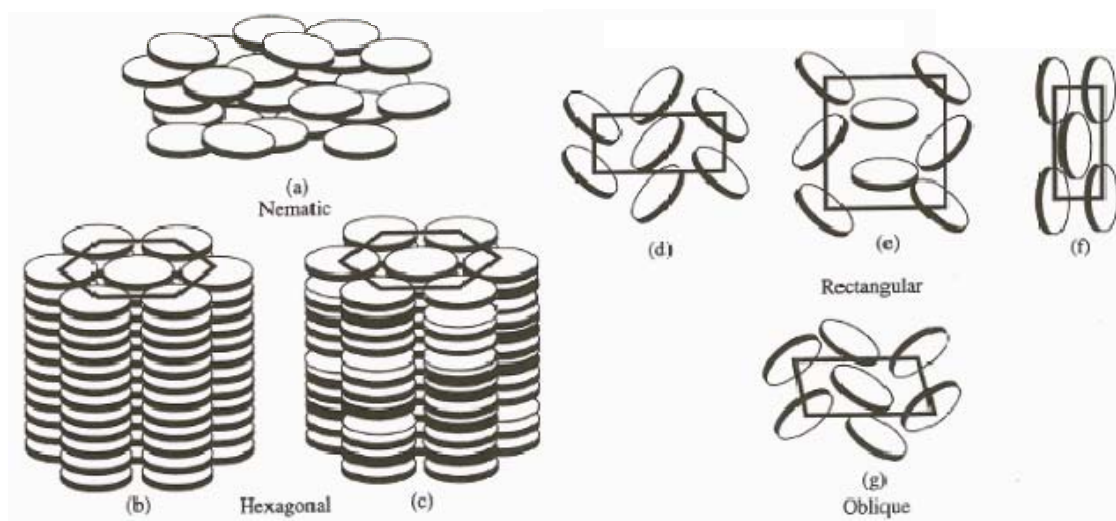


Figure 1-13. Types of mesophases formed by discotic compounds⁵⁹: a) discotic nematic (ND), b) hexagonal ordered (Dho), c) hexagonal disordered (Dhd), d,e,f) rectangular disordered with different plane group symmetry (Drd), g) oblique (Dob)

1.4 Extended PAHs

A typical example of extended PAH, **1-34**, is shown in Figure 1-14. Due to low reaction efficiency and presence of side products, the synthesis of extended PAHs still remains a challenging task. In addition, lack of analytical techniques for insoluble materials hampers the determination of their purity. Large overlap of π -areas of these molecules results in their pronounced self-association and therefore does not allow to resolve properly the aromatic region in the ^1H NMR spectra.⁶⁰⁻⁶²

The largest extended PAHs, shown in Figure 1-15, have recently been synthesized via the cyclodehydrogenation of suitable oligophenylene precursors.^{60, 62} PAH with a size of 72 aromatic carbon atoms (**1-34**) is, so far, the largest clearly characterized by NMR PAH.⁴⁸

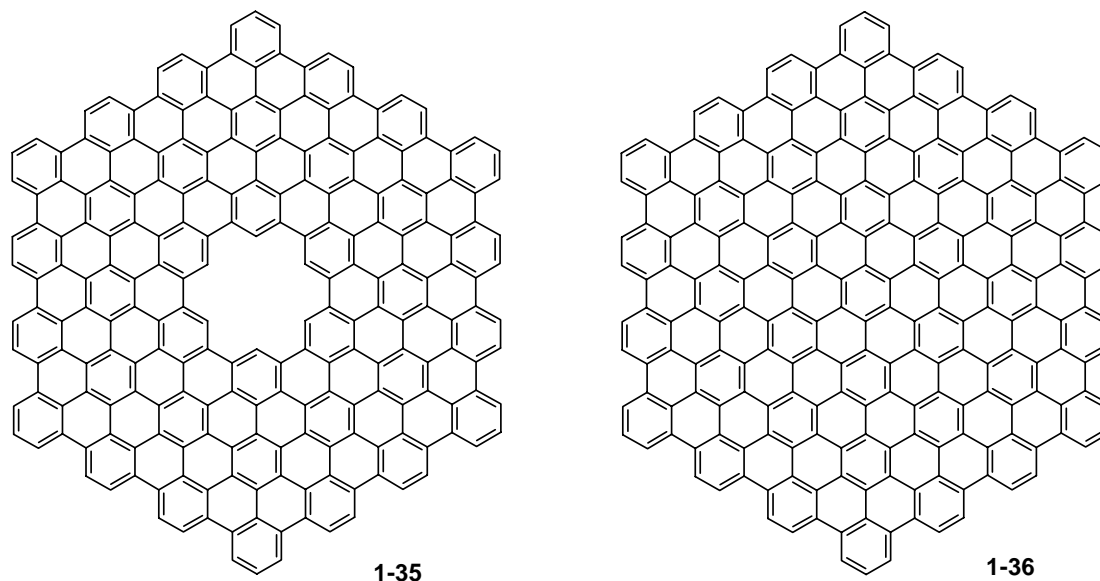


Figure 1-15. Chemical structures of the largest extended PAHs

1.5 Metal-PAH complexes

Metal derivatives of PAHs are gaining interest because the presence of the metal atom may substantially affect magnetic and optical properties of these materials.^{63, 64} Metal-PAH complexes are also important models for catalysis and surface science.⁶⁵ Increasing interest in metal-PAH systems has motivated many synthetic chemists to synthesize these species by different methods. There is a lot of information available on coordination of polymers or low molecular weight compounds with different metal ions. In particular, Ru(II) complexes with polypyridine ligands are well studied because of their efficient photophysical and photoelectrochemical properties for their potential applications in electronic and photomolecular devices.⁶⁶

1.6 Motivation and Objectives

The world demand in energy consumption is predicted to double by 2050. Natural resources, e.g. crude oil and gas, are limited and will be exhausted by the end of this century (rough estimates for oil is about 50 years from now). Therefore, finding alternative sources of energy is one of the most important tasks of our society.

Solar energy is probably one of the promising and still realistic approaches to gain additional energy. The other ways, e.g. wind power, hydrolysis of water, cold fusion, have either limited capacities or are yet technologically underdeveloped. A simple estimate shows that more solar energy strikes the Earth ($4.3 \cdot 10^{20}$ J) than all energy consumed on the planet in a year ($4.1 \cdot 10^{20}$ J).⁶⁷ Yet, the used solar energy comprises less than 1% of the world energy consumption.

At the moment, devices for conversion of solar energy (solar cells) are based on inorganic silicon and metals. The main drawback of these devices, which prevents their mass production, is their price. Hence, the main challenge in converting sunlight to electricity via photovoltaic solar cells is to reduce the cost/watt of delivered solar electricity - by approximately a factor of 5-10 to compete with fossil and nuclear electricity and by a factor of 25-50 to compete with primary fossil energy. New materials to efficiently absorb sunlight, new techniques to harness the full spectrum of wavelengths in solar radiation, and new approaches based on nanostructured architectures can revolutionize the technology used to produce solar electricity.⁶⁷

To be competitive with inorganic semiconductors, organic materials should possess similar *physical* properties, such as high conductivity, chemical and thermal stability, and appropriate HOMO-LUMO gap. Once the *electronic* properties are matched, one can take a full advantage of *mechanical* properties of organic materials. Many of them are easily processable, which allows to employ large area printing, and hence a whole range of new electronic devices to be developed - thin, lightweight, and flexible - displays, sensors, memory, field-effect transistors, solar cells, and light emitting diodes.

Due to their physical properties, such as self-organization, high charge mobility along the columns, self-healing abilities, organic materials based on extended polycyclic aromatic hydrocarbons are naturally one of the most promising candidates to be used as an active component in many organic electronic devices. A representative example is synthetically

prepared hexa-*peri*-hexabenzocoronene (HBC).⁶⁸ When substituted appropriately, HBCs form columnar mesophases.⁶⁹ The overlap of the molecular π -systems within columns allows charge carriers to hop between the disc-like molecules, with the overall mobilities up to $1 \text{ cm}^2 / \text{V sec}$.^{42, 70} These materials can be efficiently used in field-effect transistors, injection layers, or solar cells.^{68, 71}

Another typical example is pyrene, perhaps the most extensively studied member of the polycyclic aromatic hydrocarbon family. It has interesting photophysical properties, such as long excited state lifetime, high quantum yield of fluorescence, and pronounced ability to form excimers.⁷² Pyrene exhibits sensitive solvatochromic behavior, with the relative intensity of emission bands that depends on the solvent polarity.⁷² Pyrene and its derivatives form π -stacks in solution and in the solid state, similar to the derivatives of HBCs.^{47, 72} By incorporating pyrene into conjugated oligomers or polymers it is possible to obtain materials with unique photophysical properties.^{73, 74}

Studies of these two compounds, as well as the other PAHs, have shown that the periphery, functionalization, and overall size of PAHs are crucial parameters which significantly alter their electronic structure and chemical reactivity.²⁶ In particular, a large aromatic core results in a better overlap of the molecular π -systems, which might increase charge mobility of a corresponding material (cf. triphenylenes and hexabenzocoronenes).⁴⁷ Therefore, the major directions for synthetic chemistry are: synthesis and characterization of *extended* PAHs - with different functional groups improving their processability,⁶² various chemical dopings tuning the electronic structure (e.g. B-N doped systems)⁷⁵, and periphery changing their chemical reactivity.^{76, 77} Another direction is synthesis of metal-PAH complexes, where the metal atom may sufficiently influence physical properties of these materials.^{63, 64}

The main objective of this work is to develop novel synthetic concepts, which allow huge nanographenes to be synthesized starting from a small PAH building block. Following this method, it shall be possible to synthesize various extended nanographenes, including those containing heteroatoms in the core part. The second objective is to introduce metal centers into these nanographenes by complexing “super-ligands” with copper or ruthenium. The third objective is to achieve easily processable (soluble) compounds, by

choosing appropriate substitutions (bulky tert-butyl groups) which distort the aromatic core by reducing the usually very pronounced aromatic π -stacking.

1.7 References

1. Müller, R. S. T. I. K., *Device Electronics for Integrated Circuits*. Wiley: New York, 1986.
2. Cao, X. F.; Jiang, J. P.; Bloch, D. P.; Hellwarth, R. W.; Yu, L. P.; Dalton, L., *J. Appl. Phys.* **1989**, 65, (12), 5012-5018.
3. Dimitrakopoulos, C. D.; Malenfant, P. R. L., *Advanced Materials* **2002**, 14, (2), 99-117.
4. Gelinck, G., *Nature* **2007**, 445, (7125), 268-270.
5. Tanaka, K.; Ohzeki, K.; Nankai, S.; Yamabe, T.; Shirakawa, H., *Journal of Physics and Chemistry of Solids* **1983**, 44, (11), 1069-1075.
6. <http://nobelprize.org>
7. Zander, M., *Handbook of Polycyclic Aromatic Hydrocarbons*. New York, 1983.
8. Clar, E., *Polycyclic Hydrocarbons*. New York, 1964; Vol. 1, 2.
9. Dias, J. R., *Polycyclic Aromatic Compounds* **2005**, 25, 113-127.
10. Henning, T.; Salama, F., *Science* **1998**, 282, (5397), 2204-2210.
11. www.nasa.gov
12. Herndon, W. C.; Connor, D. A.; Lin, P. P., *Pure and Applied Chemistry* **1990**, 62, (3), 435-444.
13. Herndon, W. C.; Nowak, P. C.; Connor, D. A.; Lin, P. P., *J. Am. Chem. Soc.* **1992**, 114, (1), 41-47.
14. Schleyer, P. V.; Kiran, B.; Simion, D. V.; Sorensen, T. S., *J. Am. Chem. Soc.* **2000**, 122, (3), 510-513.
15. Schleyer, P. V.; Jiao, H. J.; Hommes, N. J. R. V.; Malkin, V. G.; Malkina, O. L., *J. Am. Chem. Soc.* **1997**, 119, (51), 12669-12670.
16. Zander, M., *Polycyclische Aromaten*. B.G.Teubner Verlag: Stuttgart, 1995.
17. Lehmann, E.; Auffarth, J.; Hager, J.; Rentel, K. H.; Altenburg, H., *Staub Reinhaltung Der Luft* **1986**, 46, (3), 128-131.

18. Strewe, K.; Neumann, H. J., *Erdol & Kohle Erdgas Petrochemie* **1983**, 36, (5), 231-231.
19. Sullivan, R. F.; Boduszynski, M. M.; Fetzer, J. C., *Energy & Fuels* **1989**, 3, (5), 603-612.
20. Scholl, R.; Seer, C., *Justus Liebigs Annalen Der Chemie* **1912**, 394, (1/3), 111-177.
21. Scholl, R.; Seer, C., *Berichte Der Deutschen Chemischen Gesellschaft* **1911**, 44, 1233-1240.
22. Scholl, R.; Seer, C.; Weitzenbock, R., *Berichte Der Deutschen Chemischen Gesellschaft* **1910**, 43, 2202-2209.
23. Clar, E., *Berichte Der Deutschen Chemischen Gesellschaft* **1929**, 62, 1574-1582.
24. Clar, E., *Berichte Der Deutschen Chemischen Gesellschaft* **1929**, 62, 350-359.
25. Clar, E.; John, F.; Hawran, B., *Berichte Der Deutschen Chemischen Gesellschaft* **1929**, 62, 940-950.
26. Clar, E.; Wallenstein, H.; Avenarius, R., *Berichte Der Deutschen Chemischen Gesellschaft* **1929**, 62, 950-955.
27. Clar, E.; Zander, M., *J. Chem. Soc.* **1958**, (Apr), 1577-1579.
28. Clar, E.; Zander, M., *J. Chem. Soc.* **1957**, (Nov), 4616-4619.
29. Clar, E.; Ironside, C. T.; Zander, M., *Tetrahedron* **1959**, 6, (4), 358-363.
30. Davies, W.; Porter, Q. N., *J. Chem. Soc.* **1957**, (Dec), 4967-4970.
31. Müller, M.; Kübel, C.; Müllen, K., *Chem. Eur. J.* **1998**, 4, (11), 2099-2109.
32. Berliner, E., *Organic Reactions* **1948**, 5, 229-289.
33. Harvey, R. G.; Pataki, J.; Cortez, C.; Diraddo, P.; Yang, C. X., *J. Org. Chem.* **1991**, 56, (3), 1210-1217.
34. Diederich, F.; Staab, H. A., *Angew. Chem., Int. Ed. Engl.* **1978**, 17, (5), 372-374.
35. Krieger, C.; Diederich, F.; Schweitzer, D.; Staab, H. A., *Angew. Chem., Int. Ed. Engl.* **1979**, 18, (9), 699-701.
36. Staab, H. A.; Diederich, F., *Chemische Berichte-Recueil* **1983**, 116, (10), 3487-3503.
37. Caronna, T.; Sinisi, R.; Catellani, M.; Malpezzi, L.; Meille, S. V.; Mele, A., *Chemical Communications* **2000**, (13), 1139-1140.

38. Behm, H.; Lourens, A. F.; Beurskens, P. T.; Prinsen, W. J. C.; Hajee, C. A. J.; Laarhoven, W. H., *Journal of Crystallographic and Spectroscopic Research* **1988**, 18, (4), 465-470.
39. Xiao, S. X.; Myers, M.; Miao, Q.; Sanaur, S.; Pang, K. L.; Steigerwald, M. L.; Nuckolls, C., *Angew. Chem., Int. Ed.* **2005**, 44, (45), 7390-7394.
40. Scott, L. T.; Cheng, P. C.; Hashemi, M. M.; Bratcher, M. S.; Meyer, D. T.; Warren, H. B., *J. Am. Chem. Soc.* **1997**, 119, (45), 10963-10968.
41. Scott, L. T.; Hashemi, M. M.; Meyer, D. T.; Warren, H. B., *J. Am. Chem. Soc.* **1991**, 113, (18), 7082-7084.
42. Scott, L. T.; Boorum, M. M.; McMahon, B. J.; Hagen, S.; Mack, J.; Blank, J.; Wegner, H.; de Meijere, A., *Science* **2002**, 295, (5559), 1500-1503.
43. Müller, M.; Kübel, C.; Morgenroth, F.; Iyer, V. S.; Müllen, K., *Carbon* **1998**, 36, (5-6), 827-831.
44. Morgenroth, F.; Kübel, C.; Müller, M.; Wiesler, U. M.; Berresheim, A. J.; Wagner, M.; Müllen, K., *Carbon* **1998**, 36, (5-6), 833-837.
45. Müller, M.; Iyer, V. S.; Kübel, C.; Enkelmann, V.; Müllen, K., *Angew. Chem., Int. Ed. Engl.* **1997**, 36, (15), 1607-1610.
46. Stabel, A.; Herwig, P.; Müllen, K.; Rabe, J. P., *Angew. Chem., Int. Ed. Engl.* **1995**, 34, (15), 1609-1611.
47. Watson, M. D.; Fechtenkötter, A.; Müllen, K., *Chem.Rev.* **2001**, 101, (5), 1267-1300.
48. Wasserfallen, D.; Kastler, M.; Pisula, W.; Hofer, W. A.; Fogel, Y.; Wang, Z. H.; Müllen, K., *J. Am. Chem. Soc.* **2006**, 128, (4), 1334-1339.
49. Whitesides, G. M.; Grzybowski, B., *Science* **2002**, 295, (5564), 2418-2421.
50. Brunsveld, L.; Folmer, B. J. B.; Meijer, E. W.; Sijbesma, R. P., *Chem. Rev.* **2001**, 101, (12), 4071-4097.
51. Pak, C.; Lee, H. M.; Kim, J. C.; Kim, D.; Kim, K. S., *Structural Chemistry* **2005**, 16, (3), 187-202.
52. Collings, P. J., Hird, M., *An Introduction to Liquid Crystals: Chemistry and Physics*. Taylor&Francis: London, 1997.

53. Destrade, C.; Foucher, P.; Gasparoux, H.; Tinh, N. H.; Levelut, A. M.; Malthete, J., *Molecular Crystals and Liquid Crystals* **1984**, 106, (1-2), 121-146.
54. Foucher, P.; Destrade, C.; Tinh, N. H.; Malthete, J.; Levelut, A. M., *Molecular Crystals and Liquid Crystals* **1984**, 108, (3-4), 219-229.
55. Dean, J. A., *The Analytical Chemistry Handbook*. McGraw Hill, Inc.: New York, 1995; p 15.1-15.5.
56. Cherodian, A. S.; Davies, A. N.; Richardson, R. M.; Cook, M. J.; Mckeown, N. B.; Thomson, A. J.; Feijoo, J.; Ungar, G.; Harrison, K. J., *Molecular Crystals and Liquid Crystals* **1991**, 196, 103-114.
57. Leroy, A. E., *X-ray Diffraction Methods in Polymer Science* Krieger: 1985.
58. Xia, Y. D.; Mokaya, R., *Microporous and Mesoporous Materials* **2006**, 94, (1-3), 295-303.
59. Mckeown, N. B., *Phthalocyanine Materials*. University press: Cambridge, 1998.
60. Simpson, C. D.; Brand, J. D.; Berresheim, A. J.; Przybilla, L.; Räder, H. J.; Müllen, K., *Chem. Eur. J.* **2002**, 8, (6), 1424-1429.
61. Tomovic, Z.; Watson, M. D.; Müllen, K., *Angew. Chem., Int. Ed.* **2004**, 43, (6), 755-758.
62. Kastler, M. *Discotic Materials for Organic Electronics*. Johannes Gutenberg-Universität, Mainz, 2006.
63. Braga, D.; Grepioni, F.; Biradha, K.; Pedireddi, V. R.; Desiraju, G. R., *J. Am. Chem. Soc.* **1995**, 117, (11), 3156-3166.
64. Long, N. J., *Angew. Chem., Int. Ed. Engl.* **1995**, 34, (1), 21-38.
65. Nakagawa, K.; Nishimoto, H.; Enoki, Y.; Egashira, S.; Ikenaga, N. O.; Kobayashi, T.; Nishitani-Gamo, M.; Ando, T.; Suzuki, T., *Chem. Lett.* **2001**, (5), 460-461.
66. Barigelletti, F.; Flamigni, L.; Balzani, V.; Collin, J. P.; Sauvage, J. P.; Sour, A.; Constable, E. C.; Thompson, A. M. W. C., *Coord. Chem. Rev.* **1994**, 132, 209-214.
67. www.sc.doe.gov/bes/reports/files/SEU_rpt.pdf
68. Kastler, M.; Pisula, W.; Wasserfallen, D.; Pakula, T.; Müllen, K., *Journal of the American Chemical Society* **2005**, 127, (12), 4286-4296.

69. Wasserfallen, D.; Kastler, M.; Pisula, W.; Hofer, W. A.; Fogel, Y.; Wang, Z. H.; Müllen, K., *Journal of the American Chemical Society* **2006**, 128, (4), 1334-1339.
70. van de Craats, A. M.; Warman, J. M.; Fechtenkötter, A.; Brand, J. D.; Harbison, M. A.; Müllen, K., *Adv. Mater.* **1999**, 11, (17), 1469-1472.
71. Schmidt-Mende, L.; Fechtenkötter, A.; Müllen, K.; Moons, E.; Friend, R. H.; MacKenzie, J. D., *Science* **2001**, 293, (5532), 1119-1122.
72. Winnik, F. M., *Chem. Rev.* **1993**, 93, (2), 587-614.
73. Leroy-Lhez, S.; Fages, F., *Eur. J. Org. Chem.* **2005**, (13), 2684-2688.
74. Leroy-Lhez, S.; Parker, A.; Lapouyade, P.; Belin, C.; Ducasse, L.; Oberle, J.; Fages, F., *Photochemical & Photobiological Sciences* **2004**, 3, (10), 949-958.
75. Harriman, A.; Izzet, G.; Ziessel, R., *J. Am. Chem. Soc.* **2006**, 128, (33), 10868-10875.
76. Wang, Z., Tomovic, Z., Kastler, M., Pretsch, R., Negri, F., Enkelmann, V., Müllen, K., *J. Am. Chem. Soc.* **2004**, 126, 7794-7795.
77. Kastler, M., Schmidt, J., Pisula, W., Sebastiani, D., Müllen, K., *J. Am. Chem. Soc.* **2006**, 128, (29), 9526-9534.

2 From Pyrene towards Graphite Ribbons

2.1 Synthesis of Graphite Ribbons

Already in early 1960s several research groups (Air Force Materials Laboratory¹⁻⁴, STILLE'S⁵⁻⁷ and MARVEL'S⁸⁻¹⁰ groups) started to develop synthetic methods to obtain numerous *ladder* or *double-stranded* polymers. Structure-wise, these materials fill in the gap between single-stranded (one-dimensional) conjugated polymers and two-dimensional graphite and combine useful characteristics of both. The ladder or ribbon-type backbone structure has a two-dimensional, planar conformation, resulting in a high delocalization of electrons along the backbone and, correspondingly, high conductivities. However, synthesis and characterization of these compounds is still a challenge in synthetic chemistry. In fact, there are only a few examples of defect-free, soluble hydrocarbon ribbon polymers.^{11, 12} Discrete nanoscale two-dimensional graphite subunits with different shapes and sizes have already been prepared in the group of MÜLLEN.¹³⁻²² The synthetic strategy involves two key steps: (1) synthesis of three-dimensional branched oligophenylenes by repetitive DIELS-ALDER cycloaddition of tetraphenylcyclopentadienones with arylolethylenes or by cobalt-catalyzed cyclotrimerization of diarylethylenes; (2) cyclodehydrogenation of the obtained polyphenylene precursors with FeCl₃ or Cu(OTf)₂-AlCl₃ to obtain graphitic molecules. An appropriate molecular design of branched polyphenylenes suitable for full cyclodehydrogenation is crucial for making 2D graphite ribbons with extended conjugation. SHIFRINA *et al.*^{5, 23, 24} demonstrated that the repetitive DIELS-ALDER cycloaddition of bis(tetraphenylcyclopentadienone)benzene (**2-1**) and 1,4-diethynylbenzene (**2-2**) results in high molecular weight branched polyphenylenes (Figure 2-1). The cycloaddition product of **2-1** and **2-2** has three structural isomeric repeat units as well as the gaps in between them, without phenyl rings. This prevents obtaining continuous ribbon structures of a regular width after planarization. Rotation around phenyl-phenyl single bonds along the main chain further complicates the intramolecular cyclodehydrogenation, which yields only partial planarization, with incoherent and relatively small PAH segments along the polymer backbone.

2 From Pyrene towards Graphite Ribbons

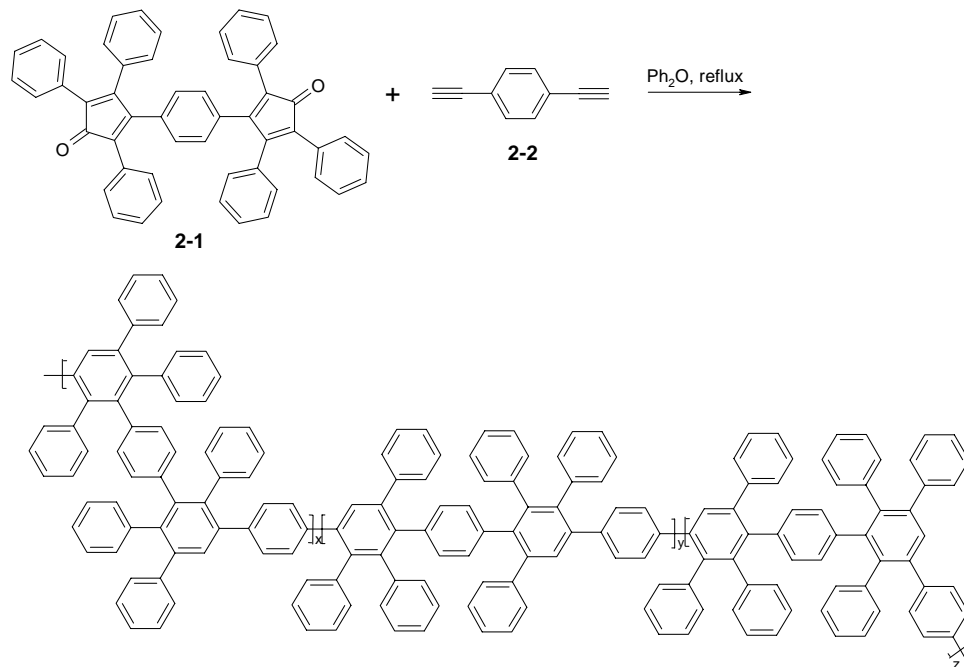


Figure 2-1. Diels-Alder cycloaddition route to branched polyphenylenes

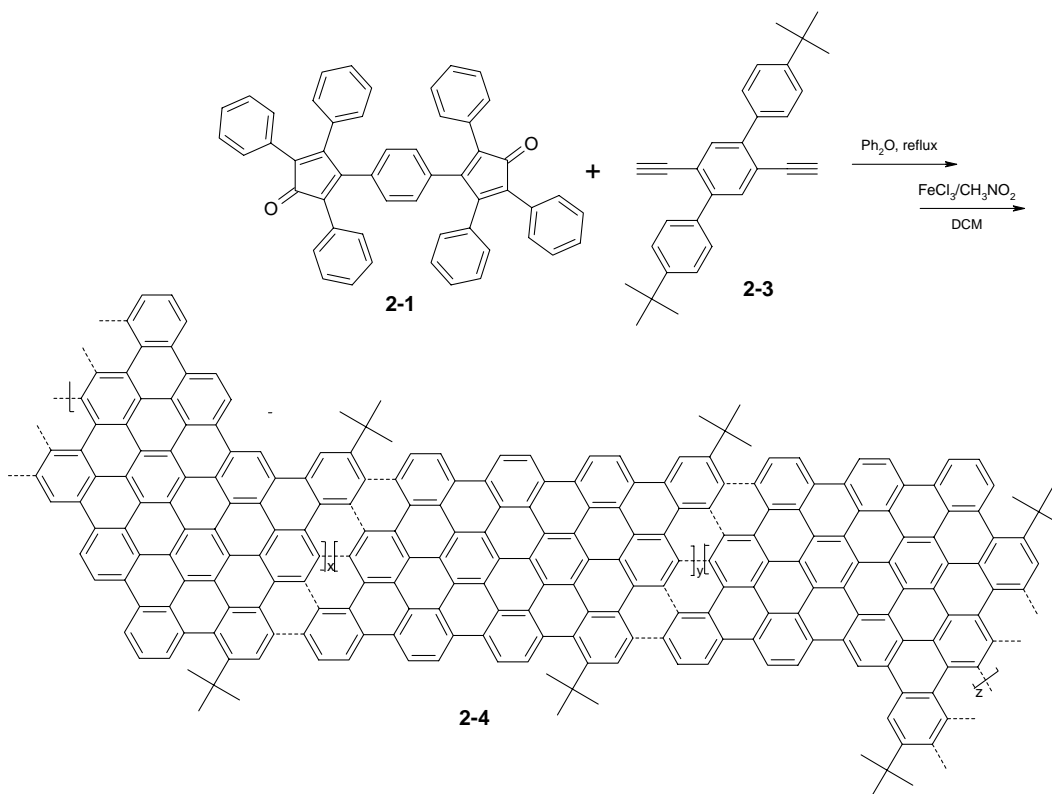


Figure 2-2. Synthetic route towards the graphite ribbons

reduce the amount of partially cyclized products.²⁷ Bis-cyclopentadienone synthesis is shown in Figure 2-4. The first step is to functionalize 2,7-di-*tert*-butylpyrene, *i.e.* to introduce keto-groups, which then participate in the KNOEVENAGEL condensation and yield the bis-cyclopentadienone block.

The classical synthetic procedure to prepare 2,7-di-*tert*-butylpyrene-4,5-dione and 2,7-di-*tert*-butylpyrene-4,5,9,10-tetraone usually involves three steps: bromination of 2,7-di-*tert*-butylpyrene, preparation of 2,7-di-*tert*-butyl-4,5,9,10 tetramethoxypyrene and further demethylation with BBr₃.²⁸ One-step attempts were normally unsuccessful, since sites other than C(4) and C(5) oxidize more readily.^{29, 30} Only recently HARRIS *et al.*³¹ suggested a significantly simplified procedure, which includes treatment of pyrene with a heterogeneous mixture of ruthenium(III) chloride (RuCl₃) and sodium periodate (NaIO₄) in methylene chloride (CH₂Cl₂), water, and acetonitrile (CH₃CN). By varying the amount of the oxidant and temperature, the reaction can be controlled in a way that only the 4- and 5- or 4-, 5-, 9-, and 10 positions of pyrene are oxidized.

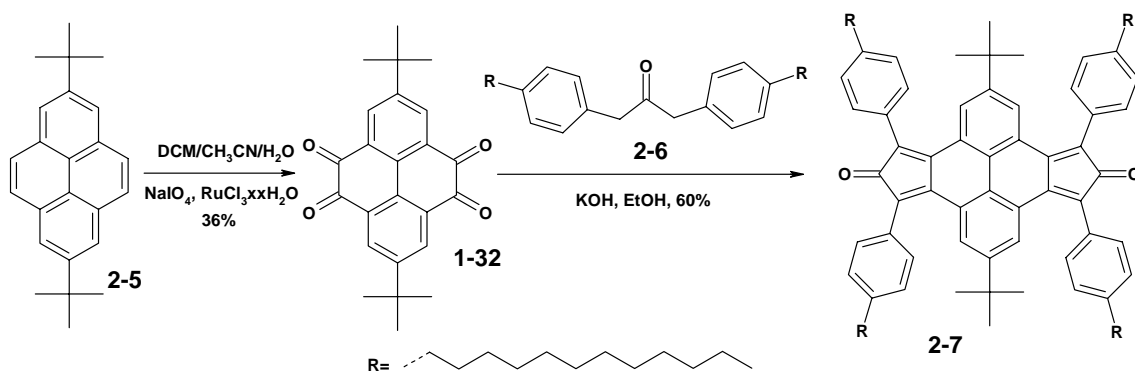


Figure 2-4. Synthesis of the building block **2-7**

Using this method, 2,7-di-*tert*-butylpyrene-4,5,9,10-tetraone (**1-32**) was synthesized with the yield of 36%. The KNOEVENAGEL condensation of the obtained **1-32** with 1,3-bis-(4-*n*-dodecyl-phenyl)propan-2-one (**2-6**) furnished the desired 2,7-di-*tert*-butyl-4,5,9,10-bis(2,5-di-*p*-dodecyl-phenylcyclopenta)-[*e,l*]pyren-5,11-dione (**2-7**).²⁷ Optimization of the reaction conditions such as time (3 h), temperature (60 °C) and ratio of starting materials (1(**1-32**):2.7(**2-6**):1.5(KOH)) resulted in 60% yield of **2-7** (see Experimental Section).

The other building block, 2''-ethynyl-2,3,4,5-tetrakis(4-dodecylphenyl)-[1,1';2',1'']terphenyl (**2-10**), was synthesized via stoichiometrically controlled DIELS – ALDER reaction between 2,3,4,5-tetrakis(4-dodecyl-phenyl)cyclopenta-2,4-dienone (**2-9**) and 2,2'-diethynylbiphenyl (**2-8**)^{32, 33} (Figure 2-5). This reaction was carried out in toluene at 110°C. Two products were separated using column chromatography.

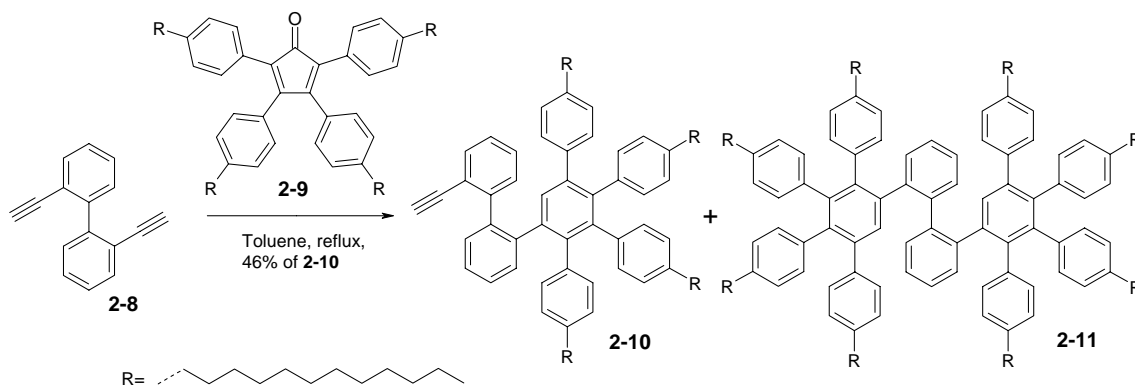


Figure 2-5. Diels-Alder cycloaddition towards **2-10**

After the synthesis of the two building blocks, **2-7** and **2-10**, their DIELS-ALDER reaction was carried out in toluene in a CEM Discover microwave at 300 W and activated cooling, keeping the temperature at 110 °C for 1 h (see Figure 2-6). Two products, the cyclopentadienone derivative **2-12** and the first ribbon **2-13** were separated by column chromatography using a gradient of PE and DCM mixture as eluent (4:1 for isolation of **2-13** and 2:1 - **2-12**). Thus, the ribbon **2-13** was obtained in 21% yield.

According to this reaction setup the maximum theoretically achievable yield of **2-13** is 50%. Additionally, taking all aspects associated with the stoichiometrically controlled DIELS-ALDER reaction (ratio of building blocks, temperature, thermal instability of bis-cyclopentadienone **2-7** and further workup) into account, the 21% yield is satisfactory.

The cyclopentadienone derivative **2-12** was obtained in 28% yield. Due to its thermal instability, the building block **2-12** was immediately used in the next DIELS-ALDER reaction, without full characterization (only MALDI TOF mass spectrometry was used). The cycloaddition between **2-12** and **2-8** provided, after necessary workup (column

chromatography and additionally, preparative TLC plates), **2-14** in 25% and the target ribbon **2-15** in 15% yield.

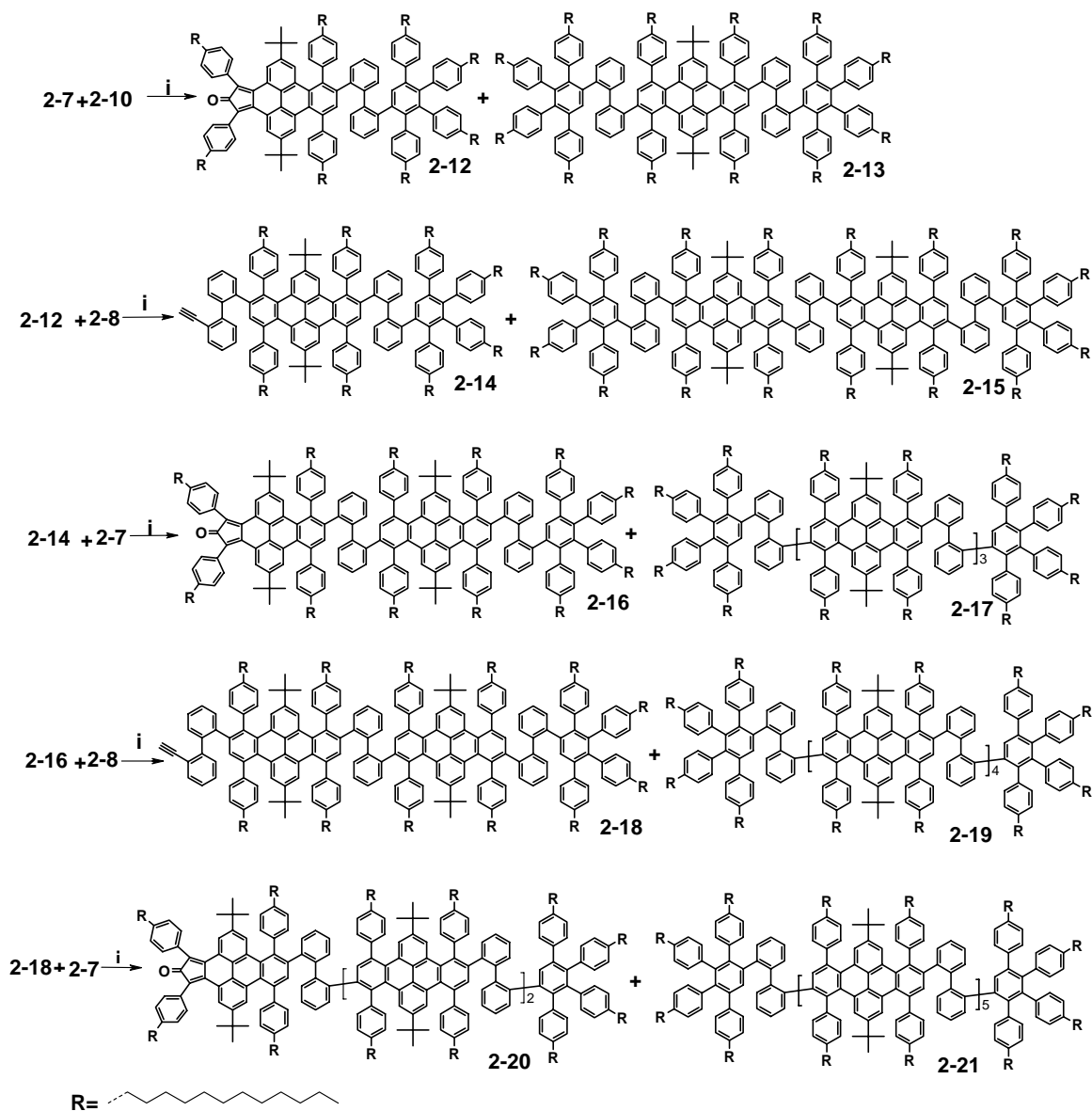


Figure 2-6. Iterative synthetic route towards a homologue series of ribbons with $n=5$. Reaction conditions: (i) CEM Discover microwave, 300 W, toluene, 110 °C

Repeating the abovementioned protocols, i.e. the stoichiometrically controlled DIELS-ALDER reaction (toluene, 110 °C, CEM Discover microwave at 300 W and activated cooling, 1 h) between corresponding building blocks - **2-14** and **2-7**; **2-16** and **2-8**; and finally **2-18** and **2-8**, compounds up to **2-21** (five ribbons of different sizes) were synthesized (see Table 2-1).

Table 2-1. Summarized results of DIELS-ALDER reactions towards five polyphenylene ribbons

DIELS-ALDER reaction between		Obtained products	Yields, % (50 % -max)
2-7	2-10	2-12	28
		2-13	21
2-8	2-12	2-14	25
		2-15	15
2-7	2-14	2-16	29
		2-17	15
2-8	2-16	2-18	34
		2-19	15
2-7	2-18	2-21	10

Note that all cyclopentadienone derivatives (**2-7**, **2-12**, **2-16** and **2-20**) are thermally unstable. Hence, they were used in the reactions without full characterization (only MALDI TOF mass spectrometry). All obtained ethynyl derivatives (**2-10**, **2-14** and **2-18**) were stable and were characterized by the standard analytical techniques: MALDI TOF and NMR spectroscopy. The larger the ethynyl building block is, the more complicated the purification of the corresponding compounds is. Synthetic details for all compounds are included in the Experimental Section.

All ribbons (**2-13**, **2-15**, **2-17**, **2-19**, see Figure 2-7) up to the longest one, **2-21**, with 372 skeletal atoms, possessed very good solubility in common organic solvents. This is due to

their branched structure and solubilizing alkyl chains. Hence, their characterization was performed using standard analytical techniques.

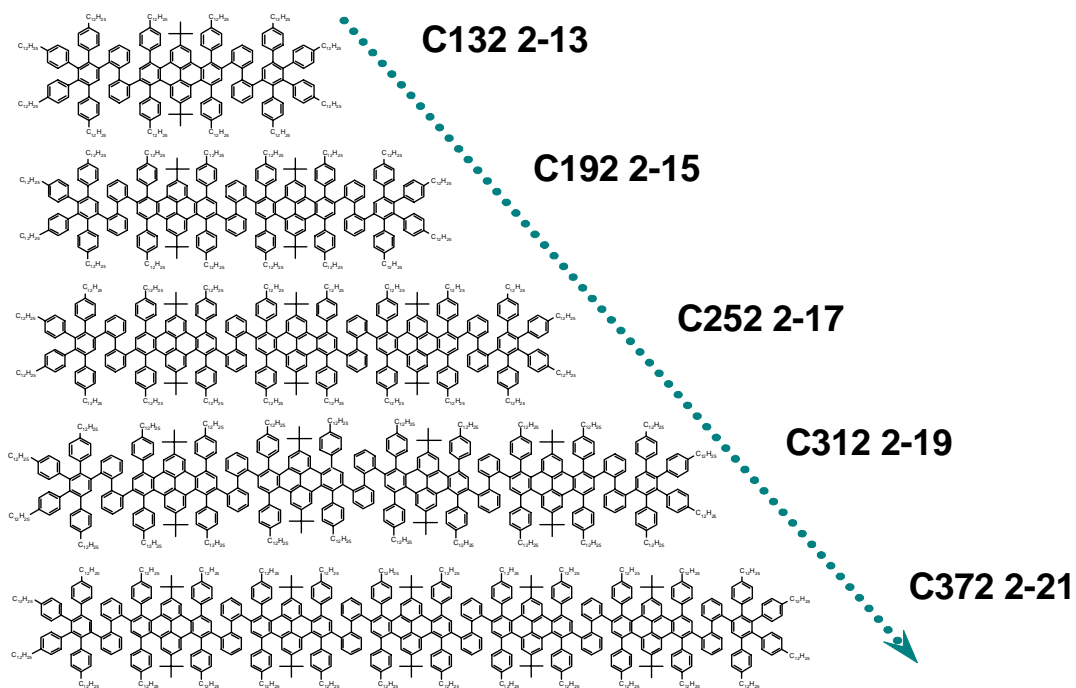


Figure 2-7. The series of ribbons from 2-13 up to 2-21

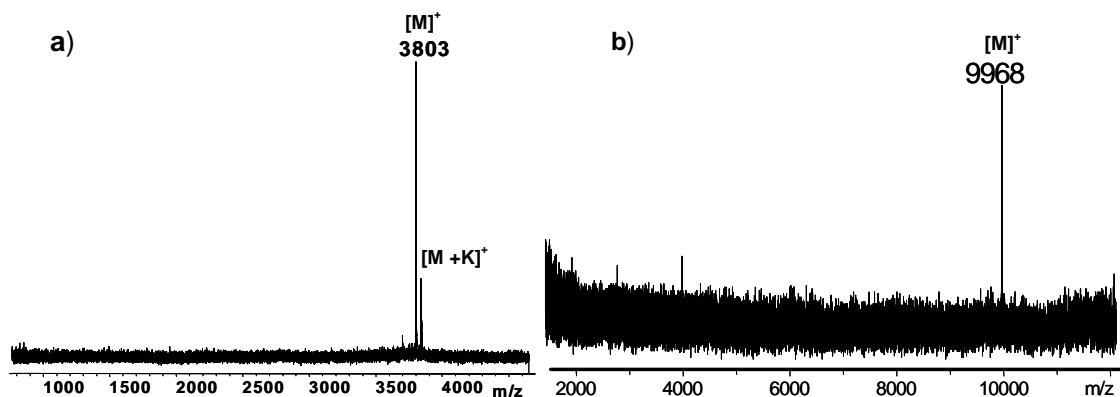


Figure 2-8. MALDI-TOF mass spectrum of 2-13 (a) and 2-21 (b)

Characterization by MALDI-TOF mass spectrometry (using dithranol as a matrix, and in some cases, adding a suitable cationization agent) and NMR spectroscopy unequivocally proved the proposed molecular structures of all synthesized molecules **2-13**, **2-15**, **2-17**, **2-19** and **2-21**. As a representative example, the MALDI-TOF mass spectra of the shortest and the longest ribbons (**2-13** and **2-21**) are shown in Figure 2-8, a and b, respectively. The spectra exhibit strong molecular peaks at m/z 3803 and 9968 Da.

NMR spectroscopy was performed in THF- d_8 . Figure 2-9 shows the ^1H NMR spectrum of **2-13** which is typical also for higher molecular weight ribbons. However, NMR signals broaden going from **2-13** to **2-21** as in the case of polymers. High temperature NMR-measurements did not provide better resolution of the peaks.

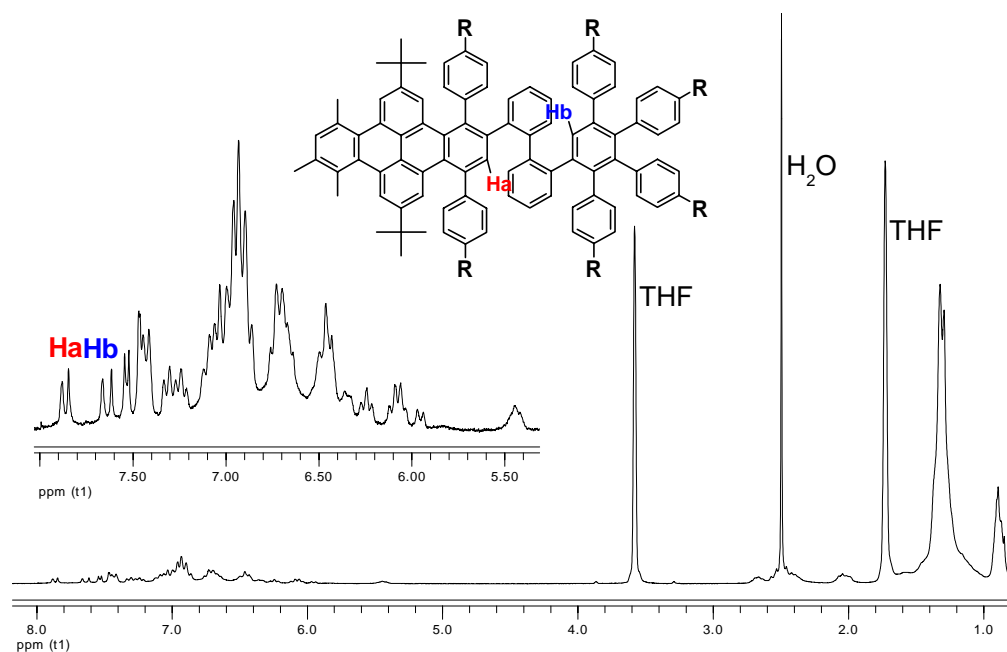


Figure 2-9. ^1H NMR-spectrum of **2-13** in THF- d_8 at room temperature (250 MHz)

The aromatic region of **2-13** is already quite broad, the proton resonances overlap, and hence only some of the signals could be distinguished. The integration of the peak intensities, however, agreed well with the calculated values. The two proton resonances, Ha of dibenzo[*e,l*]pyrene moiety appeared as a doublet at 7.86 ppm. For two protons, Hb,

located on the tetraphenyl benzene rings, two singlets were detected at 7.66 and 7.61 ppm. These two specific protons are typical for the NMR spectra of polyphenylene dendrimers, where they reflect the layer-by-layer build-up of the dendrimers³⁴. In the case of the alkyl substitutions in the periphery of the ribbons, the intensity ratios between aromatic and aliphatic signals corresponded to the expected values (see the Experimental Section).

Analysis by gel permeation chromatography (GPC) showed the monodisperse nature of the ribbons. High-performance liquid chromatography confirmed the ribbons purity.

2.3 Synthesis of Ladder Polymers

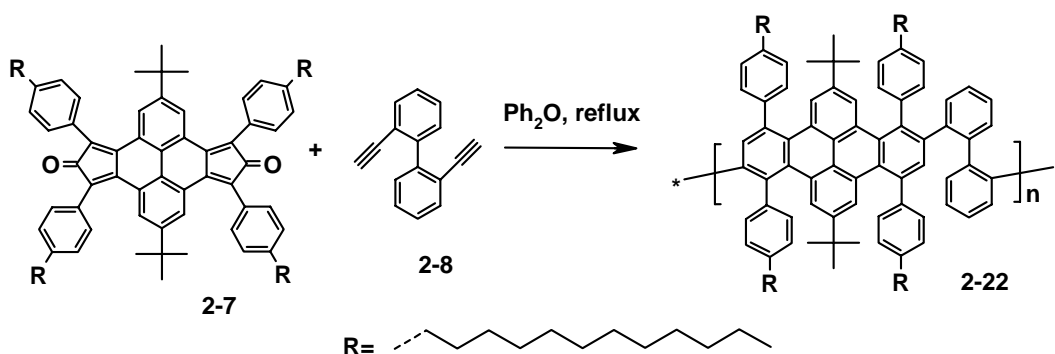


Figure 2-10. Synthetic route towards a polymer structure **2-22**

Bis-cyclopentadienone **2-7** can also be used directly for synthesis of ladder-type polymers, as shown in Figure 2-10. A microwave-assisted (300 Watt and activated cooling) DIELS-ALDER reaction between **2-7** and bis-substituted acetylene **2-8** in 1:1 ratio was carried out at 230°C in diphenylether for 12 h under inert atmosphere. Before heating the reaction mixture was thoroughly degassed in order to exclude traces of oxygen, which could prevent the polymerization. The reaction was monitored by mass spectrometry, i.e. every 2 h a sample from the reaction mixture was taken and analyzed by using MALDI TOF. After 12 h the recorded MALDI-TOF spectrum (Figure 2-11) showed the presence of polyphenylene oligomers, up to twelve repeat units long. Prolongation of the reaction did not yield a higher molecular weight polymer.

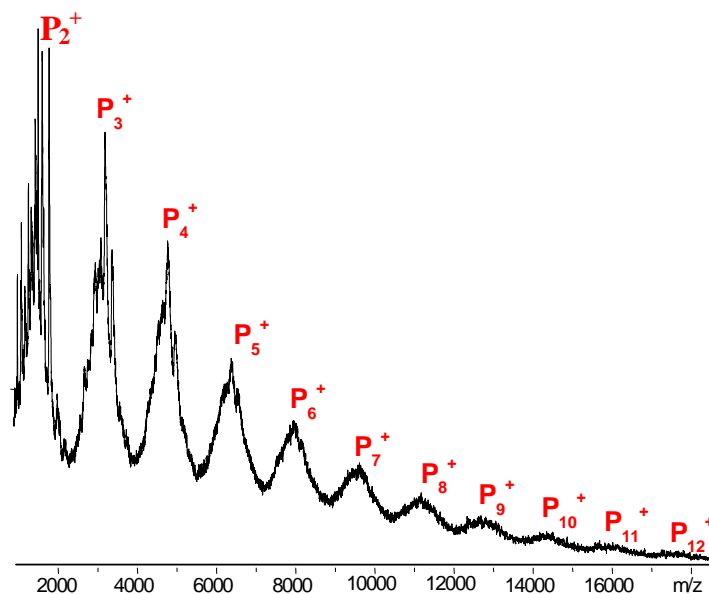


Figure 2-11. MALDI-TOF spectrum (linear mode) of the attempted polymerization

There could be several reasons why the polymerization reaction did not give higher molecular weight polymers. First, the starting material **2-7** and the reaction intermediates (different cyclopentadienone (diene) derivatives) are thermally unstable, as it has been observed earlier in the synthesis of the polyphenylene ribbons. Second, since **2-7** is unstable, it is difficult to quantify its purity. However, it is an important factor, because the ratio of the precursors in the polymerization reaction must be 1:1. Finally, traces of oxygen could inhibit the reaction. The abovementioned points make this approach ineffective. Longer polymer chains can be synthesized using step by step DIELS-ALDER method, where the abovementioned points do not play so dramatic roles.

In total, five polyphenylene ribbons (**2-13**, **2-15**, **2-17**, **2-19** and **2-21**) were synthesized in order to obtain two-dimensional ladder-type graphenes of different length. The properties of 2D graphenes such as self-organization, chemical and electronic should be strongly depended on their sizes. The larger the molecule is the better the π - π overlap of the molecules in a stack is, and therefore, efficiency of charge transport.

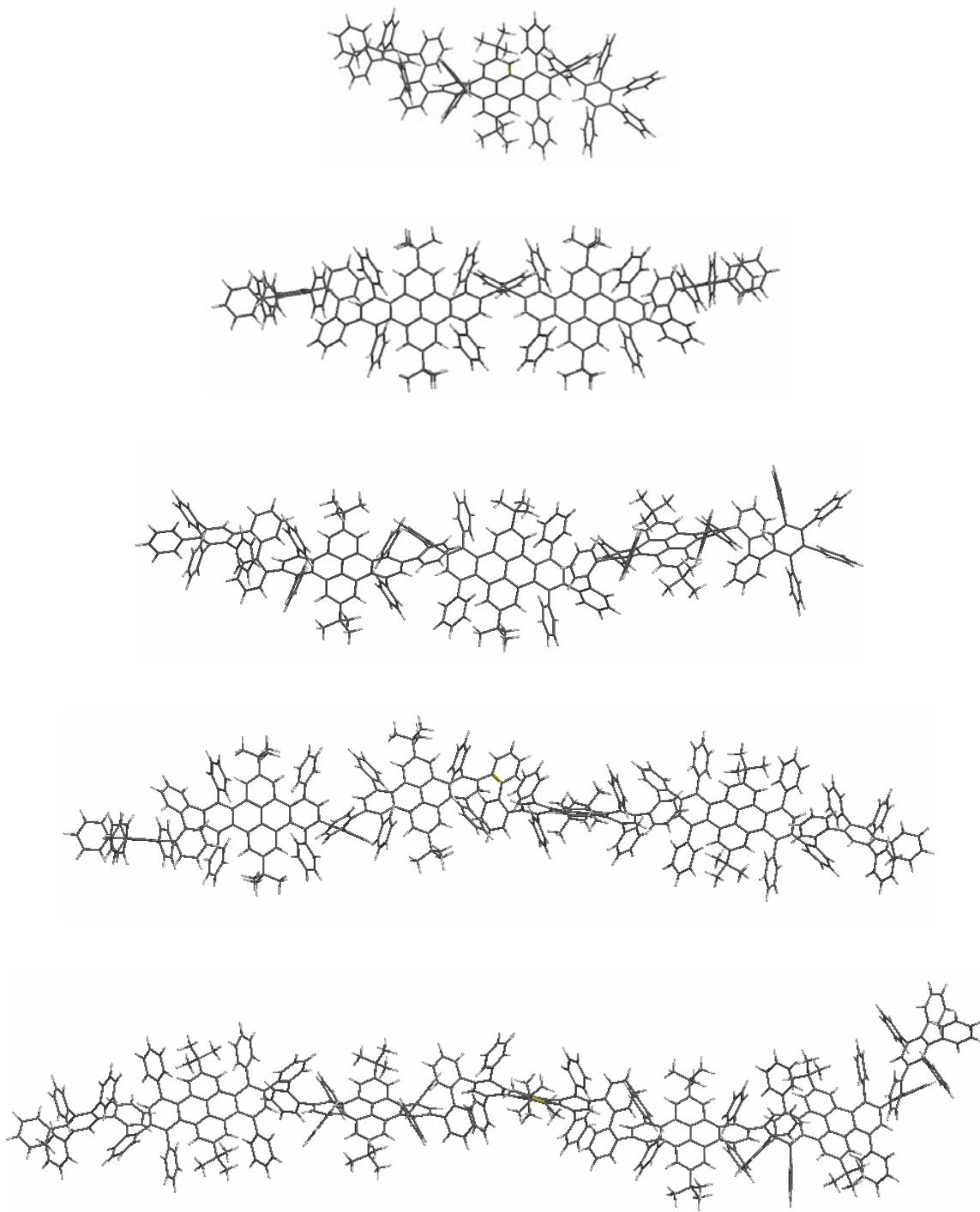


Figure 2-12. Minimized (with molecular mechanics force field available as a part of the Spartan package) structures of polyphenylene ribbons without *n*-dodecyl alkyl chains

Even prior to the cyclodehydrogenation, it is important to identify the shape and size of the oligophenylene precursors. The branched structure of a dendrimer should lead to molecular architectures with spherical symmetry with the small aspect ratio. Rigid dibenzo[*e,l*]pyrene moieties bias rod-like shape with the high aspect ratio. And as it is well-known, high aspect ratio micro/nano-structures are becoming very important for applications in the field of nanotechnology. From simple molecular mechanics of ribbon structures using force field available as a part of the Spartan package (Figure 2-12), one could observe the branched nature of the molecules. However, the presence of dibenzo[*e,l*]pyrene moieties makes them rigid possessing rod-like shape with high aspect ratio. The length of the largest ribbon **2-21**, according calculations, is around 10 nm.

A few analytical techniques (solution and solid) could provide with the information about shape/size of the molecules. The dynamic light scattering technique uses the scattered light to measure the rate of diffusion of the particles. This motion data is conventionally processed to derive a size distribution for the sample, where the size is given by the "Stokes radius" or "hydrodynamic radius" of the particle. This hydrodynamic size depends on both mass and shape (conformation). However, light scattering has not been successful in determining the average molecular size and shape, even for the largest ribbons, and merely indicated that the ribbons do not aggregate in the solution (THF, 10^{-5} mol·L⁻¹), in spite of the fact that pyrene moieties readily self-organize and form π -stacks, similar to HBC.^{13, 18} While dynamic scattering is, in principle, capable of distinguishing whether a polymer is a monomer or dimer, it cannot resolve monomer from small oligomers, and cannot quantitate fractions of small oligomers.

Since the ribbons do not aggregate in the solution, the next logical step would be the solid state characterization, i.e. transmission electron microscopy (TEM).

2.4 Transmission Electron Microscopy of Ribbons

TEM is based on the same principle as the ordinary light microscope; the difference is that TEM uses electrons instead of photons. Since electrons have much lower wavelength, it is possible to obtain a significantly (thousands times) better resolution than

the resolution of an optical microscope. In some cases, even atomistic details can be visualized.

TEM measurements were performed to visualize packing, conformations, and dimensions of ribbons on a carbon-covered copper substrate. Sample preparation was performed by drop casting from THF solution of ribbons on a carbon covered copper grid, which led to the formation of nanoscale particles after the solvent evaporation. Interestingly, there was a correlation between the particle size and the length of the ribbon: the larger the molecule is, the smaller the formed particle is. Particles obtained from **2-21** had an average diameter of 20 nm (Figure 2-13), while particles of about 300 nm were formed from the compound **2-17**. Typically, particles were interconnected with each other forming a network-like architecture.

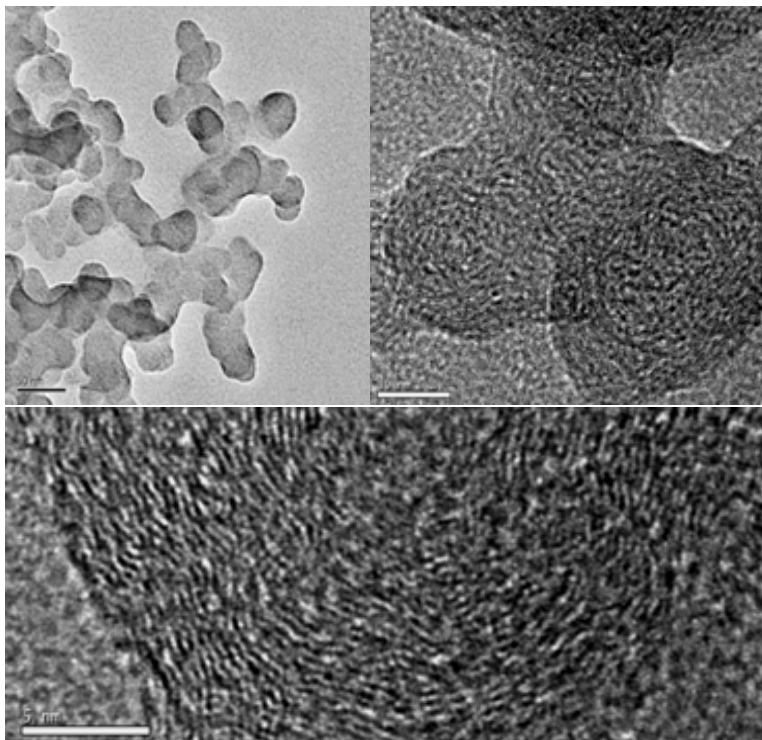


Figure 2-13. TEM-images of **2-21**. Resolution: 50 nm, 10 and 5 nm, respectively

Because of the extremely high tendency of ribbons to aggregate after solvent evaporation, it was impossible to visualize a single chain even at very dilute concentrations (10^{-8} mol/L). High resolution TEM (HRTEM) disclosed that the particles were constructed by

orderly packed wire-like structures (Figure 2-13). The wire-like structures were further organized into an onion-like pattern with a distance of ca. 0.36 nm between the wires. The separation between “wires” is similar to the distance between graphene sheets, which suggests packing of the ribbons due to intermolecular π - π interactions. Finally, the calculated length of **2-21** is about 10 nm, therefore, one can conclude that the observed nanowires are single molecules.

Already polyphenylene precursors are capable to self-organize (in a solid state). Hence, one might expect that, when cyclodehydrogenated, graphite ribbons will preserve (or even improve, due to increased VAN DER WAALS interactions) their self-organizing abilities, while remaining soluble, due to the distortion of the core from planarity by *tert*-butyl groups and the presence of solubilising dodecyl chains (Figure 2-14).

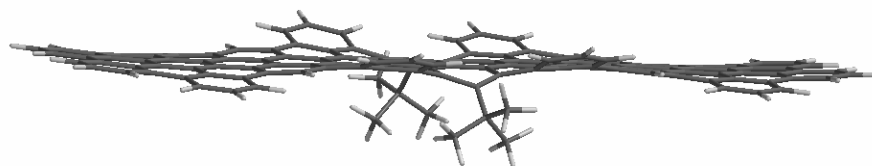


Figure 2-14. Minimized (with molecular mechanics) structure of graphite analogue of the smallest ribbon **2-13** without *n*-dodecyl alkyl chains

2.5 Cyclodehydrogenation of Ribbons

Oligophenylene precursors can be planarized by an intramolecular SCHOLL reaction with aluminum(III)chloride and copper(II) trifluoromethanesulfonate in carbon disulfide.³⁵ These conditions have been used successfully to fuse non-alkylated oligophenylene precursors. However, for alkyl-substituted oligophenylenes the cyclodehydrogenation reaction is accompanied by the cleavage or migration of alkyl side chains, which leads to side-products.³⁶ By exchanging the Lewis acid aluminum(III)chloride with the weaker agent iron(III)chloride WEHMEIER *et al.* suppressed these effects.³⁷ This type of conditions was first used by KOVACIC to synthesize poly-*p*-phenylenes.³⁸⁻⁴⁰

using hot toluene as an eluent. Solubility could be increased as was proposed before due to the presence of many solubilizing long alkyl chains and slight distortion from planarity by *tert*-butyl groups. However, in spite of good solubility the characterization with solution NMR technique failed. Even elevated temperatures did not show any resolved signals in the aromatic region. It is very difficult to obtain well resolved NMR data for PAHs larger than HBCs. Large overlap of π -areas of extended PAHs results in their pronounced self-association and therefore does not allow to resolve properly the aromatic region in the ^1H NMR spectra.^{22, 27, 41}

MALDI TOF mass characterization of the final product was done in solid state using as a matrix *trans*-2-[3-(4-*tert*-butylphenyl)-2-methyl-2-propenylidene]malononitrile (DCTB).³¹ This matrix was specially developed to identify the presence of partially fused side-products. The main peak of the MALDI-TOF spectrum at 3759 Da (see the inset to Figure 2-16) is the by far predominant product and agrees well with the calculated mass distribution of the target graphite molecule **2-23**. At the same time, the presence of the other peaks indicated that the compound contains side-products. At higher molecular weight (3773 Da) a peak of about 10% relative intensity can be assigned to a partially cyclized product with about 6-7 bonds unclosed. At lower molecular weight another peak of also approximately 10% relative intensity could be detected, which corresponds to the loss of a C4 fragment (*tert*-butyl chain). It is unlikely, that this cleavage in the benzylic position occurred during the cyclodehydrogenation. Most probably, it took place during mass measurements. The possibility that it took place during the DIELS-ALDER reaction could be excluded because of the low temperature, which was applied for synthesis of the polyphenylene precursor **2-13**. Such a detailed analysis of this reaction product by MALDI-TOF mass spectrometry, however, could not provide an exact quantification (different desorption probabilities), thus the purity of **2-23** can not be reasonably estimated.

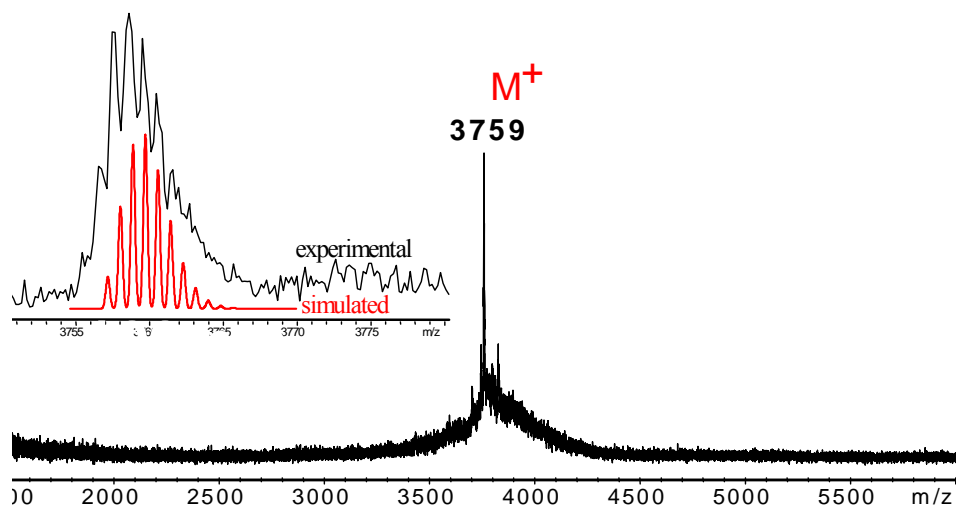


Figure 2-16. MALDI-TOF spectrum of the cyclodehydrogenated product.

The above characterization of the final product shows that fusion does occur but the target graphene molecule coexists with partially cyclised products. The partial cyclodehydrogenation can be rationalized as follows: there are two potential fusion routes for **2-13**.³² The first or “inside-out” pathway goes via formation of central bonds followed by the formation of the bonds at the rim. The second or “outside-in” starts from the bonds at the rim and proceeds with the central bonds. Both pathways are depicted in Figure 2-17. The first formation of an aryl-aryl bond can occur anywhere between two appropriate phenyl rings. If this initial bond formation occurs towards the center of the oligophenylene precursor, the next aryl-aryl bond formation has to overcome only the steric hindrance of the two hydrogens to reach a planar conformation. The cyclodehydrogenation can then continue at the rim of the already planarized core. If the bonds at the rim of the precursor molecule are formed first by the so called “outside-in” pathway, one gains two panels.³² In this situation, the molecule has to overcome the steric repulsion of six hydrogens. This leads to a kinetic barrier, resulting in partially closed species. The system **2-13** already contains a preplanarized (dibenzo[*e,l*]pyrene) core. Hence, one might expect the cyclodehydrogenation process to start at this core and proceed further, following the first route. Indeed, this scenario has been observed for **1-34**^{27, 32} and also for the model compound **2-26** (see Figure 2-18). However, the two

biphenyl-moieties can twist out-of the molecular plane, as depicted in Figure 2-17 with red arrows and have been also seen by minimization of the ribbons in Figure 2-12, thus, probably, complicating the cyclodehydrogenation reaction.

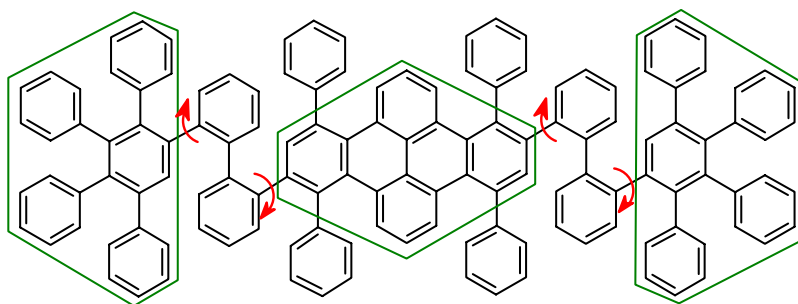


Figure 2-17. Possible panel formation

To demonstrate that the preplanarized core is being advantageous, a model compound **2-26**, was synthesized. The synthesis was done in two steps: first, microwave-assisted DIELS-ALDER reaction between **2-7** and **2-24**, yielded **2-25** in 55%.

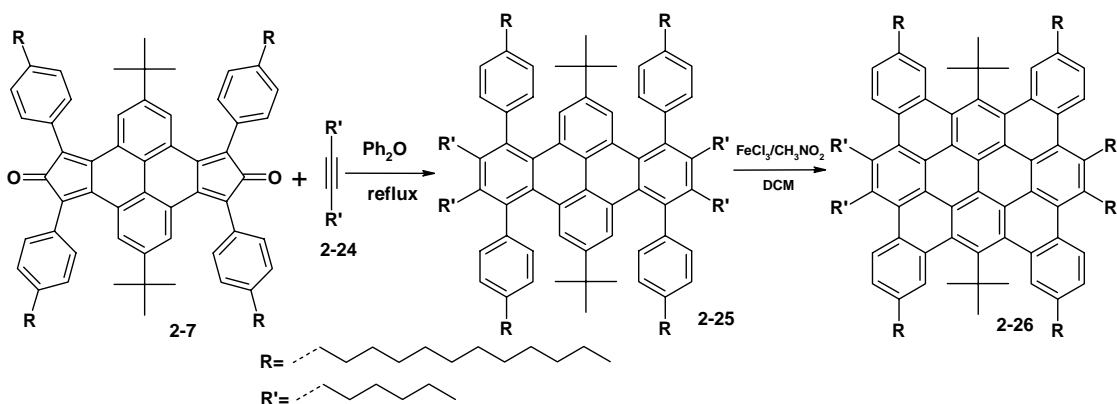


Figure 2-18. Synthesis of the model compound **2-26**

Then, the cyclodehydrogenation was carried out with 8.0 equivalents of iron(III)chloride per aryl-aryl bond (reaction time 1.5 hour). **2-26** was precipitated from the reaction mixture by addition of methanol, washed with water and methanol. Due to reasonably good solubility of the model compound, the purification was done by column chromatography: the crude product was dissolved in hot toluene and filtered over a short silica column. The yield was 80%.

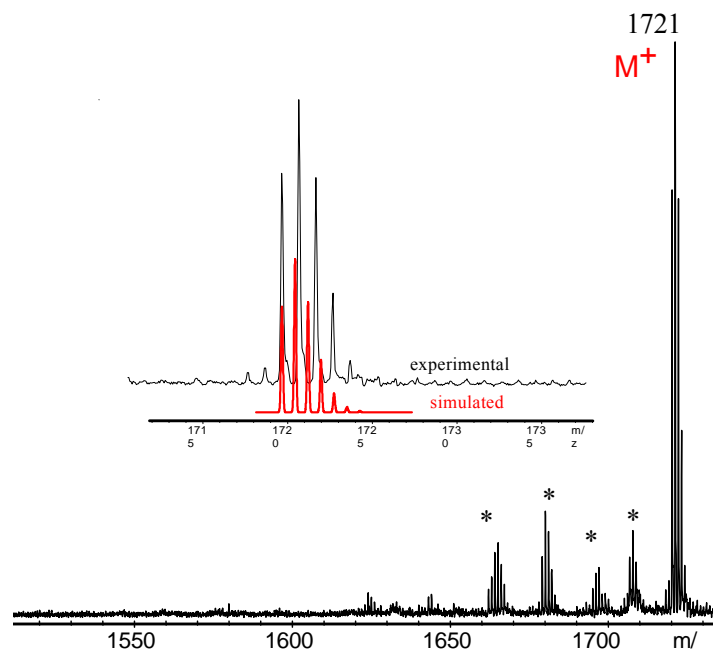


Figure 2-19. MALDI-TOF-spectrum of **2-26** (DCTB as a matrix)

Since NMR techniques failed again, the model molecule was characterized by MALDI TOF mass spectrometry. The MALDI-TOF spectrum agreed well with the simulated spectrum, as shown in Figure 2-19. However, in this case there were no side-peaks except those which belong to fragmentations during the mass-measurement (they are marked with asterix). Fragmentation due to the ionization, which in this case is the cleavage not only of *tert*-butyl groups (as it have been seen for **2-23**) but also longer alkyl chains (C12 or C6) has been checked by increasing the laser intensity. Higher laser intensity resulted in the decrease of the product signal and corresponding increase of the intensity of the side peaks.

The further attention then turned to the characterization of the electronic properties of **2-23** and their comparison to those of the model compound **2-26** and **1-34**.

2.6 UV/Vis-Spectroscopy of Graphite Molecules

Absorption spectra of **2-23** and the model compound **2-26** were recorded in THF at room temperature. The spectrum of **2-23**, presented in Figure 2-20, is rather broad and has

three distinct bands, denoted as α , β and p-bands, according to CLAR's nomenclature.⁴⁴ The weak α -band appears at the highest wavelength of the three and corresponds to a transition from the second highest occupied molecular orbital (HOMO-1) to the lowest unoccupied molecular orbital (LUMO).⁴⁵ The very intense β -band possesses the lowest wavelength of the three and corresponds to a transition from the highest occupied molecular orbital (HOMO) to the second lowest unoccupied orbital (LUMO+1).⁴⁵ The p-band is of intermediate wavelength and intensity and can be assigned to a transition from HOMO to LUMO.⁴⁵

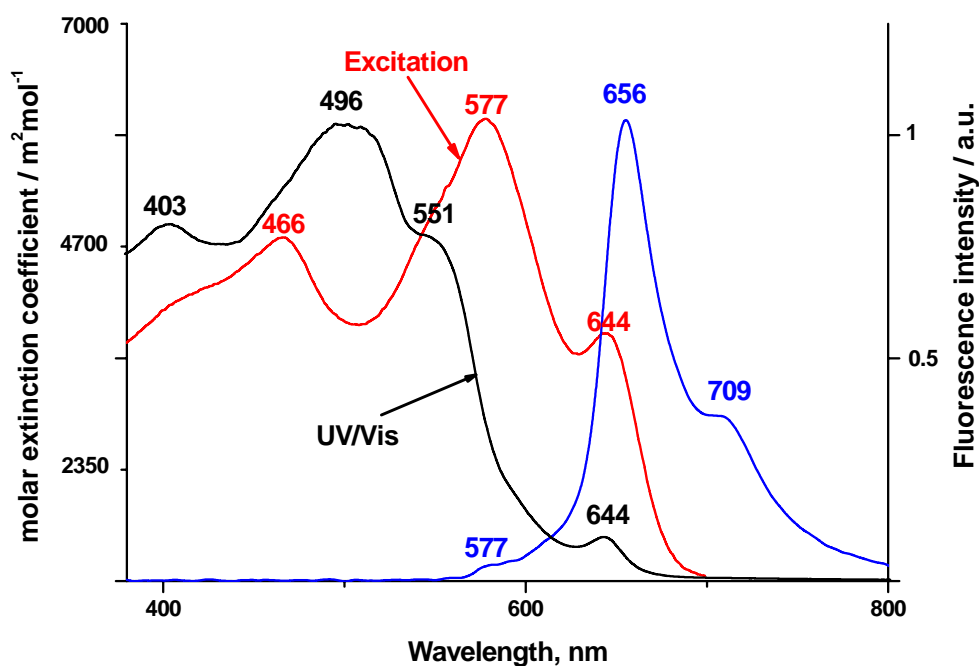


Figure 2-20. Absorption (black) and emission (blue) spectra of **2-23**

Semi-empirical calculations (PM3 ZINDOS) were performed to label the bands. These calculations are required, since for acenes, for example, the p-band can be suppressed, or can shift to longer wavelengths, exchanging the places with the α -band, as shown in Figure 2-21.⁴⁴ The calculations indicated that the band at 644 nm corresponds to the α -transition. The β -band (the most intense) has the lowest wavelength, 496 nm. The p-band has an intermediate wavelength (551 nm) and intensity.

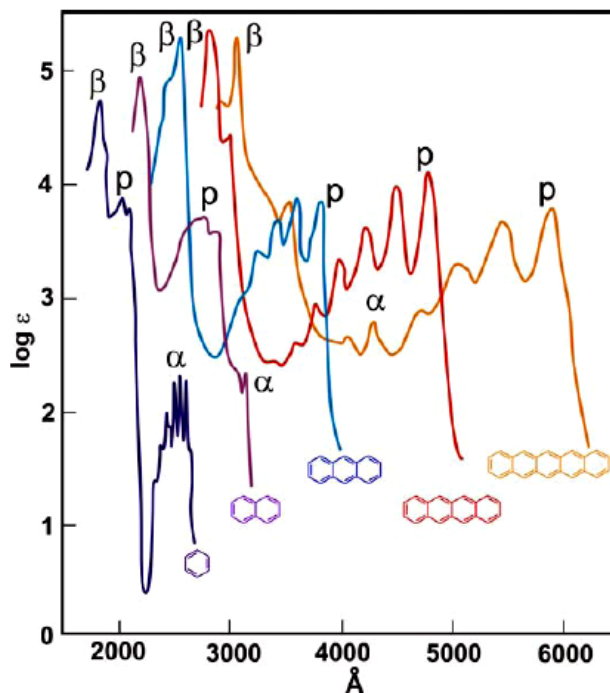


Figure 2-21. UV/vis-spectra of the acene series

The absorption spectrum of **2-23** was compared to the spectra of **1-34**⁴⁶ and **2-26**. This comparison can serve as indirect evidence whether the molecule consists of several independent, non-communicating subunits (partial cyclodehydrogenation), or has an extended conjugated core.

Indeed, comparing the absorption spectrum of the model compound **2-26**, shown in Figure 2-23 with the absorption spectrum of **1-34**, depicted in Figure 2-22, one can see the bathochromic shift between the α -bands of approximately 78 nm (602 nm in case of **1-34** and 524 nm in case of **2-26**). This is due to the larger conjugated system of **1-34**, which has, in addition to **2-26**, two HBC-like panels. Semi-empirical calculations (PM3 ZINDOS) also were performed to label the bands for the model compound **2-26**.

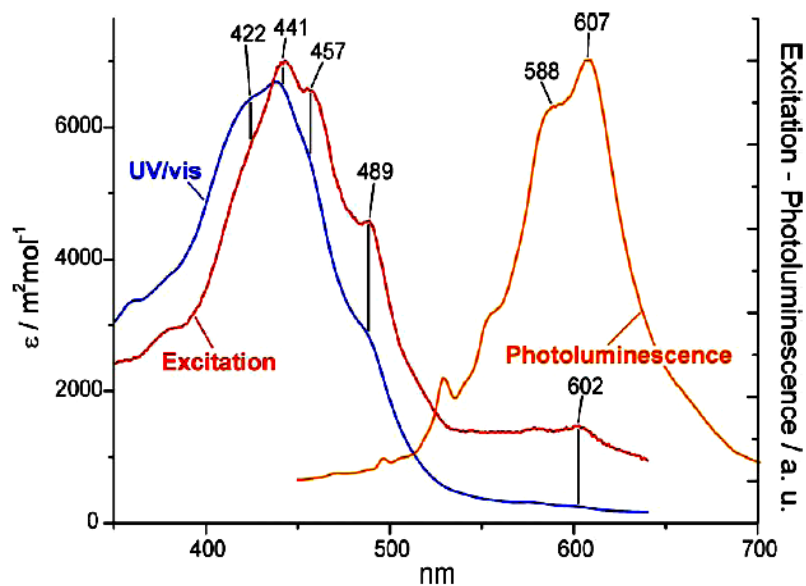


Figure 2-22. Electronic spectra of **1-34** in THF at room temperature³²

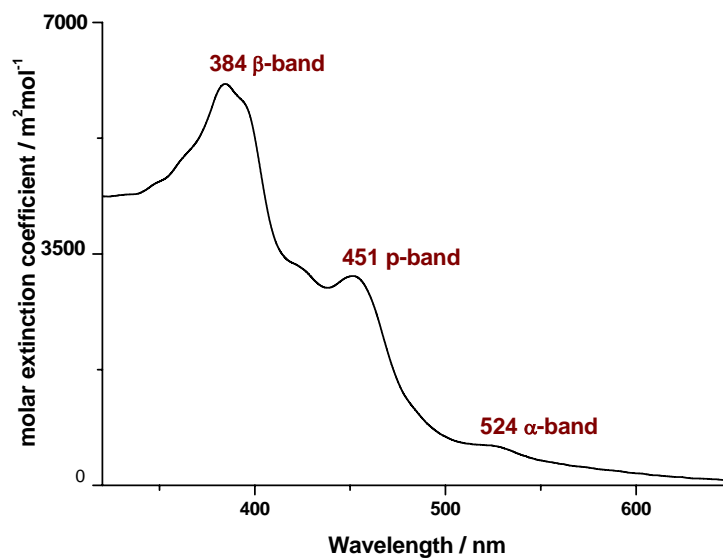


Figure 2-23. Absorption spectrum of **2-27**, recorded in THF at room temperature

Similar analysis of the adsorption spectrum of **2-23**, shown in Figure 2-20, also reveals the bathochromic shift of 42 nm with respect to **1-34**. In fact, this shift is in agreement

with the theoretical prediction of 30 nm for the compound **2-23**. Large bathochromic shift can be used as indirect evidence that the product **2-23** has a larger conjugated π -system than **1-34**.

Finally, the absorption spectrum of **2-23** is bathochromically shifted by 120 nm with respect to **2-26** (see Figure 2-23). This shift suggests fusion of not only the preplanarized core (dibenzo[*e,l*]pyrene), but also two HBC-like moieties at the rims of **2-13**, (see Figure 2-17).

Normalized emission of **2-23**, excited at 577 nm is shown in Figure 2-20 (blue line). The emission band has a rather sharp, well defined maximum, similar to emission band of fully cyclized **1-34**.

2.7 Summary

In this chapter a new design of polyphenylene ribbons, containing *n*-substituted dibenzo[*e,l*]pyrene with propeller-like dendritic backbone, is presented. A special kind of bis-cyclopentadienone building block **2-7**, possessing dibenzo[*e,l*]pyrene core was obtained and further utilized in the *stoichiometrically* controlled DIELS-ALDER reaction with aim to obtain a series of very long polyphenylene ribbons with up to 10 nm linear size. The presence of alkyl chains of different sizes along with the branched nature of the dendritic backbone led to good solubilities of all synthesized molecules in common organic solvents allowing their characterization by standard analytical techniques. Calculated linear size and rod-like shape of the ribbons was confirmed by HRTEM, which analysis also disclosed strong aromatic interactions between molecules in the solid state. TEM-images revealed nano-sized interconnected particles continue of packed ribbons within the onion-like architecture.

The evaluation of rigid dibenzo[*e,l*]pyrene moieties for the cyclodehydrogenation to obtain two-dimensional ladder-type graphene was done for the smallest ribbon **2-13**. According to the direct characterization methods the cyclodehydrogenated product **2-23** coexists with partially cyclised compounds. However, it is hard to identify by MALDI-TOF mass spectroscopy their quantity. At the same time, indirect methods and theoretical predictions demonstrated the clear presence of a fully cyclized product **2-23**.

2.8 References

1. Arnold, F. E.; Vanduse.Rl, *Macromolecules* **1969**, 2, (5), 497-&.
2. Arnold, F. E.; Vanduse.Rl, *Journal of Applied Polymer Science* **1971**, 15, (8), 2035-2047.
3. Sicree, A. J.; Vanduse.Rl; Arnold, F. E., *Journal of Polymer Science Part a-Polymer Chemistry* **1974**, 12, (2), 265-272.
4. Vanduse.Rl, *Journal of Polymer Science Part B-Polymer Letters* **1966**, 4, (3Pb), 211-&.
5. Stille, J. K.; Harris, F. W.; Rakutis, R. O.; Mukamal, H., *J. Polym. Sci. Pol. Lett.* **1966**, 4, (10PB), 791-&.
6. Stille, J. K.; Freeburg.Me, *Journal of Polymer Science Part B-Polymer Letters* **1967**, 5, (11PB), 989-992.
7. Imai, K.; Kurihara, M.; Mathias, L.; Wittmann, J.; Alston, W. B.; Stille, J. K., *Macromolecules* **1973**, 6, (2), 158-162.
8. Deschryv.F; Marvel, C. S., *Journal of Polymer Science Part a-1-Polymer Chemistry* **1967**, 5, (3Pa1), 545-552.
9. Kellman, R.; Marvel, C. S., *Journal of Polymer Science Part a-Polymer Chemistry* **1975**, 13, (9), 2125-2131.
10. Danziger, J.; Dodelet, J. P.; Lee, P.; Nebesny, K. W.; Armstrong, N. R., *Chemistry of Materials* **1991**, 3, (5), 821-829.
11. Loffler, M.; Schluter, A. D.; Gessler, K.; Saenger, W.; Toussaint, J. M.; Bredas, J. L., *Angew. Chem., Int. Ed. Engl.* **1994**, 33, (21), 2209-2212.
12. Scherf, U.; Müllen, K., *Makromolekulare Chemie-Rapid Communications* **1991**, 12, (8), 489-497.
13. Watson, M. D.; Fechtenkötter, A.; Müllen, K., *Chem. Rev.* **2001**, 101, (5), 1267-1300.
14. Samori, P.; Fechtenkötter, A.; Jackel, F.; Bohme, T.; Müllen, K.; Rabe, J. P., *J. Am. Chem. Soc.* **2001**, 123, (46), 11462-11467.
15. Schmidt-Mende, L.; Fechtenkötter, A.; Müllen, K.; Moons, E.; Friend, R. H.; MacKenzie, J. D., *Science* **2001**, 293, (5532), 1119-1122.

16. Iyer, V. S.; Yoshimura, K.; Enkelmann, V.; Epsch, R.; Rabe, J. P.; Müllen, K., *Angew. Chem., Int. Ed.* **1998**, *37*, (19), 2696-2699.
17. Dotz, F.; Brand, J. D.; Ito, S.; Gherghel, L.; Müllen, K., *J. Am. Chem. Soc.* **2000**, *122*, (32), 7707-7717.
18. Fechtenkötter, A.; Saalwachter, K.; Harbison, M. A.; Müllen, K.; Spiess, H. W., *Angew. Chem., Int. Ed.* **1999**, *38*, (20), 3039-3042.
19. Stabel, A.; Herwig, P.; Müllen, K.; Rabe, J. P., *Angew. Chem., Int. Ed. Engl.* **1995**, *34*, (15), 1609-1611.
20. Iyer, V. S.; Wehmeier, M.; Brand, J. D.; Keegstra, M. A.; Müllen, K., *Angew. Chem., Int. Ed. Engl.* **1997**, *36*, (15), 1604-1607.
21. Müller, M.; Iyer, V. S.; Kübel, C.; Enkelmann, V.; Müllen, K., *Angew. Chem., Int. Ed. Engl.* **1997**, *36*, (15), 1607-1610.
22. Simpson, C. D.; Brand, J. D.; Berresheim, A. J.; Przybilla, L.; Räder, H. J.; Müllen, K., *Chem. Eur. J.* **2002**, *8*, (6), 1424-1429.
23. Shifrina, Z. B.; Averina, M. S.; Rusanov, A. L.; Wagner, M.; Müllen, K., *Macromolecules* **2000**, *33*, (10), 3525-3529.
24. Stille, J. K.; Noren, G. K., *J. Polym. Sci. Pol. Lett.* **1969**, *7*, (7Pb), 525-&.
25. Wu, J. S.; Gherghel, L.; Watson, M. D.; Li, J. X.; Wang, Z. H.; Simpson, C. D.; Kolb, U.; Müllen, K., *Macromolecules* **2003**, *36*, (19), 7082-7089.
26. Wu, J. Liquid Crystalline Graphite Molecules as Material of Molecular Electronics: Versalite Synthesis and Self-assembly. Johannes Gutenberg-Universität Mainz, 2004.
27. Wasserfallen, D.; Kastler, M.; Pisula, W.; Hofer, W. A.; Fogel, Y.; Wang, Z. H.; Müllen, K., *J. Am. Chem. Soc.* **2006**, *128*, (4), 1334-1339.
28. Yamato, T.; Fujimoto, M.; Miyazawa, A.; Matsuo, K., *Journal of the Chemical Society-Perkin Transactions 1* **1997**, (8), 1201-1207.
29. Oberender, F. G.; Dixon, J. A., *Journal of Organic Chemistry* **1959**, *24*, (9), 1226-1229.
30. Dewar, M. J. S., *Journal of the American Chemical Society* **1952**, *74*, (13), 3357-3363.
31. Meier, M. A. R.; Schubert, U. S., *Review of Scientific Instruments* **2005**, *76*, (6), -.

32. Wasserfallen, D. *Synthetical Engineering of Supramolecular Properties of Large Polycyclic Aromatic Hydrocarbons*. Johannes Gutenberg-Universität, Mainz, 2006.
33. Müller, M.; Kübel, C.; Morgenroth, F.; Iyer, V. S.; Müllen, K., *Carbon* **1998**, 36, (5-6), 827-831.
34. Bernhardt, S. *Polyphenylene Dendrimers - Design and Synthesis of Monodisperse Functional Nanoparticles* Johannes Gutenberg-Universität, Mainz, 2006.
35. Balaban, T. N., C.D., *In Friedel-Crafts and Related Reactions*. Wiley&Sons: New York, 1964; Vol. 2.
36. Olah, G. A.; Schillin, P.; Gross, I. M., *J. Am. Chem. Soc.* **1974**, 96, (3), 876-883.
37. Wehmeier, M. *Synthese und Charakterisierung ausgedehnter polycyclischer aromatischer Kohlenwasserstoffe*. Johannes Gutenberg-Universität, Mainz, 1999.
38. Kovacic, P.; Koch, F. W., *J. Org. Chem.* **1963**, 28, (7), 1864-&.
39. Kovacic, P.; Koch, F. W., *J. Org. Chem.* **1965**, 30, (9), 3176-&.
40. Kovacic, P.; Jones, M. B., *Chem. Rev.* **1987**, 87, (2), 357-379.
41. Tomovic, Z.; Watson, M. D.; Müllen, K., *Angew. Chem., Int. Ed.* **2004**, 43, (6), 755-758.
42. Tomovic, Z. *New Discotic Liquid Crystals Based on Large Polycyclic Aromatic Hydrocarbons as Materials for Molecular Electronics*. Johannes Gutenberg-Universität, Mainz, 2004.
43. Przybilla, L.; Brand, J. D.; Yoshimura, K.; Räder, H. J.; Müllen, K., *Analytical Chemistry* **2000**, 72, (19), 4591-4597.
44. Clar, E., *Polycyclic Hydrocarbons*. New York, 1964; Vol. 1, 2.
45. Fetzer, J. C., *Large (C_n≥24) Polycyclic Aromatic Hydrocarbons*. John Wiley&Sons: New York, 2000.

3 From Pyrene to Polycyclic Aromatic Hydrocarbons Containing Nitrogen

3.1 Clar rule and Peripheries

Both experiments and theory tell us that electronic properties of PAHs depend not only on their molecular size¹⁻³ but also on their topology and periphery⁴⁻⁶. A representative example is triphenylene, which is shown in Figure 3-1. Triphenylene possesses properties, which are distinctly different from the other four-benzene-ring PAHs isomers: the highest resonance energy,⁷ ionization potential,⁸ and the largest HOMO-LUMO gap.⁸ Out of all isomers it is the most thermally stable and least chemically reactive compound. Another typical example is hexa-*peri*-hexabenzocoronene (HBC).^{2, 9-12} HBC is the next fully benzenoid homologue of benzene with D_{6h} symmetry.

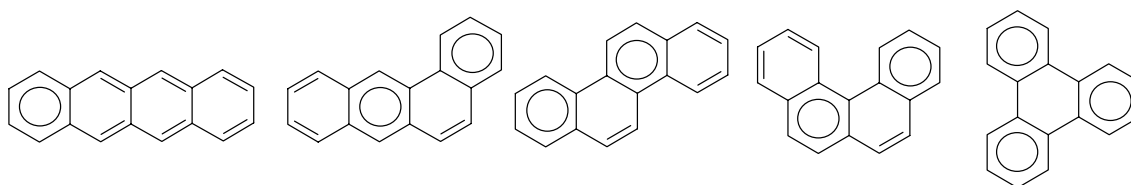


Figure 3-1. Structure of PAH isomers with four benzene rings

Chemical reactivity as well as many other properties of PAH could be understood in terms of localization of the aromatic sextets present in the molecules. According to CLAR^{13, 14} the π -electron sextets can be attributed to discrete benzene rings and the remaining π -electrons to double bonds. Sextet rings are usually depicted using solid circles (Robinson rings). Fully benzenoid PAHs can be drawn only with Robinson rings without isolated double bonds and are kinetically very stable and inert.

The PAHs with isolated double bonds can have a different CH perimeter (see Figure 3-2), with different reactivity.¹⁵⁻¹⁷ For example, the “acene”- or “zigzag edge” are rather reactive, and can be used for oxidation; the presence of “phenanthrene” or “armchair edge” indicates that the aromatic system is rather inert, as it is in triphenylene. Most of

the extended PAHs with more than 40 aromatic carbon atoms are fully-benzenoid with the “arm-chair” periphery.¹⁶

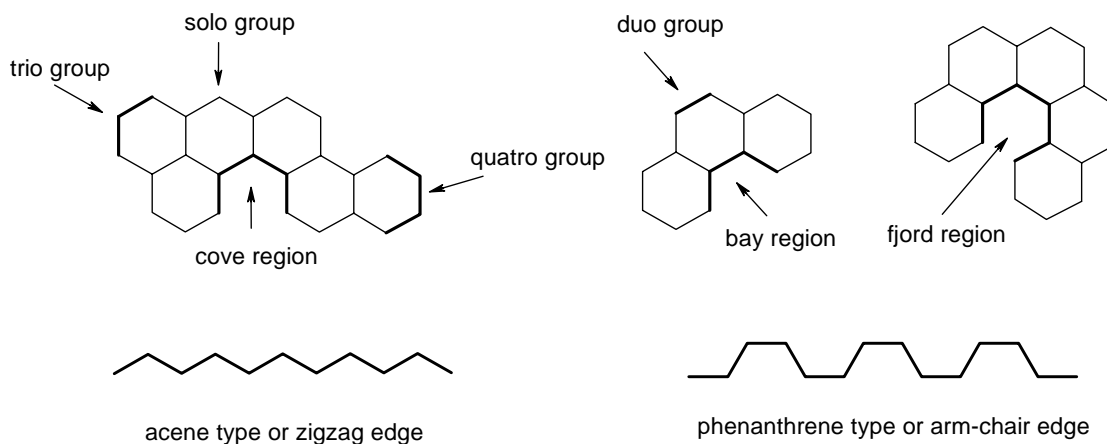
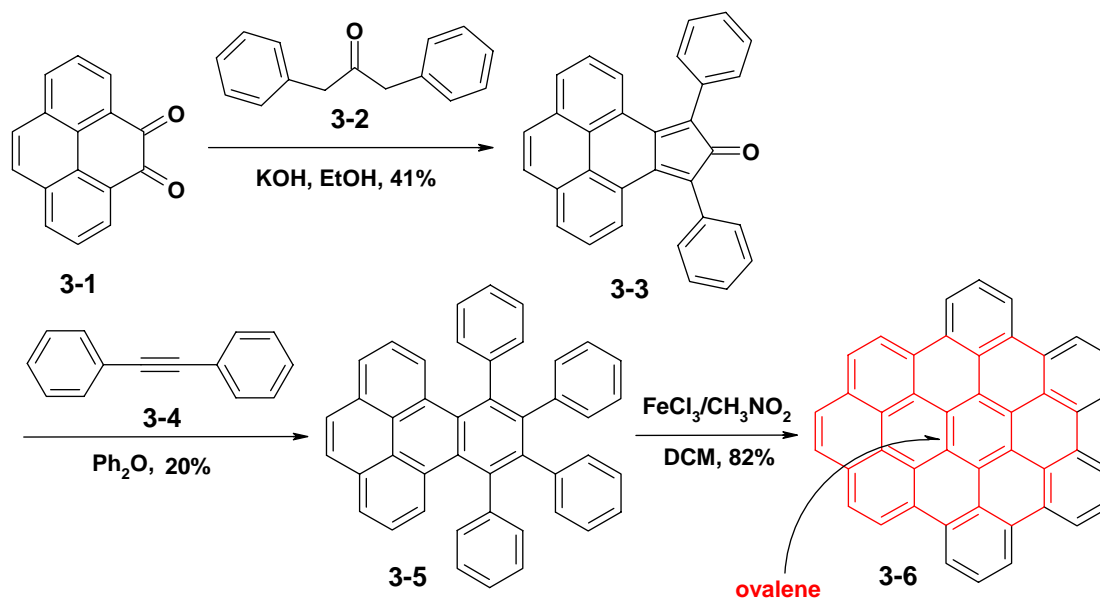


Figure 3-2. Schematic representation of the structural parameters in PAH and the different type of edges according to Dias^{15,16}

The chemical reactivity of particular peripheries can be used to extend the size of PAHs, which is then an alternative to the cyclodehydrogenation¹⁸ route. In some cases it can be more advantageous than the cyclodehydrogenation reaction, which is known to have a range of problems, such as reproducibility, solubility and purification of the PAHs.¹⁹

In fact, there have already been several attempts to introduce a “zigzag” edge into PAHs.^{20, 21} It was first introduced into cyclopentadienone **3-3** using KNOEVENAGEL condensation of pyrene-4,5-dione (**3-1**) with 1,3-diphenylpropan-2-one (**3-2**) (Figure 3-3). The microwave assisted DIELS-ALDER reaction with diphenylacetylene **3-4** gave the precursor **3-5**. The SCHOLL reaction with iron(III) chloride allowed then to obtain tetrabenzo[bc,ef,hi,uv]ovalene (TBO) **3-6**. The drawback of this method was insufficient solubility of TBO, which did not allow obtaining high quality NMR spectra as well as prohibited further oxidation of the “zigzag” edge. However, both solubility problem and thermally stability of **3-3** can be resolved by introducing *tert*-butyl groups to pyrene-4,5-dione (**3-1**).²²

Figure 3-3. Synthetic route towards **3-6**

In this chapter a new type of graphitic molecules with “reactive” double bond at the periphery is introduced. It is shown that this periphery with localized high electron density is suitable for further functionalization. Using a new synthetic concept, extended nanographenes were prepared based on the quinoxaline condensation.²³ Thus, it is possible to grow PAH structures up to 104 atoms in the core part. A distortion of the aromatic core by adequately placed bulky *tert*-butyl groups efficiently reduces the usually very pronounced aromatic π -stacking. Even the largest presented example in this study exhibits good solubility in common organic solvents and could thus be purified by standard laboratory techniques. All extended PAH are fully characterized by NMR spectroscopy, UV/vis, MALDI-TOF and cyclic voltammetry (CV).

3.2 Synthesis of the Building Block 3-13

In what follows, the synthesis of a six-fold *tert*-butylated tetrabenzo[*bc,ef,hi,uv*]ovalene (TBO) building block is introduced by incorporating a pyrene into cyclopentadienone; TBO is further oxidized to α -diketone; the latter is then used to synthesize a number of extended PAHs.

3 From Pyrene to Polycyclic Aromatic Hydrocarbons Containing Nitrogen

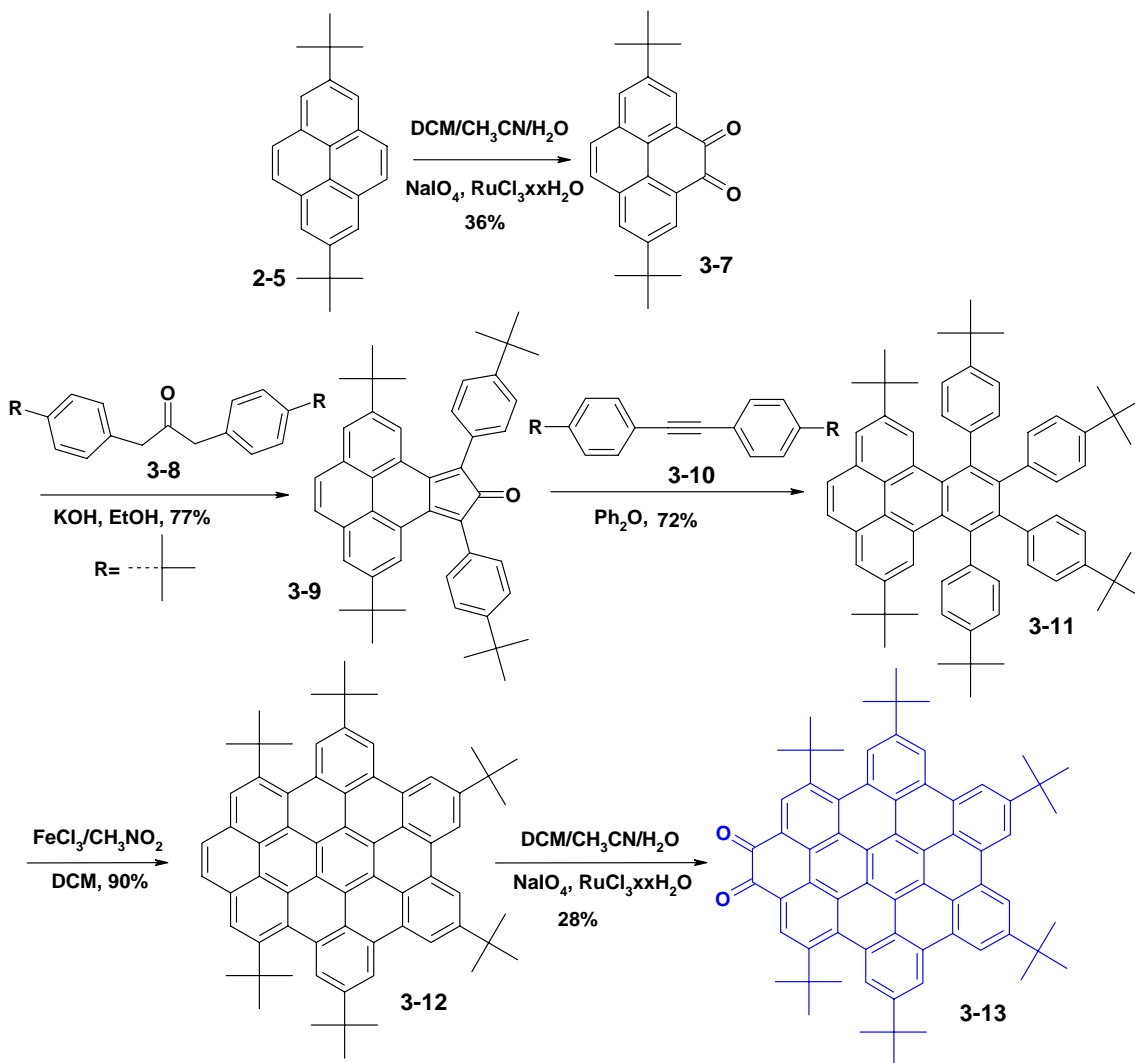


Figure 3-4. Synthetic route to 1,6-di-*tert*-butyl-8,11,14,17-tetra(*t*-butyl)tetrabenzo[*bc,ef,hi,uv*]ovalene-3,4-dione **3-13**

2,7-Di-*tert*-butylpyrene (**2-5**) was obtained using FRIEDEL-CRAFTS alkylation of pyrene with almost quantitative yield (Figure 3-4).²⁴ K-region oxidation of **2-5** towards 2,7-di-*tert*-butylpyrene-4,5-dione (**3-7**) was done by applying an oxidative procedure described in Chapter 2. The KNOEVENAGEL condensation of **3-7** with 1,3-bis(4-*tert*-butylphenyl)propan-2-one (**3-8**) gave the cyclopentadienone building block **3-9**. **3-8** was prepared by treating 4-bromomethyl-*tert*-butylbenzene with $\text{Fe}(\text{CO})_5$.²⁵ DIELS-ALDER reaction between 2,7-di-*tert*-butyl-4,5-bis(4-*tert*-butylphenyl)-cyclopentapyren-5-one (**3-9**) and di-*tert*-butyldiphenylacetylene (**3-10**), which was obtained as a product of the HAGIHARA-SONOGOSHIRA coupling between 4-*tert*-

butylphenylacetylene and 4-*tert*-butyliodobenzene²⁶, resulted in the corresponding 2,7-di-*tert*-butyl-9,10,11,12-tetrakis(4-*tert*-butyl-phenyl)benzopyrene (**3-11**) in relatively good yield (72%). A six-fold *tert*-butylated TBO **3-12** was obtained by the cyclodehydrogenation of **3-11** with FeCl₃ and Lewis acid. The yield was nearly quantitative after reductive workup. Compound **3-12** possessed good solubility in common organic solvents.

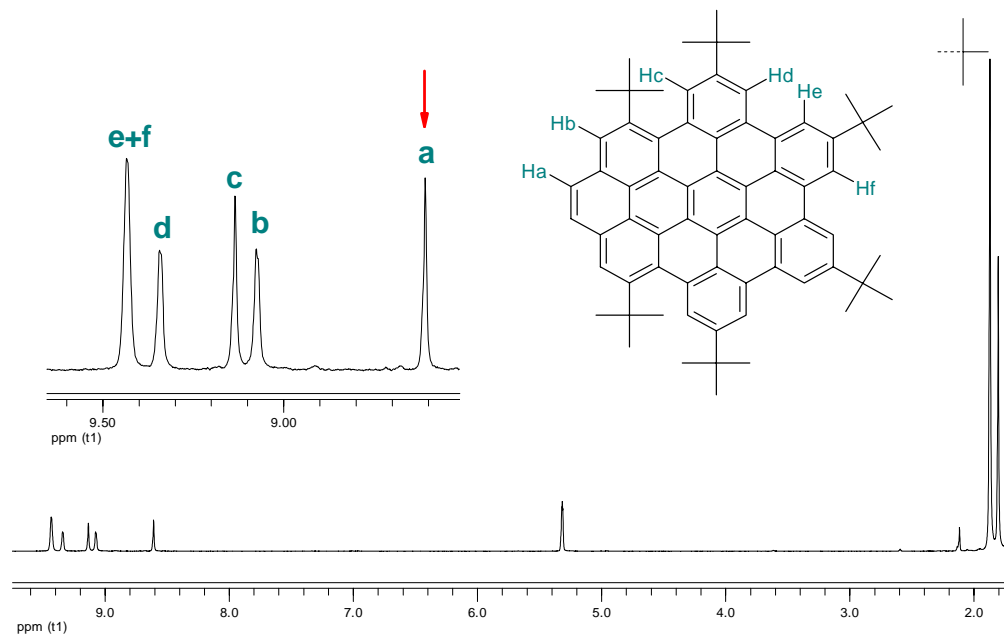


Figure 3-5. ¹H NMR spectrum of **3-12**, recorded at room temperature in dichloromethane-*d*₂ (250 MHz)

¹H, NOESY, H,H COSY NMR spectra of **3-12** were obtained in tetrachloroethane-*d*₂; the ¹H NMR spectrum is shown in Figure 3-5. The resonance of the two protons located at the “zigzag” edge was observed at 8.64 ppm (marked by a red arrow), i.e., significantly shielded compared to the aromatic “armchair” protons, which are singlets between 9.1 and 9.5 ppm.

Crystals suitable for X-ray structure analysis were obtained by slow evaporation of a hexane solution of **3-12** at room temperature.²² Crystal structure analysis suggests that the “outer rings” are alternatively bent up and down by approximately 15° each, as shown in Figure 3-6, which is due steric interaction of the *tert*-butyl groups.²⁷

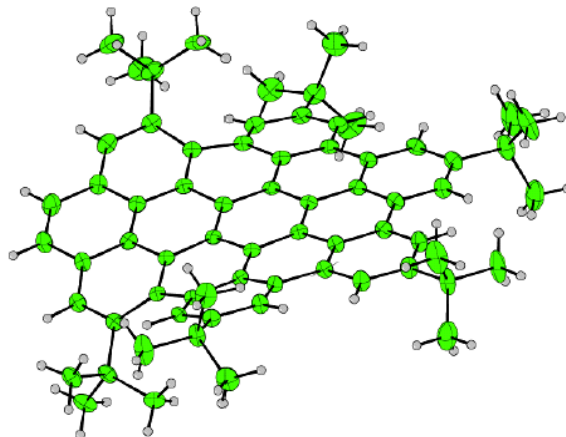


Figure 3-6. Single crystal structure of **3-12**

3-12 was further oxidized towards α -diketone **3-13**. Modification of the previously reported oxidation conditions for the generation of the α -diketone **3-13** led to a significant increase in the reaction yield.^{22, 28} The use of $\text{RuCl}_3/\text{NaIO}_4$ in aqueous mixture of solvents $\text{CH}_2\text{Cl}_2/\text{CH}_3\text{CN}$ instead of $\text{RuO}_2/\text{NaIO}_4$ in aqueous N,N -dimethylformamide was found to be beneficial, in terms of both the yield and the reaction time. Taking all of the difficulties associated with the direct oxidation of the K-region into account the 28% yield is satisfactory. Compound **3-13** exhibited good solubility in common organic solvents presumably due to a distortion of the aromatic core from planarity by bay region *tert*-butyl groups (see Figure 3-7).²⁹

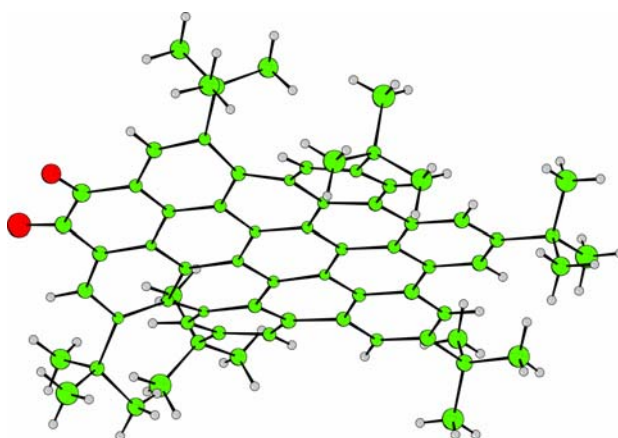


Figure 3-7. Single crystal structure of **3-13**

Purification was achieved by using column chromatography.

The ^1H -NMR spectrum of **3-13** was recorded in tetrachloroethane- d_2 (Figure 3-8) and is similar to the spectrum of **3-12**. According to the integration, there are 10 aromatic protons in this spectrum. Consistent with H,H COSY (Figure 3-9) and NOESY two proton resonances (H_c) are shifted to the higher field and appear at the same ppm value as the resonances of the two protons of the “zigzag” edge H_a of **3-12**.

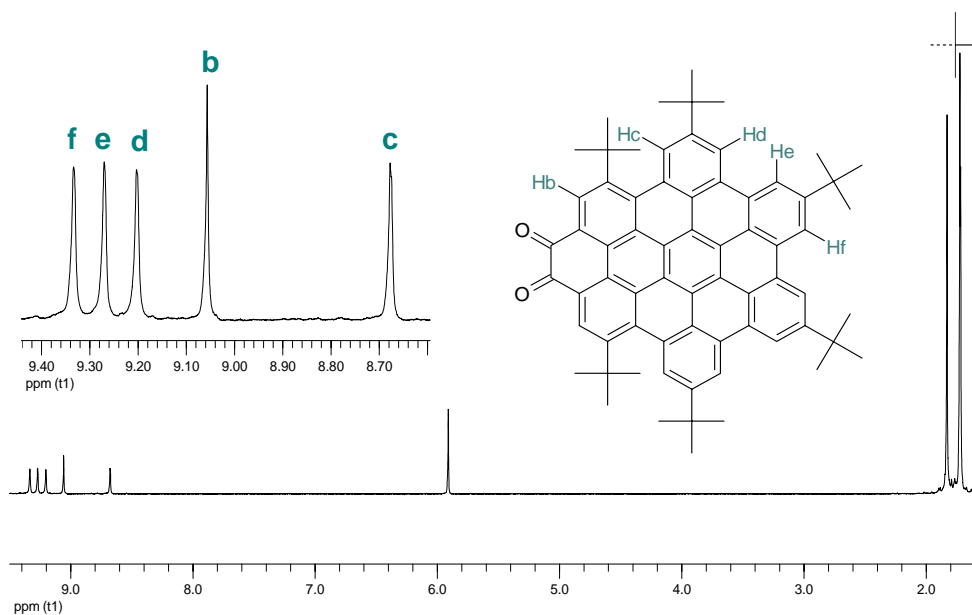


Figure 3-8. ^1H NMR of **3-13**, recorded at room temperature in tetrachloroethane- d_2 (500 MHz)

The combination of good solubility and the presence of the α -diketone render compound **3-13** as a promising building block for the construction of larger aromatic and heteroaromatic systems.

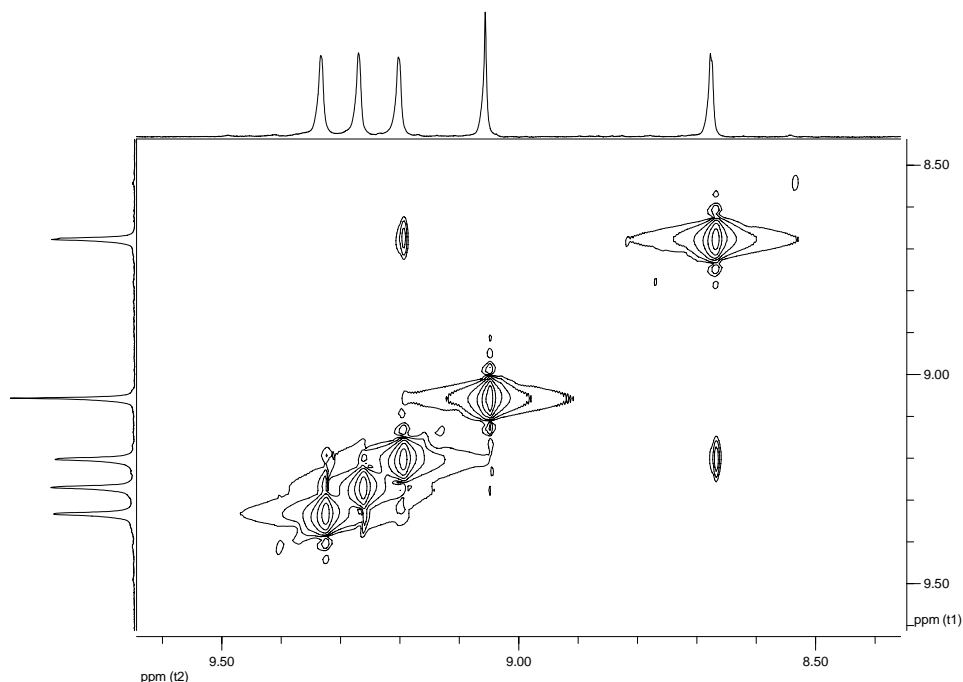


Figure 3-9. H,H COSY (right) spectra of **3-13**, recorded at room temperature in tetrachloroethane- d_2 (500 MHz)

3.3 Synthesis of Extended PAHs

The quinoxaline-ring formation between α -diketone and *o*-phenylenediamines is known as a high-yielding reaction, which has even been used for synthesis of polymers.^{23, 30-32} To test the condensation conditions for our systems, compound **3-13** was treated with *o*-phenylenediamine dihydrochloride in boiling acetic acid (Figure 3-10).³³ The extended quinoxaline-containing PAH **3-18** was isolated in 55% yield after 7 hours of reaction. Significant amounts of the starting material **3-13** (up to 20%) were recovered. 3 days of reaction furnished 76% of **3-18** and 5% of **3-13**. Eventually, the α -diketone unit **3-13** is not very reactive. The PAHs **3-19** and **3-20** were obtained after the analogous treatment of **3-13** with 3,3'-diaminobenzidine tetrahydrochloride and 1,2,4,5-benzenetetraamine tetrahydrochloride, respectively. **3-21** was synthesized within 5 hours by refluxing **3-17** with **3-13** in acetic acid and furnished in 57% yield.

3 From Pyrene to Polycyclic Aromatic Hydrocarbons Containing Nitrogen

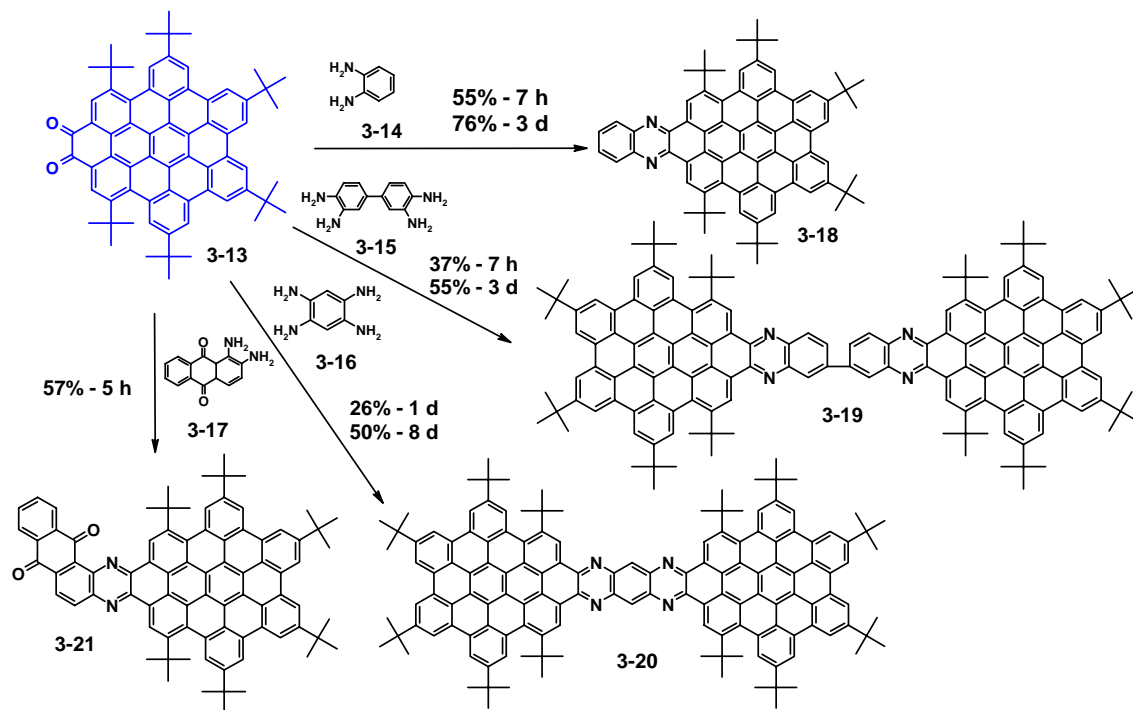


Figure 3-10. Synthesis of novel extended PAHs molecules **3-18** - **3-21**

The synthesized compounds are shown in Figure 3-10. All of them have an extended π -system (electron donor, D) and a quinoxaline bridge (electron acceptor, A). The presence of both donor and acceptor groups in one molecule often leads to an efficient intramolecular charge transfer interactions,³⁴ and can be used for artificial photosynthesis³⁵, semiconducting materials³⁶⁻³⁸, various molecular electronics^{39, 40} and photovoltaic⁴¹ devices. Charge transfer between D and A groups characterizes the low-energy physics of these molecules and is responsible for the appearance of low-energy excitations with large transition and/or mesomeric dipole moments.^{42, 43}

All PAHs showed good solubilities of up to 20 mg/mL in common organic solvents such as toluene, THF or dichloromethane and could thus be purified using standard chromatography methods. Unlike all other PAHs of this size, these nanographenes do not have solubilizing long alkyl chains on the corona. The calculated (B3LYP/6-31g*, vacuum) structure of **3-20** has significant deviations from planarity, whereas the analogous arene without the *tert*-butyl groups was calculated to have a perfectly planar aromatic framework (Figure 3-11). Thus the good solubility arises from either the nonplanarity of the PAH, the presence of the *tert*-butyl groups, or both effects.

3 From Pyrene to Polycyclic Aromatic Hydrocarbons Containing Nitrogen



Figure 3-11. Optimized geometries of **3-20** with (left) and without (right) tert-butyl groups (B3LYP/6-31g*, vacuum).

Good solubilities allow, contrary to most extended PAHs (i.e. larger than HBC)^{3, 21}, to record MALDI-TOF (dithranol matrix), structure rich UV/vis and resolved ¹H NMR spectra of these compounds. The MALDI-TOF spectrum of **3-18** is shown in Figure 3-12.

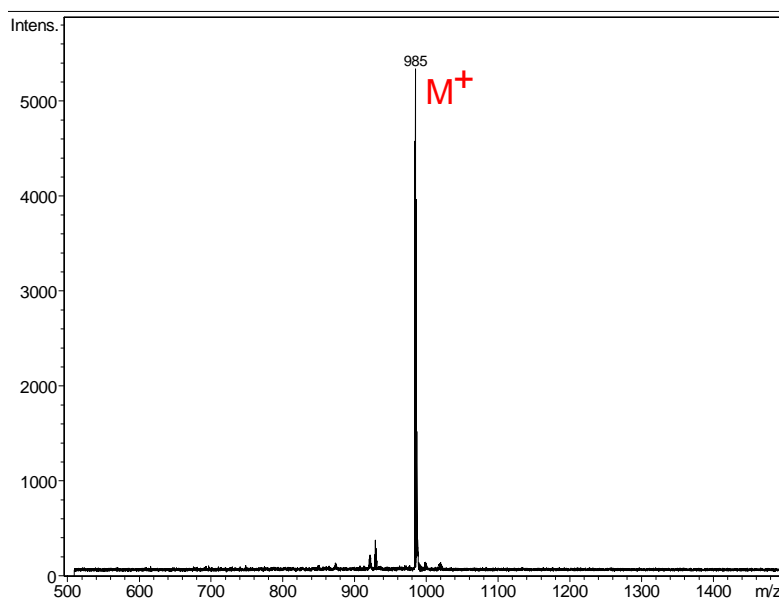


Figure 3-12. MALDI-TOF-spectrum of the compound **3-18** (dithranol matrix).

The ¹H NMR spectra of four novel extended PAHs were recorded in tetrachloroethane-d₂ or dichloromethane-d₂ and showed the sharp aromatic resonances, which imply a low self-association propensity in solution. Typically the signals for such systems are broad due to pronounced interactions between the aromatic π -systems.¹⁹ The two examples of the ¹H NMR spectra of **3-18** and **3-20** are presented in Figure 3-13 and Figure 3-14,

3 From Pyrene to Polycyclic Aromatic Hydrocarbons Containing Nitrogen

respectively.

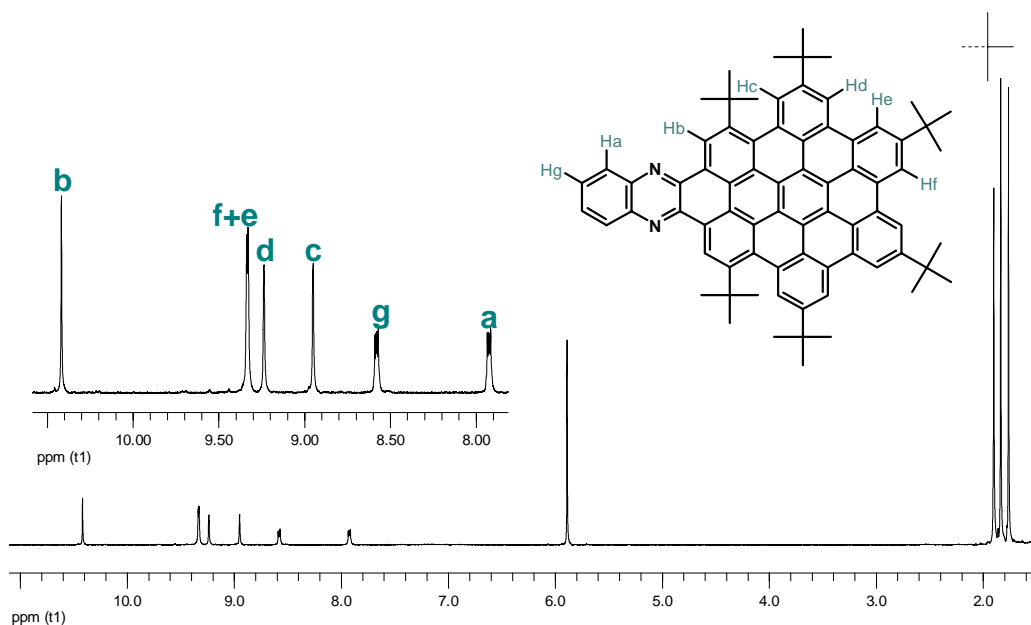


Figure 3-13. ^1H NMR spectrum of **3-18**, recorded in tetrachloroethane- d_2 at 100°C (500 MHz)

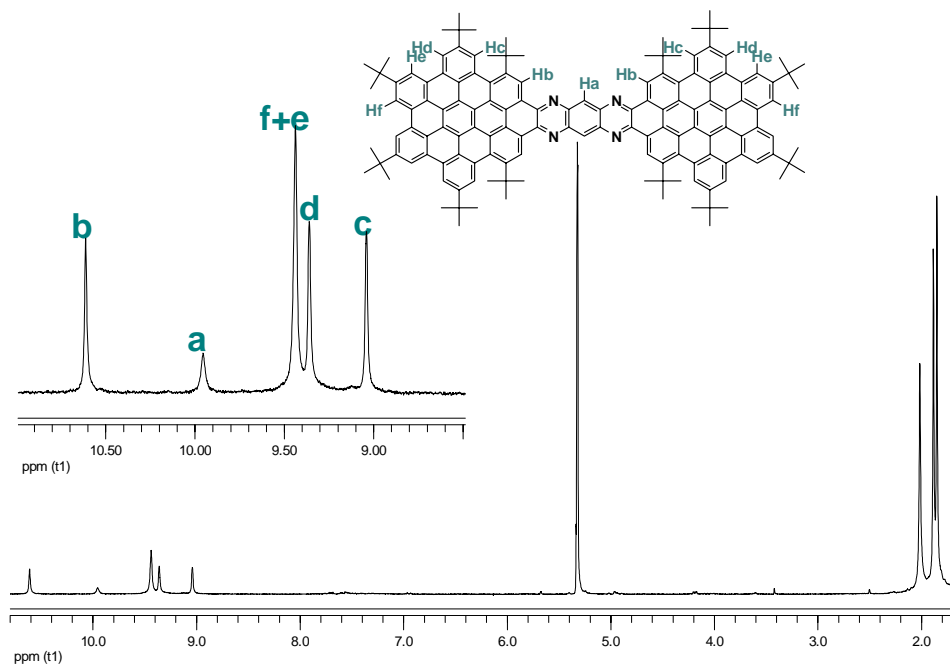


Figure 3-14. ^1H NMR spectrum of **3-20**, recorded in dichloromethane- d_2 at room temperature (250 MHz)

All proton resonances could be assigned to their corresponding nuclei using two dimensional NMR experiments (H,H COSY and NOESY). The analysis reveals that in all cases the two proton resonances H_b are shifted to the lower field compared to H_b of **3-12**. The ¹H NMR spectrum of **3-19** (not shown) is very similar to the one of **3-18**, which is expected since **3-19** represents the dimer-structure of **3-18**. However, the H_b proton resonances are appearing as a doublet, which suggests the reduction of the molecular symmetry. In all cases the ¹H NMR spectra did not reveal any impurity.

3.4 Spectroscopic and Electrochemical Properties

A UV/vis absorption spectrum of **3-12**, shown in Figure 3-15, was recorded in chloroform. It has three bands (α , β and γ) which are typically observed in aromatic hydrocarbons^{4, 44}.

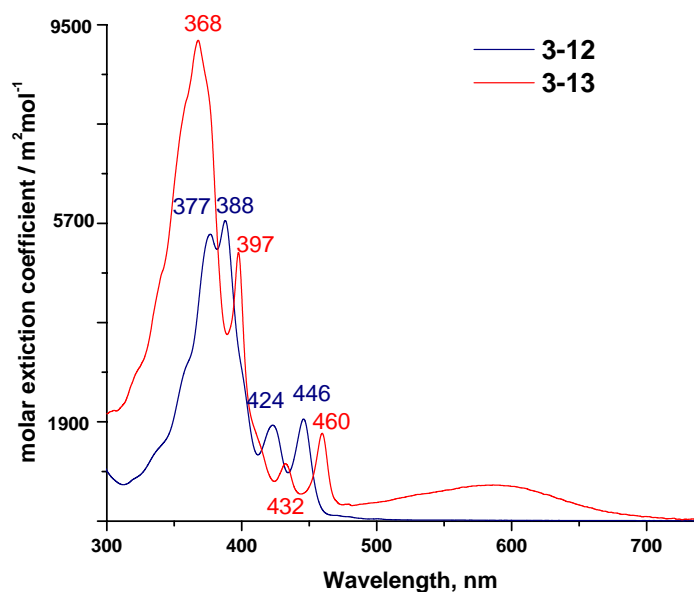


Figure 3-15. UV/vis-spectra of **3-12** and **3-13**, recorded at room temperature in chloroform ($1.05 \cdot 10^{-5}$ mol/L)

The absorption spectrum of **3-13** (Figure 3-15) has similar bands to its precursor **3-12**; the absorption maximum of **3-13** ($\lambda_{\text{max}}=368$ nm) is hypsochromically shifted with respect to the corresponding band of **3-12** ($\lambda_{\text{max}}=377$ nm). However, in addition, the absorption

spectrum of **3-13** has an $n-\pi^*$ transition, which manifests itself as a broad weak band at 470-700 nm. This band is due to the excitation of the lone pair of electrons (designed n) on the oxygen atom to the LUMO of the carbonyl group.⁴⁵

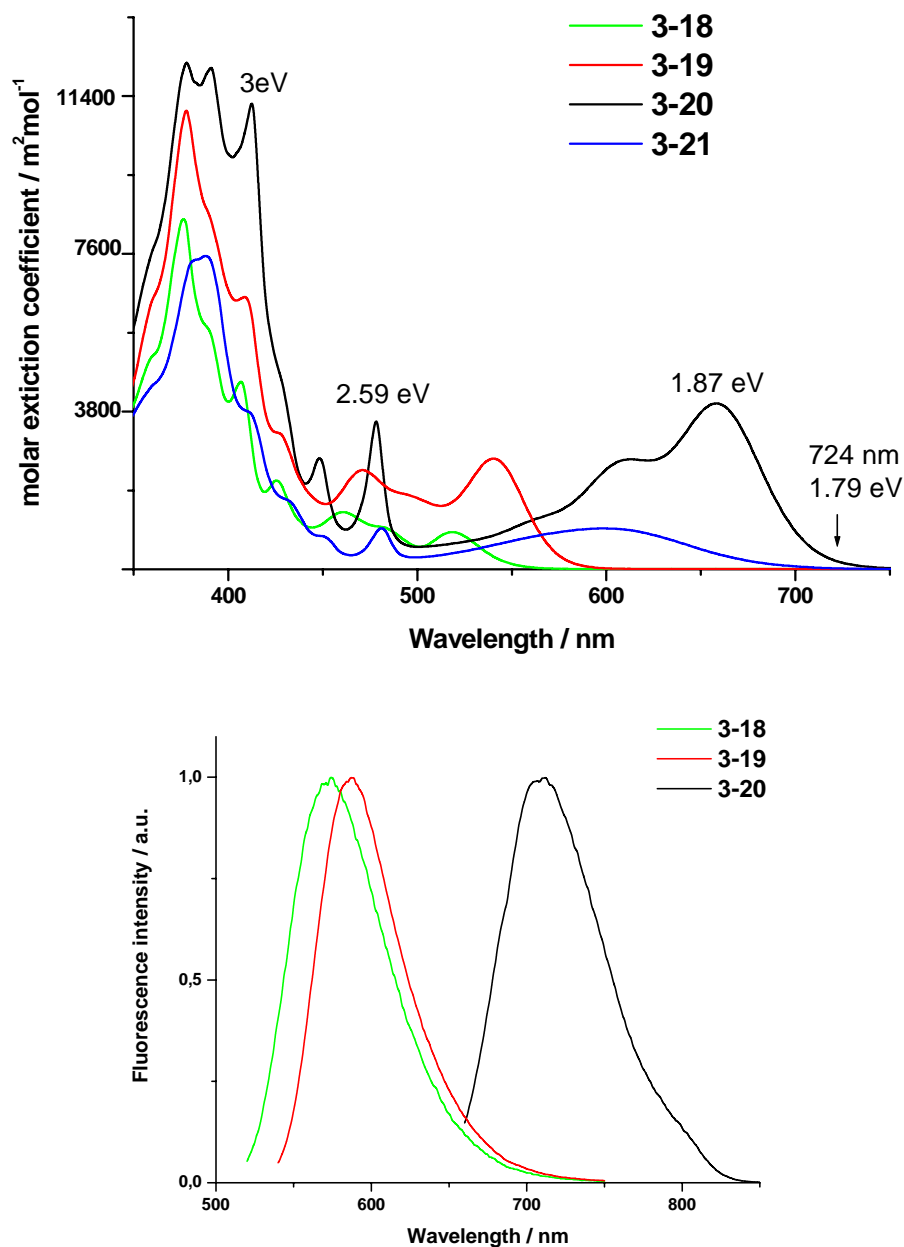


Figure 3-16. Absorption and emission spectra of compounds **3-18** - **3-21** in chloroform at room temperature

UV/vis absorption spectra of PAHs **3-18** - **3-21** were recorded in chloroform at concentration of 10^{-5} mol/L (Figure 3-16). PAH **3-18** has a similar absorption spectrum to that of D_{6h} -symmetric HBC.⁴⁶ However, the usually weak α -transition is more intense, since the symmetry of **3-18** (C_2) is lower. The absorption spectrum of **3-19** is very similar to that of **3-18**, but with a small bathochromic shift (23 nm) of the absorption bands. This is expected since **3-19** is comprised of two units of **3-18** connected by a C-C single bond (biaryl linkage). As in most biaryl systems, the electron interaction between the two arenes is relatively small.

In contrast, when two aromatic moieties become fused, as in the nanographene **3-20**, the absorption spectrum changes dramatically. The longest absorption band shifts bathochromically by about 150 nm. The emission spectra follow a similar trend: the emission maximum of **3-20** is considerably bathochromically shifted, compared to those of **3-18** and **3-19**, which differ only slightly ($\Delta\lambda=124$ nm).

To determine the excitation energies, DFT calculations were performed. The structures of PAHs **3-18** - **3-21** were first optimized at the B3LYP 6-31g* level of theory and the ZINDO method was then conducted. The calculations are in good agreement with the experimentally determined peak positions (Table 3-1), and the error is within the expected range for this type of method.⁴⁷

Both the calculations and the UV/vis data show that an increase in the size of the aromatic system leads to smaller band gaps. With the asymmetric increase of the aromatic system in going from **3-18** to **3-20**, the α - and p-bands exchange their positions. This phenomenon is well-known for the acene series (see Chapter 2).⁴ The energy of β -transitions in the investigated cases does not exhibit a dependence upon the size of the aromatic system.

3 From Pyrene to Polycyclic Aromatic Hydrocarbons Containing Nitrogen

Table 3-1. Comparison between the calculated excitation energies (E) and oscillator strengths (f) and the experimentally determined energies of the PAHs **3-18** - **3-21**

	Transition	E(eV) exp.	E(eV) calc.	f (calc)
3-18	α	2.39	2.58	0.07
	p	2.56	2.70 ^a	0.03
	β	3.05	2.94	1.19
3-19	α	2.50	2.57	0.05
	p	2.25	2.52 ^b	0.80
	β	3.03	2.94	0.38
3-20	α	2.59	2.48	0.11
	p	1.71	2.29	2.19
	β	3.02	3.09	0.0031

^aWave function composition: -0.34 (H-1 - L+1), 0.49 (H - L)

^bWave function composition: 0.21 (H-1 - L+1), 0.38 (H - L), 0.13 (H - L+1)

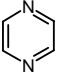
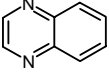
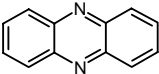
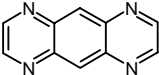
In order to determine the electron affinity and thus the LUMO levels of the novel PAHs **3-13**, **3-18** - **3-21**, CV was performed (Table 3-2). Cyclic voltammetry is a type of potentiodynamic electrochemical measurement. To obtain a cyclic voltammogram, the voltage is varied in a solution and the change in current is measured with respect to the change in voltage. It is a specific type of voltammetry used for studying the redox properties of chemicals and interfacial structures.

The cyclic voltammogram of **3-18** has two reversible one-electron reductions, with which a LUMO level of -3.53 eV could be determined. This suggests a reduction of the pyrazine ring, similar to the known model system quinoxaline and phenazine.^{48, 49} Using the optical bandgap of 2.56 eV for compound **3-18**, the HOMO level was determined to be

3 From Pyrene to Polycyclic Aromatic Hydrocarbons Containing Nitrogen

-6.08 eV, which is slightly higher than that of the model system (-6.14 eV). In going from **3-18** to the biaryl system **3-19**, no pronounced changes of the redox potentials were observed. However, both reduction processes of **3-19** now involve the transfer of two electrons.

Table 3-2. Redox Potentials. Pt electrode vs Ag/AgCl, nBu₄NClO₄ 0.1M in CH₃CN, $\nu = 100\text{mV/s}$, films were prepared from DCM-solution. HOMO values as well as HOMO-LUMO gap were calculated from UV/vis data.

	E _{1red} (V)	E _{2red} (V)	E _{3red} (V)	LUMO (eV)	HOMO- LUMO gap (eV)	HOMO (eV)
pyrazine 	-2.07 (1e)			-2.33	3.75	-6.08
quinoxaline 	-1.62 (1e)	-2.46 (1e)		-2.78	3.92	-6.70
phenazine 	-1.17 (1e)	-1.84 (1e)		-3.23	2.91	-6.14
pyrazino[2,3-g]quinoxaline 	-0.96 (2e)	-1.54 (2e)		3.44	3.48	-6.92
3-13	-0.66 (1e)	-1.27 (1e)		-3.74		
3-18	-0.87 (1e)	-1.38 (1e)		-3.53	2.56	-6.08
3-19	-0.92 (2e)	-1.35 (2e)		-3.48	2.25	-5.73
3-20	-0.70	-1.10		-3.70	1.71	-5.41

	(2e)	(2e)				
3-21	-0.64	-1.25	-1.70	-3.76		
	(1e)	(1e)	(2e)			

Although the LUMO energies of **3-19** are very similar to those of **3-18**, the HOMO level was determined to be significantly higher (-5.64 eV). Thus the increase in the size of PAH results in arising of the HOMO level and very little change in the position of the LUMO level. PAH **3-20** shows two reversible reductions appearing at a more positive potentials than those of the other two PAHs and pyrazino[2,3-g]quinoxaline^{50, 51}, indicating a lower lying LUMO. The extended PAH moieties are in conjugation and thus the HOMO level is shifted to a higher level (-5.41 eV). Also in this case, as compare to the reduction behaviors of pyrazino[2,3-g]quinoxaline and **3-18** (values of the peak potentials), two electrons are transferred in both reduction processes. Worthy of note is that nanographene **3-20** exhibits similar a electron affinity to perylenetetracarboxydiimides, which are the most thoroughly studied n-type organic semiconductors.⁵² PAH **3-20** is therefore holds promise for use as an n-type organic semiconductor.

3-13 shows two one-electron processes, which suggest the reduction of two carbonyl-centers into the ketyls. **3-21** also has two one-electron processes; however, there is an additional one-electron process which corresponds to the reduction of the pyrazine ring, which is shifted to more negative value as compared to other PAHs. The parent compound **3-12** does not show any reduction, due to its donating nature, similar to HBC which can store up to six electrons.⁵³

Compound **3-20** could be also considered as a quadrupolar (D-A-D) molecule.^{43, 54} Dipolar (D-A),^{43, 55} quadrupolar (D-A-D or A-D-A),^{56, 57} or more generally, multipolar molecules⁵⁸ are organic molecules, where electron donor (D) and acceptor (A) groups are linked by π -conjugated bridges. Because of their highly symmetric structure, all of these systems have no permanent dipole moment. However, for many of these chromophores, experimental data suggest the existence of polar excited states. For example, strong fluorescence solvatochromism has been observed for quadrupolar systems, revealing the existence of highly dipolar excited states. Usually such systems show a moderately

intense absorption band in their UV/vis spectra, which can be assigned to an intramolecular charge transfer (CT) transition from a localized HOMO into a differently localized LUMO state.^{56, 57, 59-61} In the system **3-20**, the CT band could be found at a wavelength of 657 nm (Figure 3-18). ZINDO calculations show that this band could be assigned to the intramolecular charge transfer (CT) transition from the HOMO, delocalized over the HBC framework, to the LUMO, localized on the tetraazaanthracene unit (Figure 3-17).

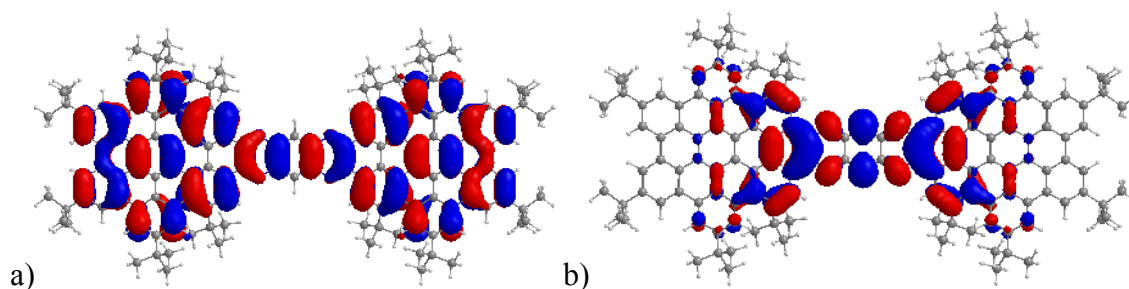


Figure 3-17. Pictorial presentation of a) HOMO and b) LUMO of **3-20** calculated at the B3LYP/6-31g* level in vacuum

Another characteristic feature for small quadrupolar molecules, as it have been already mentioned above, is that the emission is known to shift depending on the solvent polarity.^{56, 57, 59-61} UV/vis and emission spectra of compound **3-20** were recorded in solvents of different polarities, going from cyclohexane to toluene to THF and finally to a mixture of acetonitrile/THF (1/1 by volume). The position of absorption maximum in the UV/vis spectra (Figure 3-18, left) was found to be insensitive to the solvent polarity (4 nm range). In contrast, the emission maximum undergoes a pronounced bathochromic shift with increasing solvent polarity. The fluorescence spectrum, recorded in cyclohexane, exhibits a very intense emission at a wavelength of 658 nm (Figure 3-18, right), which shifts to 684 nm in toluene, 709 nm in THF and 740 nm in a mixture of THF and acetonitrile. This indicates that, even though **3-20** has no permanent dipole moment (because of its symmetric structure), similar to many families of quadrupolar chromophores, it has a polar excited state.^{56, 59, 61} Hence, the phenazine bridge in the D-A-D system **3-20** can function as a π -electron-accepting unit only in the excited state. In this

context, **3-20** is now the largest known PAH system exhibiting fluorescence solvatochromism.

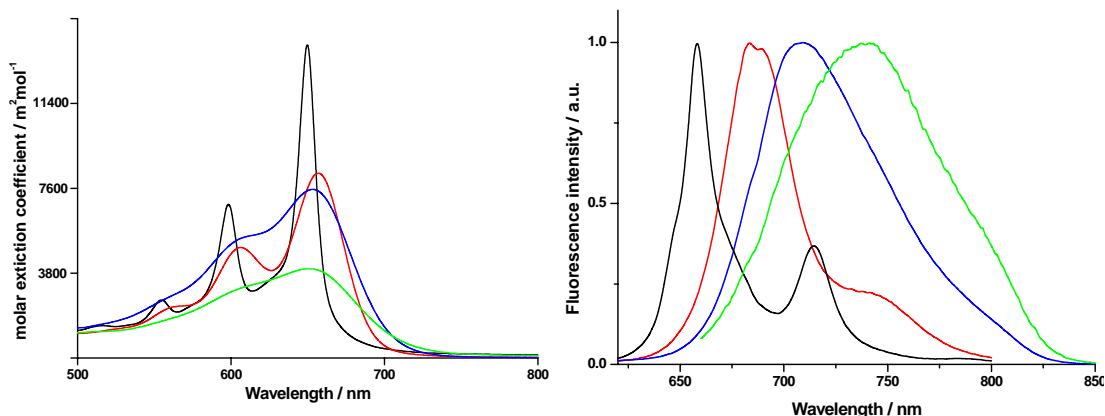


Figure 3-18. Absorption spectra (left) and normalized emission spectra (right) of **3-20**, recorded in cyclohexane (black line), toluene (red line), THF (blue line) and in mixture of THF/CH₃CN=1/1 (green line).

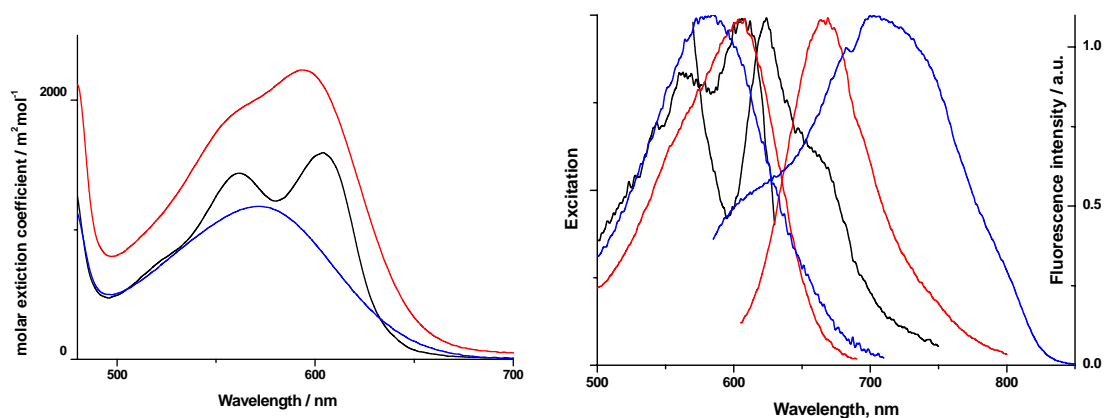


Figure 3-19. Absorption (left) and emission (right) spectra of **3-21** in cyclohexane (black line), toluene (red line) and in THF (blue line)

Contrary to **3-20**, the compound **3-21** has one donor and one acceptor unit, i.e. has a permanent dipole moment. This manifests itself in the UV/vis spectrum of **3-21** as a broad absorption band at 500-700 nm, and indicates charge-transfer, due to conjugation of donor and acceptor moieties. This is further confirmed by the absorption spectra of **3-21** (Figure 3-19), which show that the maximum position and intensity change with the

3 From Pyrene to Polycyclic Aromatic Hydrocarbons Containing Nitrogen

solvent polarity. The absorption spectra, recorded in cyclohexane reveal absorption at a wavelength of 604 nm ($1597 \text{ m}^2 \cdot \text{mol}^{-1}$), which shifts hypsochromically: 594 nm ($2232 \text{ m}^2 \cdot \text{mol}^{-1}$) in toluene and 571 nm ($1180 \text{ m}^2 \cdot \text{mol}^{-1}$) in THF. The emission spectra of **3-21**, excited at 600 nm, are also shown in Figure 3-19. One can clearly see a strong bathochromic shift as a function of the solvent polarity: in cyclohexane, it exhibits a very intense emission at a wavelength of 624 nm, which shifts to 669 nm in toluene and 704 nm in THF. This indicates that the **3-21** has the dipole moment also in the excited state.

3.5 Reductive protonation and alkylation of 3-20

In compounds with pyrazine or tetraazaanthracene bridges the bridging ligand can serve as an electron acceptor unit. This implies that once protonated, such units are capable of driving proton-coupled, multi-electron-transfer reactions which can be used for facile H_2 production.

3 From Pyrene to Polycyclic Aromatic Hydrocarbons Containing Nitrogen

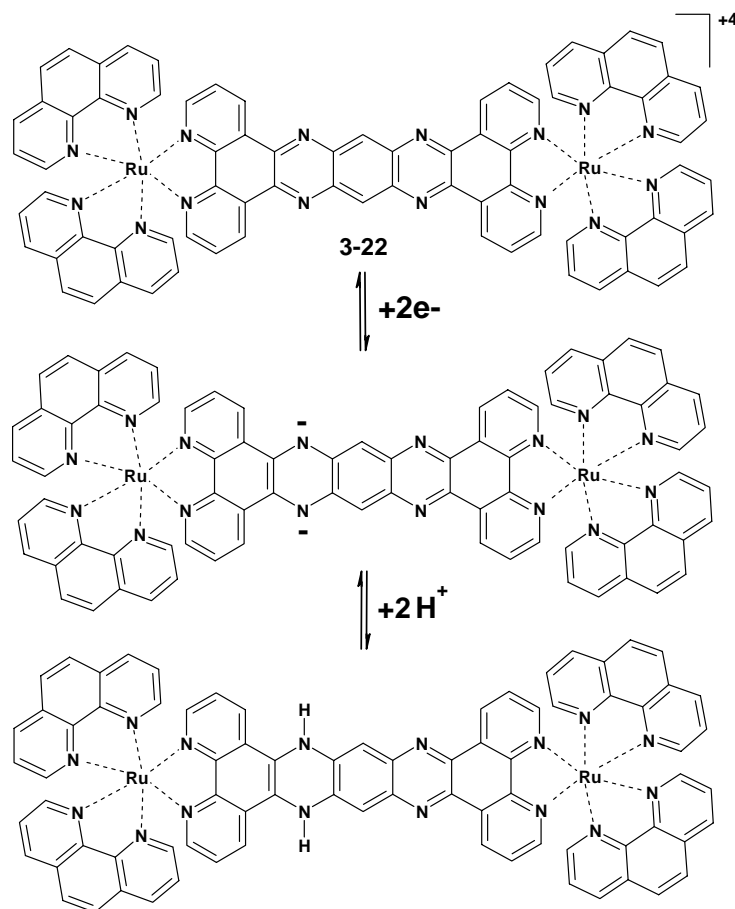


Figure 3-20. Chemical structure of Ru-complex **3-22** and the related redox and protonated isomers

For example, MACDONNELL *et al.*^{62, 63} reported that dinuclear Ru(II) complex $[(\text{phen})_2\text{Ru}(\text{tatpp})\text{Ru}(\text{phen})_2]^{+4}$ **3-22** was capable of photochemical to undergo two sequential one-electron reductions (to form the singly reduced and the doubly reduced) and protonations, upon visible-light irradiation in the presence of sacrificial reducing agents (Figure 3-20).

In what follows the reduction behavior of **3-20** is presented. All experiments were performed in situ, using quartz tubes, which allow measuring UV/vis directly from the reaction solution.

3 From Pyrene to Polycyclic Aromatic Hydrocarbons Containing Nitrogen

3.5.1 Reduction of 3-20 by using Co(Cp)₂

To test the ability of the system **3-20** for reduction, the MACDONNELL's method was firstly applied. Addition of cobaltocene to an acetonitrile solution of **3-20** did not change the adsorption spectra, i.e. no visible improvement of creating of any charge species as it was described by MACDONNELL *et al.*^{62, 63}

After addition of trifluoroacetic acid (TFA) as a protonation agent, the color of the solution changed to dark-green and a broad red shifted band appeared in the absorption spectrum (not shown). However, the intensity of that band was far lower than that of the initial compound and than that, which assigned the creation of protonation products of the Ru-complex **3-22**.^{62, 63} It was hard to judge, which protonated product was obtained, since it was impossible to perform mass spectroscopy. Therefore, other reduction methods were chosen.

3.5.2 Reduction of 3-20 by using SnCl₂

YAMAMOTO *et al.*^{64, 65} discovered that the imine groups in dendritic polyphenylazomethines coordinate strongly to various metal ion, particular SnCl₂. These complexes could be further reduced to the corresponding amines in the presence of NaBH₄. Following this procedure, compound **3-20** was dissolved in a DCM:acetonitrile mixture (1:1) under inert atmosphere (argon). SnCl₂ was added directly to the mixture, which led to an immediate change of the color of the solution from green to yellow. UV/vis spectra showed a strong bathochromic shift, indicating complexation with SnCl₂ (Figure 3-21 and Figure 3-22).

3 From Pyrene to Polycyclic Aromatic Hydrocarbons Containing Nitrogen

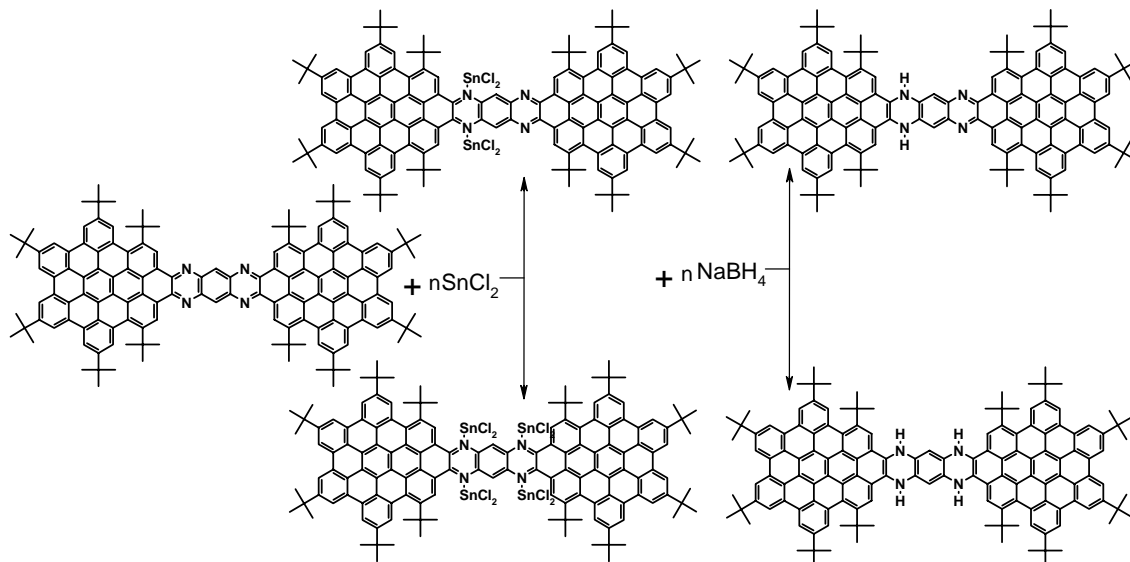


Figure 3-21. Selective reduction of imines in **3-20** complexed with SnCl_2

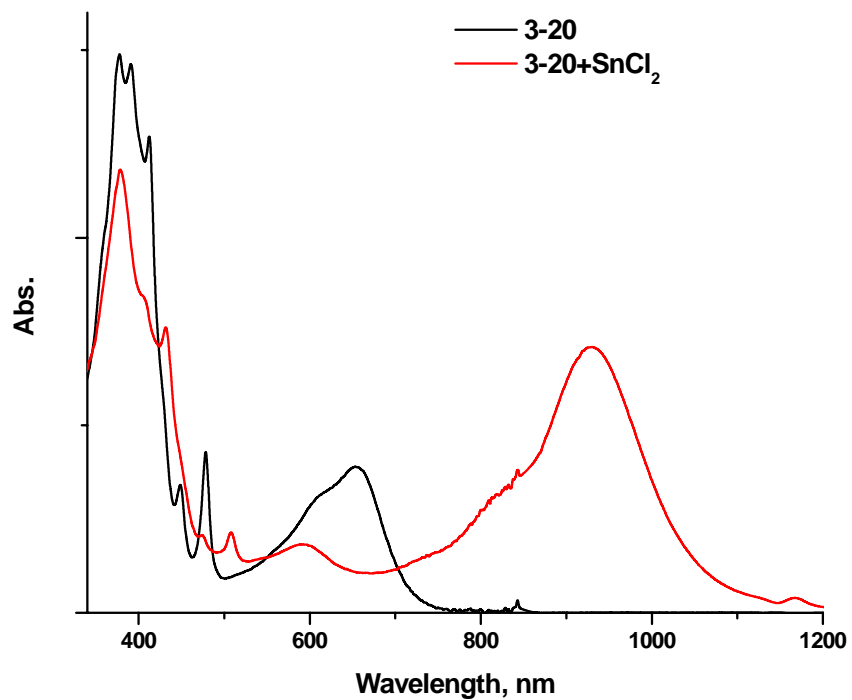


Figure 3-22. UV/vis spectrum of **3-20** complexed with SnCl_2

However, further addition of NaBH_4 did change neither the adsorption spectra nor the color of the solution, i.e. did not yield the protonated product. Apparently, the good

stability of the complex of **3-20** with SnCl_2 (stable even in air) prevented further reduction of imine groups. FD- or MALDI-TOF-mass spectrometry showed only the presence of the initial compound **3-20**, i.e. the complex was not stable enough to survive MALDI ionization. ^1H NMR spectra was recorded in dichloromethane- d_2 and showed broadening of the aromatic peaks. This has also been observed for dendritic polyphenylazomethines, where the peaks broaden on addition of SnCl_2 .^{64, 65}

3.5.3 Reduction of 3-20 by using PhLi

DIETRICH *et al.*⁶⁶ used phenyllithium (PhLi) in combination with phenyliodine (PhI) and catalytic amount of copper to introduce phenyl rings into phenazine derivatives. The same procedure was attempted with the aim to introduce phenyl rings into **3-20** (Figure 3-23).

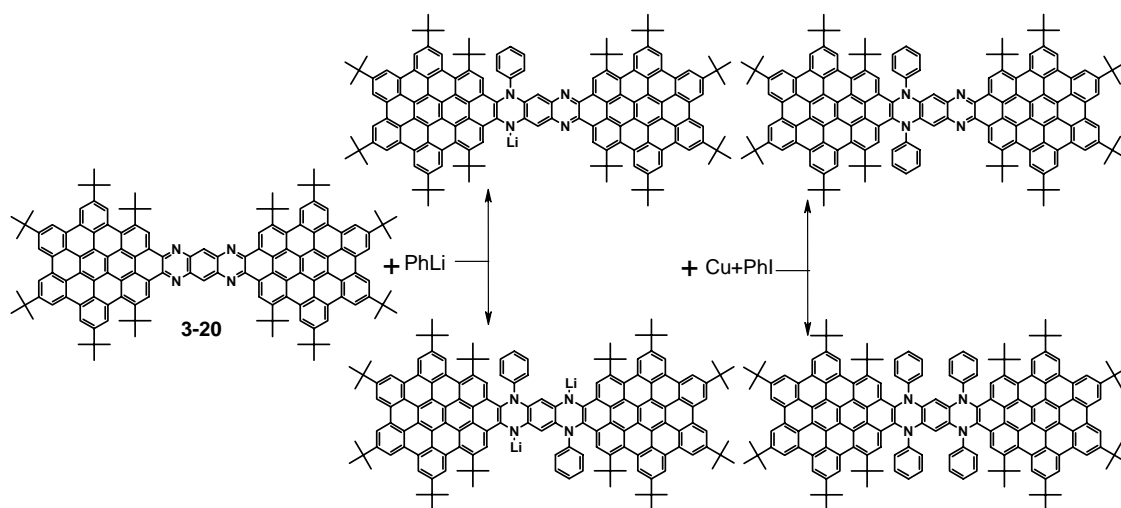


Figure 3-23. Possible mechanism of phenylation according to Dietrich⁶⁶

The neutral compound **3-20** was dissolved in dry degassed THF, after which a solution of PhLi was added. The solution color changed immediately; the UV/vis spectrum revealed an intense red-shifted band (Figure 3-24, red). Further addition of copper with PhI caused a hypsochromic shift in the spectrum (green line) and after 15 min the solution became dark green and the hypsochromic shifted band became more intense (blue line). After one hour, a small red shift was observed (brown line), indicating possible formation of one of the phenylated products (Figure 3-23). The characterization of the product by MALDI

TOF was impossible due to on air the color of the sample changed immediately suggesting its instability.

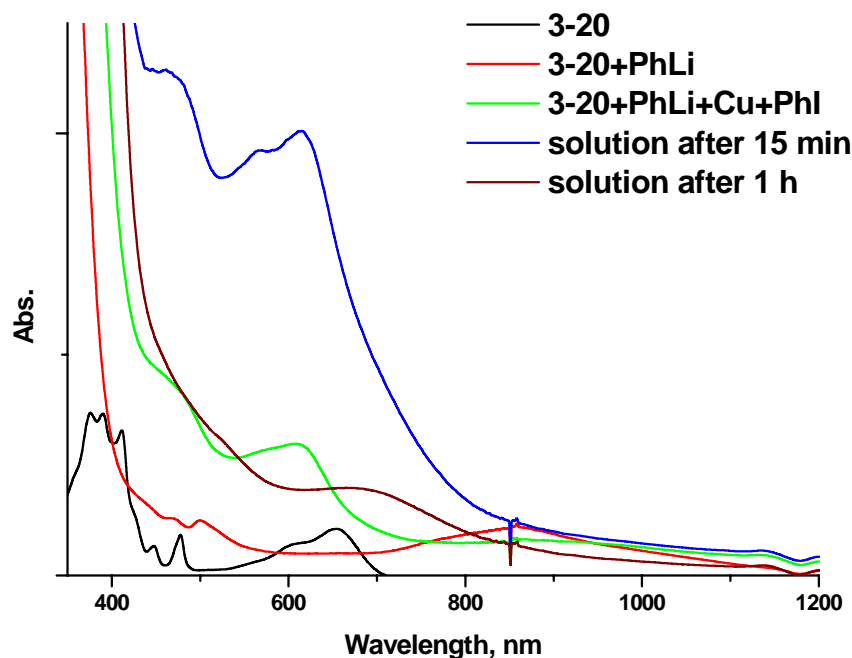


Figure 3-24. UV/vis spectra presenting of phenylation of **3-20**

3.6 Summary

In this chapter a new type of graphitic molecules with “reactive” double bond at the periphery was presented. It was shown that this periphery with localized high electron density was suitable for further functionalization. Therefore, the selective oxidation of the perimeter of a six-fold *tert*-butylated tetrabenzob[*bc,ef,hi,uv*]ovalene **3-12**, led to the formation of an α -diketone **3-13**. Thus synthesized building block **3-13** was able to react with di- or tetraaminobenzenes in quinoxaline reactions to obtain four extended hetero PAHs containing up to 104 skeletal atoms. The distortion from planarity of the aromatic frameworks by bulky *tert*-butyl groups brought extraordinarily high solubility (up to 20 mg/mL), presumably through the suppression of the molecular aggregation and allowing their purification and characterization to be performed by standard methods.

Well-resolved ^1H NMR spectra were recorded for all nanographenes. The sharp resonances in the aromatic region implied low self-association propensities in solution. The experimental and computed UV/vis spectra are in good agreement and reveal that the positions of the α and p bands depend strongly on the overall size of the aromatic system. According to cyclic voltammetry, the introduction of the quinoxaline or tetraazaanthracene bridges into the large aromatic moiety significantly reduced the LUMO level, thus rendering them electron acceptor systems.

The novel nanographene **3-20** with 98 atoms in the aromatic core is so far the largest known PAH with resolved ^1H NMR spectra and exhibits strong fluorescence solvatochromism. The emission of **3-20** shifts with the polarity of the solvent suggesting that, in the excited state, such system can work as the π -electron-accepting unit. The material has a good electron affinity compared to the established systems with similar energy gaps such as PDIs, which makes it promising for use in FETs. Reductive protonation (alkylation) of **3-20** in situ was performed to obtain system, containing two or four protons (phenyl-groups). By use of UV/vis spectroscopy it was possible to detect the formation of protonated or phenylated products. However, due to lack stability of these systems it was hard to characterize them.

It has been shown that the introduction of electron-acceptor groups leads to a donor-acceptor compound **3-21** with intramolecular charge transfer, which can be used in artificial photosynthesis.³⁵

3.7 References

1. Debije, M. G.; Piris, J.; de Haas, M. P.; Warman, J. M.; Tomovic, Z.; Simpson, C. D.; Watson, M. D.; Müllen, K., *J. Am. Chem. Soc.* **2004**, 126, (14), 4641-4645.
2. Watson, M. D.; Fechtenkötter, A.; Müllen, K., *Chem. Rev.* **2001**, 101, (5), 1267-1300.
3. Tomovic, Z.; Watson, M. D.; Müllen, K., *Angew. Chem., Int. Ed.* **2004**, 43, (6), 755-758.
4. Clar, E., *Polycyclic Hydrocarbons*. New York, 1964; Vol. 1, 2.
5. Stein, S. E.; Brown, R. L., *J. Am. Chem. Soc.* **1987**, 109, (12), 3721-3729.

3 From Pyrene to Polycyclic Aromatic Hydrocarbons Containing Nitrogen

6. Tyutyulkov, N.; Müllen, K.; Baumgarten, M.; Ivanova, A.; Tadjer, A., *Synthetic Metals* **2003**, 139, (1), 99-107.
7. Hess, B. A.; Schaad, L. J., *J. Am. Chem. Soc.* **1971**, 93, (2), 305-310.
8. Biermann, D.; Schmidt, W., *J. Am. Chem. Soc.* **1980**, 102, (9), 3173-3181.
9. Herwig, P.; Kayser, C. W.; Müllen, K.; Spiess, H. W., *Adv. Mater.* **1996**, 8, (6), 510-&.
10. Stabel, A.; Herwig, P.; Müllen, K.; Rabe, J. P., *Angew. Chem., Int. Ed. Engl.* **1995**, 34, (15), 1609-1611.
11. Fechtenkötter, A.; Saalwächter, K.; Harbison, M. A.; Müllen, K.; Spiess, H. W., *Angew. Chem., Int. Ed.* **1999**, 38, (20), 3039-3042.
12. Fechtenkötter, A.; Tchegotareva, N.; Watson, M.; Müllen, K., *Tetrahedron* **2001**, 57, (17), 3769-3783.
13. Clar, E., *The Aromatic Sextet*. New York, 1972.
14. Zander, M., *Handbook of Polycyclic Aromatic Hydrocarbons*. New York, 1983.
15. Dias, J. R., *Polycyclic Aromatic Compounds* **2005**, 25, 113-127.
16. Dias, J. R., *Jornal of Chemical Information and Modeling* **2005**, 45, 562-571.
17. Ruiz-Morales, Y., *Jornal of Physical Chemistry A* **2002**, 106, 11283-11308.
18. Watson, M. D.; Fechtenkötter, A.; Müllen, K., *Chemical Reviews* **2001**, 101, (5), 1267-1300.
19. Wasserfallen, D.; Kastler, M.; Pisula, W.; Hofer, W. A.; Fogel, Y.; Wang, Z. H.; Müllen, K., *J. Am. Chem. Soc.* **2006**, 128, (4), 1334-1339.
20. Pascal, R. A.; Mcmillan, W. D.; Vanengen, D.; Eason, R. G., *J. Am. Chem. Soc.* **1987**, 109, (15), 4660-4665.
21. Duong, H. M.; Bendikov, M.; Steiger, D.; Zhang, Q. C.; Sonmez, G.; Yamada, J.; Wudl, F., *Org. Lett.* **2003**, 5, (23), 4433-4436.
22. Wang, Z. H.; Tomovic, E.; Kastler, M.; Pretsch, R.; Negri, F.; Enkelmann, V.; Müllen, K., *J. Am. Chem. Soc.* **2004**, 126, (25), 7794-7795.
23. Stille, J. K., Mainen, E. L., *Macromolecules* **1968**, 1, (1), 36-42.
24. Miura, Y.; Yamano, E.; Miyazawa, A.; Tashiro, M., *J. Chem. Soc. Perkin Trans. 2* **1996**, (3), 359-364.

25. Han, G. Y.; Han, P. F.; Perkins, J.; Mcbay, H. C., *J. Org. Chem.* **1981**, 46, (23), 4695-4700.
26. Herwig, P. T.; Enkelmann, V.; Schmelz, O.; Müllen, K., *Chem. Eur. J.* **2000**, 6, (10), 1834-1839.
27. The minority component of the disordered tert-butyl group (C502, C., and C522) has been removed for clarity). Space group, Pcab, $a = 17.2333(6)$, $b = 24.8954(8)$, $c = 29.6704(9)$ Å, $\alpha = 90$, $\beta = 90$, $\gamma = 90^\circ$, $V = 12729.5(7)$ Å³, $Z = 8$, $D_x = 1.102$ g/cm³, unique reflections measured 11285, 6943 reflections observed ($I > 3\sigma(I)$), $R = 0.0804$, $R_w = 0.0943$. (This crystal contains a substantial amount of disordered solvent (2 hexane molecules per ring), which is partially disordered even at 120 K. This is why no significant data were observed at scattering angles $\theta > 65^\circ$. In addition, one of the tert-butyl groups is also disordered. The data parameter ratio of 8.93 is the consequence of this disorder.
28. Hu, J.; Zhang, D.; Harris, F. W., *J. Org. Chem.* **2005**, 70, (2), 707-708.
29. Spacegroup, P., $a = 13.4680(5)$, $b = 22.3670(7)$, $c = 25.1580(8)$ Å, $\alpha = 90$, $\beta = 101.4200(15)$, $\gamma = 90^\circ$, $V = 7428.5(4)$ Å³, $Z = 4$, $D_x = 1.482$ g/cm³, unique reflections measured 13050, 1062 reflections observed ($I > 2\sigma(I)$), $R = 0.0493$, $R_w = 0.0282$.
30. Fox, M. A., Voynick, T.A., *J.Org.Chem.* **1981**, 46, (7), 1235-1239.
31. Jenekhe, S. A., *Macromolecules* **1991**, 24, (1), 1-10.
32. Sawtschenko, L., Jobst, K., Neudeck, A., Dunsch, L., *Electrochim.Acta* **1996**, 41, (1), 123-131.
33. Fogel, Y., Kastler, M., Wang, Z., Andrienko, D., Bodwell, G. J., Müllen, K., *submitted* **2007**.
34. Dumur, F.; Gautier, N.; Gallego-Planas, N.; Sahin, Y.; Levillain, E.; Mercier, N.; Hudhomme, P.; Masino, M.; Girlando, A.; Lloveras, V.; Vidal-Gancedo, J.; Veciana, J.; Rovira, C., *J. Org. Chem.* **2004**, 69, (6), 2164-2177.
35. Fox, M. A., Chanon, M., *Photoinduced Electron Transfer*. Amsterdam, 1988.
36. Prasad, P. N., Williams, D. J., *Introduction to Nonlinear Optical Effects in Molecules and Polymers*. New York, 1991.
37. Wong, M. S.; Bosshard, C.; Pan, F.; Günter, P., *Adv. Mater.* **1996**, 8, (8), 677-&.
38. Nalwa, H. S., *Adv. Mater.* **1993**, 5, (5), 341-358.

39. Launay, J. P., *Molecular Electronics. In Granular Nanoelectronics*. Plenum Press: New York, 1991.
40. Petty, M. C., Bryce, M. R., Bloor, D., *Introduction to Molecular Electronics*. Oxford University Press: New York, 1995.
41. Martin, N., Sanchez, L., Illescas, B., Perez, I., *Chem.Rev.* **1998**, 98, 2527.
42. Reichardt, C., *Chem. Rev.* **1994**, 94, (8), 2319-2358.
43. Kanis, D. R.; Ratner, M. A.; Marks, T. J., *Chem. Rev.* **1994**, 94, (1), 195-242.
44. Platt, J. R., *J.Chem.Phys.* **1949**, 17, 484-496.
45. Williams, D. H., Fleming, I., *Spectroscopic Methods in Organic Chemistry* Third ed.; McGRAW-HILL Book Company (UK) Limited: 1980.
46. Kastler, M., Schmidt, J., Pisula, W., Sebastiani, D., Müllen, K., *J. Am. Chem. Soc.* **2006**, 128, (29), 9526-9534.
47. Parac, M.; Grimme, S., *Chem. Phys.* **2003**, 292, (1), 11-21.
48. Alwair, K.; Archer, J. F.; Grimshaw, J., *J. Chem. Soc. Perkin Trans. 2* **1972**, (11), 1663.
49. Baba, H.; Yamazaki, I., *Journal of Molecular Spectroscopy* **1972**, 44, (1), 118-&.
50. Kobayashi, T.; Kobayashi, S., *Eur. J. Org. Chem.* **2002**, (13), 2066-2073.
51. Ono, K.; Okazaki, Y.; Ohkita, M.; Saito, K.; Yamashita, Y., *Heterocycles* **2004**, 63, (10), 2207.
52. Li, J. L.; Dierschke, F.; Wu, J. S.; Grimsdale, A. C.; Müllen, K., *Journal of Materials Chemistry* **2006**, 16, (1), 96-100.
53. Gherghel, L.; Brand, J. D.; Baumgarten, M.; Müllen, K., *J. Am. Chem. Soc.* **1999**, 121, (35), 8104-8105.
54. Terenziani, F.; Painelli, A.; Katan, C.; Charlot, M.; Blanchard-Desce, M., *J. Am. Chem. Soc.* **2006**, 128, (49), 15742-15755.
55. Marder, S. R.; Beratan, D. N.; Cheng, L. T., *Science* **1991**, 252, (5002), 103-106.
56. Charlot, M.; Izard, N.; Mongin, O.; Riehl, D.; Blanchard-Desce, M., *Chem. Phys. Lett.* **2006**, 417, (4-6), 297-302.
57. Chung, S. J.; Rumi, M.; Alain, V.; Barlow, S.; Perry, J. W.; Marder, S. R., *J. Am. Chem. Soc.* **2005**, 127, (31), 10844-10845.

3 From Pyrene to Polycyclic Aromatic Hydrocarbons Containing Nitrogen

58. Beljonne, D.; Wenseleers, W.; Zojer, E.; Shuai, Z. G.; Vogel, H.; Pond, S. J. K.; Perry, J. W.; Marder, S. R.; Bredas, J. L., *Adv. Funct. Mater.* **2002**, 12, (9), 631-641.
59. Abbotto, A.; Beverina, L.; Bozio, R.; Facchetti, A.; Ferrante, C.; Pagani, G. A.; Pedron, D.; Signorini, R., *Org. Lett.* **2002**, 4, (9), 1495-1498.
60. Ventelon, L.; Charier, S.; Moreaux, L.; Mertz, J.; Blanchard-Desce, M., *Angew.Chem.,Int.Ed.* **2001**, 40, (11), 2098-2101.
61. Woo, H. Y.; Liu, B.; Kohler, B.; Korystov, D.; Mikhailovsky, A.; Bazan, G. C., *J. Am. Chem. Soc.* **2005**, 127, (42), 14721-14729.
62. de Tacconi, N. R.; Lezna, R. O.; Konduri, R.; Ongeri, F.; Rajeshwar, K.; MacDonnell, F. M., *Chem. Eur. J.* **2005**, 11, (15), 4327-4339.
63. Konduri, R.; de Tacconi, N. R.; Rajeshwar, K.; MacDonnell, F. M., *J. Am. Chem. Soc.* **2004**, 126, (37), 11621-11629.
64. Higuchi, M.; Tsuruta, M.; Chiba, H.; Shiki, S.; Yamamoto, K., *J. Am. Chem. Soc.* **2003**, 125, (33), 9988-9997.
65. Yamamoto, K.; Higuchi, M.; Shiki, S.; Tsuruta, M.; Chiba, H., *Nature* **2002**, 415, (6871), 509-511.
66. Gilman, H.; Dietrich, J. J., *J. Am. Chem. Soc.* **1957**, 79, (23), 6178-6179.

4 From Pyrene to the Largest Phthalocyanines

4 From Pyrene to the Largest Phthalocyanines

4.1 Synthesis and physical properties of phthalocyanines

Phthalocyanine (Pc) was first found as a highly colored by-product in the chemical conversion of *ortho*-1,2-disubstituted benzene derivatives. In 1907 BRAUN and TCHERNIAK¹ obtained a dark insoluble material during the preparation of *ortho*-cyanobenzamide from phthlalimide and acetic acid. Later, in 1927, DE DIESBACH and VON DER WEID² observed an exceptionally stable bluish material during the reaction of *ortho*-dibromobenzene with copper cyanide in refluxing pyridine.

However, the full structure of Pc was not elucidated until 1928 when, during the industrial preparation of phthalimide from phthalic anhydride, a stable insoluble blue-green pigment was obtained.³ LINSTED,⁴⁻⁷ in collaboration with Imperial Chemical Industries, applied a combination of elemental analysis, ebullioscopic molecular mass determination and oxidative degradation, and showed that Pc is a symmetric macrocycle composed of four iminoisoindoline units with a central cavity of a sufficient size to accommodate various metal ions (Figure 4-1).

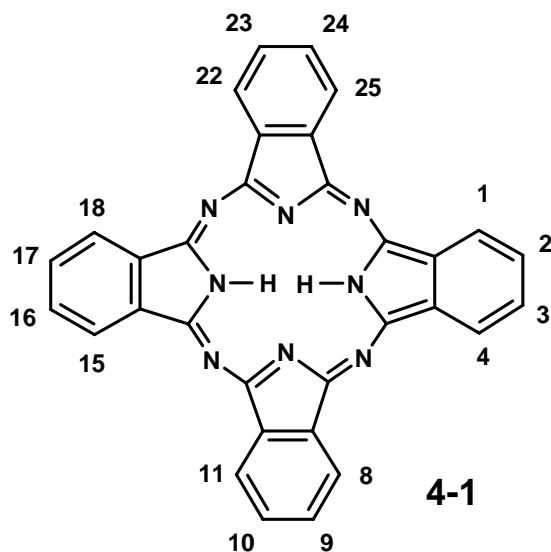


Figure 4-1. The structure of phthalocyanine **4-1** with each of the possible sites of substitution at the benzo-positions numbered using the accepted notation

In addition to the structural description, LINSTEAD's series of papers contained the details of the preparation of Pcs from phthalonitrile (*ortho*-dicyanobenzene), which is still the best precursor for Pc synthesis on a laboratory scale. LINSTEAD also introduced the name *phthalocyanine* by combining the prefix *phthal*, from the Greek *naphtha* (rock oil, to emphasize the association with its various phthalic acid-derived precursors), and the Greek *cyanine* (blue).

4.1.1 Synthesis

Several *ortho*-disubstituted benzene derivatives can act as Pc precursors (see Figure 4-2). However, phthalonitrile **4-2** (1,2-dicyanobenzene) is suitable for a laboratory synthesis.

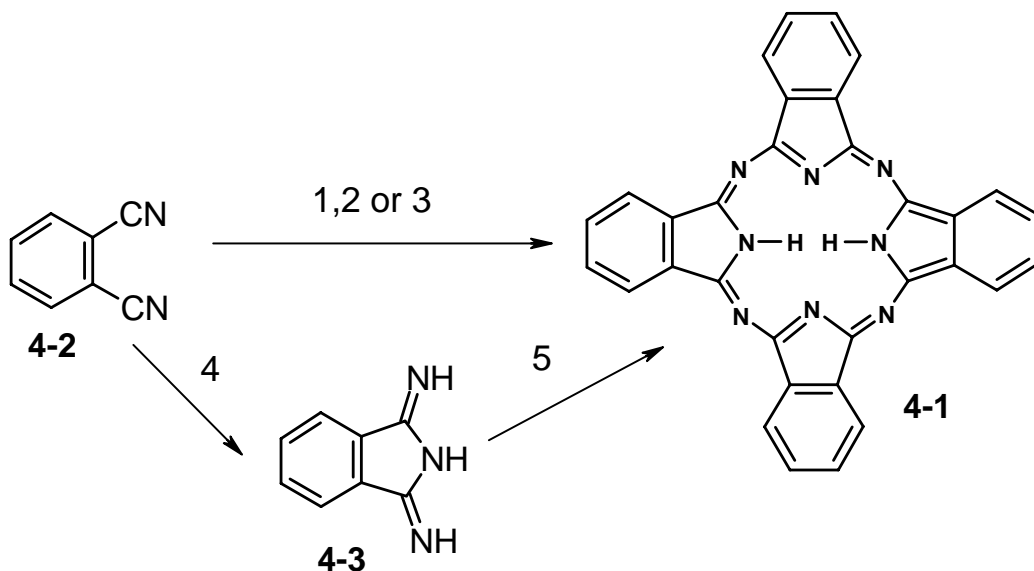


Figure 4-2. Synthetic routes to H₂Pc **4-1**; reagents and conditions: 1. Lithium, refluxing pentanol, followed by aqueous hydrolysis. 2. Fuse with hydroquinone. 3. Heat with 1,8-diazobicyclo[4.3.0]non-5-ene (DBN) in a melt or in pentanol solution. 4. Ammonia (NH₃), refluxing methanol, sodium methoxide. 5. Reflux in a high-boiling-point alcohol

There are several methods of cyclotetramerisation of phthalonitrile **4-2** to form **4-1**. These include the initial formation of diiminoisoindole **4-3**, by the reaction of **4-2** with ammonia. **4-3** condenses under relatively mild conditions to form H₂Pc.⁸ Cyclotetramerisation of **4-2** in the melt with hydroquinone (4:1 by weight) as the

necessary reducing agent allows preparation of phthalocyanine **4-1** in the absence of any metal ions that may be incorporated into the product as MPc impurities.⁹ Similarly, a non-nucleophilic hindered base such as 1,5-diazabicyclo[4.3.0]non-5-ene (DBN) is an efficient reagent for cyclotetramerisation of **4-2** in a melt or pentanol solution.¹⁰ In addition, H₂Pc **4-1** is conveniently prepared from **4-2** using a refluxing solution of lithium metal dissolved in pentanol to form Li₂Pc, which can be readily made to undergo demetallation using dilute aqueous acid.¹¹

4.1.2 Synthesis of metal-ion-containing Pcs (MPc)

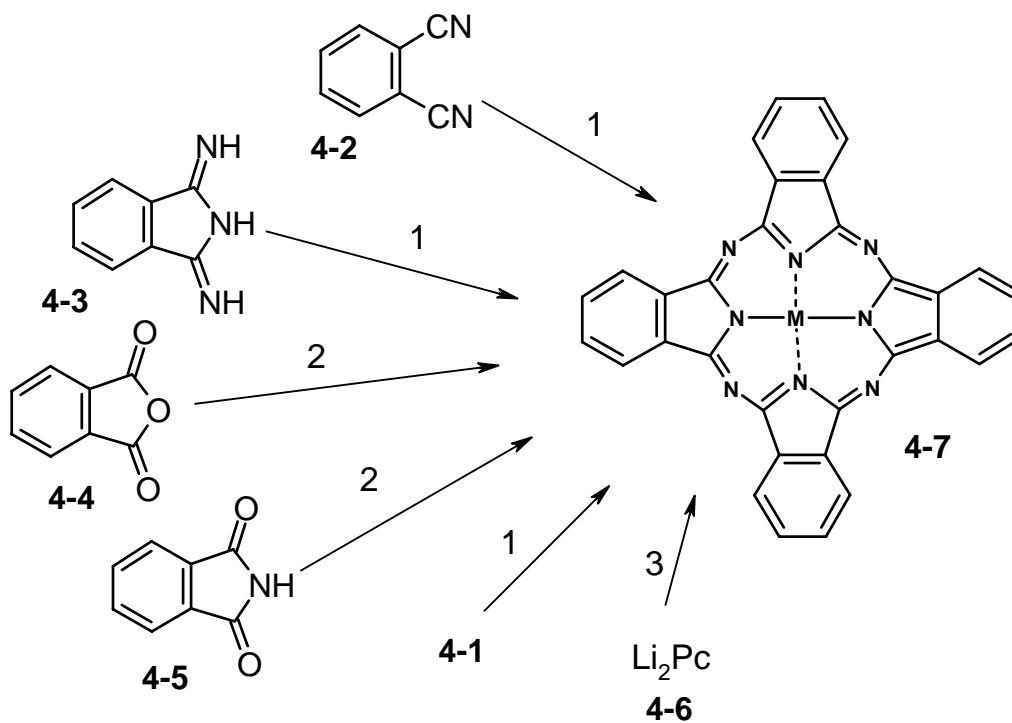


Figure 4-3. Synthetic routes to MPc **4-7**; reagents and conditions: 1. Heating in a high-boiling-point solvent with metal salt. 2. Heating in a high-boiling-point solvent with metal salt and urea. 3. Heating in ethanol with metal salt

The simplest metal-ion-containing Pcs **4-7** are prepared directly from **4-2** or **4-3** using the metal ion as a template for cyclotetramerisation (Figure 4-3). Phthalic anhydride **4-4** or phthalimide **4-5** can be also used as a precursor in the presence of a metal salt (e.g. copper(II) acetate or nickel(II) chloride) and a source of nitrogen (urea). Alternatively,

the reaction between H₂Pc **4-1** or Li₂Pc **4-6** and an appropriate metal salt produces most of MPc **4-7**. However, the insolubility of **4-1** in any organic solvents requires the use of a high-boiling aromatic solvent such as chloronaphthalene or quinoline in order to ensure complete metallation.

4.1.3 The crystal structure of phthalocyanines

Fabrication of optoelectronic devices requires defects free crystalline phase of Pc materials. Already LINSTED showed that H₂Pc and many other MPcs can be purified by sublimation in vacuum and form large single crystals with a well-defined crystal structure.^{12, 13}

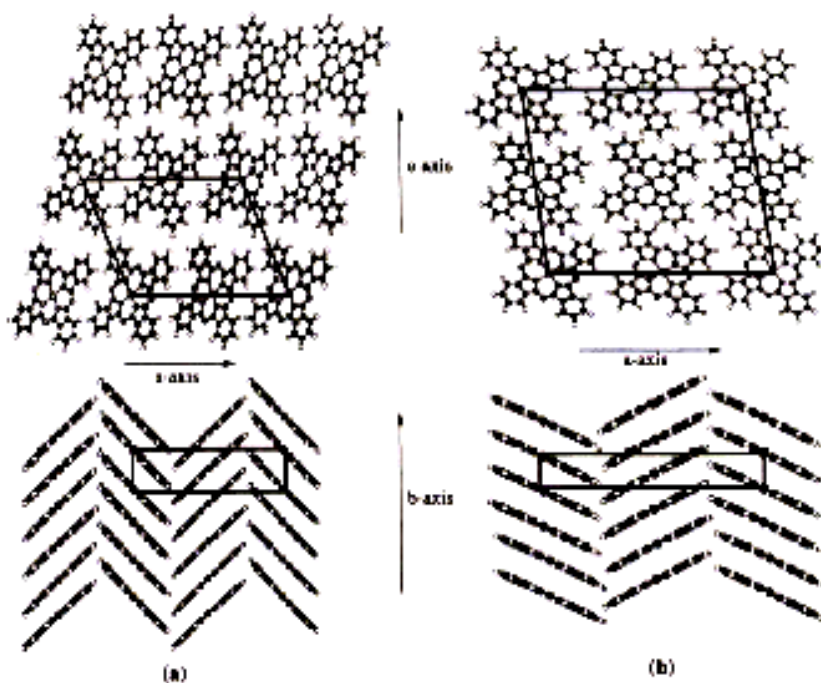


Figure 4-4. Crystal structures of MPc: a) the β -form of crystal; b) the α -form of crystal¹⁴

The common crystal type obtained by sublimation is the β -form, monoclinic with two Pc molecules per unit cell. The β -form is the thermodynamically most stable polymorph of H₂Pc and the most planar MPc with metal ions as Cu²⁺, Co²⁺, Mn²⁺, Ni²⁺, Zn²⁺ and Fe²⁺. In each case the Pc stacks make an angle of between 45° and 49° with the *b*-axis of the crystal unit cell.¹⁵ The Pc molecules in neighbouring stacks are roughly orthogonal,

producing a herringbone arrangement. Pc molecules also exhibit α -type polymorphs, for example the industrially important pigment form of CuPc. The main difference between these two forms is the smaller tilt angle (about 27-30°) of the molecules relative to the b -axis of the crystal. The α -phase has a monoclinic crystal structures with four molecules per unit cell, see Figure 4-4.^{16, 17}

4.1.4 Spectroscopic properties

The absorption of light gives Pcs their clear blue or green colors. Naturally, these compounds were immediately used as pigments and dyes soon after their discovery, and are still of immense commercial importance.

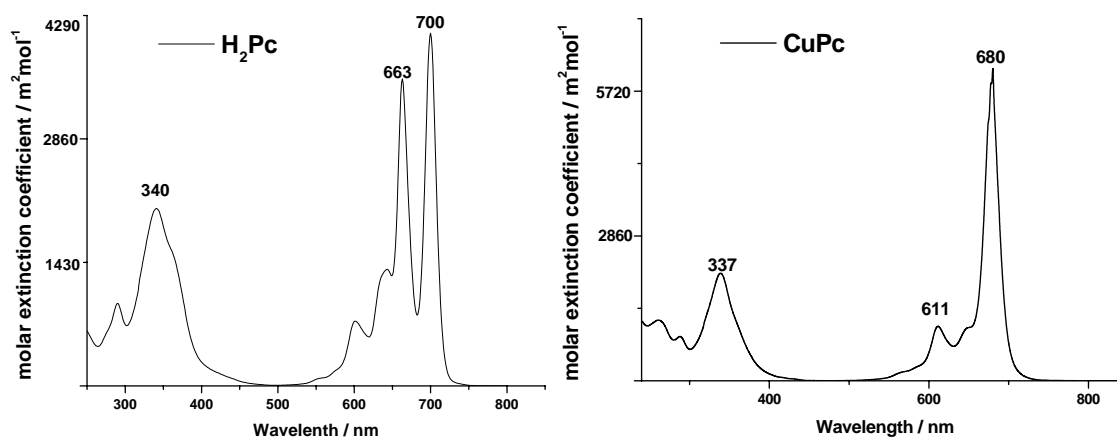


Figure 4-5. The absorption spectra of solutions of H₂Pc and CuPc

The characteristic absorption spectra for H₂Pc and CuPc in solution are shown in Figure 4-5. In both cases there is a strong absorption band between 670 and 690 nm, termed the Q-band. This band is responsible for the intense blue (or blue-green) color of the compound. It is very sensitive to substitutions and environment of the Pc macrocycle. The weak absorption bands at about 611 nm are vibrational overtones of the Q-band. In addition there is a strong absorption band in the ultra-violet region between 320 and 370 nm, which is the Soret or B-band.

The Q-band absorption was assigned to the transition from the HOMO to LUMO.¹⁸ The splitting of the Q-band of H₂Pc is due to its lower symmetry, D_{2h} compared D_{4h} of planar MPcs, which results in the consequent loss of the degeneracy of the LUMO orbital.¹⁹

4.1.5 Discotic and columnar mesophases of Pcs

Mesogenicity of Pcs was first demonstrated in CuPc-*op*-C₁OC₁₂ by Piechocki and Simon²⁰ in 1982. This compound displays a mesophase with a remarkably large thermal range, from 53° up to 300 °C. In fact, it decomposes before reaching the isotropic state. A powder X-ray diffraction study revealed that this mesophase has a two-dimensional hexagonal arrangement of columnar stacks. The lack of a sharp reflection at an intramolecular distance of 3.4 Å indicated that there is no long-range periodicity along the axes of the columns. The mesophase symmetry was classified as D_{hd}.

The columnar architecture suggested that these materials could serve as anisotropic electronic conductors. Charge transport along the columns would be facilitated by the substantial π - π orbital overlap of the aromatic cores, whereas conductivity perpendicular to the columnar axes would be hindered by the molten insulating alkyl chains.

Since the first discovery a number of mesogenic Pcs have been prepared with different numbers, lengths and positions of the flexible substituents. It has been shown that the linking group attaching side-chains to the Pc core as well as the central metal-ion have a strong influence on the structure and thermal stability of the resultant mesophase. For example, Pcs with straight alkyl side-chains of length 4 do not form mesophases and melt directly from the crystalline state into an isotropic liquid. Initial melting temperatures are very sensitive to the chain length; longer chains reduce the temperature of crystal-mesophase transition considerably.²¹ In fact, this behavior is typical for most discotics: another representative example is HBC substituted with flexible alkyl chains, which form stable mesophases in a wide temperature range, up to 200 °C.

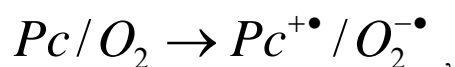
4.1.6 Conductivity of Pcs

Pc materials are extrinsic conductors, i.e. their conductivity is due to doping, or addition of impurities, contrary to intrinsic conductors, where the conductivity arises from thermal

excitations. Electronic conductivity in organic materials with Pcs was first demonstrated by ELEY²².

Conductivity measurements of pure single β -type crystals of Pcs showed that H₂Pc and most planar divalent MPcs have a bandgap of approximately 2 eV; the room-temperature conductivity is in the range of 10^{-14} - 10^{-16} S·cm⁻¹²³ and the mobility of charge carriers along the b-axis is 0.1-2.0 cm²·V⁻¹·s⁻¹.²⁴ Since impurities affect the electronic behavior of Pcs, commercially available Pcs require extensive purification.^{9, 25}

Charge-transfer complexes between unsubstituted Pcs and suitable acceptors, for example, iodine are known for their high conductance.²⁶⁻²⁸ In addition, various ambient gases can be used as dopants, especially O₂. For example, the conductivity of a single crystal of β -CuPc is two orders of magnitude higher when measured in O₂



where the complex with oxidizing species is acting as a p-dopant and the conductivity is extrinsic in character, with holes being the dominant charge carriers.^{29, 30}

Early studies of columnar phases of Pc derivatives suggested that the cofacial arrangement of aromatic cores can be used for one-dimensional conductivity along columns.²⁰ However, later studies proved that even intrinsic semiconductors, such as LiPc and LuPc₂, when purified, act as insulators in their mesomorphic states.³¹

This chapter first introduces the synthesis of the two largest copper phthalocyanines from two building blocks, each of which is, itself, an extended PAH. Later, long alkyl side-chains are introduced at the periphery of Pcs with the aim to self-organize mesogens into a columnar mesophase. Finally, the resulting compounds are characterized with standard methods: their spectroscopic, structural, and electrochemical properties are presented.

4.2 Synthesis of extended Pcs

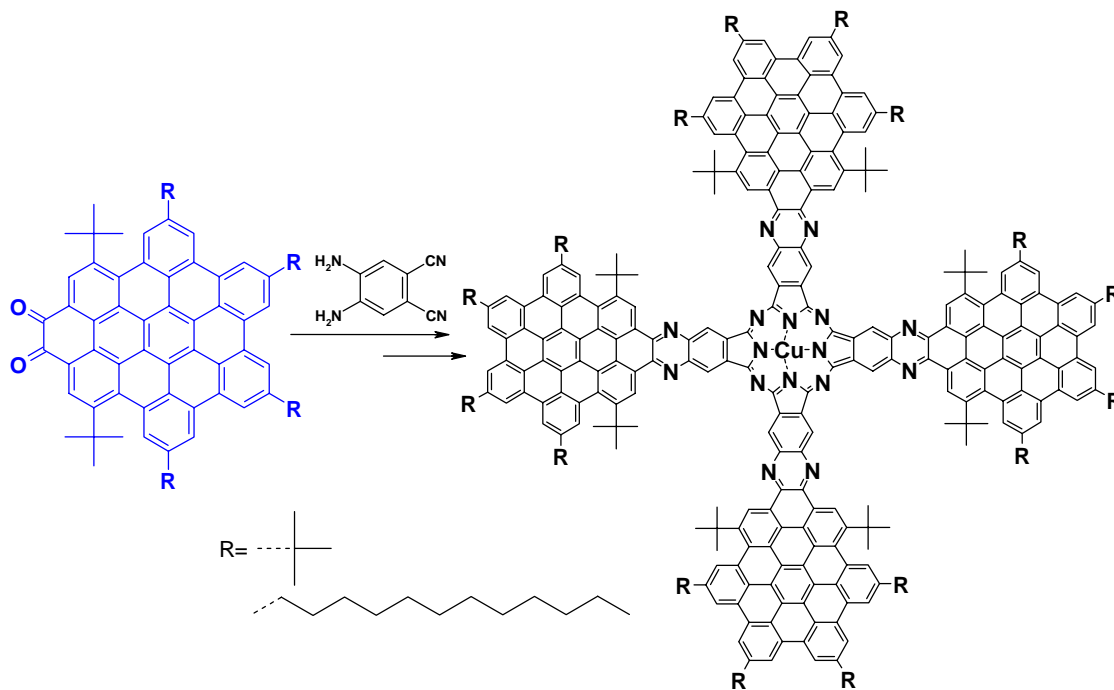
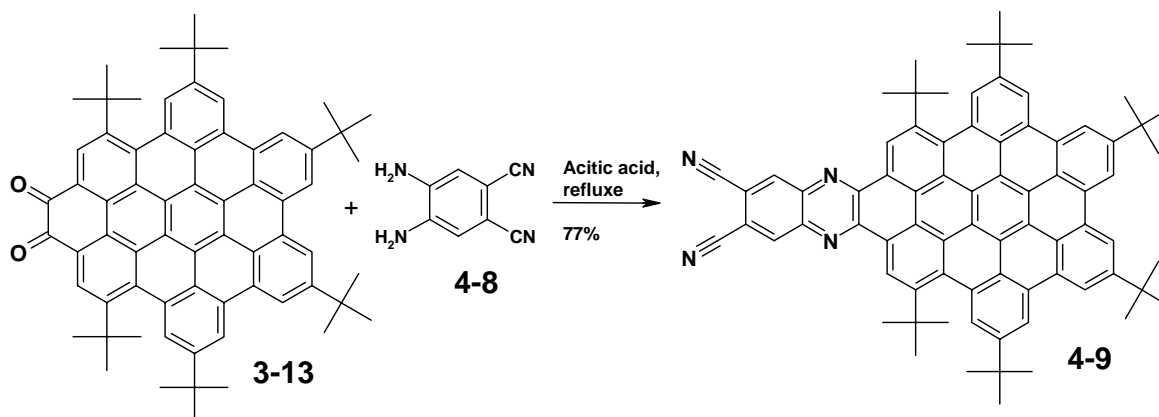


Figure 4-6. General synthetic way towards giant phthalocyanines

In the previous chapter it has been shown that the quinoxaline ring-formation between **3-13** and *ortho*-diamino-derivatives can be used to extend PAHs. Here, the same concept is applied to obtain an *ortho*-cyano-derivative necessary for further phthalocyanine synthesis (Figure 4-6).

Figure 4-7. Synthesis of dicyano-derivative **4-9**

Condensation between **3-13** and 1,2-diamino-4,5-dicyanobenzene (**4-8**) towards **4-9** (Figure 4-7) was carried out in acetic acid at 130 °C for 6 hours. The yield of the condensation was 77 %. The desired product **4-9** was soluble in common organic solvents and its purification was done by column chromatography. The structure characterization was performed with MALDI-TOF spectrometry and NMR spectroscopy.

Figure 4-8 shows the ^1H NMR spectrum of **4-9**, recorded in tetrachloroethane- d_2 at 100°C. As it has already been shown for extended PAHs that the two proton resonances H_b are always shifted towards lower field, while H_a resonances to the higher one. H,H COSY (Figure 4-9) and NOESY were recorded at 100 °C and allowed to assign all protons in the molecule.

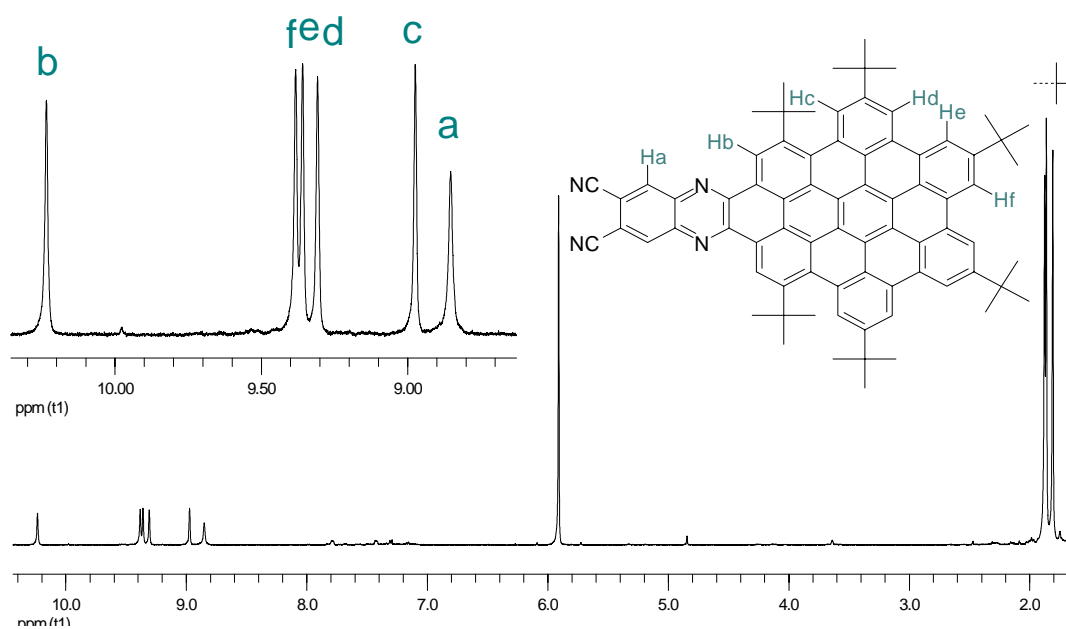


Figure 4-8. ^1H NMR of **4-9**, recorded in tetrachloroethane- d_2 at 100 °C (500 MHz)

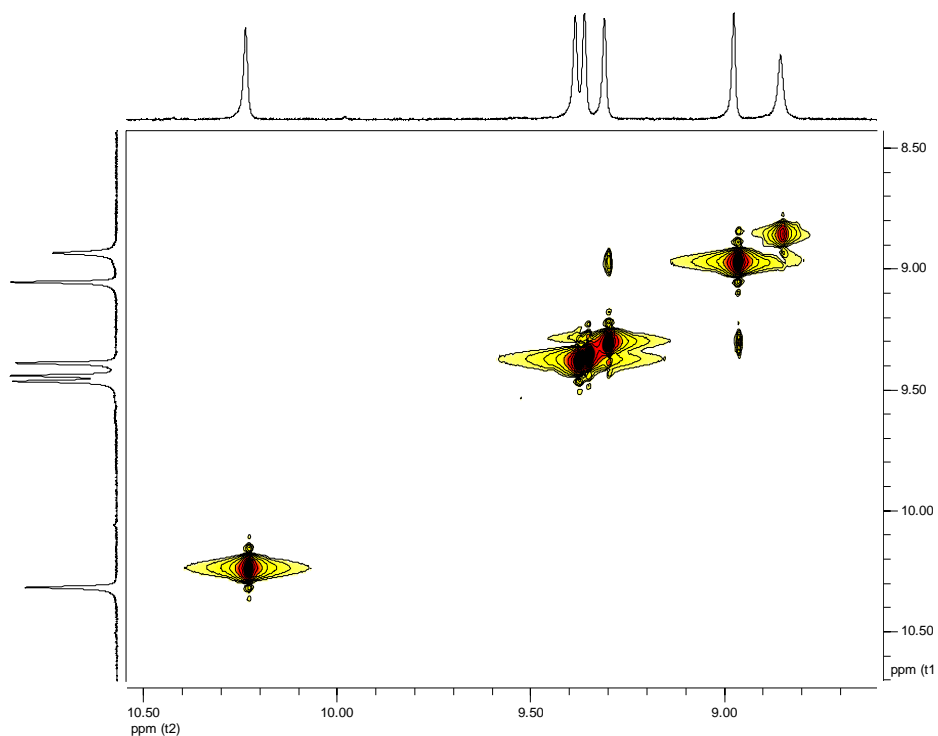


Figure 4-9. H,H COSY of **4-9**, recorded in tetrachloroethane- d_2 at 100°C (500 MHz)

Further cyclotetramerisation of **4-9** with the aim to form the corresponding metal-containing phthalocyanine was performed in a high boiling solvent - quinoline in the presence of urea and Cu(II) salt (Figure 4-10). The reaction mixture was heated overnight and purification of the final dark-brown product was done by column chromatography with mixture of the solvents (DCM:THF=10:1). Additional washing of the final product with methanol was required for the total removal of quinoline. The largest known 1,6-di-*tert*-butyl-8,11,14,17-tetra(*t*-butyl)tetrabenz[*jk,mn,pq,st*]-benzo[1,2-*a*]pyrazine[2,3-*d*]ovalenocyanine (**4-10**) (224 atoms in the aromatic skeleton) was obtained in 7% yield.^{14, 32} No product was found in the absence of urea. Variation of the temperature, concentration and reaction time, as well as the use of microwave irradiation did not lead to an improvement of the yield. The low yield is, in fact, in the same range as those for other ‘large’ phthalocyanines, e.g. one containing 104 skeletal atoms (4%) (Figure 4-11).³³ Most of the unreacted starting material could be recovered.

4-10 showed surprisingly good solubility in common organic solvents, most probably due to distortion of the aromatic core by bulky *tert*-butyl groups, which suppress the self-

aggregation (see Figure 4-12). This made possible the characterization of phthalocyanine **4-10** using standard analytical methods.

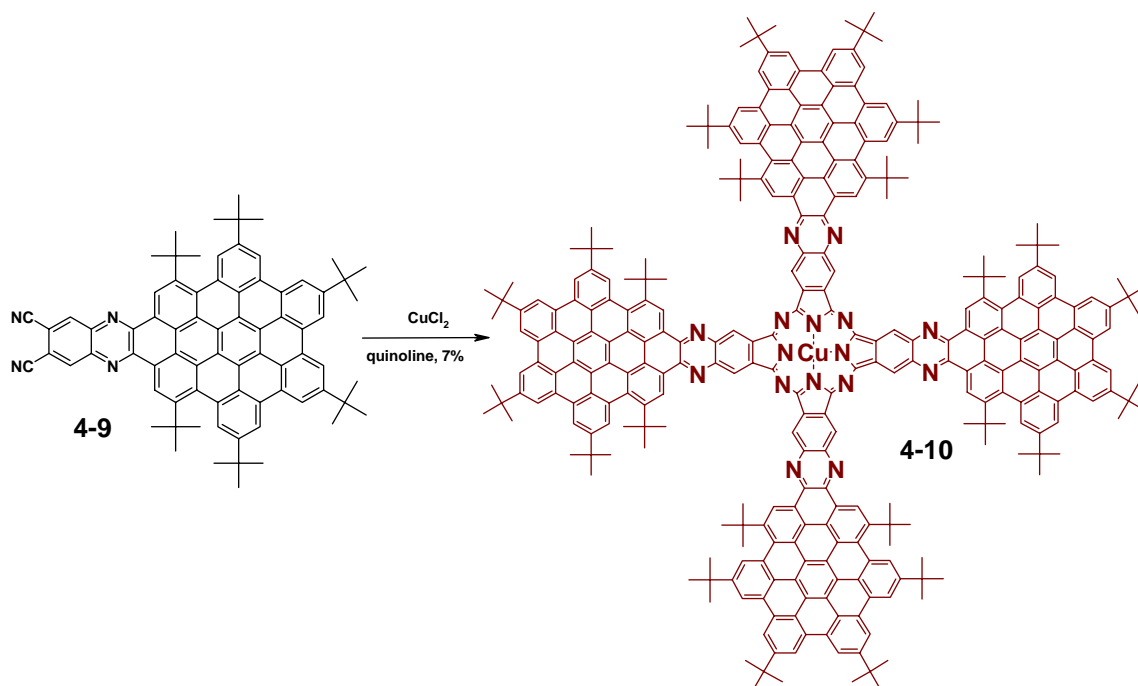


Figure 4-10. Synthetic route to the giant phthalocyanine **4-10**

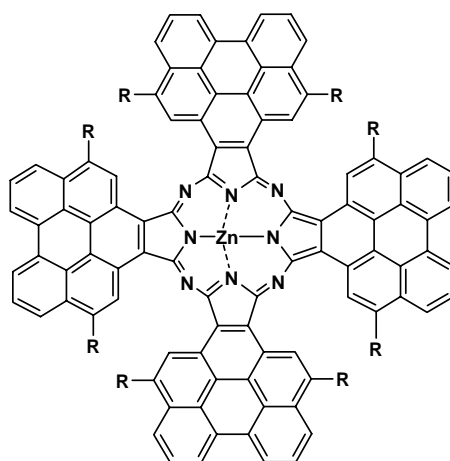


Figure 4-11. Phthalocyanine derivative containing 104 skeletal atoms

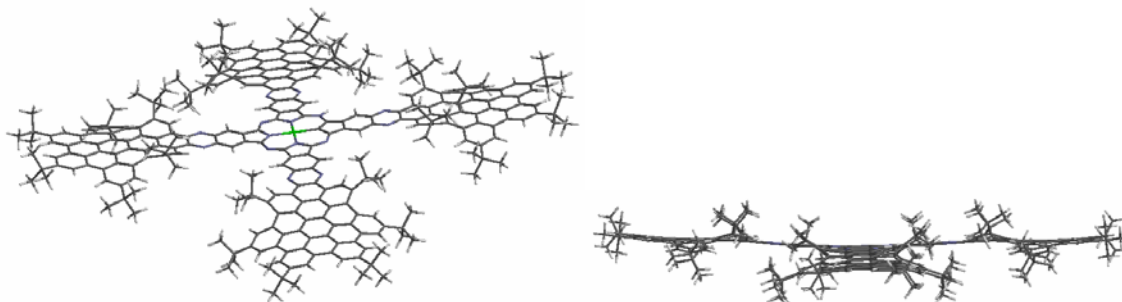


Figure 4-12. Minimized (with molecular mechanics force field available as a part of the Spartan package) structure of phthalocyanine **4-10**

4.3 Characterization of extended Pc

MALDI TOF mass measurements of phthalocyanine **4-10** were done in the solid state by using DCTB as a matrix.

The MALDI TOF mass spectrum, shown in Figure 4-13, has an expected peak at 4207 Da. An additional peak at 2112 Da corresponds to the double charged molecule ion. There are also a few peaks next to the main peak, due to cleavage of *tert*-butyl groups during measurements. Possible structures after cleavage are given in Figure 4-14.

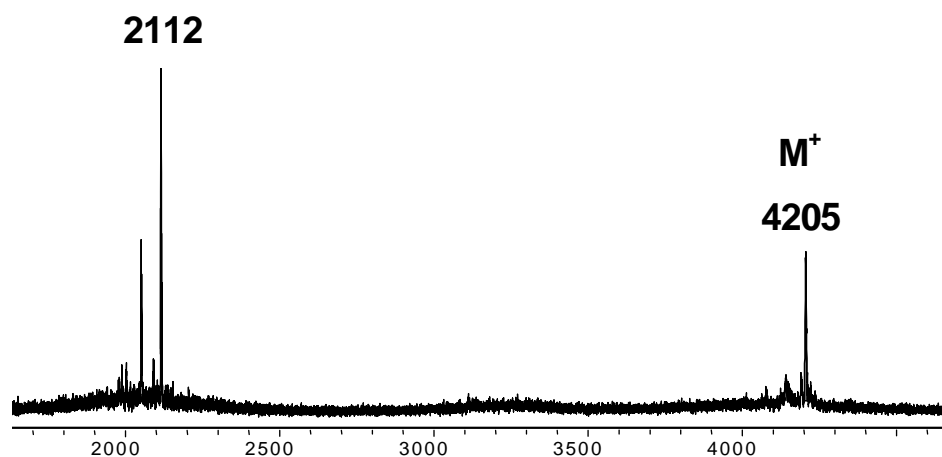


Figure 4-13. MALDI-TOF-mass-spectrum of **4-10**

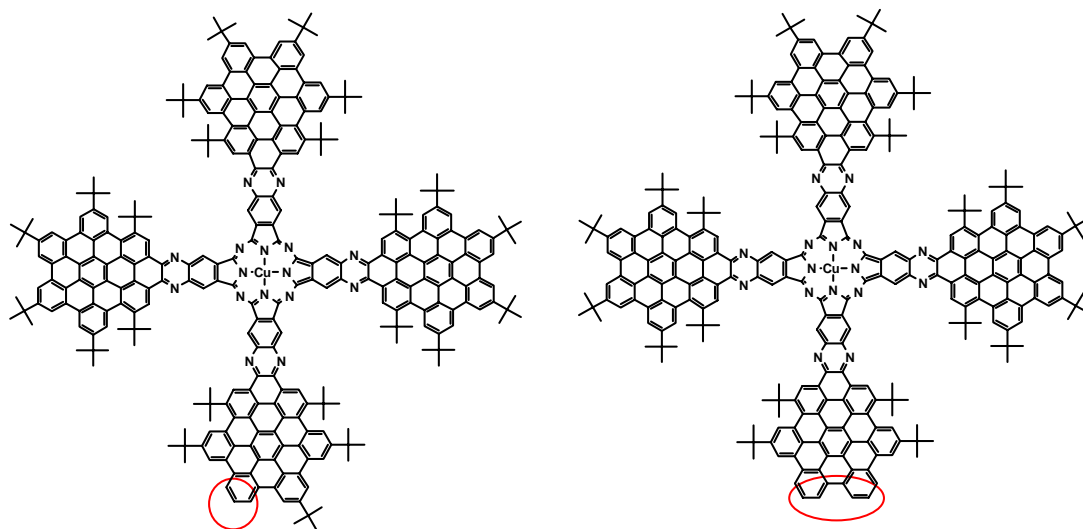


Figure 4-14. Possible structures which can be obtained during mass-measurements

Since copper(II)-complexes are paramagnetic materials^{34, 35}, they possess small positive magnetic susceptibility, due to the presence of unpaired electrons. Magnetic field realigns unpaired electronic orbitals and induces magnetic moment in the bulk of the material. Once the external field is removed, the induced magnetic moment disappears. Due to this fact, the standard NMR spectroscopy cannot be used to further characterize the structure of phthalocyanine **4-10**.

The UV/vis absorption spectrum of **4-10** was recorded in chloroform and exhibits the two characteristic bands for phthalocyanines (B- and Q-bands at 379 and 869 nm, respectively) along with bands originated from the PAH **3-18** moieties (Figure 4-15).¹⁴ The weak absorption band at about 780 nm is a vibrational overtone of the Q-band.¹⁴ The Q-band, which corresponds to a $\pi\text{-}\pi^*$ transition from the HOMO to LUMO is red-shifted by about 190 nm from that of commercially available copper-tetra-*tert*-butylphthalocyanine (CuPc). The extended phthalocyanine shown in Figure 4-11 exhibits a Q-band around 797 nm in its UV/vis spectrum.³³ It is well known that the intensity of the Q-band is very sensitive to substitution and aggregation.^{14, 36, 37} For **4-10**, the Q-band is less intense than that of CuPc, which might be due to the distortion from planarity of the aromatic units and the presence of acceptor moieties around the Pc center.^{38, 39}

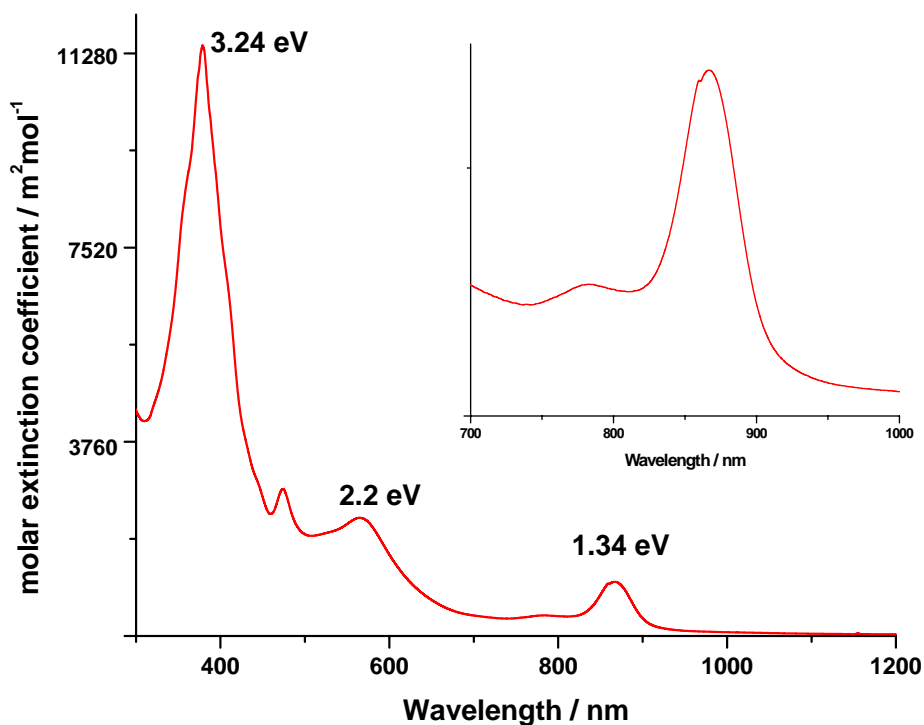


Figure 4-15. Absorption spectra of **4-10** in chloroform at room temperature

The other typical absorption band, the B or Soret-band,¹⁴ was observed at 379 nm. The B-band is assigned to a π - π^* transition of the aromatic units fused to the Pc macrocycle. Because of the extended PAH systems in **4-10**, this band is about two times more intense than those of CuPc. Using cyclovoltammetry and the optical bandgap, the energies of the HOMO (-3.59 eV) and LUMO (-4.93 eV) of **4-10** were obtained. The energy gap of **4-10** is much smaller than that of small Pc derivatives.^{23, 24}

4.4 Introduction of n-dodecyl chains

4.4.1 Synthesis

As it has already been mentioned in the introduction to this chapter, Pcs decorated with linear alkyl side-chains made of four carbon atoms, do not exhibit columnar mesophases.²¹ To enhance mesogenic properties of the phthalocyanine **4-10**, longer alkyl chains (*n*-dodecyl) should be introduced to its periphery.

The first attempts to introduce *n*-dodecyl chains into TBO were done by KASTLER with the aim to increase solubility and obtain columnar mesophases.^{40, 41} However, in his case the KNOEVENAGEL reaction of pyrene-4,5-dione (**3-1**) with 1,3-bis(4-*n*-dodecyl-phenyl)propan-2-one (**2-6**) did not give the desired cyclopentodienone **4-11**, since the product decomposes (Figure 4-16).

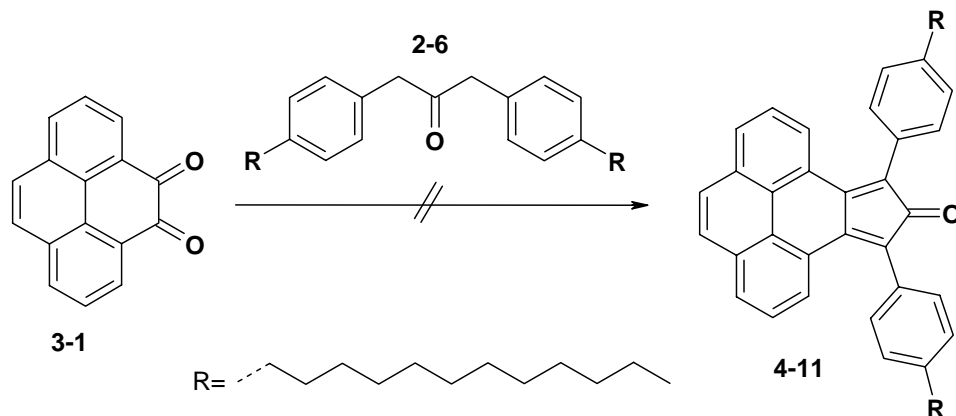


Figure 4-16. Attempted synthesis of an alkylated cyclopentadienone-derivative **4-11**

As was shown in Chapter 3 that the presence of *tert*-butyl groups stabilizes the cyclopentadienone derivatives, and therefore, to introduce dodecyl chains into TBO, the KNOEVENAGEL condensation of 2,7-di-*tert*-butyl-pyrene-4,5-dione (**3-7**) with 1,3-bis(4-*n*-dodecyl-phenyl)propan-2-one (**2-6**) (see Figure 4-17) gave the cyclopentadienone building block **4-12** in a yield of 57%. This cyclopentadienone derivative is thermally unstable and starts to decompose after about 1 h reaction time.

DIELS-ALDER reaction between 2,7-di-*tert*-butyl-4,5-bis(4-*n*-dodecyl-phenyl)-cyclopenta[*e*]pyren-5-one (**4-12**) and di-*n*-dodecyl-butyldiphenylacetylene (**4-13**), resulted in 2,7-di-*tert*-butyl-4,5,6,7-tetrakis(4-*n*-dodecyl-phenyl)-benzo[*e*]pyrene (**4-14**) in 21% yield. The low yield is due to thermal instability of the cyclopentadienone building block **4-12**.

For synthesis of 1,6-di-*tert*-butyl-8,11,14,17-tetra-*n*-dodecyl-tetrabenzo[*bc,ef,hi,uv*]ovalene (**4-15**) the same reaction conditions were applied as for cyclodehydrogenation of **3-12**, except now the amount of FeCl₃ was enlarged on 1.5. A new member of the graphite family with “reactive” double bond at the periphery **4-15**

was obtained in nearly quantitative yield after reductive workup. **4-15** showed good solubility in common organic solvents.

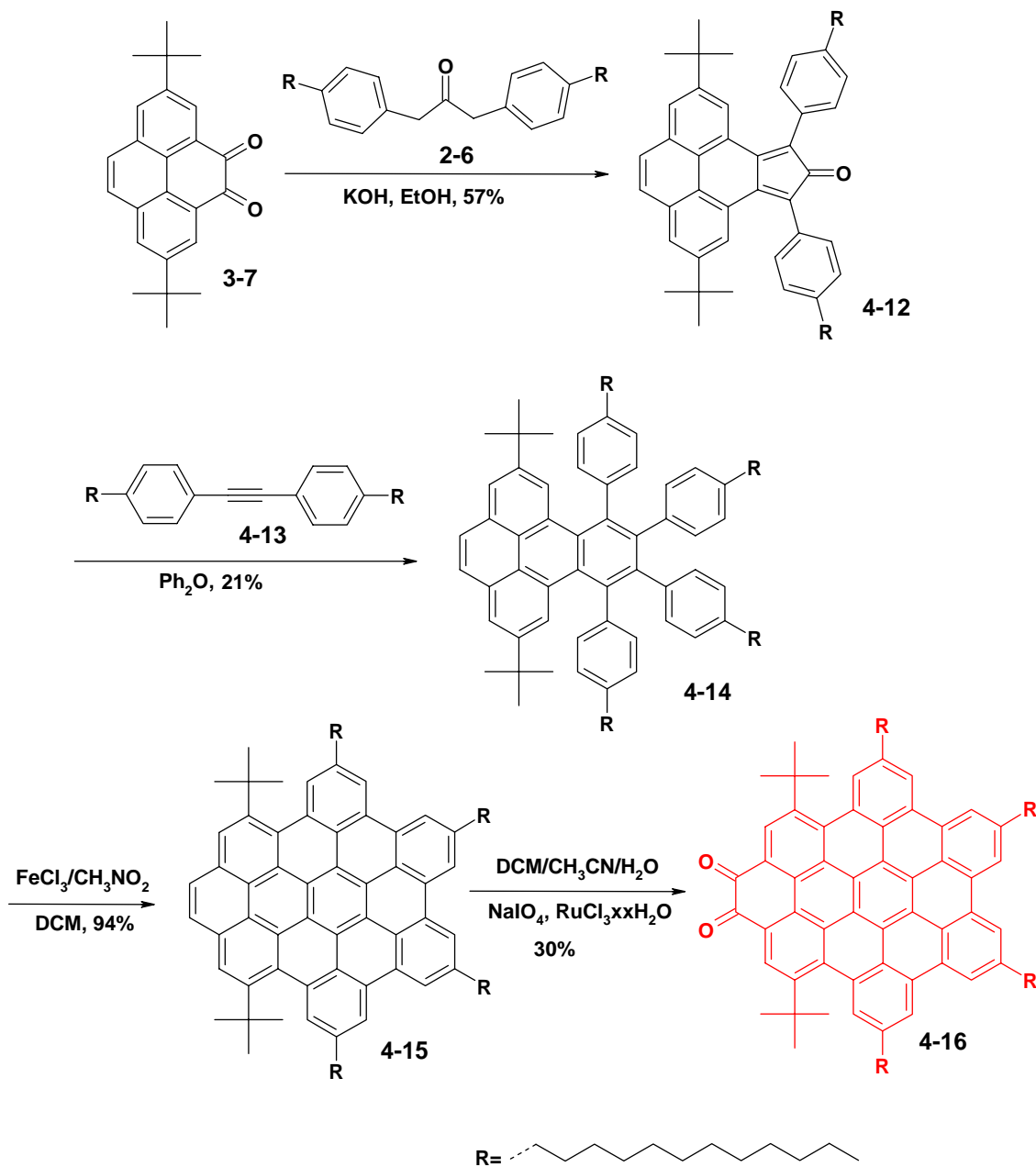


Figure 4-17. Synthetic route for the introduction of n-dodecyl-chains to the periphery of “zigzag” PAHs

^1H , NOESY, H,H COSY spectra of **4-15** were recorded in tetrachloroethane- d_2 at 100 °C. High temperature was chosen to suppress aggregation and sharpen proton signals. The resonances of the two protons located at the “zigzag” edge were observed at $\delta=8.53$ ppm, i.e. they are significantly shielded with respect to the aromatic “armchair” protons, which appear as singlets between 9.0 and 8.7 ppm (Figure 4-18).

Figure 4-19 shows NOESY of **4-15**. All protons are sketched. Proton resonances of H_a and H_b appear at the highest and at the lowest fields, respectively. The proton resonances belonging to the HBC-moiety appear between 8.90 and 8.60 ppm.

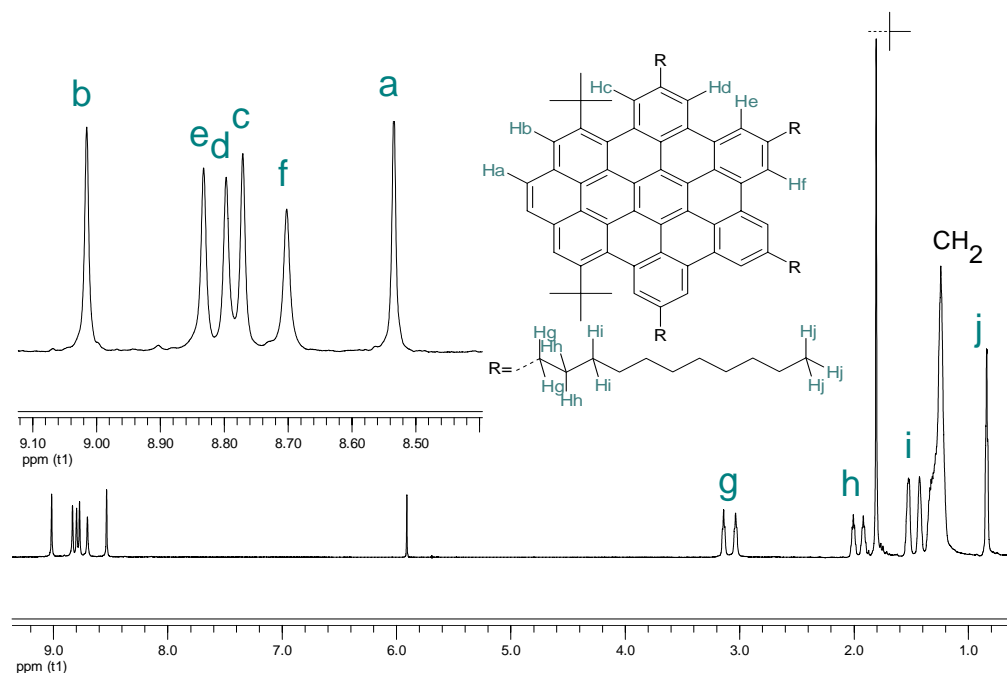


Figure 4-18. ^1H NMR of **4-15**, recorded in tetrachloroethane- d_2 at 100 °C (500 MHz)

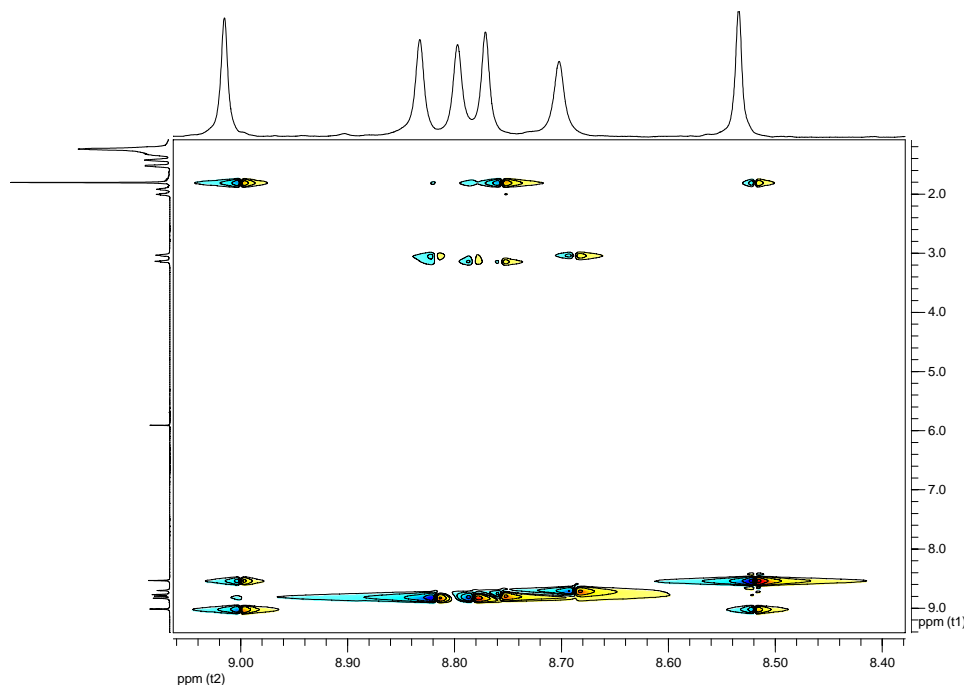


Figure 4-19. NOESY of **4-15**, recorded in tetrachloroethane- d_2 at 100°C (500 MHz)

The selective oxidation of the “zigzag” edge to its corresponding diketo-structure **4-16** was achieved by the same oxidative method as for six-fold *tert*-butyl TBO **3-12**, using ruthenium (III) chloride (RuCl_3) and sodium periodate (NaIO_4) under very mild conditions. The yield of this reaction was 30%, which is slightly larger (2%) as the yield of 1,6-di-*tert*-butyl-8,11,14,17-tetra(*t*-butyl)tetrabenzo[*bc,ef,hi,uv*]ovalene-3,4-dione (**3-13**). **4-16** showed good solubility in common organic solvents, due to the presence of long alkyl chains. The characterization was finalized by MALDI-TOF mass spectrometry and NMR spectroscopy. Experimentally determined and calculated m/z ratios agree perfectly with predictions for the synthesized compound **4-16**, within the range of accuracy of the instrument.

The ^1H NMR as well as H,H COSY and NOESY of **4-16** were recorded in tetrachloroethane- d_2 at 100 °C. Figure 4-20 shows that the two proton resonances, H_c , are shifted to lower ppm, similar to **3-13** which has only *tert*-butyl groups in the periphery. Analysis of H,H COSY (Figure 4-21) and NOESY allows to identify all protons of aromatic and aliphatic regions.

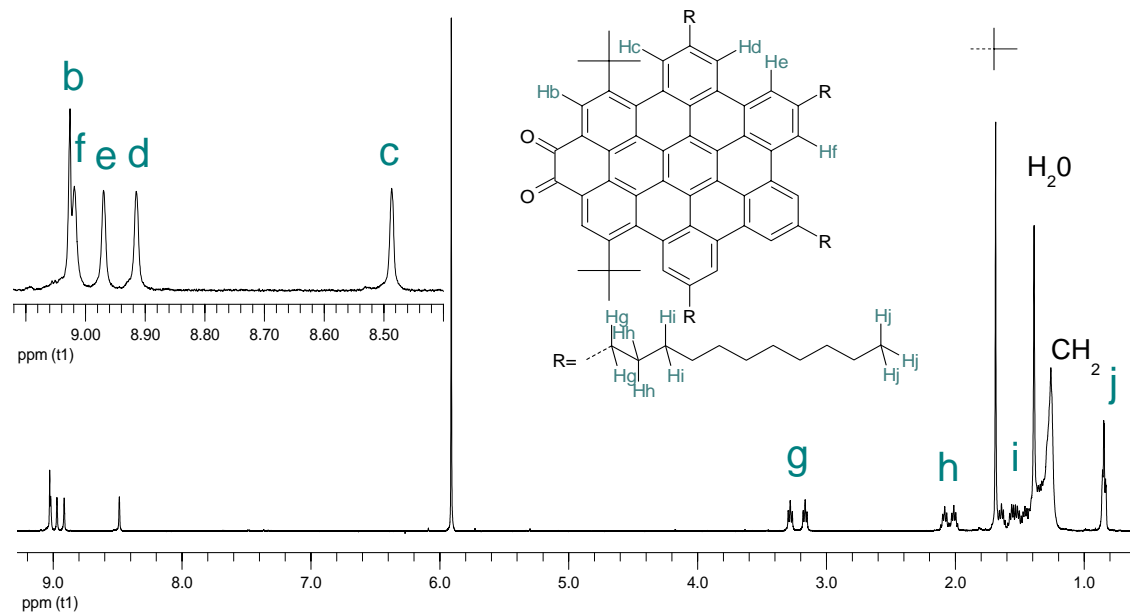


Figure 4-20. ^1H NMR of **4-16**, recorded in tetrachloroethane- d_2 at 100 °C (500 MHz)

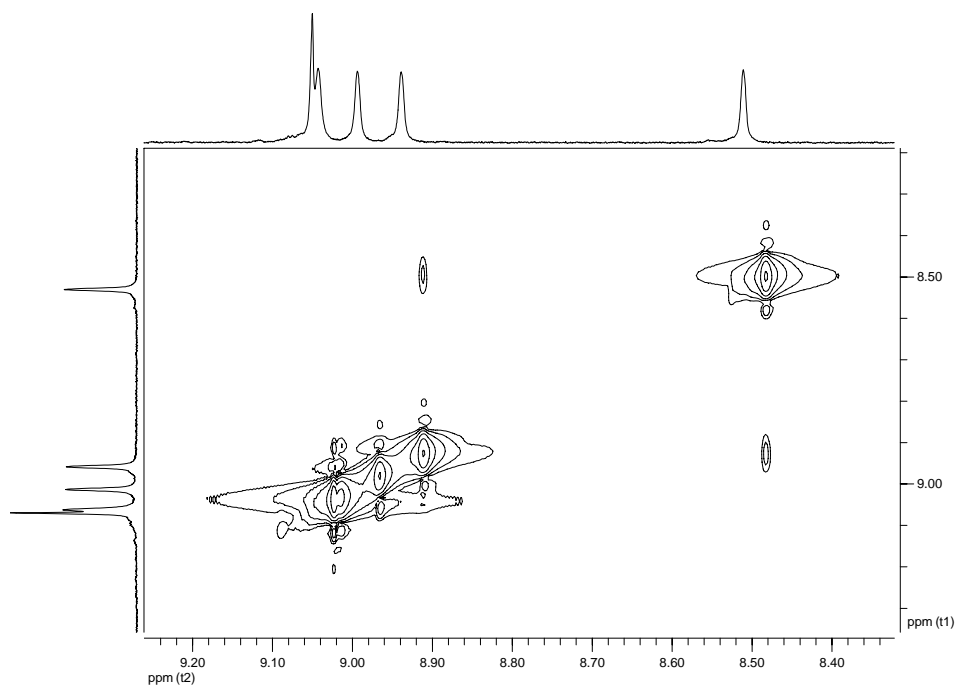


Figure 4-21. H,H COSY of **4-16**, recorded in tetrachloroethane- d_2 at 100 °C (500 MHz)

The resonances of two other protons, H_b and H_f appear next to each other, which is probably due to the absence of a strong distortion from planarity of the aromatic core by

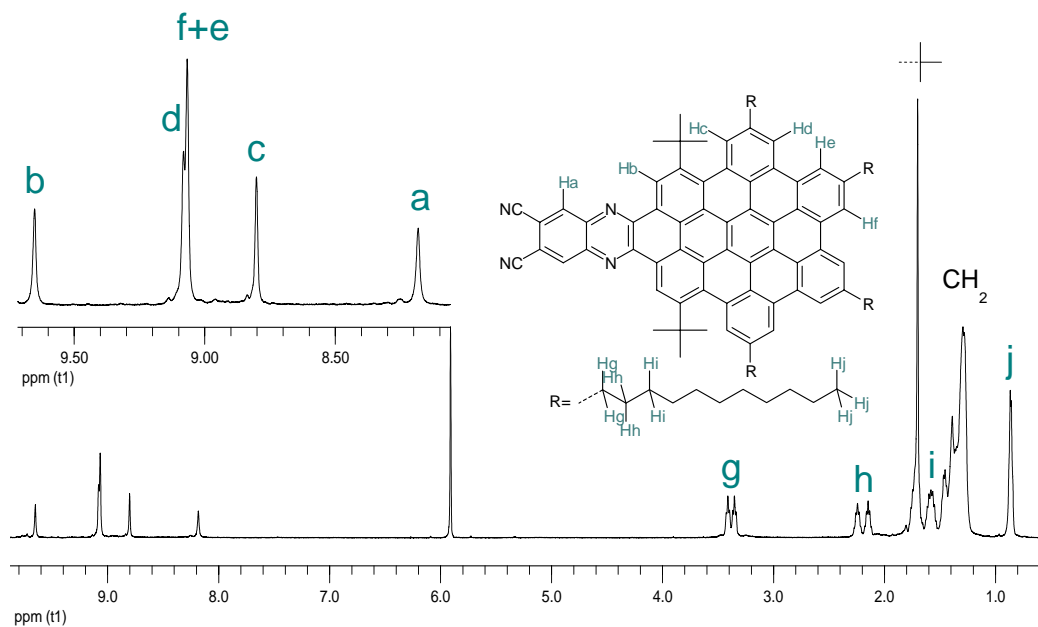


Figure 4-23. ^1H NMR of **4-17**, recorded in tetrachloroethane- d_2 at 100 °C (500 MHz)

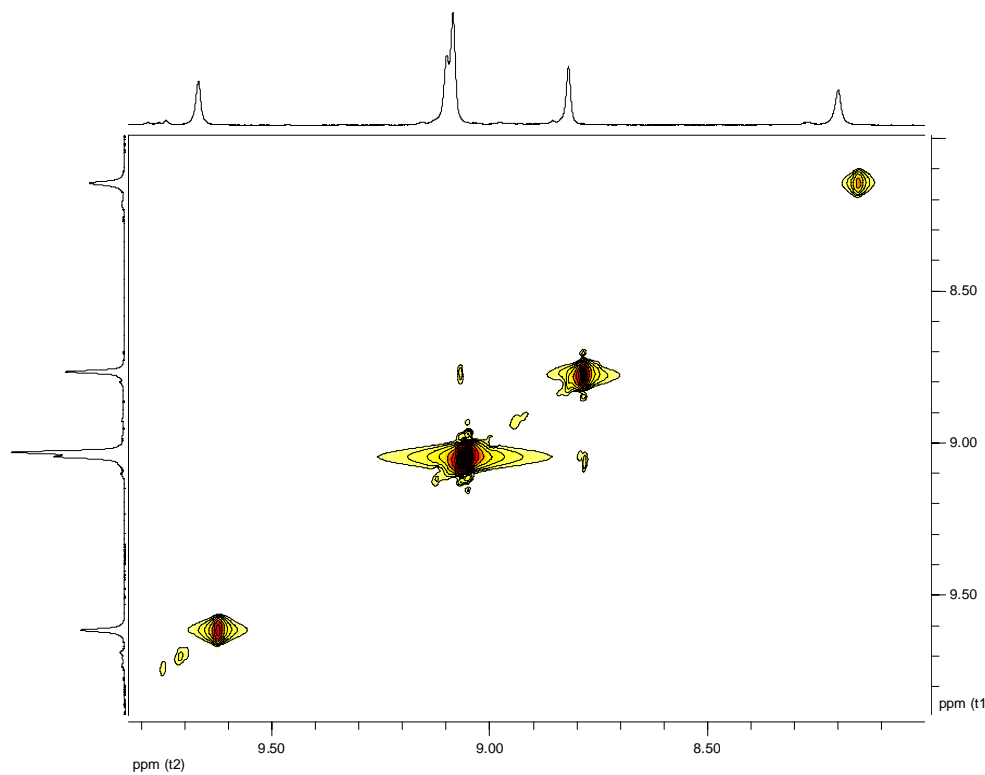


Figure 4-24. H,H COSY (right) of **4-17**, recorded in tetrachloroethane- d_2 at 100 °C (500 MHz)

To form metal-ion-containing phthalocyanine, cyclotetramerisation of **4-17** was performed in a high boiling solvent - quinoline in the presence of urea and Cu(II) salt (Figure 4-25). Purification was accomplished by column chromatography with the mixture of two solvents (DCM:THF=10:1). Thus, the second largest known 1,6-di-*tert*-butyl-8,11,14,17-tetra-*n*-dodecyl-tetrabenzo[*jk,mn,pq,st*]benzo[1,2-*a*]pyrazine[2,3-*d*]ovalenocyanine (**4-18**) was obtained in 7% yield (30 mg), which is the same range as for **4-10**.

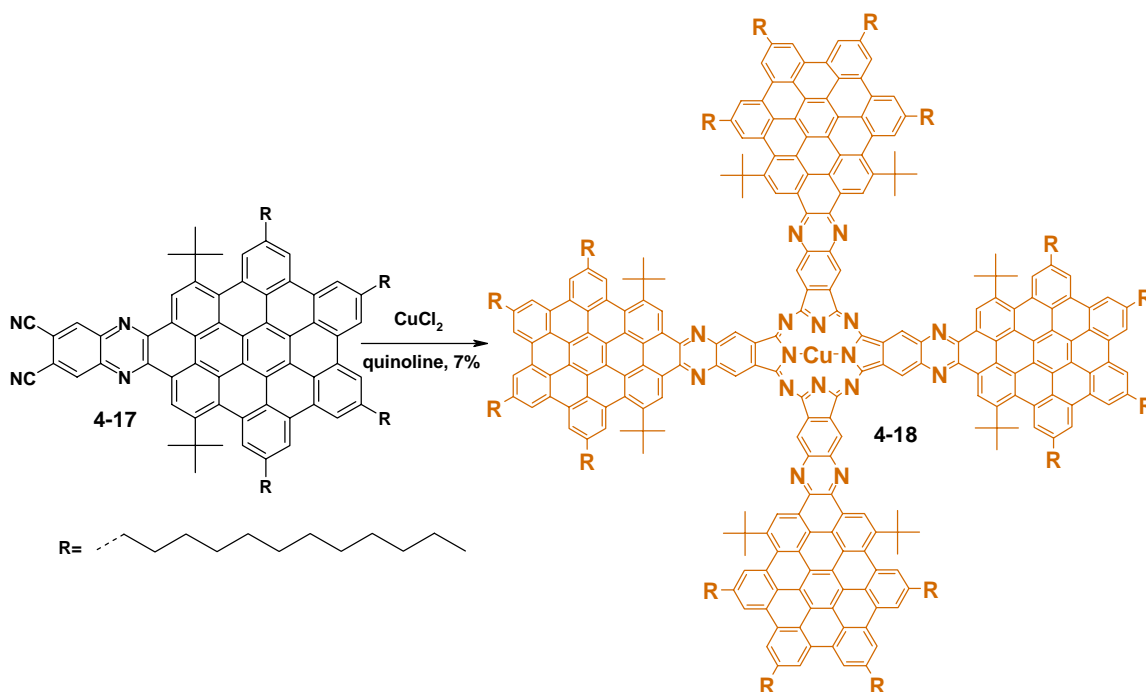


Figure 4-25. Synthetic route to **4-18**

Phthalocyanine **4-18** showed good solubility in common organic solvents, due to the solubilising alkyl-chains. However, the distortion from planarity of the aromatic core by bulky *tert*-butyl groups is still present (see Figure 4-26, left), which is probably suppressing self-aggregation as in the case of **4-10**. Without any substitution such phthalocyanine derivative would remain planar, which is known for CuPc.

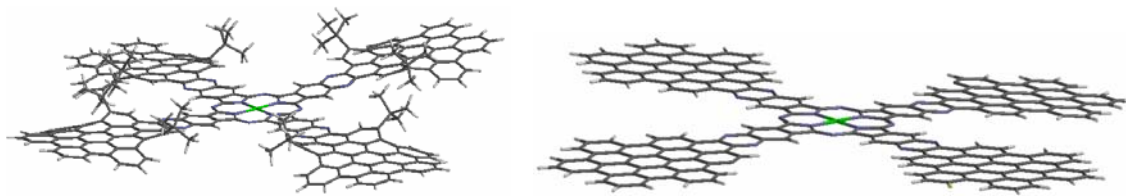


Figure 4-26. Minimized (with molecular mechanics force field available as a part of the Spartan package) structures of phthalocyanines: without *n*-dodecyl alkyl chains, which can serve as a model of **4-18** (left) and without any substitutions (right)

4.4.2 Characterization of second extended Pc

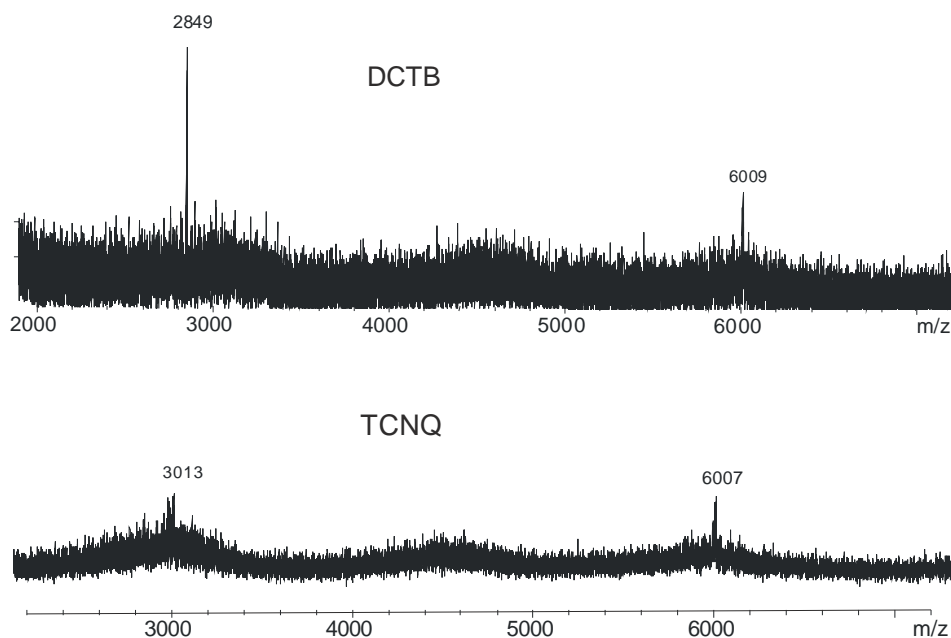


Figure 4-27. MALDI-TOF-mass-spectrum of **4-18**, using different matrixes

MALDI-TOF-mass measurements were done in a solid state, using *trans*-2-[3-(4-*tert*-butylphenyl)-2-methyl-2-propenylidene]malononitrile (DCTB) and 7,7,8,8-tetracyanoquinodimethane (TCNQ) as a matrixes. MALDI-TOF-mass-spectra, which are shown in Figure 4-27, have an expected peak at 6007 (6009) Da. The other peak at 3013 (2849) Da belongs to the double-charged molecular ion as it was also observed in the case of **4-10**. The lower laser intensity in both measurements was applied with aim to decrease fragmentation (cleavage of alkyl chains as was seen for **4-10**). However, the

quality of the spectra suffered dramatically. Mass measurements were also performed in solutions using Dithranol as a matrix since **4-18** possess good solubility in common organic solvents. However, no peaks of the final product were found.

It is also interesting to compare spectroscopic properties of both synthesized phthalocyanines. Thus, absorption spectra were recorded for the same concentrations of phthalocyanines **4-10** and **4-18** and are shown in Figure 4-28. There are two characteristic bands for **4-18** (Figure 4-28, orange line): the Q-band is found at 874 nm and the B-band at 379 nm along with bands originating from **3-18**. A small bathochromic shift of 5 nm is observed as compared to phthalocyanine **4-10**, which is, probably, due to the relatively weak donor effect of dodecyl chains. The weak absorption band at 780 nm belongs to a vibrational overtone of Q-band of **4-18**, which is also detected for **4-10**. Both spectra are well matched, which could be an indirect structure proof.

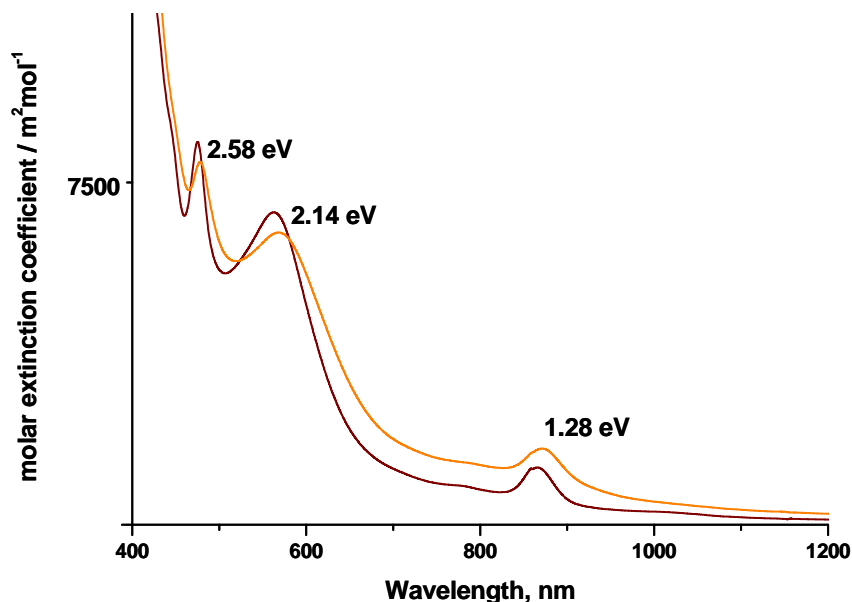


Figure 4-28. UV/Vis-spectra of the two largest phthalocyanine derivatives: **4-10** and **4-18** (orange line)

4.4.3 DSC and TGA

Differential scanning calorimetry measurements were performed in the temperature range from -150 °C to 220 °C with the rate 10 °C/min. First heating of **4-18** showed two

potential phase transitions. However, these transitions do not occur during cooling or second heating. Hence, these transitions are due to the reorganization of *n*-dodecyl-chains, and the material does not undergo any phase-transitions after the thermal reorganization of the side chains.

Thermogravimetric analysis revealed that **4-18** is stable up to *ca.* 450 °C. At 450 °C attached alkyl substituents start to decompose.

4.4.4 2D-WAXS

Fibers of the **4-18** were measured using a two-dimensional wide-angle X-ray scattering. The sample was prepared by filament extrusion, i.e. the material was heated up to a phase at which it becomes plastically deformable and is extruded as thin filament by a constant-rate motion of the piston along the cylinder.⁴² The resulting X-ray pattern is shown in Figure 4-29(a). If one compares it to a typical X-ray pattern of, for example, alkyl-substituted HBC (see Figure 4-29(b)) it becomes clear that there is practically no long-range ordering in the system of **4-18**. This is due to a poor self-organization, which has already been observed for other large PAHs.⁴³⁻⁴⁵

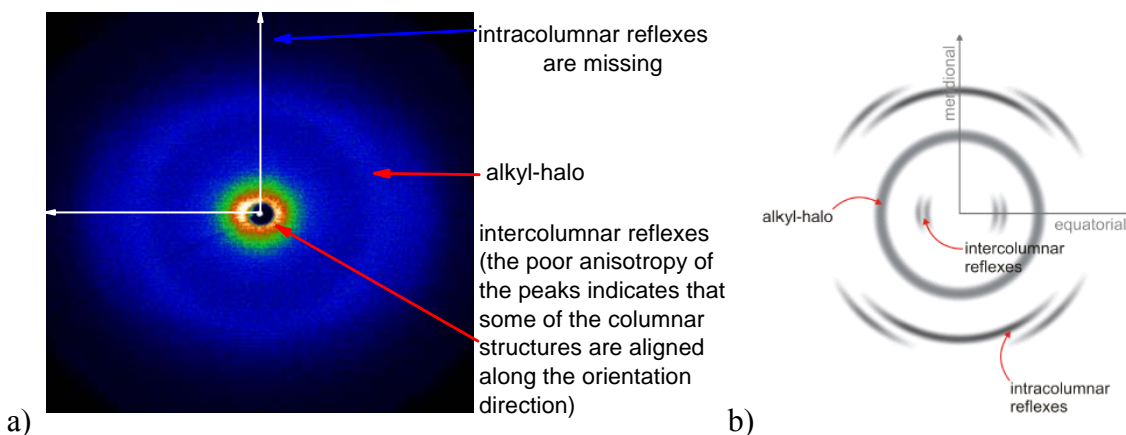


Figure 4-29. (a) X-ray pattern obtained for extruded filaments of **4-18** (b) typical X-ray pattern obtained for extruded filaments of alkyl substituted HBCs: the intercolumnar correlation is identified by the reflexes on the equatorial plane; intracolumnar correlations lead to meridional reflexes.

4.5 Summary

In this chapter, the synthetic route towards the two largest phthalocyanine derivatives was presented. In spite of the huge molecular size of these materials, they demonstrate good solubility in common organic solvents. This is due to probable distortion from planarity of aromatic cores by bulky *tert*-butyl groups (which is the case for **4-10**); as well as the presence of solubilizing long alkyl chains attached to the corona for **4-18**.

The presence of long alkyl chains, however, did not lead to the formation of columnar mesophases. *Tert*-butyl groups, which distort the planarity of the molecules, not only prevent their aggregation but also disfavor the formation of self-organized structures.

Stable, infrared-absorbing Pc dyes can adsorb light of cheap semiconductor (e.g. gallium arsenide) lasers working at 800-1000 nm. Their stability and optical compatibility can be utilized in long-term archival storage devices, such as write-once, read-many-times discs. The absorption band of **4-10** and **4-18** at 869 nm combined with their excellent chemical stability make them attractive materials for such devices.⁴⁶

Many Pcs can be used in photovoltaic cells, electrochromic displays, and photoconductive plates. Compared to smaller planar metal containing phthalocyanines (CuPc), both **4-10** and **4-18** have higher molar extinction coefficient, bathochromically shifted absorption profile and a smaller HOMO-LUMO gap, which can be advantageous for these devices.⁴⁷

4.6 References

1. Braun, A.; Tcherniac, J., *Berichte Der Deutschen Chemischen Gesellschaft* **1907**, 40, 2709-2714.
2. De Diesbach, H., von der Weid, E., *Helvetica Chemica Acta* **1927**, 10, 886-7.
3. Cronshaw, C. J. T., *Nature* **1935**, 135, 996-997.
4. Byrne, G. T.; Linstead, R. P.; Lowe, A. R., *J. Chem.Soc.* **1934**, 1017-1022.
5. Dent, C. E.; Linstead, R. P.; Lowe, A. R., *J. Chem.Soc.* **1934**, 1033-1039.
6. Linstead, R. P.; Lowe, A. R., *J. Chem.Soc.* **1934**, 1031-1033.
7. Linstead, R. P.; Lowe, A. R., *J. Chem.Soc.* **1934**, 1022-1027.
8. Leznoff, C. C.; Hall, T. W., *Tetrahedron Lett.* **1982**, 23, (30), 3023-3026.

9. Thompson, J. A.; Murata, K.; Miller, D. C.; Stanton, J. L.; Broderick, W. E.; Hoffman, B. M.; Ibers, J. A., *Inorg. Chem.* **1993**, 32, (16), 3546-3553.
10. Wohrle, D.; Eskes, M.; Shigehara, K.; Yamada, A., *Synthesis-Stuttgart* **1993**, (2), 194-196.
11. Mckeown, N. B.; Chambrier, I.; Cook, M. J., *J. Chem.Soc. Perkin Trans. 1* **1990**, (4), 1169-1177.
12. Robertson, J. M.; Woodward, I., *J. Chem. Soc.* **1937**, 219-230.
13. Robertson, J. M.; Woodward, I., *J. Chem. Soc.* **1940**, 36-48.
14. Mckeown, N. B., *Phthalocyanine Materials*. University press: Cambridge, 1998.
15. Mason, R.; Williams, G. A.; Fielding, P. E., *J. Chem.Soc. Dalton Trans.* **1979**, (4), 676-683.
16. Ashida, M.; Suito, E., *Journal of Electron Microscopy* **1964**, 13, (1), 50-50.
17. Suito, E.; Ashida, M., *Journal of Electron Microscopy* **1964**, 13, (4), 222-222.
18. Schaffer, A. M.; Gouterma, M.; Davidson, E. R., *Theoretica Chimica Acta* **1973**, 30, (1), 9-30.
19. Orti, E.; Bredas, J. L.; Clarisse, C., *J. Chem. Phys.* **1990**, 92, (2), 1228-1235.
20. Piechocki, C.; Simon, J.; Skoulios, A.; Guillon, D.; Weber, P., *J. Am. Chem. Soc.* **1982**, 104, (19), 5245-5247.
21. Clarkson, G. J.; Hassan, B. M.; Maloney, D. R.; McKeown, N. B., *Macromolecules* **1996**, 29, (5), 1854-1856.
22. Eley, D. D., *Nature* **1948**, 162, (4125), 819-819.
23. Usov, N. N.; Bendersk.Va, *Physica Status Solidi* **1970**, 37, (2), 535-7.
24. Cox, G. A.; Knight, P. C., *Journal of Physics C-Solid State Physics* **1974**, 7, (1), 146-156.
25. Houdayer, A.; Hinrichsen, P. F.; Belhadfa, A.; Crine, J. P.; Marsan, B., *Journal of Materials Science* **1988**, 23, (11), 3854-3860.
26. Schramm, C. J.; Stojakovic, D. R.; Hoffman, B. M.; Marks, T. J., *Science* **1978**, 200, (4337), 47-48.
27. Schramm, C. J.; Scaringe, R. P.; Stojakovic, D. R.; Hoffman, B. M.; Ibers, J. A.; Marks, T. J., *J. Am. Chem. Soc.* **1980**, 102, (22), 6702-6713.
28. Marks, T. J., *Science* **1985**, 227, (4689), 881-889.

29. Heilmeyer, G. H.; Harrison, S. E., *Phys. Rev.* **1963**, 1, (5), 2010-&.
30. Kasuga, K., Mihara, T., Nakao, T., Takahashi, K., *Inorg. Chemica Acta* **1991**, 189, 11-12.
31. Belarbi, Z.; Sirlin, C.; Simon, J.; Andre, J. J., *J. Phys. Chem.* **1989**, 93, (24), 8105-8110.
32. Tomoda, H.; Saito, S.; Shiraishi, S., *Chemistry Letters* **1983**, (3), 313-316.
33. Cammidge, A. N.; Gopee, H., *Chemistry-a European Journal* **2006**, 12, (33), 8609-8613.
34. Assour, J. M.; Harrison, S. E., *Physical Review a-General Physics* **1964**, 136, (5A), 1368-&.
35. Boguslavskii, E. G.; Prokhorova, S. A.; Nadolinnyi, V. A., *Journal of Structural Chemistry* **2005**, 46, (6), 1014-1022.
36. Cook, M. J.; Dunn, A. J.; Daniel, M. F.; Hart, R. C. O.; Richardson, R. M.; Roser, S. J., *Thin Solid Films* **1988**, 159, 395-404.
37. Cook, M. J.; Dunn, A. J.; Howe, S. D.; Thomson, A. J.; Harrison, K. J., *Journal of the Chemical Society-Perkin Transactions I* **1988**, (8), 2453-2458.
38. Kudrevich, S. V.; vanLier, J. E., *Coordination Chemistry Reviews* **1996**, 156, 163-182.
39. Saito, T.; Sisk, W.; Kobayashi, T.; Suzuki, S.; Iwayanagi, T., *J. Phys. Chem.* **1993**, 97, (30), 8026-8031.
40. Kastler, M. *Discotic Materials for Organic Electronics*. Johannes Gutenberg-Universität, Mainz, 2006.
41. Takada, J.; Awaji, H.; Koshioka, M.; Nakajima, A.; Nevin, W. A., *Appl. Phys. Lett.* **1992**, 61, (18), 2184-2186.
42. Pisula, W. Control of the Supramolecular Long-Range Self-Organization of Polycyclic Aromatic Hydrocarbons for Device Applications. Johannes Gutenberg-Universität Mainz, 2005.
43. Tomovic, Z. New Discotic Liquid Crystals Based on Large Polycyclic Aromatic Hydrocarbons as Materials for Molecular Electronics. Johannes Gutenberg-Universität, Mainz, 2004.

44. Simpson, C. *Nanoscale Polycyclic Aromatic Hydrocarbons-Synthesis and Characterization*. Johannes Gutenberg-Universität, Mainz, 2003.
45. Jung, S. H.; Pisula, W.; Rouhanipour, A.; Räder, H. J.; Jacob, J.; Müllen, K., *Angew. Chem., Int. Ed.* **2006**, 45, (28), 4685-4690.
46. Emmelius, M.; Pawlowski, G.; Vollmann, H. W., *Angewandte Chemie-International Edition in English* **1989**, 28, (11), 1445-1471.
47. Schmidt-Mende, L.; Fechtenkötter, A.; Müllen, K.; Moons, E.; Friend, R. H.; MacKenzie, J. D., *Science* **2001**, 293, (5532), 1119-1122.

4 From Pyrene to the Largest Phthalocyanines

5 From Pyrene towards Phenanthroline Ligands for Metal Complexation

5.1 Ruthenium (II) Complexes

In green plants and purple bacteria, photosynthetic units harvest light to induce electron transfer to finally initiate consecutive chemical conversion.¹ Even though photosynthesis converts only 0.02-0.05% of the incident solar energy of about 1022 kJ per year into biological material, this is 100 times more than the food needed for mankind.²

The possibility of light harvesting explains a considerable interest in ruthenium polypyridyl complexes.³ Indeed, ruthenium based dyes have found wide application in the manufacturing of solar cells based on TiO₂, with the famous N3 dye as an example, see Figure 5-1. These devices have high photon-to-current conversion efficiencies, up to 10% under AM 1.5 solar conditions.⁴

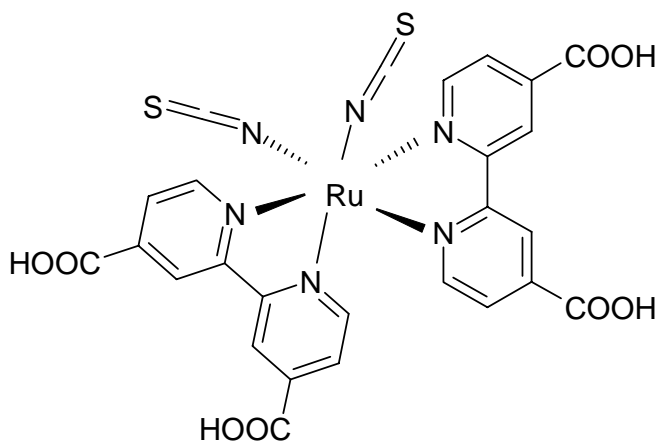


Figure 5-1. Ruthenium dye N3

The photophysical properties of the dye shall be tuned for a particular application. This can be achieved by mixing in a single dye molecule anchoring or electron donating groups. For example, good π -acceptor ligands bearing a low-lying π^* orbital can lead to red-shifting of the metal-to-ligand charge-transfer (MLCT) absorption bands.^{5,6} In dyads, where donor and acceptor components are connected by appropriate bridging groups,

intercomponent energy or electron-transfer processes can be triggered by light excitation. Dyads with rigid bridges have the advantage that energy-/electron-transfer can be studied more systematically, due to precise structural definition. Therefore, dyads based on fully aromatic fused-ring bridging ligands are intensively studied; typical ligands of this type are the azaaromatic systems.⁷⁻¹²

LAUNAY *et al.*^{7, 13} studied rigid and conjugated dimetallic systems, with fully conjugated tetrapyrrophenazine (tpphz) **5-1** ligands (Figure 5-2). Known intermetallic distances allowed for accurate measurements of the rate constants of electron and energy transfer processes.

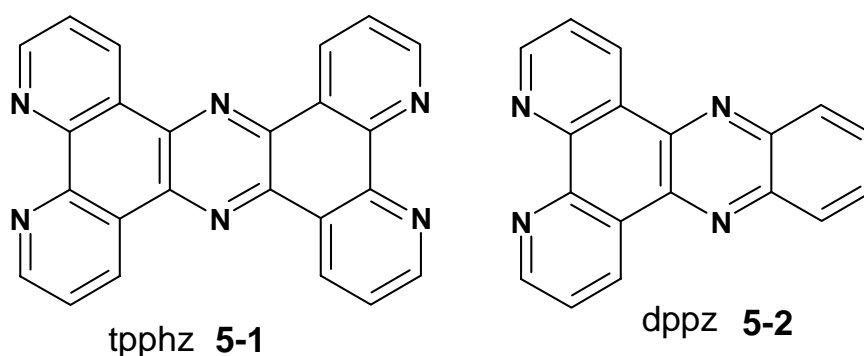


Figure 5-2. Structures of rigid ligands

Another intensively studied ligand is dppz **5-2** (dppz=dipyridophenazine), which is used to form $[L_2M(dppz)]^{2+}$ (L=bpy, phen; M= RuII, OsII) or $[(4-Mepy)(CO)_3Re^I(dppz)]^+$ complexes. These compounds are used as molecular light switches for DNA¹⁴⁻²⁰ and micelle solutions²¹ or for the study of fast electron transfer through DNA.²²

The rigid bridging groups do not only assist in determining structural information, but their nature also significantly affects the electron- and energy-transfer rates. Using an appealing similarity, these bridges are sometimes called “molecular wires”.²³

MACDONNELL *et al.*^{12, 24} presented a detailed photophysical study of homonuclear tatpp **5-3** complexes of Ru(II) **3-22** and Os(II) **5-4** (Figure 5-3).

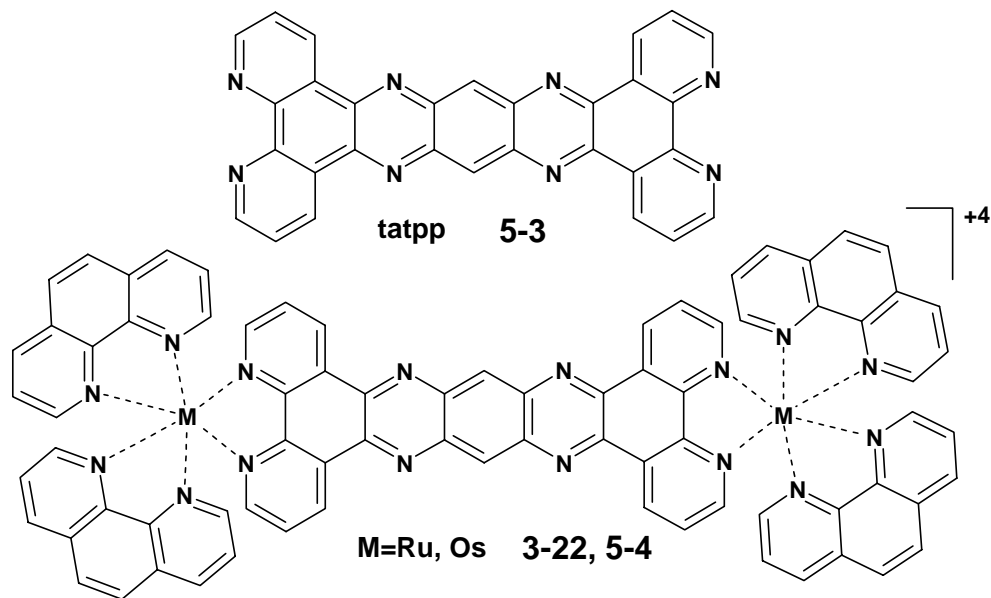


Figure 5-3. Chemical structures of **tatpp 5-3** and its complexes with Ru(II) **3-22** and Os(II) **5-4**

It was shown that for a number of bridging ligands, the photophysical behavior of binuclear Ru(II) and Os(II) complexes is qualitatively similar. The main differences between the Ru(II) and Os(II) systems are quantitative, particularly in the metal-to-ligand charge-transfer (MLCT) state lifetime being shorter for the Os(II) system because of lower excited-state energy (energy-gap law).

However, for polyquinoxaline bridges, this holds only for complexes of the shortest member of the series, **tpphz 5-1**.^{10, 12, 25} When longer **tatpp** systems, e.g. **5-3**, are considered, the behavior of the Ru(II) complex **3-22** differs dramatically from that of the Os(II) one.

Even larger, polyaromatic bridges provide relatively strong intercomponent electronic coupling. Therefore, they are very convenient connectors for the construction of polynuclear metal complexes, especially for studying long-range energy- and/or electron-transfer processes.²⁶⁻²⁸ A bridging ligand of this type, **dppz(11-11')dppz 5-5**, was studied by NATARAJAN *et al.*²⁹ and is shown in Figure 5-4. This is not a single example, however: polynuclear Ru(II) complexes of polypyridyl ligands similar to **5-6** and **5-7** are now actively studied both by chemists and photophysicists.³⁰⁻³⁵

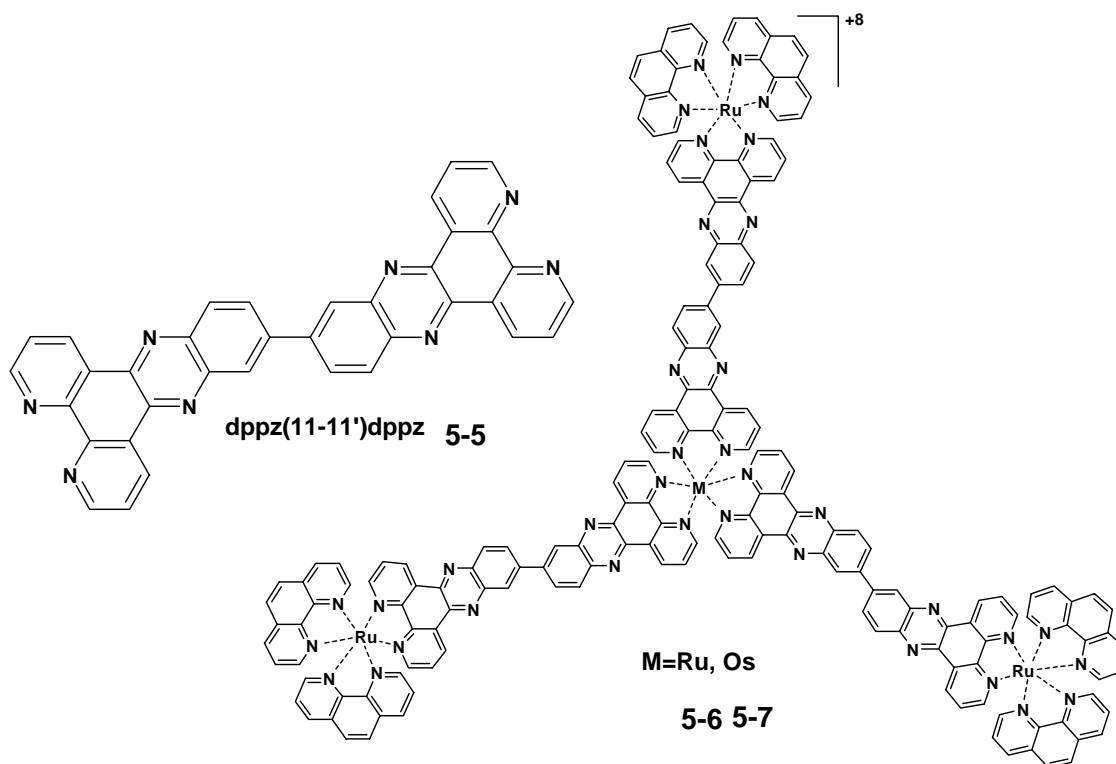
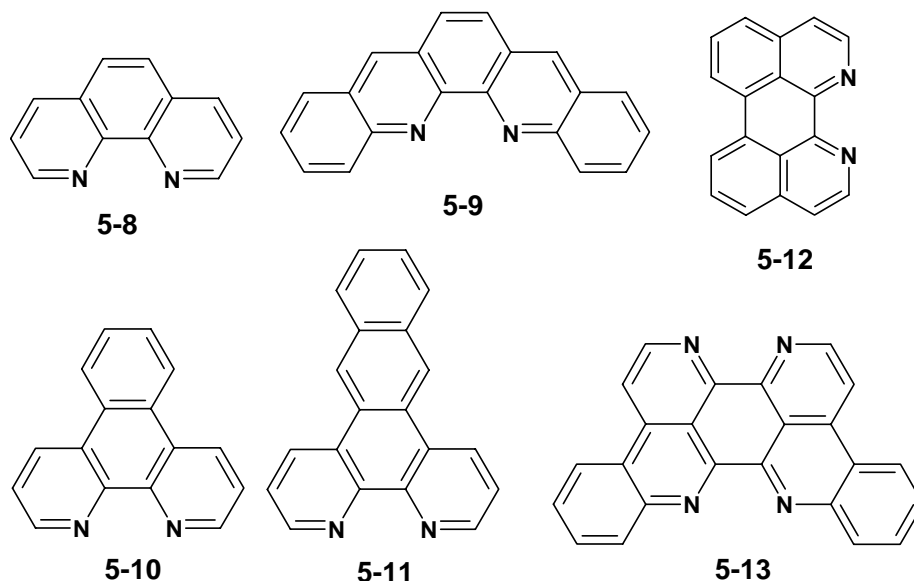


Figure 5-4. Chemical structures of a bridging ligand **5-5** and its corresponding complexes **5-6** and **5-7**

In addition to elongation of bridging ligands, THUMMEL *et al.*³⁶ performed modifications of the phenanthroline (phen) ligand **5-8**, increasing the π -delocalization while retaining the C_2 -symmetry. This was accomplished by benzo fusion, leading to the benzo- and naphtho-fused phens **5-9**³⁷⁻³⁹ and **5-10**^{40, 41}, as well as the dibenzo-fused phen **5-11**⁴² and 1,12-diazaperylene (DAP, **5-12**)^{43, 44}, all shown in Figure 5-5.

Among large ligands, a special place has the biological compound eilatin, **5-13**, Figure 5-5, which can serve as a bridging ligand with nonequivalent binding sites for Ru(II).⁴⁵⁻⁴⁹ Eilatin combines several unique features: (a) large, planar fused-aromatic surface; (b) two distinct binding sites, a bpy-type “head” and a biq-type “tail” (biq) 2,2'-biquinoline; and (c) a low-lying π^* orbital, which renders it as an exceptionally good π -acceptor ligand.⁴⁸

Figure 5-5. Modified structures of 1,10-phenanthroline **5-8**

Apart from ruthenium (II), copper(II) complexes are intensively studied, mostly due to their biological relevance.⁵⁰⁻⁵³ They can also be immobilized on electrodes in order to obtain new catalytically active surfaces.⁵⁴ Copper (II) ion forms various oxygen-activating copper-diimine complexes of 2,2'-bipyridine and 1,10-phenanthroline and their derivatives. In transition metal complexes, the coordination of the metal ion and steric as well as electronic effects provided by the ligand play a critical role in the catalytic performance. The coordination of the central ion and the electronic effects of the complexes can be altered by adding different substituents to the ligand. The electron transfer reactions of Cu(I/II) species and the coordination geometry of Cu-diimine complexes have been recently reviewed by RORABACHER⁵⁵.

Ideally, an efficient light-harvesting material should combine in one molecule both photophysical properties of metal complexes (e.g. efficient light absorption) with charge conducting properties of self-assembled PAHs, described in Chapter 3. Metal binding can be viewed as a new synthetic way to construct extended PAHs with or without heteroatoms or/and metal centers.⁵⁶

In the following chapter the synthesis and characterization of three new phenanthroline ligands suitable for metal complexation are presented.

5.2 Synthesis of Phenanthroline Ligands

Chapters 3 and 4 demonstrated that the quinoxaline-ring formation reaction is an appropriate method for the synthesis of extended PAHs with heteroatoms in the aromatic core. In addition, the synthesis of two dicyano-derivatives **4-9** and **4-17**, showed that this reaction can be successfully used for PAH functionalization. In this chapter, the same method will be employed to synthesize three new phenanthroline ligands suitable for metal binding.

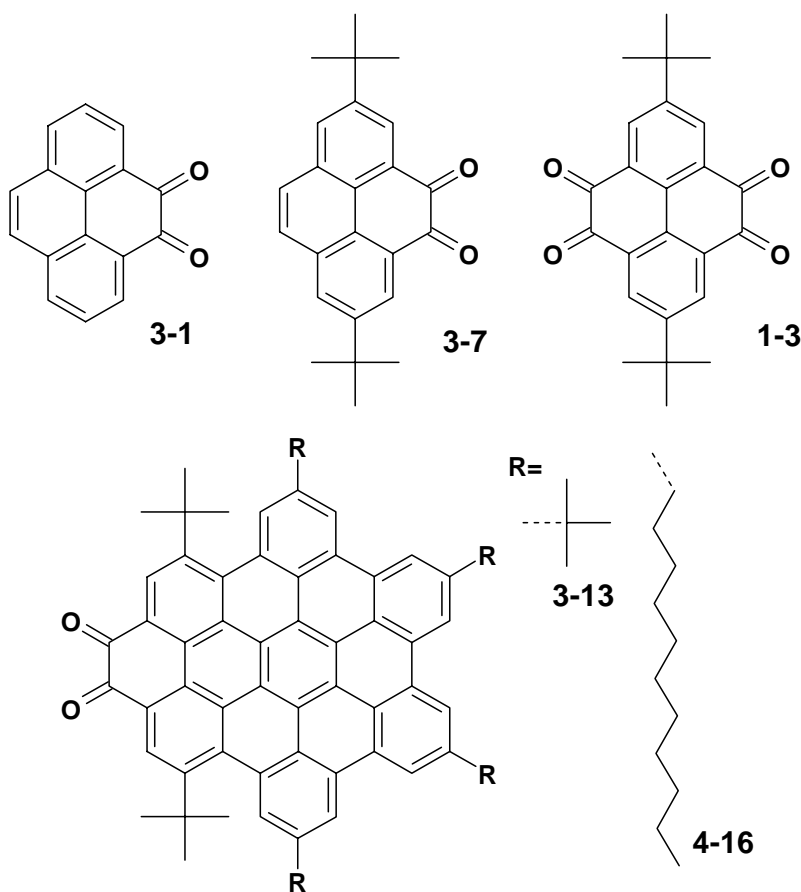


Figure 5-6. Choice of the 1,2-dicarbonyl-derivatives for the synthesis of the phenanthroline ligands

The quinoxaline ring-formation reaction is a condensation between *o*-diamines and a 1,2-dicarbonyl.⁵⁷ In previous chapters synthesis of five different dicarbonyl-derivatives was described: 2,7-di-*tert*-butyl-pyrene-4,5-dione **3-7**, 2,7-di-*tert*-butyl-pyrene-4,5,9,10-tetraone **1-32**, pyrene-4,5-dione **3-1**, **3-13** and **4-16** (Figure 5-6). It has been shown in

Chapter 3 that pyrene-4,5-dione **3-1** does not give stable derivatives; hence, it was not considered as a possible ligand building block. At an initial stage **4-16** was also excluded, since **3-13** has similar capabilities for ligand formation. Three other dicarbonyl molecules (**3-7**, **1-32** and **3-13**) were considered as potential building blocks.

The suitable *o*-diamine derivative, 5,6-diamino-1,10-phenanthroline⁵⁸ **5-16** was obtained from commercially available phendione **5-14** (Figure 5-7). A mixture of **5-14**, $\text{NH}_2\text{OH}\cdot\text{HCl}$ and BaCO_3 was refluxed in ethanol for 16 h. After necessary workup, phenodioxiime **5-15** was obtained in 32% yield. The slurry of **5-15** and Pd-C (10%) in ethanol was heated to reflux; then a solution of $\text{N}_2\text{H}_4\cdot\text{H}_2\text{O}$ in ethanol was added and the resulting mixture refluxed for 16 h. The resulting solid was filtered and 5,6-diamino-1,10-phenanthroline **5-16** was produced in 72% yield.

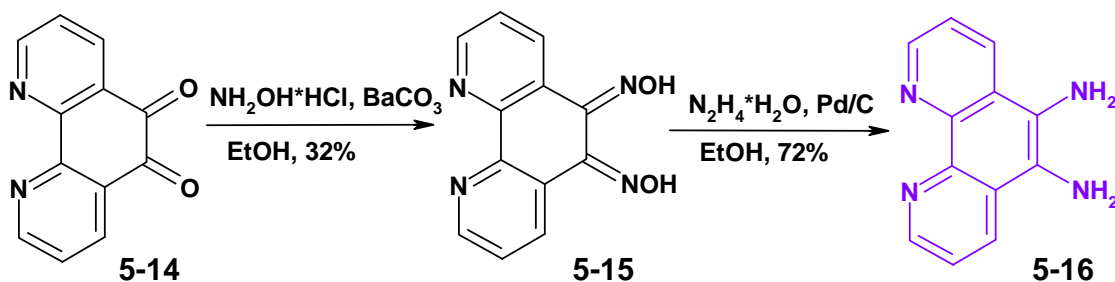


Figure 5-7. Synthetic route towards 5,6-diamino-1,10-phenanthroline **5-16**

Dried **5-16** was treated with 2,7-di-*tert*-butylpyrene-4,5-dione **3-7** in dry pyridine under inert atmosphere overnight. The yellow solid was filtrated, washed with pyridine and gave 66% yield of the desired product **5-17** (Figure 5-8). Further, **3-13** was refluxed in dry pyridine with **5-16** overnight. The final compound **5-18** was furnished in 57%.

2,7-Di-*tert*-butyl-pyrene-4,5,9,10-tetraone **1-32** was treated with 5,6-diamino-1,10-phenanthroline **5-16** in reflux pyridine for 16 h. The desired product **5-19** was obtained in 56% yield.

Products **5-17** and **5-18** are soluble in common organic solvents. Their characterization was performed using standard analytical techniques (MALDI-TOF-mass spectrometry, NMR and UV/vis spectroscopy). Since **5-19** did not show good solubility, its characterization by MALDI-TOF was done in a solid state using DCTB as a matrix.

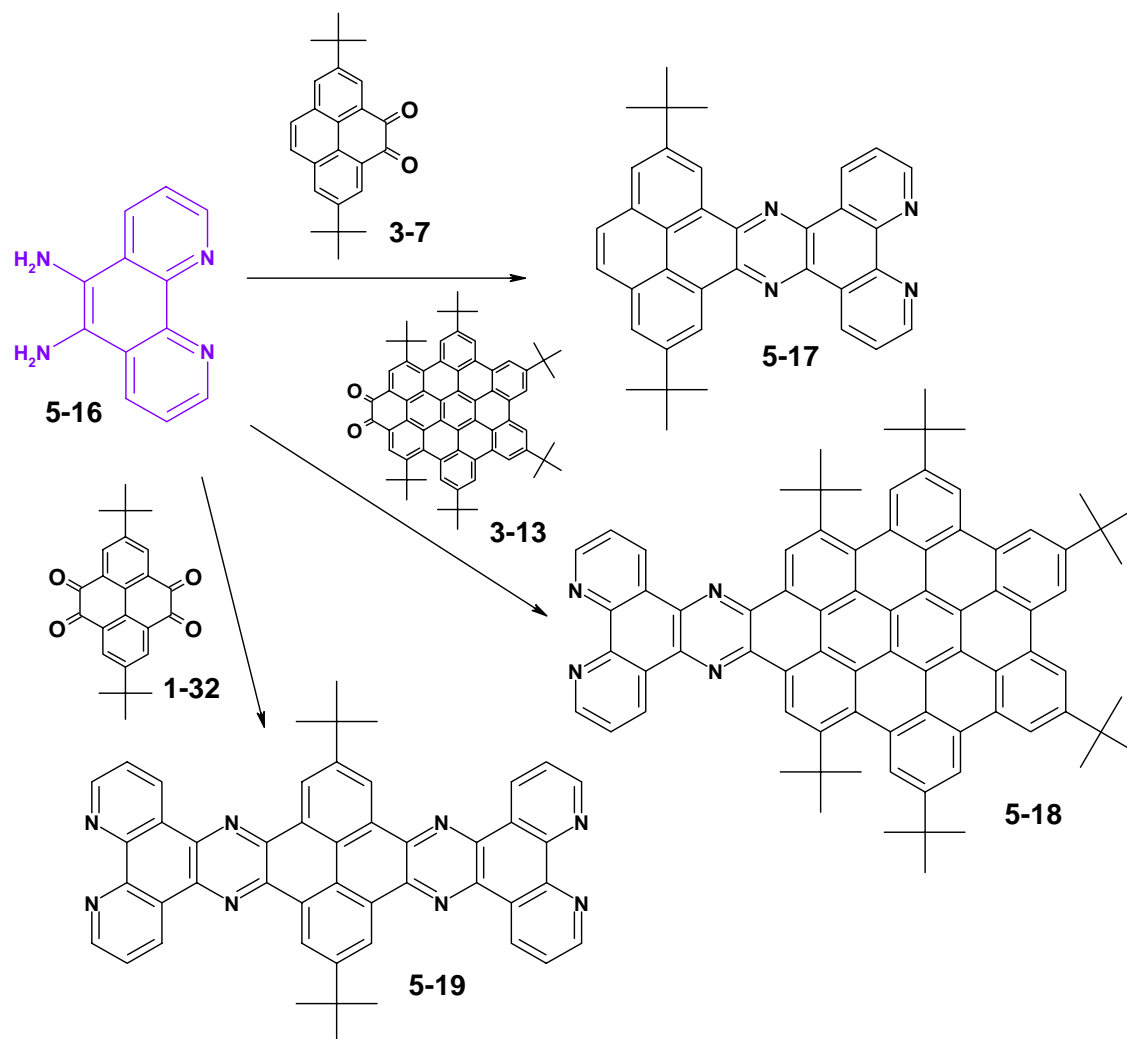


Figure 5-8. Synthetic approach towards the phenanthroline ligands

Figure 5-9 shows the ^1H NMR spectrum of **5-17**, recorded at 100°C in tetrachloroethane- d_2 . The aromatic region has six proton resonances, which can be assigned by using H,H COSY (Figure 5-10) and NOESY measurements. H,H COSY shows that the resonances of four protons, H_d and H_c , appear as one broad peak in the ^1H NMR spectra at 9.81 ppm, since they have similar positions with respect to the pyrazine ring. Two proton resonances from the “zigzag” edge could be identified at higher field at 8.02 ppm. Selected conditions of NMR measurements led to suppression of signals from phenanthroline protons. Thus, they appeared as broad singlets.

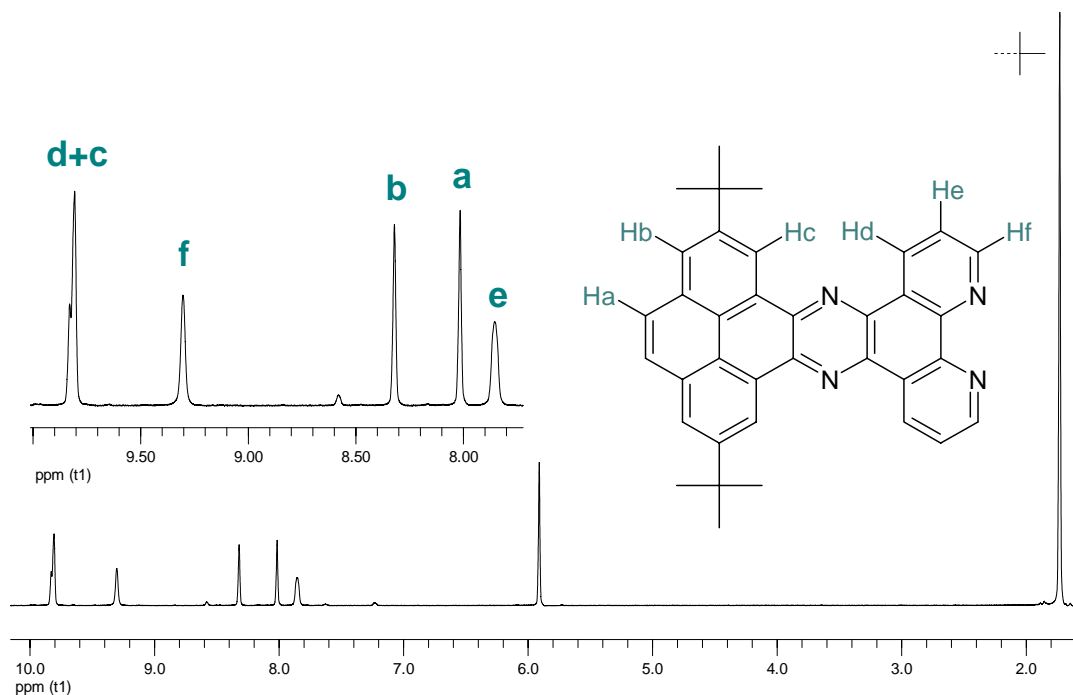


Figure 5-9. ^1H NMR of **5-17**, recorded in tetrachloroethane- d_2 at 100 °C (500 MHz)

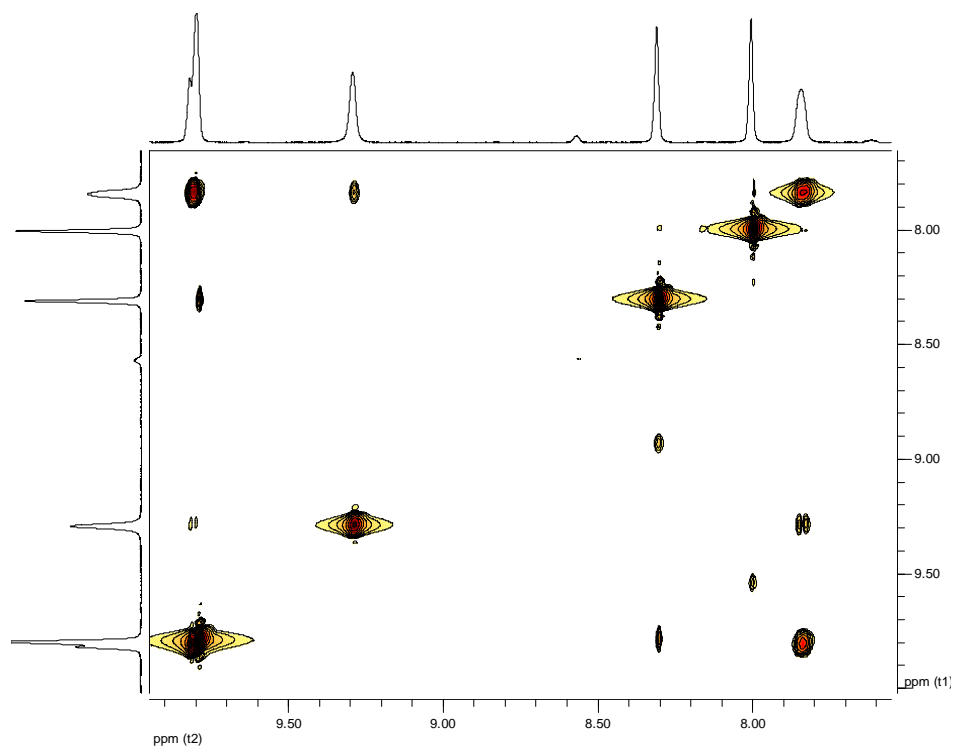


Figure 5-10. ^1H , ^1H COSY of **5-17**, recorded in tetrachloroethane- d_2 at 100 °C (500 MHz)

The ^1H NMR spectrum of **5-18** was recorded at 100 °C in tetrachloroethane- d_2 and is shown in Figure 5-11. The aromatic region has 10 proton resonances from the HBC moiety, which could also be assigned by using H,H COSY and NOESY experiments. Two proton resonances H_d are shifted towards the lower field (10.23 ppm), which is typical for PAHs with pyrazine rings, see also Chapters 3 and 4.

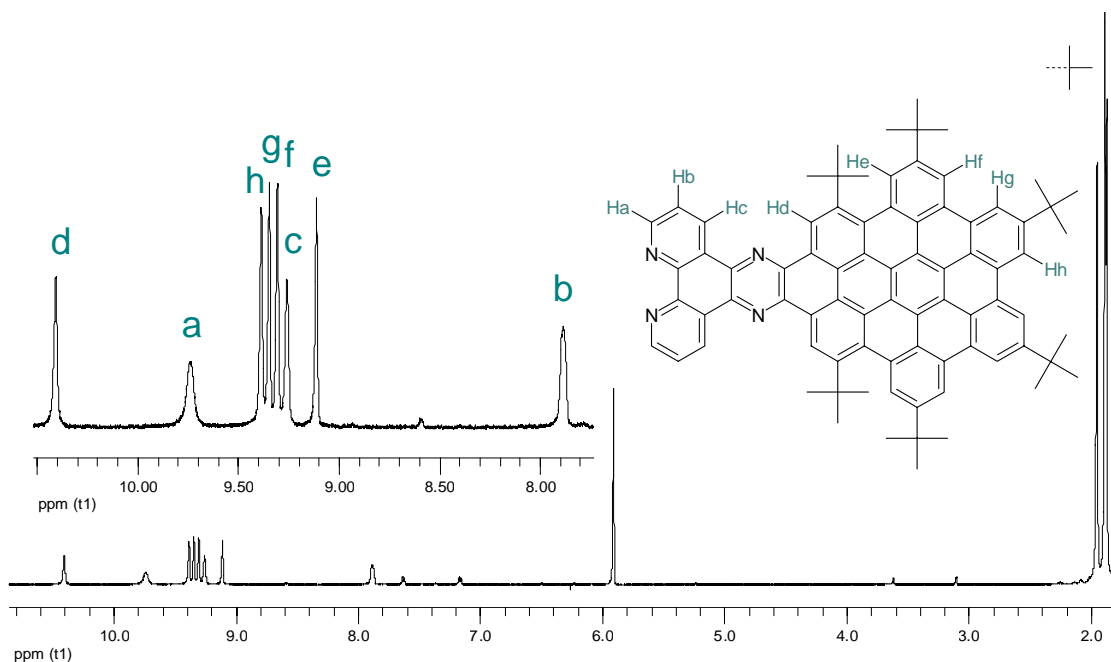


Figure 5-11. ^1H NMR of **5-18**, recorded in tetrachloroethane- d_2 at 100 °C (500 MHz)

MALDI-TOF-mass spectrum of **5-19** is shown in Figure 5-13. Experimentally determined and calculated m/z ratios agree well within the range of the accuracy of the instrument.

The ^1H NMR spectrum of **5-19** (Figure 5-14) shows that four proton resonances H_a are split in two different peaks at lower (10.52 ppm) and higher (9.28 ppm) fields. Nine proton resonances of *tert*-butyl groups could be identified as two different peaks. H,H COSY and NOESY (Figure 5-15) confirm these conclusions.

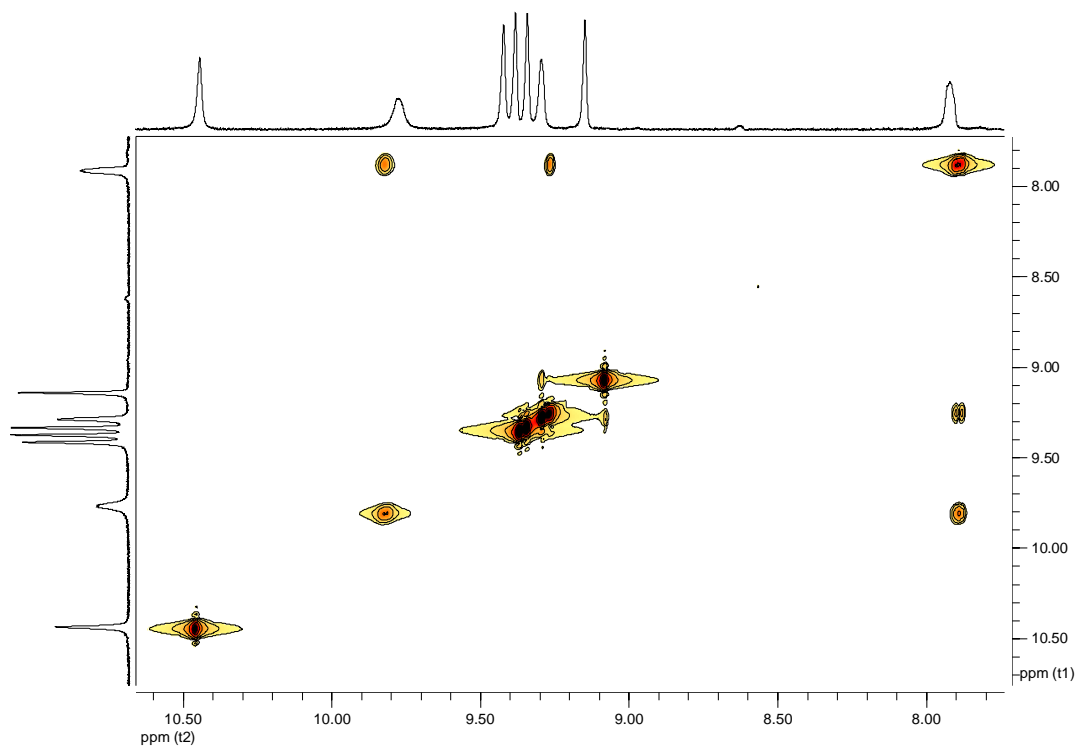


Figure 5-12. ^1H , ^1H COSY of **5-18**, recorded in tetrachloroethane- d_2 at 100 °C (500 MHz)

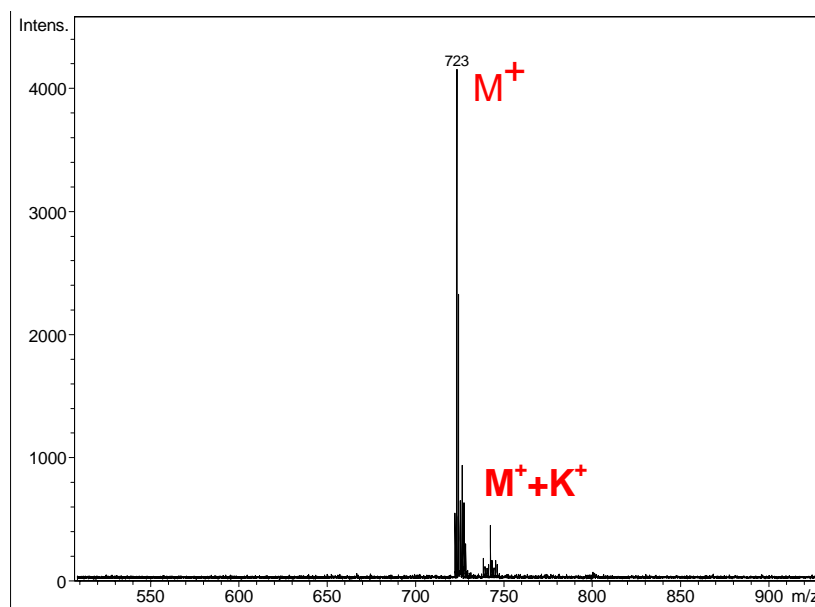


Figure 5-13. MALDI-TOF-mass spectrum of **5-19** (DCTB as a matrix)

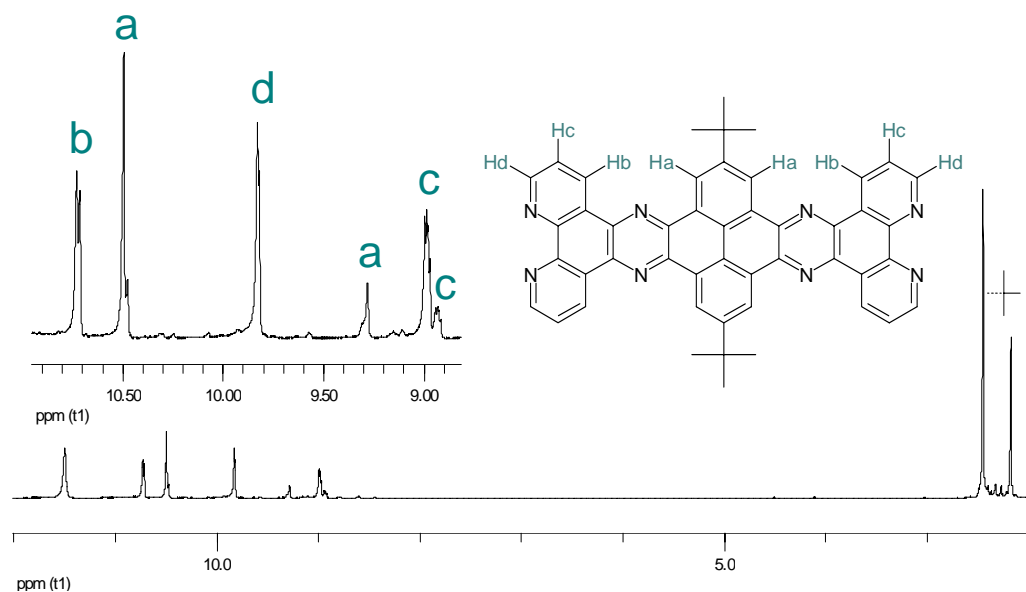


Figure 5-14. ¹H NMR, NOESY of **5-19**, recorded at 65 °C in CF₃COOD (500 MHz)

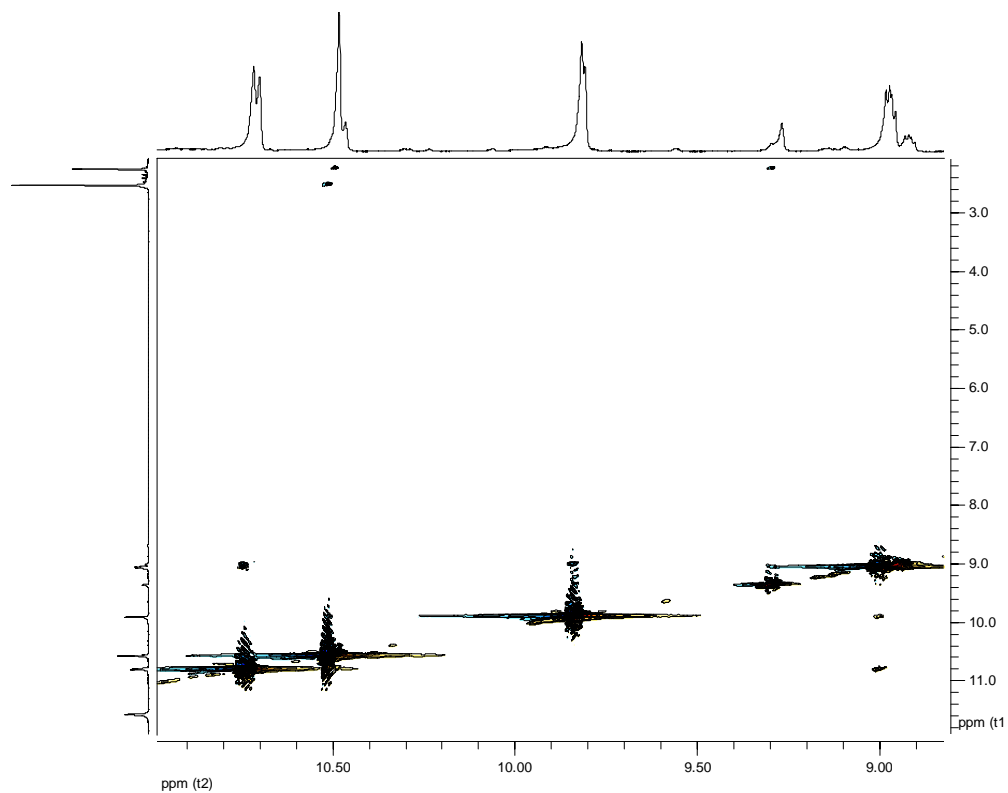
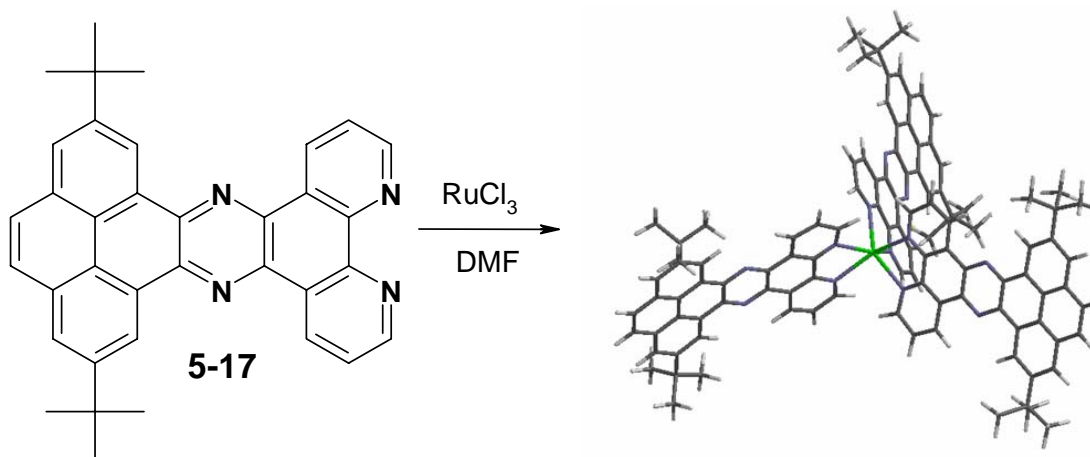


Figure 5-15. NOESY of **5-19**, recorded at 65 °C in CF₃COOD (500 MHz)

5.3 Synthesis of Ru-complexes using ligands 5-17 and 5-18

Figure 5-16. Synthetic route towards Ru(II)-complex **5-20**

The complexation reaction of **5-17** with RuCl_3 towards the Ru(II)-complex **5-20** (Figure 5-16) was carried out in refluxing DMF under inert atmosphere for 14 days. The brown product was isolated from the reaction mixture *via* precipitation as PF_6^- -salt. Repetitive precipitations from *n*-pentan allowed excluding traces of the starting compound **5-17**.

Since **5-20** was soluble in common organic solvents, tetrachloroethane- d_2 was used for NMR spectroscopy instead of acetonitrile- d_3 , which is normally used for poorly soluble Ru-complexes.

MALDI-TOF mass spectrometry was accomplished in a solid state (DCTB as a matrix). The mass-spectrum (Figure 5-17) has a peak at 1654 Da which belongs to the complex **5-20**. The peak at 1801 Da corresponds to **5-20** with hexafluorophosphate (PF_6^-) as a negative counterion. The peak at 1137 Da appears due to fragmentations occurring during mass-measurements.

The ^1H NMR spectrum, as well as H,H COSY of **5-20** are shown in Figure 5-18 and Figure 5-19, respectively. The proton resonances H_d and H_c no longer belong to a single peak, appearing at 7.98 and 9.87 ppm correspondingly. This indirectly confirms that the ligand (in which H_d and H_c are similar) became a part of a Ru complex.

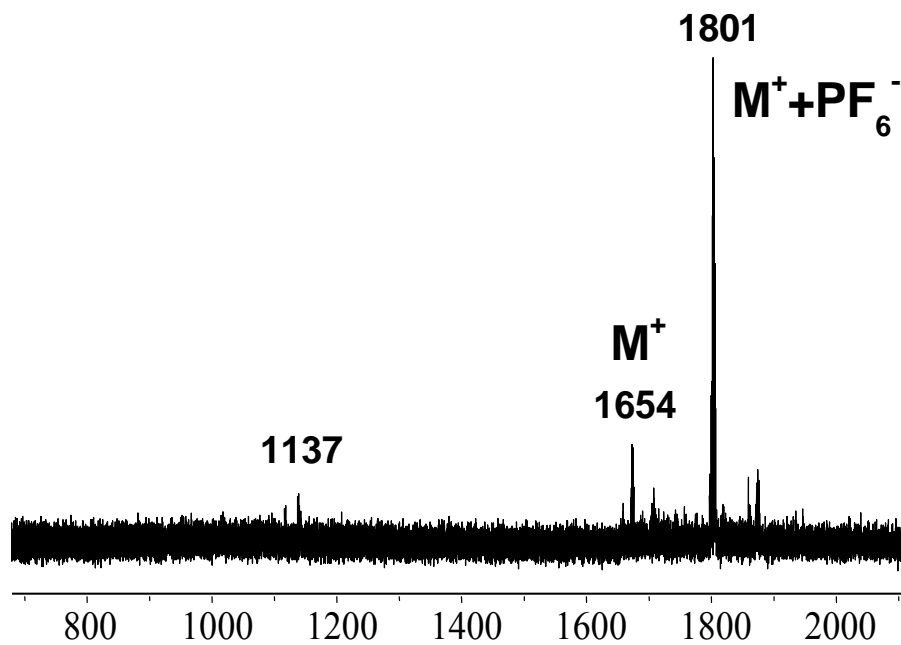


Figure 5-17. MALDI-TOF-mass spectrum of **5-20**

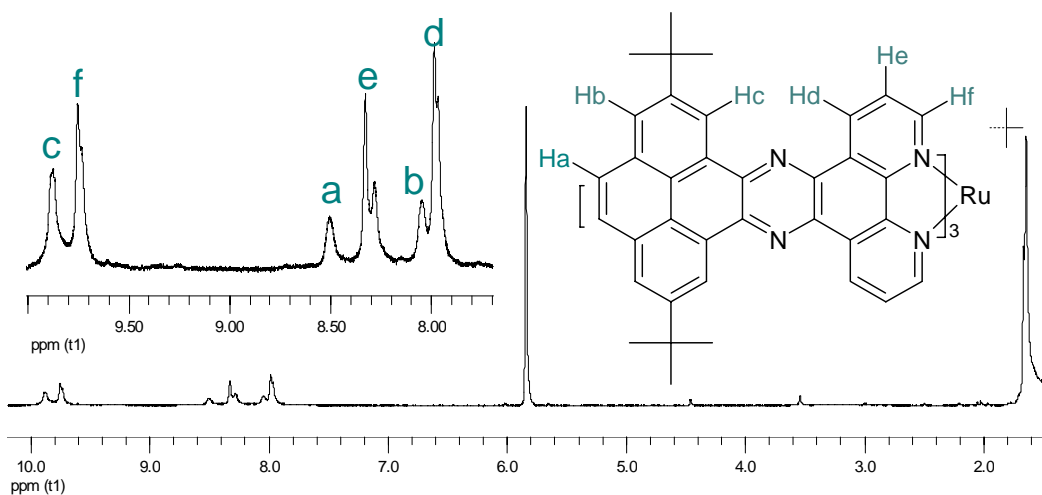


Figure 5-18. 1H NMR of **5-20**, recorded in tetrachloroethane- d_2 at 100 °C (500 MHz)

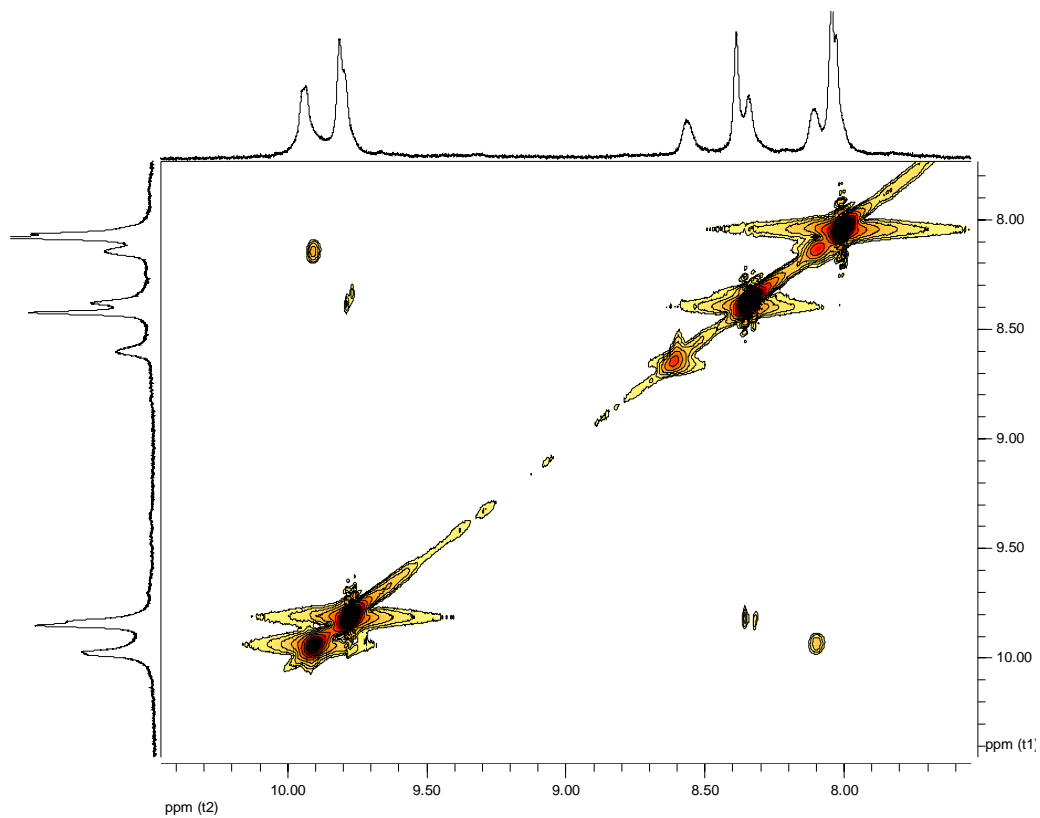


Figure 5-19. H,H COSY of **5-20**, recorded in tetrachloroethane- d_2 at 100 °C (500 MHz)

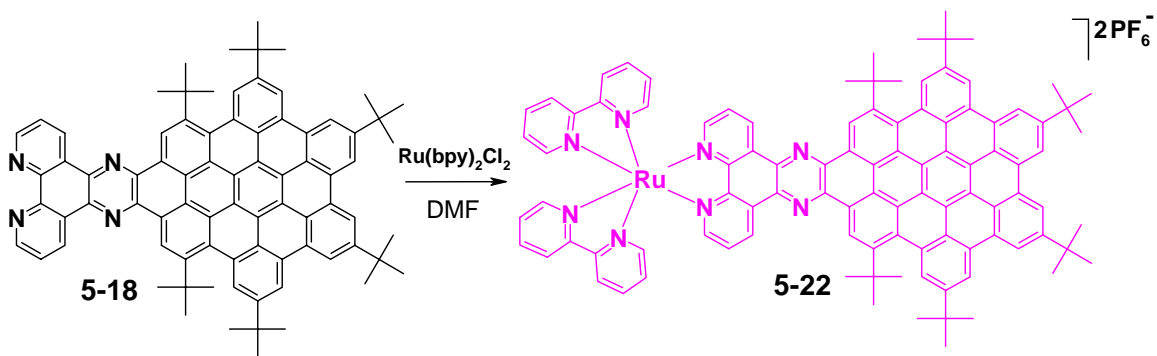


Figure 5-20. Synthesis of Ru-complex **5-22**

The same synthetic strategy was used for the ligand **5-18**. After 3 weeks of complexation with RuCl_3 , MALDI-TOF detected only a starting compound. However, a smaller complex with $\text{Ru}(\text{bpy})_2\text{Cl}_2$ (Figure 5-20) could be obtained already after 3 days, pointing out that **5-18** is suitable for complexation. This Ru-complex has good solubility due to the presence of six *tert*-butyl groups in the periphery. The purity of **5-22** was checked by MALDI-TOF spectrometry and NMR spectroscopy (see experimental part).

5.4 Synthesis of a Copper (II) complex

The complexation reaction of **5-18** towards copper(II)-complex **5-23** (Figure 5-21) was carried out in refluxing DMF under inert atmosphere for 14 days. The reaction was monitored by MALDI-TOF-mass spectrometry and the desired complex was detected already on the third day.

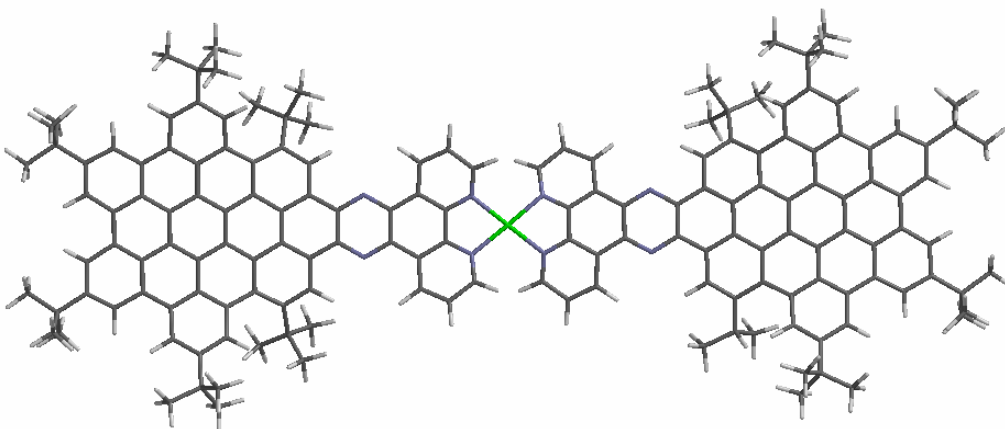
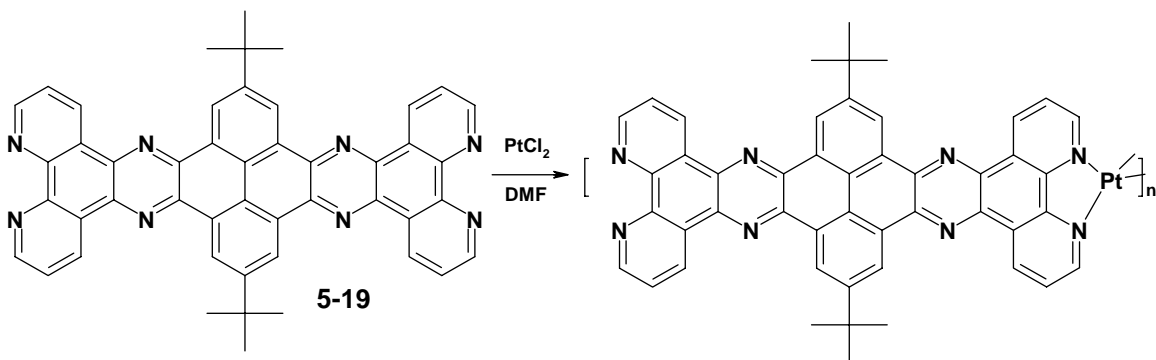


Figure 5-21. Chemical structure of the Cu(II)-complex **5-23**

After 2 weeks the dark red product was isolated *via* precipitation from *n*-pentan. The solubility of the resulting copper-complex **5-23** was poor in common organic solvents. The characterization by MALDI-TOF was done in solid-state (DCTB as a matrix) and showed traces of **5-18** in the final product.

5.5 Synthesis of a Pt(II)-complex

Figure 5-22. Synthetic route towards Pt-complexes with different n

The stoichiometrically controlled complexation reaction towards the polymer-structure (Figure 5-22) was accomplished in refluxing DMF under inert atmosphere over 1 week. A 1:1 ratio of the precursor **5-19** and PtCl_2 was taken. Characterization of the final product was done by MALDI-TOF in the solid state (DCTB as a matrix). The mass spectrum showed the presence of 4 different products (see Figure 5-23) as well as the precursor molecule **5-19**.

It was impossible to obtain extended oligomers, since the ligand **5-19** is poorly soluble and its Pt(II)-derivatives are even less soluble in DMF. As a result, they precipitate from the mixture and no longer participate in the reaction. Insolubility of the products also complicates their purification.

The ratio 2:1 of **5-19** and PtCl_2 was also tried with the aim to obtain only dimer **5-25** (Figure 5-23). After 4 days the solid state MALDI-TOF mass spectrometry showed only the presence of the ligand **5-19** and compound **5-24**. Extension of the reaction time to 14 days did not help to obtain **5-25**.

These results clearly indicate that the oligomers of **5-19** have bad solubility, which, first of all, it should be improved in the future work.

5 From Pyrene towards Phenanthroline Ligands for Metal Complexation

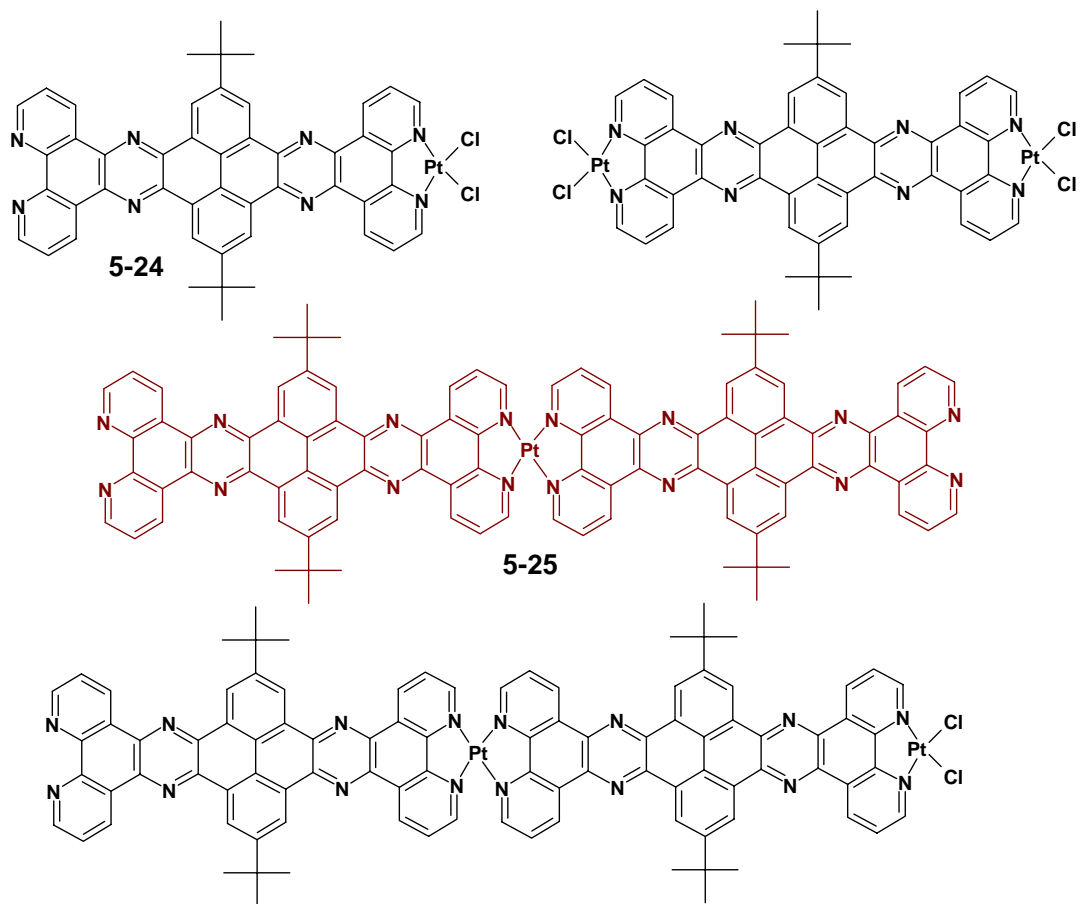


Figure 5-23. Chemical structures of the products of the complexation reaction.

5.6 Spectroscopic properties

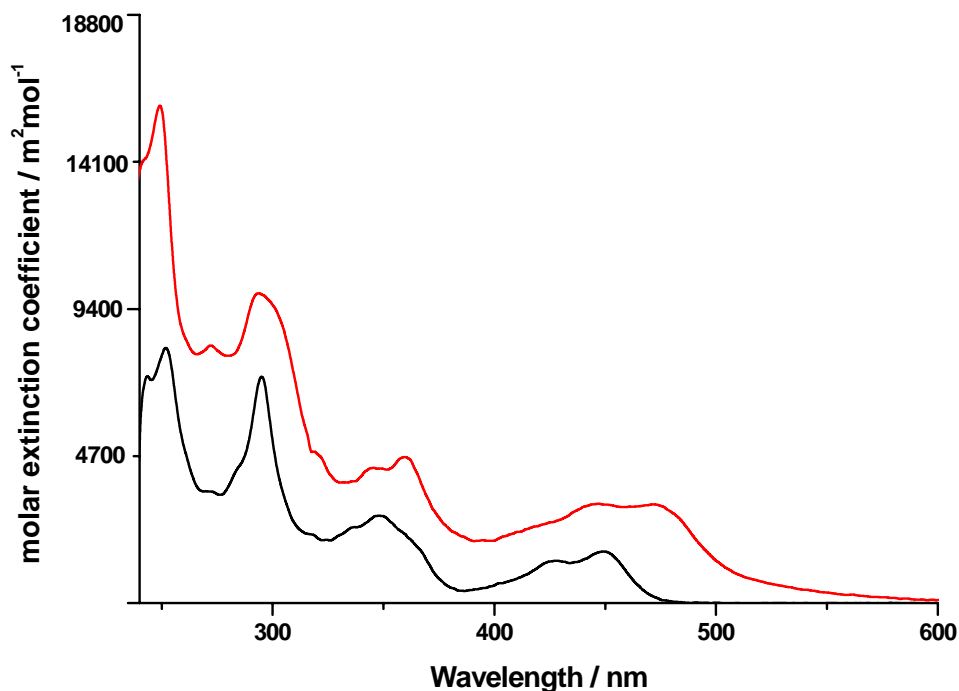


Figure 5-24. Absorption spectra of the ligand **5-17** (black) and the Ru(II)-complex **5-20** (red)

Figure 5-24 shows absorption spectra of the ligand **5-17** and the Ru(II)-complex **5-20**, which were recorded at room temperature at concentration $5.3 \times 10^{-6} \text{ mol} \cdot \text{L}^{-1}$. The UV/vis spectrum of the ligand **5-17** exhibits absorption band at 343 nm, which is similar to one of pyrene. Another band, at 443 nm, arises due to the conjugation of pyrene with the phenanthroline moiety and is assigned to $\pi - \pi^*$ transitions of **5-17**. The same transitions are present in the spectrum of the Ru(II) complex **5-20**. However, the absorption band at 443 nm is now overlapping with the $d_{\pi}(\text{Ru}) - \pi^*(\mathbf{5-17})$ metal-to-ligand charge-transfer (MLCT) transitions at 470 nm. The combination of absorptions at 443 and 470 nm renders this complex its dark red color. In particular, the band around 470 nm is similar in shape to the lowest-energy absorption band of $\text{Ru}(\text{phen})_3^{2+}$ around 440 nm, which is assigned to $d_{\pi}(\text{Ru}) - \pi^*(\text{phen})$ MLCT transition, but is bathochromically shifted over 30 nm.

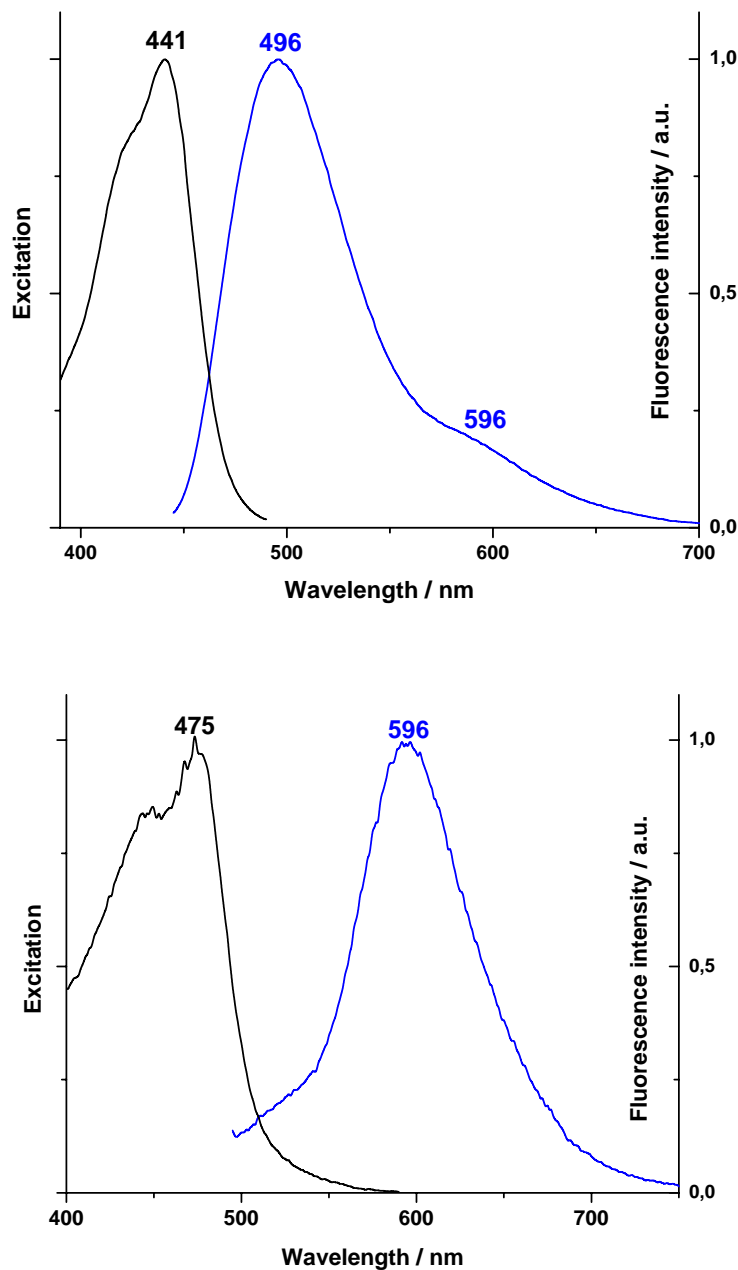


Figure 5-25. Normalized emission spectrum of **5-20**, excited at 440 nm (left) and excited at 490 nm (right)

Emission spectra of **5-20** were recorded at room temperature, excited at two wavelengths, 440 and 490 nm. Figure 5-25 (left, blue line) shows the emission spectrum of **5-20** excited at 440 nm, which is assigned to the $\pi - \pi^*$ transition of the ligand **5-17**. However,

one could also observe an additional shoulder at 596 nm, which is the MLCT transition according to the UV/vis spectrum (Figure 5-24). The difference between these two bands is approximately 100 nm. Figure 5-25 (right) shows that, if the Ru(II)-complex is excited at 490 nm, the $\pi - \pi^*$ transition from the ligand practically disappears, but instead the transition from the ligand to the metal (at 596 nm) becomes much more pronounced. This transition also manifests itself as a new band at 475 nm in the excitation spectrum (Figure 5-25, right, black line). The Stokes shift is about 120 nm.

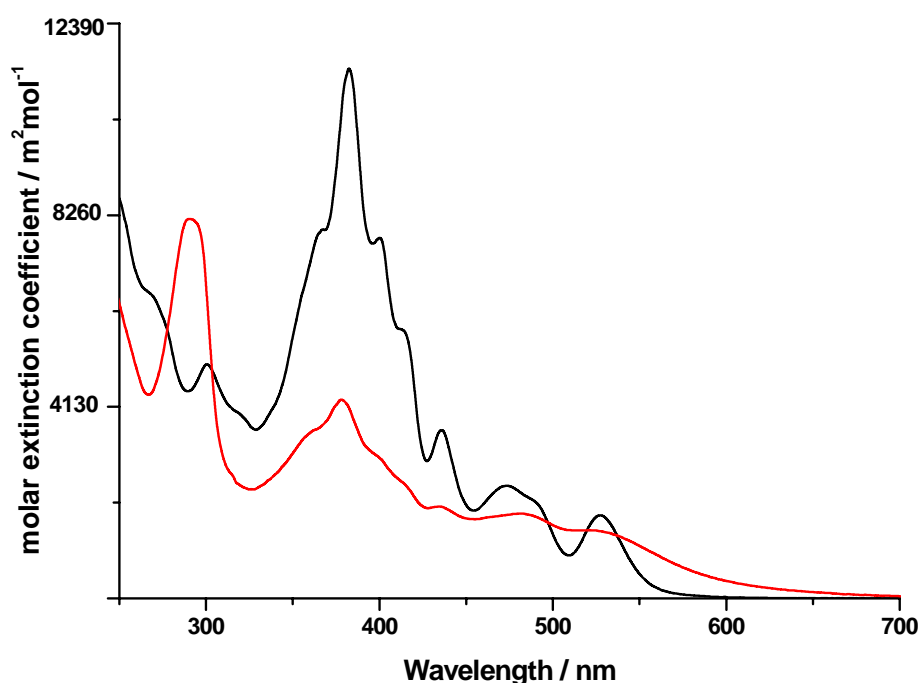


Figure 5-26. Absorption spectra of the ligand **5-20** (black) and the Ru(II)-complex **5-24** (red)

Absorption spectra of the ligand **5-18** and the Ru(II)-complex **5-22** were recorded at concentration $2.4 \times 10^{-5} \text{ mol} \cdot \text{L}^{-1}$ at room temperature and are shown in Figure 5-26. The UV/vis spectrum of the ligand **5-18** looks very similar to the absorption spectrum of PAH **3-18**, shown in Chapter 3. As before, three typical bands α , β and γ are present. Even though the phenanthroline moiety extends the conjugated system, no bathochromic shift can be observed.

The absorption spectrum of Ru(II)-complex **5-22** shows an additional band in the UV region at 290 nm, which is attributed to the ligand-centered $\pi - \pi^*$ transitions of the peripheral bpy ligands. The long tail of the absorption is due to strong overlap between transitions of the ligand and the $d\pi(\text{Ru}) - \pi^*(\mathbf{5-18})$ metal-to-ligand charge-transfer.

Emission spectra of **5-22** were recorded at room temperature, again excited at two wavelengths, 520 and 590 nm. Figure 5-27 shows the normalized emission spectrum of the Ru(II)-complex **5-22** excited at 520 nm. This wavelength is assigned to the $\pi - \pi^*$ transition of the ligand **5-18**. The emission waveband is rather broad, due to a strong overlap between electronic transitions assigned to the ligand **5-18** and MLCT. To confirm the MLCT transition another excitation wavelength was chosen, where the ligand does not contribute any more. Indeed, excitation at 590 nm gives a new band at 642 nm, which belongs to $d\pi(\text{Ru}) - \pi^*(\mathbf{5-18})$ MLCT.

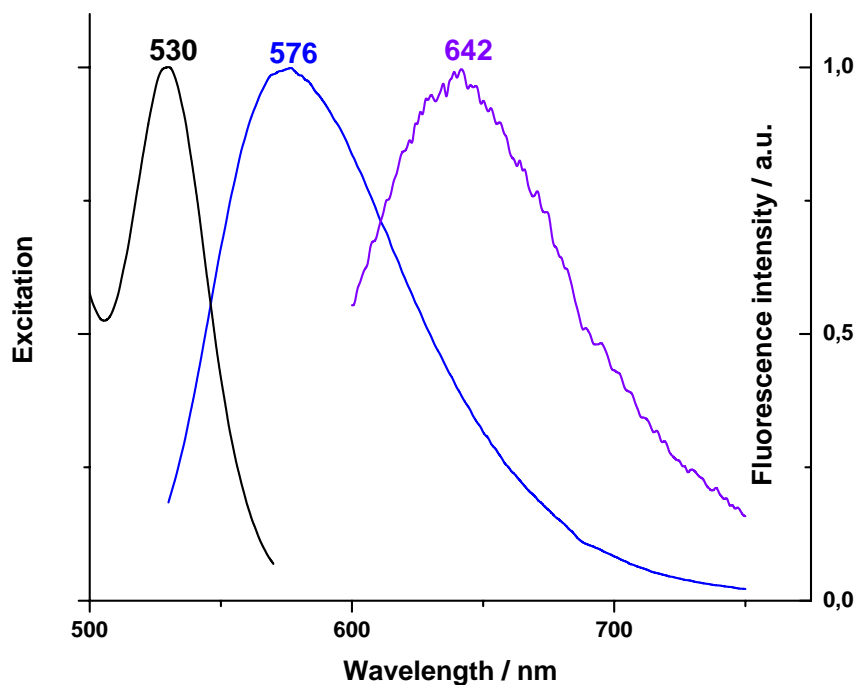


Figure 5-27. Normalized emission spectrum of **5-22**, excited at 520 (blue line) and 590 nm (violet line)

As it was mentioned before, **5-19** does not possess good solubilities in common organic solvents. However, it was possible to record absorption spectra in chloroform at concentrations (10^{-4} - 10^{-6} mol·L $^{-1}$). They are shown in Figure 5-28. Emission spectra of **5-19** were recorded at concentrations 10^{-4} and 10^{-6} mol·L $^{-1}$ and are also shown in Figure 5-28. Comparison of two spectra shows that the emission at 10^{-4} mol·L $^{-1}$ (464 nm) is bathochromically shifted on 7 nm, as well as becomes broader than the spectrum at 10^{-6} mol·L $^{-1}$ (457 nm). Such behavior can be explained by strong aggregation of **5-19**.

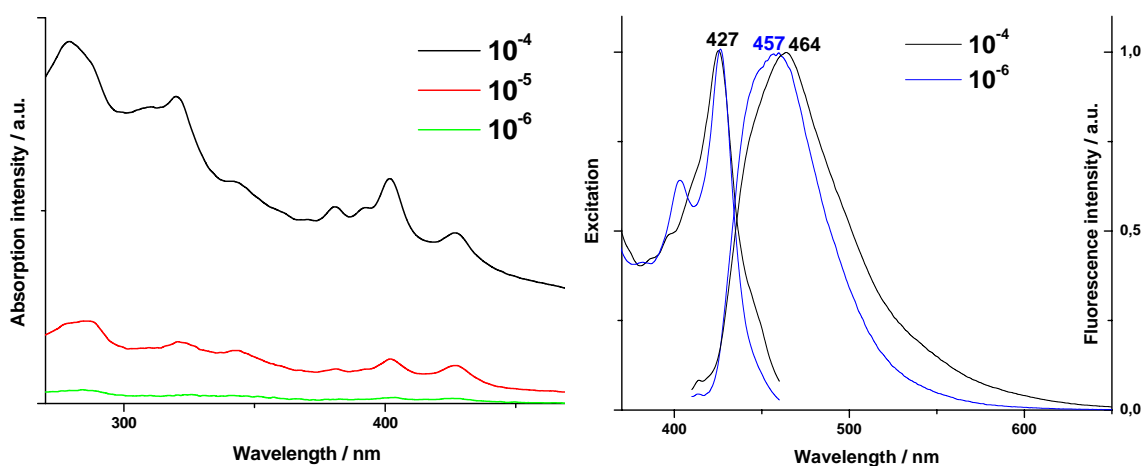


Figure 5-28. Absorption (left) and emission (right) spectra of **5-19**, recorded at concentrations 10^{-4} - 10^{-6} mol·L $^{-1}$.

5.7 Summary

In this chapter, three novel phenanthroline ligands were synthesized by using the quinoxaline reactions. Ligands **5-17** and **5-18** showed good solubility in common organic solvents and therefore were suitable for metal complexation. Thus, two new soluble (tetrachloroethane, acetonitrile) Ru(II) complexes **5-20** and **5-22** have been obtained and characterized by standard analytical techniques. The absorption and emission spectra of the synthesized complexes exhibited both the ligand-associated π - π^* and metal-to-ligand charge-transfer transitions, whose energy and relative intensity depended on the type of the ligands bound to the metal center.

The ligand **5-19** showed bad solubility in organic solvents and its characterization was done in solid state. **5-19** provided two reactive centers suitable for metal complexation (Pt(II)). However, the obtained Pt(II)-complexes were insoluble, which complicated their purification.

As a conclusion, this chapter provides not only the synthesis and characterizations of the novel ligands and their metal complexes, but also an alternative method to grow extended PAHs, containing heteroatoms and metal centers in the aromatic core.

5.8 References

1. Deisenhofer, J.; Epp, O.; Sinning, I.; Michel, H., *Journal of Molecular Biology* **1995**, 246, (3), 429-457.
2. Barber, J.; Andersson, B., *Nature* **1994**, 370, (6484), 31-34.
3. Hagfeldt, A.; Gratzel, M., *Chemical Reviews* **1995**, 95, (1), 49-68.
4. Bolink, H. J.; Cappelli, L.; Coronado, E.; Gratzel, M.; Nazeeruddin, M. K., *J. Am. Chem. Soc.* **2006**, 128, (1), 46-47.
5. Caspar, J. V.; Kober, E. M.; Sullivan, B. P.; Meyer, T. J., *Journal of the American Chemical Society* **1982**, 104, (2), 630-632.
6. Chen, P. Y.; Mecklenburg, S. L.; Duesing, R.; Meyer, T. J., *Journal of Physical Chemistry* **1993**, 97, (26), 6811-6815.
7. Bolger, J.; Gourdon, A.; Ishow, E.; Launay, J. P., *Inorg. Chem.* **1996**, 35, (10), 2937-2944.
8. Ishow, E.; Gourdon, A.; Launay, J. P.; Lecante, P.; Verelst, M.; Chiorboli, C.; Scandola, F.; Bignozzi, C. A., *Inorg. Chem.* **1998**, 37, (14), 3603-3609.
9. Ishow, E.; Gourdon, A.; Launay, J. P.; Chiorboli, C.; Scandola, F., *Inorg. Chem.* **1999**, 38, (7), 1504-1510.
10. Chiorboli, C.; Bignozzi, C. A.; Scandola, F.; Ishow, E.; Gourdon, A.; Launay, J. P., *Inorg. Chem.* **1999**, 38, (10), 2402-2410.
11. Kim, M. J.; Konduri, R.; Ye, H. W.; MacDonnell, F. M.; Puntoriero, F.; Serroni, S.; Campagna, S.; Holder, T.; Kinsel, G.; Rajeshwar, K., *Inorg. Chem.* **2002**, 41, (9), 2471-2476.

12. Campagna, S.; Serroni, S.; Bodge, S.; MacDonnell, F. M., *Inorg. Chem.* **1999**, 38, (4), 692-701.
13. Bolger, J.; Gourdon, A.; Ishow, E.; Launay, J. P., *J. Chem. Soc. Chem. Commun.* **1995**, (17), 1799-1800.
14. Friedman, A. E.; Chambron, J. C.; Sauvage, J. P.; Turro, N. J.; Barton, J. K., *J. Am. Chem. Soc.* **1990**, 112, (12), 4960-4962.
15. Chambron, J. C.; Sauvage, J. P.; Amouyal, E.; Koffi, P., *Nouveau Journal De Chimie-New Journal of Chemistry* **1985**, 9, (8-9), 527-529.
16. Gupta, N.; Grover, N.; Neyhart, G. A.; Liang, W. G.; Singh, P.; Thorp, H. H., *Angew. Chem., Int. Ed. Engl.* **1992**, 31, (8), 1048-1050.
17. Hiort, C.; Lincoln, P.; Norden, B., *J. Am. Chem. Soc.* **1993**, 115, (9), 3448-3454.
18. Haq, I.; Lincoln, P.; Suh, D. C.; Norden, B.; Chowdhry, B. Z.; Chaires, J. B., *J. Am. Chem. Soc.* **1995**, 117, (17), 4788-4796.
19. Stoeffler, H. D.; Thornton, N. B.; Temkin, S. L.; Schanze, K. S., *J. Am. Chem. Soc.* **1995**, 117, (27), 7119-7128.
20. Yam, V. W. W.; Lo, K. K. W.; Cheung, K. K.; Kong, R. Y. C., *J. Chem. Soc. Chem. Commun.* **1995**, (11), 1191-1193.
21. Chambron, J. C.; Sauvage, J. P., *Chem. Phys. Lett.* **1991**, 182, (6), 603-607.
22. Murphy, C. J.; Arkin, M. R.; Jenkins, Y.; Ghatlia, N. D.; Bossmann, S. H.; Turro, N. J.; Barton, J. K., *Science* **1993**, 262, (5136), 1025-1029.
23. Balzani, V., Venturi, M., Credi, A., *Molecular devices & machines*. Wiley-VCH: 2003.
24. Chiorboli, C.; Fracasso, S.; Ravaglia, M.; Scandola, F.; Campagna, S.; Wouters, K. L.; Konduri, R.; MacDonnell, F. M., *Inorg. Chem.* **2005**, 44, (23), 8368-8378.
25. Chiorboli, C.; Rodgers, M. A. J.; Scandola, F., *J. Am. Chem. Soc.* **2003**, 125, (2), 483-491.
26. Balzani, V.; Juris, A.; Venturi, M.; Campagna, S.; Serroni, S., *Chem. Rev.* **1996**, 96, (2), 759-833.
27. Schlicke, B.; Belser, P.; De Cola, L.; Sabbioni, E.; Balzani, V., *J. Am. Chem. Soc.* **1999**, 121, (17), 4207-4214.

28. Barigelletti, F.; Flamigni, L.; Collin, J. P.; Sauvage, J. P., *Chem. Commun.* **1997**, (4), 333-338.
29. Bilakhiya, A. K.; Tyagi, B.; Paul, P.; Natarajan, P., *Inorg. Chem.* **2002**, 41, (15), 3830-3842.
30. Balzani, V., Scandola, F., *Supramolecular Photochemistry*. Horwood: Chichester, U.K., 1991.
31. De Cola, L.; Belser, P., *Coord. Chem. Rev.* **1998**, 177, 301-346.
32. Belser, P.; Bernhard, S.; Blum, C.; Beyeler, A.; De Cola, L.; Balzani, V., *Coord. Chem. Rev.* **1999**, 192, 155-169.
33. Barigelletti, F.; Flamigni, L., *Chem. Soc. Rev.* **2000**, 29, (1), 1-12.
34. El-ghayoury, A.; Harriman, A.; Khatyr, A.; Ziessel, R., *Angew. Chem., Int. Ed.* **2000**, 39, (1), 185-+.
35. Juris, A.; Prodi, L.; Harriman, A.; Ziessel, R.; Hissler, M.; El-ghayoury, A.; Wu, F. Y.; Riesgo, E. C.; Thummel, R. P., *Inorg. Chem.* **2000**, 39, (16), 3590-3598.
36. Chouai, A.; Wicke, S. E.; Turro, C.; Bacsá, J.; Dunbar, K. R.; Wang, D.; Thummel, R. P., *Inorg. Chem.* **2005**, 44, (17), 5996-6003.
37. Thang, D. C.; Jacquignon, P.; Dufour, M., *Journal of Heterocyclic Chemistry* **1976**, 13, (3), 641-644.
38. Steemers, F. J.; Verboom, W.; Reinhoudt, D. N.; van der Tol, E. B.; Verhoeven, J. W., *Journal of Photochemistry and Photobiology a-Chemistry* **1998**, 113, (2), 141-144.
39. Steemers, F. J.; Verboom, W.; Hofstraat, J. W.; Geurts, F. A. J.; Reinhoudt, D. N., *Tetrahedron Lett.* **1998**, 39, (41), 7583-7586.
40. Albano, G.; Belser, P.; Daul, C., *Inorg. Chem.* **2001**, 40, (7), 1408-1413.
41. Albano, G.; Belser, P.; De Cola, L.; Gandolfi, M. T., *Chem. Commun.* **1999**, (13), 1171-1172.
42. Wu, F. Y.; Thummel, R. P., *Inorganica Chimica Acta* **2002**, 327, 26-30.
43. Schmelz, O.; Mews, A.; Basche, T.; Herrmann, A.; Mullen, K., *Langmuir* **2001**, 17, (9), 2861-2865.
44. Glazer, E. C.; Tor, Y., *Angew. Chem., Int. Ed.* **2002**, 41, (21), 4022-4026.
45. Leudtke, N. W.; Hwang, J. S.; Glazer, E. C.; Gut, D.; Kol, M.; Tor, Y., *ChemBiochem* **2002**, 3, (8), 766-771.

46. Gut, D.; Rudi, A.; Kopilov, J.; Goldberg, I.; Kol, M., *J. Am. Chem. Soc.* **2002**, 124, (19), 5449-5456.
47. Bergman, S. D.; Reshef, D.; Frish, L.; Cohen, Y.; Goldberg, I.; Kol, M., *Inorg. Chem.* **2004**, 43, (13), 3792-3794.
48. Rudi, A.; Kashman, Y.; Gut, D.; Lellouche, F.; Kol, M., *Chem. Commun.* **1997**, (1), 17-18.
49. Bergman, S. D.; Reshef, D.; Groysman, S.; Goldberg, I.; Kol, M., *Chem. Commun.* **2002**, (20), 2374-2375.
50. Malem, F.; Mandler, D., *Analytical Chemistry* **1993**, 65, (1), 37-41.
51. Karlin, K. D., *Science* **1993**, 261, (5122), 701-708.
52. Strizhak, P. E.; Basylchuk, A. B.; Demjanchyk, I.; Fecher, F.; Schneider, F. W.; Munster, A. F., *Phys. Chem. Chem. Phys.* **2000**, 2, (20), 4721-4727.
53. Hanaki, A., *Bulletin of the Chemical Society of Japan* **1995**, 68, (3), 831-837.
54. Zhang, J. J.; Anson, F. C., *Journal of Electroanalytical Chemistry* **1993**, 348, (1-2), 81-97.
55. Rorabacher, D. B., *Chem. Rev.* **2004**, 104, (2), 651-697.
56. Jung, S. H.; Pisula, W.; Rouhanipour, A.; Räder, H. J.; Jacob, J.; Müllen, K., *Angewandte Chemie-International Edition* **2006**, 45, (28), 4685-4690.
57. Stille, J. K.; Mainen, E. L., *Macromolecules* **1968**, 1, (1), 36-42.
58. Bodige, S.; MacDonnell, F. M., *Tetrahedron Lett.* **1997**, 38, (47), 8159-8160.

5 From Pyrene towards Phenanthroline Ligands for Metal Complexation

6 Conclusions and Outlook

Organic-based electronic devices require materials with well-tuned physical properties, such as chemical and thermal stability, appropriate HOMO-LUMO gap and high conductivity. Of special interest is adjusting HOMO and LUMO levels of the molecules, which are often responsible for charge carrier mobilities, charge ejection from electrodes, etc. Studies of polycyclic aromatic hydrocarbons have shown that the overall size, periphery, and functionalization of PAHs are crucial parameters which significantly alter their electronic structure and chemical reactivity. Therefore, the major directions for this thesis are the synthesis and characterization of *extended* PAHs - with different functional groups improving their processability, periphery changing their chemical reactivity and inclusion of different metal ions, which influence physical properties.

The cyclodehydrogenation reaction has been applied for the newly synthesised polyphenylene ribbons with preplanarized (dibenzo[*e,l*]pyrene) moieties in the aromatic core (Figure 6-1). The synthetic strategy employed is discussed in Chapter 2 and is based on *stoichiometrically* controlled DIELS-ALDER cycloaddition. Thus, very long polyphenylene ribbons with up to 10 nm linear size, containing *n*-substituted dibenzo[*e,l*]pyrene with propeller-like dendritic backbone have been efficiently synthesized. All molecules possessed very good solubility in common organic solvents allowing their characterization by standard analytical techniques. The cyclodehydrogenation reaction was applied for the smallest ribbon in order to obtain two-dimensional ladder-type graphene and yielded the cyclodehydrogenated product **2-23** (Figure 6-1). However, according to the direct characterization methods **2-23** coexists with partially cyclised compounds.

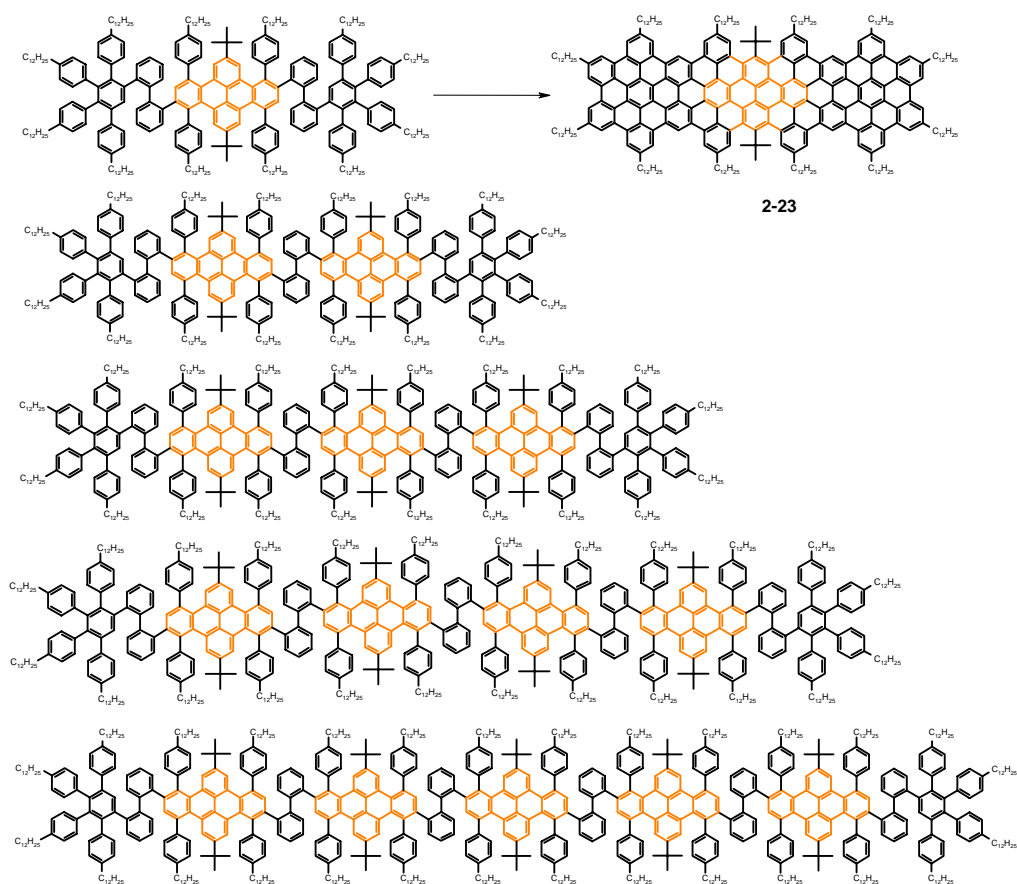


Figure 6-1. The series of the ribbons with preplanarized (dibenzo[*e,l*]pyrene) moieties in the aromatic core and attempted cyclodehydrogenation

A simple extension of the PAHs, as have been observed, leads to their pronounced tendency to self-associate, i.e. reduces solubility and complicates purification. It also affects the reproducibility of the cyclodehydrogenation reaction. Therefore, a new concept was developed to extend PAH's core - the change of the nature of the PAH's periphery. Here the introduction of "zigzag" sites, discussed in Chapter 3 was shown to lower the HOMO-LUMO gap and to result in higher chemical reactivities. This allowed, in Chapters 3, 4 and 5, further functionalizing of PAH and enlarging their aromatic cores. In particular, the selective oxidation of the "zigzag" edge of a six-fold *tert*-butylated tetrabenzo[*bc,ef,hi,uv*]ovalene **3-12** allowed the corresponding diketo building block to be made on a gram scale. The α -diketone **3-13** was then subjected to quinoxaline ring-

formation reactions; as a result the largest known heteroatom containing PAHs (up to 224 atoms in the aromatic core) have been prepared (Figure 6-2).

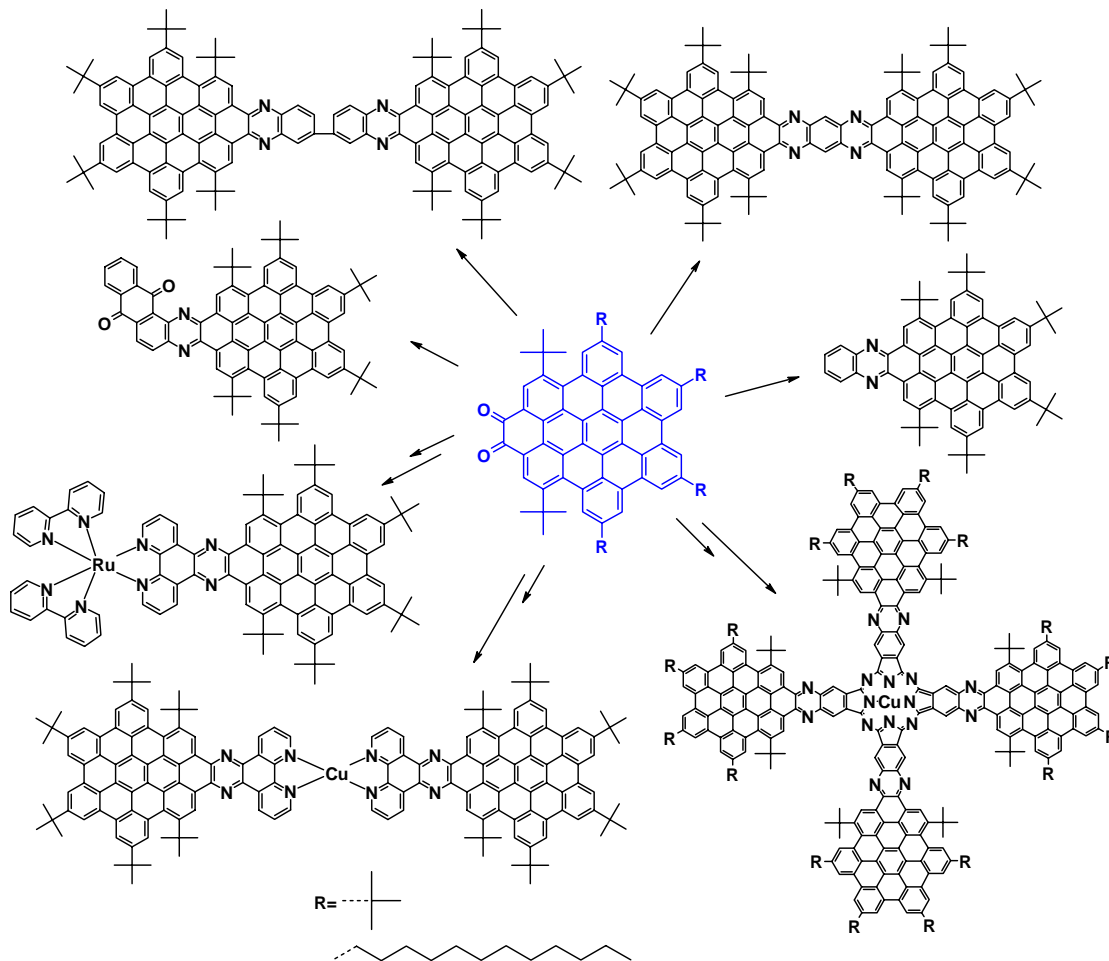


Figure 6-2. Universality of α -diketone **3-13**

Despite the size of these novel molecules, extraordinary solubilities in common organic solvents were obtained due to a distortion from planarity of the aromatic core by bulky *tert*-butyl groups, which hampered the usually very pronounced aggregation tendency of extended π -systems. Therefore, the synthesized PAHs were purified using standard chromatography. All extended PAHs possess the small HOMO-LUMO gap together with good electron affinities, which make them potential candidates for application in organic FETs.

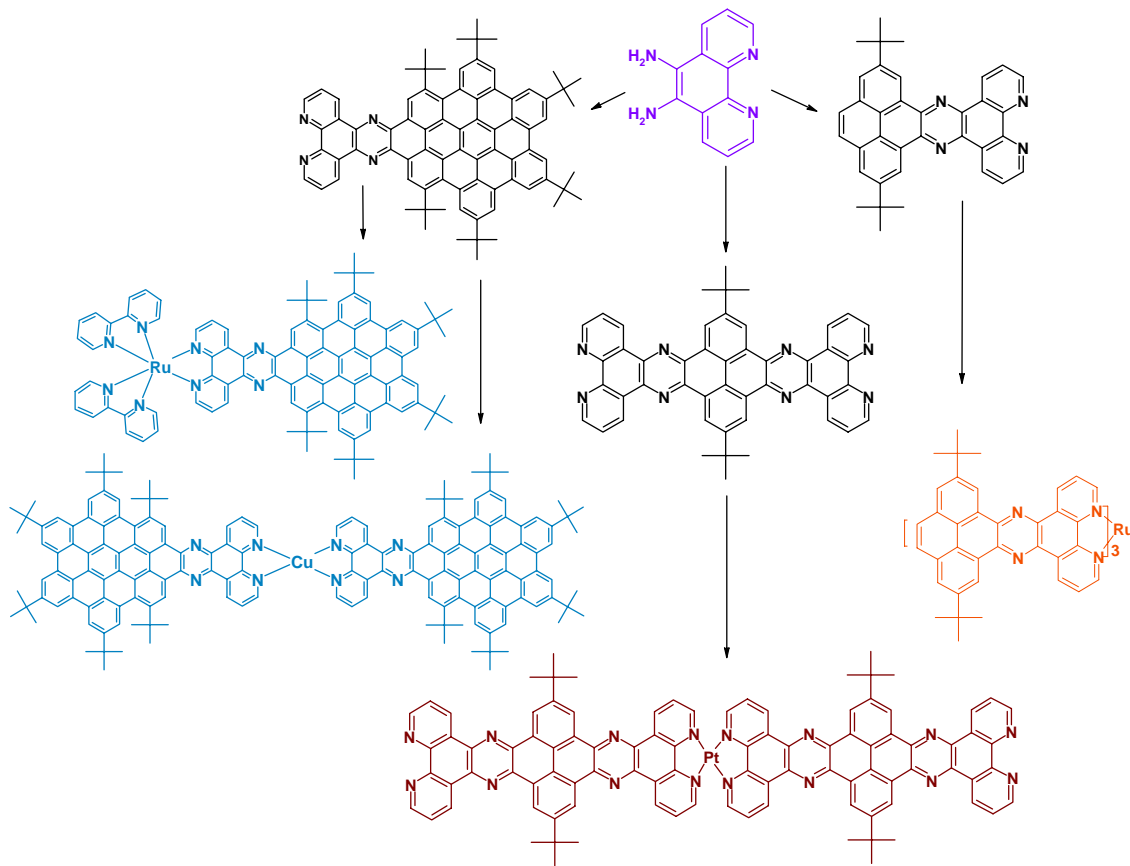


Figure 6-3. Four different metal complexes based on phenanthroline ligands

Another alternative synthetic route towards extended PAHs is the metal-PAH complexation. Ru(II) complexes 2,2'-bipyridine and 1,10-phenanthroline ligands have attracted scientific interest because of light harvesting absorption and emission characteristics, their chemical stability, and low barriers for electron and energy transfer. Using the quinoxaline methodology in Chapter 5 three new phenanthroline ligands (up to 60 skeletal atoms) to be complexed to a metal center have been synthesized and characterized (Figure 6-3). Four different (Ru(II), Cu(II) and Pt(II)) complexes were synthesized, opening the possibility to construct a range of large metal complexes by varying the metal as well as the number and nature of ligands.

7 Experimental Section

7.1 General Methods

Chemicals and Solvents

The chemicals and solvents were obtained from the companies Fluka, Sigma-Aldrich, Merck, ABCR, Lancaster and used as obtained, unless otherwise mentioned.

Chromatography

Preparative column chromatography was performed on silica gel from Merck with a grain size of 0.063-0.2 mm.

NMR spectroscopy

^1H NMR and ^{13}C -NMR spectra were recorded in CD_2Cl_2 , $\text{C}_2\text{D}_2\text{Cl}_4$ and d_8 -THF on a Bruker DPX 250, Bruker AMX 300, Bruker DRX 500 or Bruker DPX 700 with use of the solvent proton- or carbon-signal as internal standard.

Mass spectrometry

FD mass spectra were obtained on a VG Instruments ZAB 2-SE-FPD. MALDI-TOF mass spectra were measured on a Bruker Reflex II-TOF spectrometer using a 337nm nitrogen laser and 7,7,8,8-tetracyanoquinodimethane (TCNQ), or 9-nitroanthracene, 1,8,9-trihydroxy anthracene (Dithranol), trans-2-[3-(4-tert-butylphenyl)-2-methyl-2-propenylidene]malononitrile (DCTB) matrices.

UV/vis and Fluorescence spectroscopy

UV/Vis spectra were recorded at room temperature on Perkin-Elmer Lambda 9 or Perkin-Elmer Lambda 5 spectrometers. Solution fluorescence spectra were obtained on a SPEX-Fluorolog II (212) spectrometer.

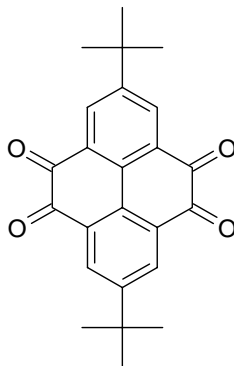
Differential scanning calorimetry (DSC) and thermogravimetric analysis (TGA)

DSC was measured on a Mettler DSC 30 with heating and cooling rates of 10 K/min. For TGA a Mettler 500 thermogravimetric analyzer was used.

2D-WAXS

Powder X-ray diffraction experiments were performed using a Siemens D 500 Kristalloflex diffractometer with a graphite-monochromatized $\text{CuK}\alpha$ X-ray beam, emitted from a rotating Rigaku RU-300 anode.

7.2 Synthesis

7.2.1 2,7-Di-*tert*-butylpyrene-4,5,9,10-tetraone (**1-32**)

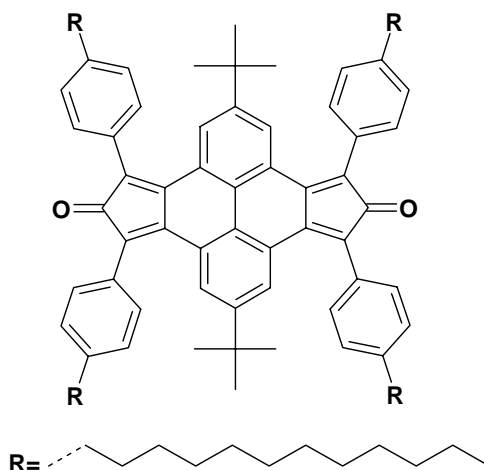
To a solution of 2,7-di-*tert*-butyl-pyrene (**2-5**) (10.00 g, 32.00 mmol) in DCM (1L) and CH₃CN (1L) were added NaIO₄ (56.00 g, 0.26 mol), H₂O (1L) and RuCl₃*xH₂O (0.80 g, 3.84 mmol).¹ The dark brown suspension was heated at 30-40 °C overnight. The reaction mixture was poured into water and extracted with DCM (3 times). The organic phase was collected and solvent was removed under reduced pressure to afford a dark orange solid. Column chromatography (DCM) gave pure product as bright orange crystals.

Yield: 3.68 g (31%)

FD-MS (8KV), m/z[ue⁻¹]: 374 (M⁺) (cal. for C₂₄H₂₂O₄ 374.44)

¹H NMR (250 MHz, CD₂Cl₂, 298 K): δ (ppm) = 8.45 (s, 4H), 1.42 (s, 18H, H_{*t*-but})

¹³C-NMR (250 MHz, CD₂Cl₂, 298 K): δ(ppm)= 178.63(CO), 155.04, 133.90, 132.56, 131.01, 35.64, 30.75

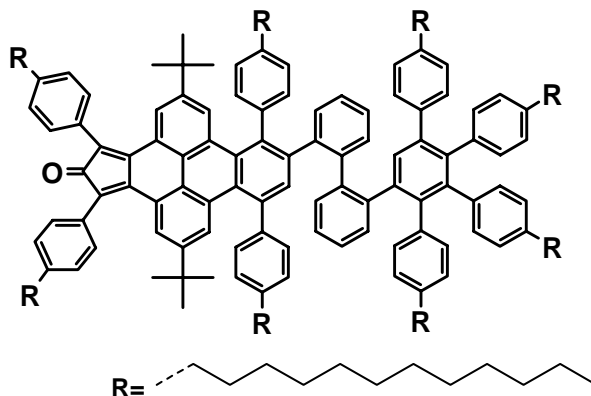
7.2.2 2,7-Di-*tert*-butyl-4,5:9,10-bis(2,5-di-*p*-dodecyl-phenylcyclopenta)-[*e,l*]pyrene-5,11-dione (**2-7**)

In the flask were added 0.50 g (0.50 mmol) of 1,3-bis(4-dodecyl)phenylacetone (**2-6**), 0.13 g (0.33 mmol) of 2,7-di-*tert*-butylpyrene-4,5,9,10-tetraone (**1-32**) and 40 ml of ethanol. The solution of sodium hydroxide (0.03 g) in methanol (1 ml) was added dropwise and reaction mixture was heating at 60 °C during 3 h. The precipitate was filtrated and subjected to column chromatography (DCM: PE=1: 3 as eluent).

Yield: 0.28g (60 %), green powder, which is unstable and was thus used without complete characterization.

FD-MS (8KV), m/z[ue⁻¹]: 1397.1 (M⁺) (cal. for C₁₀₂H₁₃₈O₂ 1396.24)

7.2.3 2,7-Di-*tert*-butyl-4,5-(2,5-di-*p*-dodecylphenyl-2',3',4',5'-tetrakis(4'-dodecylphenyl)-[1',1'';2'',3]terphenyl-dibenzo[*l*])-9,10-cyclopenta[*e*]pyrene-10-one (**2-12**)

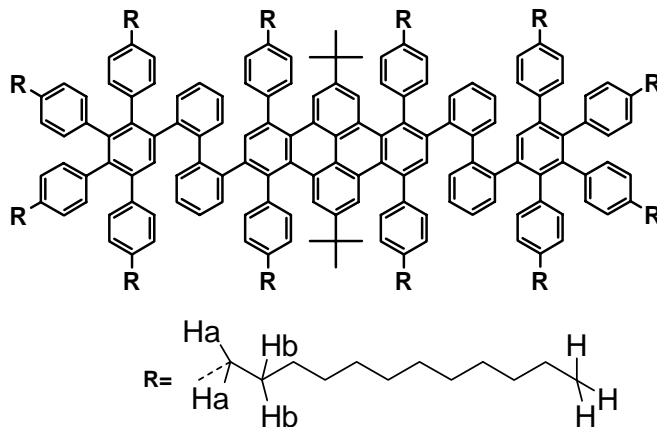


In the 10 ml tube were added 0.15 g (0.11 mmol) of ,7-di-*tert*-butyl-4,5:9,10-bis(2,5-di-*p*-dodecyl-phenylcyclopenta)[*e,l*]pyrene-5,11-dione (**2-7**), 0.13 g (0.11 mmol) of 2'-ethynyl-2,3,4,5-tetrakis(4-dodecylphenyl)-[1,1';2',1'']terphenyl (**2-10**) and 1 ml of toluene were placed in a microwave tube, which was purged with argon and sealed. The reaction was carried out in a CEM Discover microwave at 300 W and activated cooling, keeping the temperature at 110 °C for 1 h. The solvent was removed and the residue was treated via column chromatography using silica with DCM: PE=1: 2 as eluent.

Yield: 0.08 g (28%), green amorphous compound, which is unstable and was thus used without complete characterization.

FD-MS (8KV), m/z [ue^{-1}]: 2600.6 (M^+) (cal. for $C_{193}H_{264}O$ 2600.26)

7.2.4 2,7-Di-*tert*-butyl-4,5:9,10-bis(2,5-di-*p*-dodecylphenyl-2',3',4',5'-tetrakis(*p*-dodecylphenyl)-[1',1'';2'',3]terphenyl)dibenzo[*e,l*]pyrene (**2-13**)



In the 10 ml tube were added 0.15 g (0.11 mmol) of 2,7-di-*tert*-butyl-4,5:9,10-bis(2,5-di-*p*-dodecyl-phenylcyclopenta)-[*e,l*]pyrene-5,11-dione (**2-7**), 0.13 g (0.11 mmol) of 2''-ethynyl-2,3,4,5-tetrakis(4-dodecylphenyl)-[1,1';2',1'']terphenyl (**2-10**) and 1 ml of toluene were placed in a microwave tube, which was purged with argon and sealed. The reaction was carried out in a CEM Discover microwave at 300 W and activated cooling, keeping the temperature at 110 °C for 1 h. The solvent was removed and the residue was treated via column chromatography using silica with DCM: PE=1: 4 as eluent.

Yield: 0.09 g (21%), colorless oil.

MS(MALDI-TOF), m/z [ue^{-1}]: 3803 (M^+), 3842 ($M^+ + K^+$) (cal. for $C_{284}H_{390}$ 3804.27)

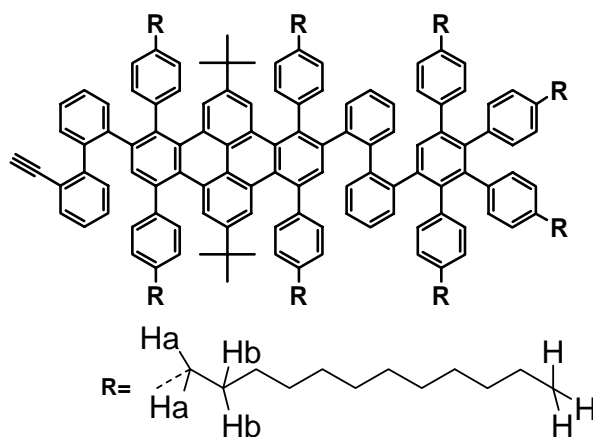
UV/vis: λ / nm (ϵ / $m^2 \cdot mol^{-1}$) = 308 (5 520), 286 (6 560), 258 (9 360)

1H -NMR (250 MHz, THF- d_8 , 298K): δ (ppm)= 7.86 (d, $^3J(H,H)=8.7$ Hz, 2H), 7.66 (s, 1H), 7.61 (s, 1H), 7.53 (d, $^3J(H,H)=5.82$ Hz, 2H), 7.45 (m, 6H), 7.27 (m, 6H), 7.11-6.86 (m, 30H), 6.72 (m, 10H), 6.46 (t, 7H), 6.24 (t, 2H), 6.09 (m, 3H), 5.95 (d, $^3J(H,H)=7.99$ Hz, 1H), 5.44 (t, 1H), 2.66 (m, 8H, $H_{CH_2-\alpha}$), 2.42 (m, 8H, $H_{CH_2-\alpha}$), 2.04 (m, 8H, $H_{CH_2-\alpha}$), 1.30 (br.s, 240H, H_{CH_2-rest}), 0.89 (br.s., 54H, $H_{CH_3} + H_{t-but}$)

^{13}C -NMR (500 MHz, THF- d_8 , 333 K): δ (ppm)= 142.57, 142.33, 140.55, 140.50, 140.42, 140.37, 140.24, 139.79, 139.53, 139.32, 139.21, 139.08, 138.86, 138.75, 138.47, 138.38, 138.03, 137.73, 137.38, 132.64, 132.40, 131.52, 131.45, 131.33, 129.78, 129.17, 128.25, 126.78, 126.63, 126.36, 126.17, 125.89, 125.20, 124.86, 35.45, 35.25, 35.13, 34.98,

31.54, 30.90, 30.75, 30.67, 30.62, 30.56, 30.52, 29.30, 29.12, 28.90, 28.63, 28.56, 22.19, 13.44

7.2.5 2,7-Di-*tert*-butyl-4,5:9,10-(2,5-di-*p*-dodecylphenyl-2',3',4',5'-tetrakis(*p*-dodecylphenyl)-[1',1'';2'',3]terphenyl-2''-ethynyl-3-biphenyl)dibenzo[*e,l*]pyrene (**2-14**)



In the 10 ml tube were added 0.11 g (0.04 mmol) of **2-12**, 0.01 g (0.04 mmol) of 2,2'-diethynyl-biphenyl (**2-8**) and 1 ml of toluene were placed in a microwave tube, which was purged with argon and sealed. The reaction was carried out in a CEM Discover microwave at 300 W and activated cooling, keeping the temperature at 110 °C for 1 h. The solvent was removed and the residue was treated via column chromatography using silica with DCM: PE=1: 4 as eluent. The final separation was accomplished by preparative TLC with DCM: PE=1: 6 as eluent.

Yield: 0.03 g (25%), colorless oil.

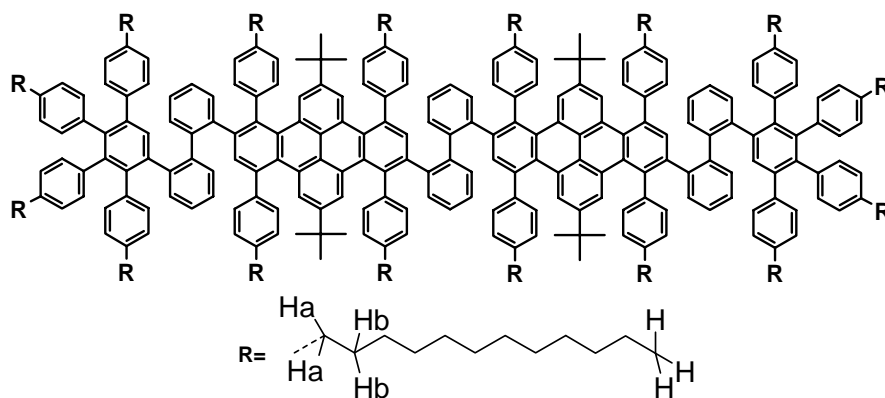
FD-MS (8KV), m/z [ue^{-1}]: 2776.6 (M^+) (cal. for $C_{208}H_{274}$ 2774.50)

1H -NMR (700 MHz, THF- d_8 , 333 K): δ (ppm)= 7.86 (t, 1H), 7.77 (m, 4H), 7.54 (s, 2H), 7.41 (t, 4H), 7.18 (m, 14H), 6.95 (m, 26H), 6.70 (m, 14H), 6.42 (s, 2H), 6.29 (s, 2H), 6.15 (m, 2H), 3.28 (s, 1H, H_{CH}), 2.63 (m, 4H, $H_{CH_2-\alpha}$), 2.54 (m, 4H, $H_{CH_2-\alpha}$), 2.47 (m, 4H, $H_{CH_2-\alpha}$), 2.37 (m, 4H, $H_{CH_2-\alpha}$), 2.26 (s, 9H, H_{t-but}), 2.00 (m, 4H, $H_{CH_2-\beta}$), 1.66 (m, 4H,

$H_{CH2-\beta}$), 1.62 (m, 4H, $H_{CH2-\beta}$), 1.55 (m, 4H, $H_{CH2-\beta}$), 1.35 (br.s, 144H, $H_{CH2-rest}$), 0.89 (s, 33H, $H_{CH3}+H_{t-but-rest}$)

^{13}C -NMR (700 MHz, THF- d_8 , 333 K): δ (ppm)= 144.81, 144.25, 143.52, 143.40, 143.28, 143.18, 142.72, 142.09, 141.99, 141.95, 141.83, 141.80, 141.54, 141.25, 141.21, 141.14, 141.00, 140.80, 140.69, 140.55, 140.48, 140.29, 140.07, 140.00, 139.66, 139.28, 139.05, 138.92, 138.62, 135.44, 135.42, 135.26, 135.22, 134.87, 134.81, 134.29, 134.20, 133.90, 133.71, 133.19, 133.03, 132.93, 132.80, 132.64, 132.26, 131.90, 131.60, 130.99, 130.54, 130.07, 129.81, 129.26, 129.02, 128.78, 128.49, 128.11, 127.72, 127.66, 127.50, 127.32, 127.21, 127.10, 126.89, 126.66, 126.24, 125.77, 84.66, 82.22, 36.85, 36.70, 36.50, 36.41, 36.25, 35.38, 35.29, 33.12, 32.81, 32.46, 32.18, 31.87, 31.79, 30.90, 30.86, 30.79, 30.75, 30.52, 30.12, 29.91, 23.76, 14.60

7.2.6 1,2'-Bis(2,7-di-*tert*-butyl-4,5:9,10-bis(2,5-di-*p*-dodecylphenyl)-2',3',4',5'-tetrakis(*p*-dodecylphenyl)-[1',1'';2'',3]terphenyldibenzo[*e,l*]pyreno)biphenyl (**2-15**)



In the 10 ml tube were added 0.112 g (0.043 mmol) of **2-12**, 0.009 g (0.043 mmol) of 2,2'-diethynyl-biphenyl (**2-8**) and 1 ml of toluene were placed in a microwave tube, which was purged with argon and sealed. The reaction was carried out in a CEM Discover microwave at 300 W and activated cooling, keeping the temperature at 110 °C for 1 h. The solvent was removed and the residue was treated via column

chromatography using silica with DCM: PE=1: 4 as eluent. The final separation was accomplished by preparative TLC with DCM: PE=1: 6 as eluent.

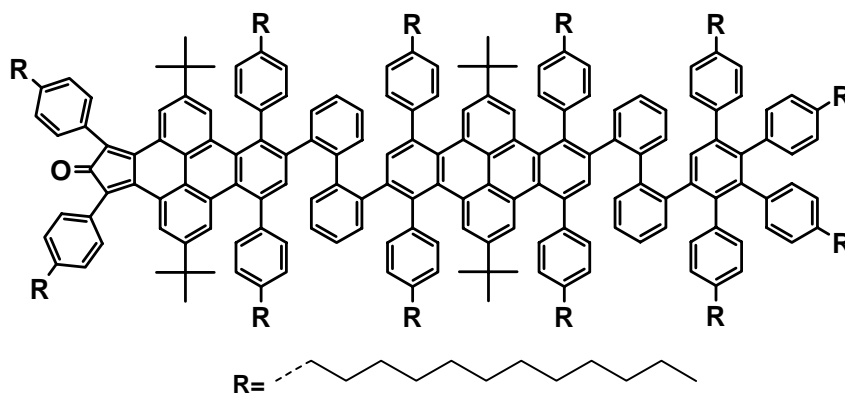
Yield: 0.06 g (15%), colorless oil.

MS(MALDI-TOF), m/z [ue^{-1}]: 5350 (M^+), 5373 (M^+K^+) (cal. for $C_{400}H_{538}$ 5346.75)

1H -NMR (700 MHz, THF- d_8 , 333 K): δ (ppm)= 8.26 (t, 1H), 8.14 (t, 3H), 8.03 (t, 1H), 7.87 (s, 4H), 7.79 (s, 4H), 7.75 (s, 2H), 7.64 (s, 6H), 7.57 (s, 4H), 7.30 (br.t, 56H), 6.97 (br.t, 28H), 6.84 (s, 6H), 6.77 (s, 6H), 6.64 (s, 4H), 6.46 (t, 3H), 6.32 (t, 2H), 6.17 (t, 1H), 5.66 (t, 1H), 2.69 (m, 6H, $H_{CH_2-\alpha}$), 2.54 (m, 8H, $H_{CH_2-\alpha}$), 2.47 (m, 6H, $H_{CH_2-\alpha}$), 2.37 (m, 12H, $H_{CH_2-\alpha}$), 2.30 (s, 18H, H_{t-but}), 2.03 (m, 6H, $H_{CH_2-\beta}$), 1.60 (m, 8H, $H_{CH_2-\beta}$), 1.57 (m, 6H, $H_{CH_2-\beta}$), 1.30 (br.s, 300H, H_{CH_2-rest}), 0.89 (s, 66H, $H_{CH_3}+H_{t-but}$)

^{13}C -NMR (700 MHz, THF- d_8 , 333 K): δ (ppm)= 143.54, 143.23, 142.97, 142.71, 141.53, 141.40, 141.25, 140.94, 140.74, 140.55, 140.42, 140.04, 139.88, 139.69, 139.03, 138.65, 138.43, 137.84, 137.65, 134.88, 134.66, 134.28, 134.22, 133.68, 133.49, 133.30, 133.11, 132.72, 132.61, 132.49, 132.38, 132.29, 131.38, 131.07, 131.01, 130.91, 130.24, 129.96, 129.48, 129.24, 128.64, 128.50, 127.50, 127.12, 126.86, 126.07, 125.85, 125.59, 125.14, 36.36, 36.10, 35.90, 34.76, 32.51, 32.29, 31.84, 31.58, 31.25, 30.52, 30.27, 29.92, 29.51, 23.16, 14.02

7.2.7 2,7-Di-*tert*-butyl-4,5-(2,5-di-*p*-dodecylphenyl)benzene-2',7'-di-*tert*-butyl-4',5':9',10'-(2',5'-di-*p*-dodecylphenyl-2'',3'',4'',5''-tetrakis(*p*-dodecylphenyl)-[1'',1''';2''',3']terphenyl-3'-biphenyl)dibenzo[*e,l*]pyreno)-9,10-cyclopenta[*e*]pyrene-10-one (**2-16**)

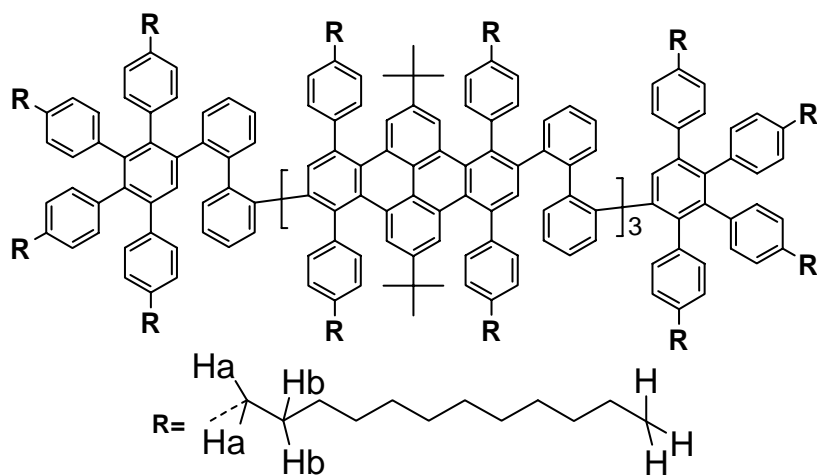


In the 10 ml tube were added 0.21 g (0.08 mmol) of **2-14**, 0.11 g (0.08 mmol) of ,7-di-*tert*-butyl-4,5:9,10-bis(2,5-di-*p*-dodecyl-phenylcyclopenta)-[*e,l*]pyrene-5,11-dione (**2-7**) and 2 ml of toluene were placed in a microwave tube, which was purged with argon and sealed. The reaction was carried out in a CEM Discover microwave at 300 W and activated cooling, keeping the temperature at 110 °C for 1 h. The solvent was removed and the residue was treated via column chromatography using silica with DCM: PE=1: 2 as eluent.

Yield: 0.09g (29%), green amorphous compound, which is unstable and was thus used without complete characterization.

MS(MALDI-TOF), m/z [$\text{u}e^{-1}$]: 4142 (M^+) (cal. for $C_{309}H_{412}$ 4142.73)

7.2.8 2,7-Di-*tert*-butyl-4,5:9,10-bis(2,5-di-*p*-dodecylphenyl-2',7'-di-*tert*-butyl-4',5':9',10'-(2',5'-di-*p*-dodecylphenyl-2'',3'',4'',5''-tetrakis(*p*-dodecylphenyl)-[1'',1''';2''',3']terphenyl-3'-biphenyl)dibenzo[*e,l*]pyreno)dibenzo[*e,l*]pyrene (**2-17**)



In the 10 ml tube were added 0.21 g (0.08 mmol) of **2-14**, 0.11 g (0.08 mmol) of ,7-di-*tert*-butyl-4,5:9,10-bis(2,5-di-*p*-dodecyl-phenylcyclopenta)-[*e,l*]pyrene-5,11-dione (**2-7**) and 2 ml of toluene were placed in a microwave tube, which was purged with argon and sealed. The reaction was carried out in a CEM Discover microwave at 300 W and activated cooling, keeping the temperature at 110 °C for 1 h. The solvent was removed and the residue was treated via column chromatography using silica with DCM: PE=1: 5 as eluent.

Yield: 0.07 g (15%), colorless oil.

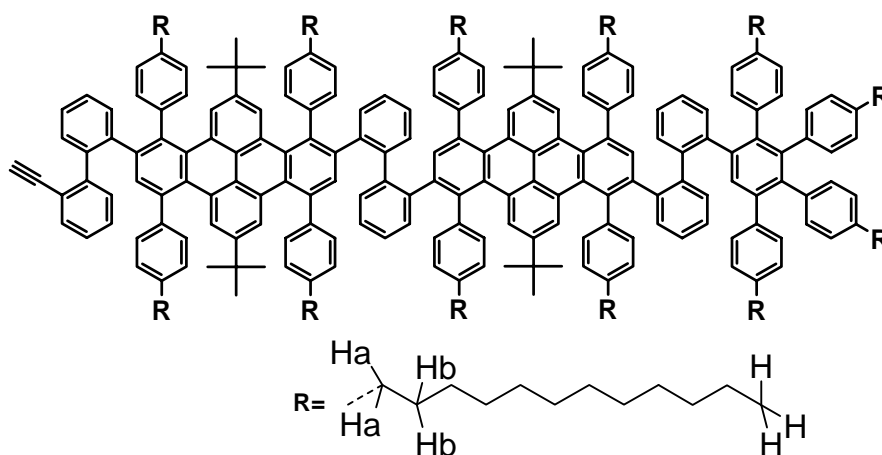
MS(MALDI-TOF), m/z [ue^{-1}]: 6889 (M^+) (cal. for $C_{516}H_{686}$ 6889.22)

UV/vis: λ / nm ($\epsilon / m^2 \cdot mol^{-1}$) = 310 (24 990), 256 (29 580)

1H -NMR (700 MHz, THF- d_8 , 338K): δ (ppm)= 7.97-7.88 (tt, 3H), 7.84-7.82 (tt, 3H), 7.79-7.76 (tt, 3H), 7.58 (br.s, 4H), 7.52-7.44 (tt, 8H), 7.37 (t, 6H), 7.30 (t, 3H), 7.24 (t, 6H), 7.18 (s, 1H), 7.17 (s, 1H), 7.13 (t, 4H), 7.08 (t, 8H), 7.02 (t, 8H), 6.92-6.85 (tt, 19H), 6.78 (br.s, 6H), 7.70-7.55 (tt, 16H), 7.47 (t, 8H), 7.32 (s, 1H), 7.27 (s, 1H), 7.20 (s, 2H), 7.09 (s, 1H), 6.01 (s, 1H), 5.97 (s, 1H), 5.86 (dd, 1H, $^3J(H,H)=5.12$ MHz), 5.42 (s, 1H), 2.68 (m, 5H, $H_{CH_2-\alpha}$), 2.51(s, 54H, H_{t-but}), 2.41 (m, 15H, $H_{CH_2-\alpha}$), 2.02 (m, 10H, $H_{CH_2-\beta}$), 1.95 (m, 10H, $H_{CH_2-\beta}$), 1.29 (br.s, 360H, H_{CH_2-rest}), 0.89 (br.s, 60H, H_{CH_3})

^{13}C -NMR (700 MHz, THF- d_8 , 338 K): $\delta(\text{ppm})= 144.09, 144.01, 143.96, 143.94, 143.89, 143.85, 143.81, 143.78, 143.74, 143.66, 143.58, 143.52, 143.44, 143.37, 143.31, 143.24, 143.22, 143.12, 143.06, 143.03, 141.97, 141.93, 141.88, 141.85, 141.75, 141.73, 141.61, 141.57, 141.50, 141.48, 141.44, 141.32, 141.22, 140.92, 140.87, 140.76, 140.55, 140.51, 140.43, 140.38, 140.25, 140.12, 139.96, 139.89, 139.81, 139.72, 139.68, 139.56, 139.27, 139.23, 139.14, 138.98, 138.90, 138.74, 138.51, 138.42, 138.34, 135.27, 135.06, 134.85, 134.81, 134.63, 134.48, 134.27, 134.04, 133.88, 133.79, 133.64, 133.49, 133.45, 133.32, 133.02, 132.70, 132.66, 132.61, 132.48, 132.23, 131.53, 131.43, 131.22, 131.20, 130.91, 130.85, 130.65, 130.57, 130.27, 130.16, 129.97, 129.92, 129.78, 129.60, 129.52, 129.42, 129.38, 129.26, 129.19, 129.11, 129.04, 128.96, 128.84, 128.80, 127.96, 127.86, 127.80, 127.67, 127.44, 127.28, 127.24, 127.16, 127.14, 126.75, 126.59, 126.53, 126.42, 126.25, 126.04, 38.56, 38.51, 38.46, 38.16, 36.83, 36.59, 36.30, 34.75, 34.46, 34.26, 33.88, 33.67, 33.00, 32.44, 31.95, 31.21, 31.09, 30.76, 30.44, 28.14, 27.75, 23.69$

7.2.9 2,7-Di-*tert*-butyl-4,5:9,10-(2,5-di-*p*-dodecylphenyl-2',7'-di-*tert*-butyl-4',5':9',10'-(2',5'-di-*p*-dodecylphenyl-2'',3'',4'',5''-tetrakis(*p*-dodecylphenyl)-[1'',1''';2'',3]terphenyl-3-biphenyl)dibenzo[*e,l*]pyreno-2''''-ethinyl-3-biphenyl)dibenzo[*e,l*]pyrene (**2-18**)



In the 10 ml tube were added 0.09 g (0.02 mmol) of **2-16**, 0.002 g (0.02 mmol) of 2,2'-diethynyl-biphenyl (**2-8**) and 1 ml of toluene were placed in a microwave tube, which

was purged with argon and sealed. The reaction was carried out in a CEM Discover microwave at 300 W and activated cooling, keeping the temperature at 110 °C for 1 h. The solvent was removed and the residue was treated via column chromatography using silica with DCM: PE=1: 4 as eluent. The final separation was accomplished by preparative TLC with DCM: PE=1: 6 as eluent.

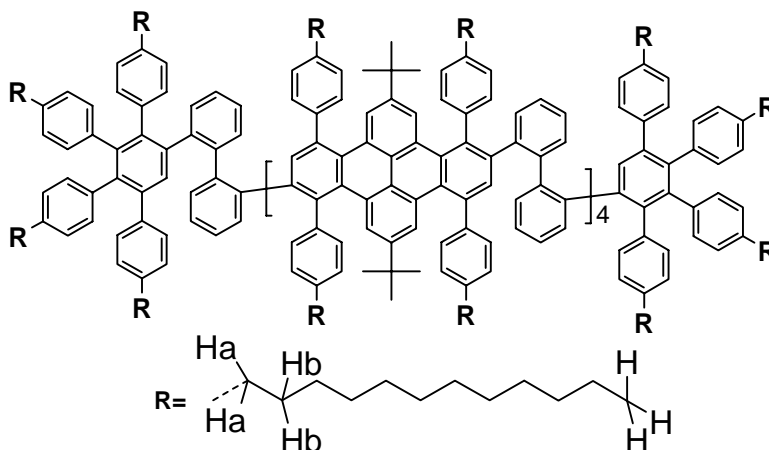
Yield: 0.03 g (34%), colorless oil.

MS(MALDI-TOF), m/z [$u\epsilon^{-1}$]: 4317 (M^+) (cal. for $C_{324}H_{422}$ 4316.98)

1H -NMR (500 MHz, THF- d_8 , 338K): δ (ppm)= 8.00 (s, 1H), 7.97 (s, 1H), 7.86 (t, 4H), 7.72 (m, 8H), 7.55 (s, 4H), 7.42 (t, 8H), 7.19 (t, 16H), 6.96 (t, 38H), 6.71 (t, 16H), 6.43 (s, 2H), 6.30 (s, 2H), 6.13 (t, 2H), 5.85 (t, 1H), 3.28 (s, 1 H_{CH}), 2.63 (m, 6H, $H_{CH2-\alpha}$), 2.55 (m, 6H, $H_{CH2-\alpha}$), 2.48 (m, 3H, $H_{CH2-\alpha}$), 2.39 (m, 6H, $H_{CH2-\alpha}$), 2.24(s, 6H, H_{t-but}), 2.03 (m, 3H, $H_{CH2-\beta}$), 1.62 (m, 12H, $H_{CH2-\beta}$), 1.29 (br.s, 228H, $H_{CH2-rest}$), 0.89 (br.s, 66H, $H_{CH3}+H_{t-but-rest}$)

^{13}C -NMR (500 MHz, THF- d_8 , 338 K): δ (ppm)= 143.99, 143.94, 143.93, 143.84, 143.72, 143.01, 141.82, 141.70, 141.67, 141.55, 141.24, 140.73, 140.70, 140.50, 140.18, 140.10, 140.00, 138.80, 138.25, 133.61, 132.88, 132.64, 131.64, 131.61, 131.29, 130.75, 130.77, 130.25, 130.18, 129.88, 129.58, 129.52, 129.41, 127.81, 127.36, 126.39, 125.95, 125.87, 36.56, 36.40, 36.12, 35.02, 32.82, 32.51, 32.17, 31.58, 31.51, 30.61, 30.22, 29.84, 23.46, 14.29

7.2.10 1,2'-Bis(bis(2'',7''-di-*tert*-butyl-4'',5''-9'',10''-bis(2'',5''-di-*p*-dodecylphenyl)-2''',3''',4''',5''')-tetrakis(*p*-dodecylphenyl)-[1''',1'''';2''''',3''']terphenyldibenzo[*e,l*]pyreno))biphenyl (**2-19**)



In the 10 ml tube were added 0.09 g (0.02 mmol) of **2-16**, 0.002 g (0.02 mmol) of 2,2'-diethynyl-biphenyl (**2-8**) and 1 ml of toluene were placed in a microwave tube, which was purged with argon and sealed. The reaction was carried out in a CEM Discover microwave at 300 W and activated cooling, keeping the temperature at 110 °C for 1 h. The solvent was removed and the residue was treated via column chromatography using silica with DCM: PE=1: 4 as eluent. The final separation was accomplished by preparative TLC with DCM: PE=1: 6 as eluent.

Yield: 0.026 g (15%), colorless oil.

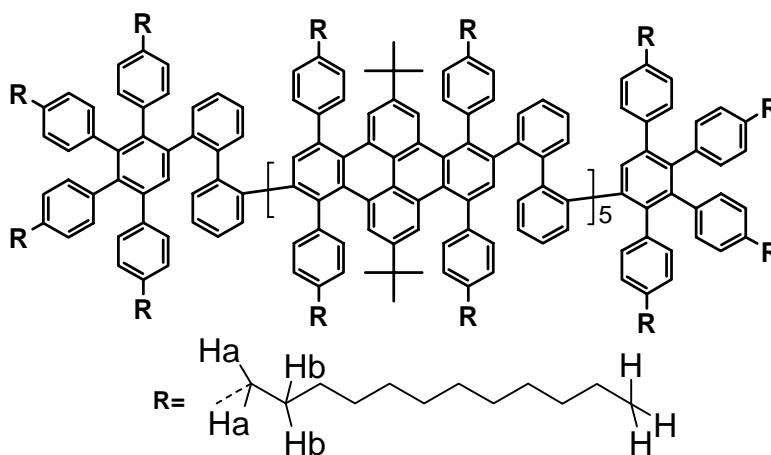
MS(MALDI-TOF), m/z [ue^{-1}]: 8430 (M^+) (cal. for $C_{632}H_{834}$ 8431.69)

1H -NMR (500 MHz, THF- d_8 , 338K): δ (ppm)= 7.93 (t, 4H), 7.78 (t, 4H), 7.68 (t, 4H), 7.55 (s, 8H), 7.46 (t, 8H), 7.34 (tt, 10H), 6.92 (t, 6H), 6.71 (br.t, 66H), 6.52 (br.t, 28H), 6.41 (s, 6H), 6.30 (s, 6H), 6.17 (t, 2H), 6.04 (t, 2H), 5.97 (t, 1H), 5.85 (t, 2H), 2.69 (m, 5H, $H_{CH2-\alpha}$), 2.55 (m, 6H, $H_{CH2-\alpha}$), 2.48 (m, 6H, $H_{CH2-\alpha}$), 2.38 (m, 8H, $H_{CH2-\alpha}$), 2.25 (s, 36H, H_{t-but}), 2.04 (m, 3H, $H_{CH2-\beta}$), 1.66 (m, 6H, $H_{CH2-\beta}$), 1.59 (m, 14H, $H_{CH2-\beta}$), 1.29 (br.s, 432H, $H_{CH2-rest}$), 0.89 (s, 108H, $H_{CH_3}+H_{t-but-rest}$)

^{13}C -NMR (500 MHz, THF- d_8 , 338 K): δ (ppm)= 144.10, 144.05, 143.98, 143.97, 143.88, 143.85, 143.78, 143.69, 143.54, 143.23, 142.97, 142.71, 141.53, 141.40, 141.25, 141.05, 140.94, 140.74, 140.55, 140.42, 140.04, 139.88, 139.78, 139.69, 139.45, 139.03, 138.65, 138.43, 137.84, 137.65, 134.88, 134.66, 134.28, 134.22, 133.68, 133.49, 133.30, 133.11,

132.72, 132.61, 132.49, 132.38, 132.29, 131.38, 131.07, 131.01, 130.91, 130.54, 130.24, 129.96, 129.76, 129.59, 129.48, 129.24, 128.85, 128.64, 128.50, 127.50, 127.12, 126.86, 126.62, 126.37, 126.07, 125.85, 125.59, 125.14, 36.36, 36.10, 35.90, 34.76, 32.51, 32.29, 31.84, 31.58, 31.25, 30.52, 30.27, 29.92, 29.51, 23.16, 14.02

7.2.11 2,7-Di-*tert*-butyl-4,5:9,10-bis(2,5-di-*p*-dodecylphenyl-bis(2',7'-di-*tert*-butyl-4',5':9',10'-(2'',5''-di-*p*-dodecylphenyl-2''',3''',4''',5'''-tetrakis(*p*-dodecylphenyl)-[1''',1''';2''',3'']terphenyl-3'-biphenyl)dibenzo[*e,l*]pyreno))dibenzo[*e,l*]pyrene (**2-21**)



In the 10 ml tube were added 0.030 g (0.007 mmol) of **2-18**, 0.01 g (0.007 mmol) of 7-di-*tert*-butyl-4,5:9,10-bis(2,5-di-*p*-dodecyl-phenylcyclopenta)-[*e,l*]pyrene-5,11-dione (**2-7**) and 0.5 ml of toluene were placed in a microwave tube, which was purged with argon and sealed. The reaction was carried out in a CEM Discover microwave at 300 W and activated cooling, keeping the temperature at 110 °C for 1 h. The solvent was removed and the residue was treated via column chromatography using silica with DCM: PE=1: 4 as eluent.

Yield: 0.007 g (10%), colorless oil.

MS(MALDI-TOF), m/z [ue^{-1}]: 9968 (M^+) (cal. for $C_{284}H_{390}$ 9974.17)

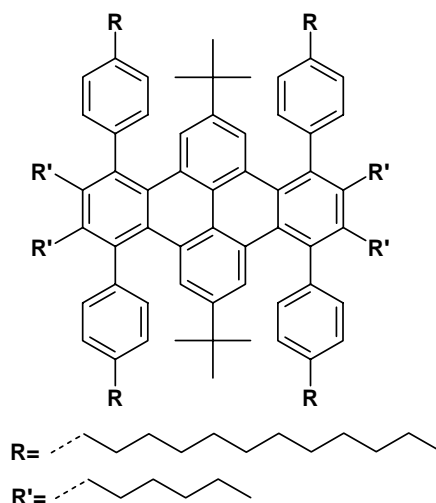
UV/vis: λ / nm ($\epsilon / m^2 \cdot mol^{-1}$) = 310 (28 500), 256 (38 500)

1H -NMR (500 MHz, THF- d_8 , 338K): δ (ppm) = peaks are very broad – 8.25-8.18 (br.m, 1H), 8.08-8.02 (br.m, 1H), 7.90 (br.s, 1H), 7.80 (br.s, 2H), 7.68 (s, 4), 7.60-7.52 (br.m,

4H), 7.51-7.47 (br.m, 6H), 7.46-7.38 (br.m, 6H), 7.37-7.16 (br.m, 28H), 7.16-6.94 (br.m, 50H), 6.93-6.81 (br.m, 28H), 6.80-6.48 (br.m, 50H), 6.45-6.34 (br.m, 8H), 6.23-6.08 (br.m, 1H), 2.68 (m, 12H, H_{CH2- α}), 2.55 (m, 22H, H_{CH2- α}), 2.04 (m, 22H, H_{CH2- α}), 1.89 (s, 27H, H_{*t*-but}), 1.60 (s, 45H, H_{*t*-but}), 1.29 (br.s, 504H, H_{CH2-rest}), 0.89 (s, 102H, H_{CH3+H_{*t*-but-rest}})

¹³C-NMR (500 MHz, THF-d₈, 338 K): amount of the compound was not enough to identify peaks

7.2.12 2,7-Di-*tert*-butyl-4,5:9,10-bis(3,4-dihexyl-2,5-di-*p*-dodecylphenyl)dibenzo[*e,l*]pyrene (**2-26**)



In the 10 ml tube were added 0.05 g (0.04 mmol) of 2,7-di-*tert*-butyl-4,5:9,10-bis(2,5-di-*p*-dodecyl-phenylcyclopenta)-[*e,l*]pyren-5,11-dione (**2-7**), 0.07 g (0.08 mmol) of **2-25** and 1.5 ml of diphenylether were placed in a microwave tube, which was purged with argon and sealed. The reaction was carried out in a CEM Discover microwave at 300 W and activated cooling, keeping the temperature at 220 °C for 1 h. The solvent was removed and the residue was treated via column chromatography using silica with DCM: PE=1:19 as eluent.

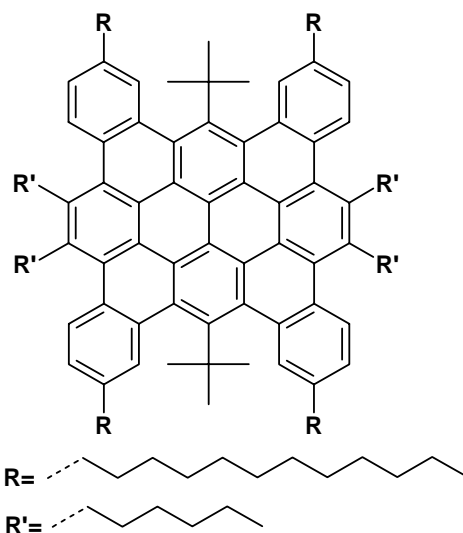
Yield: 0.03 g (55%), colorless oil.

MS(MALDI-TOF), m/z [ue^{-1}]: 1727 (M^+) (cal. for C₁₂₈H₁₉₀ 1728.94)

$^1\text{H-NMR}$ (250 MHz, THF- d_8 , 298 K): $\delta(\text{ppm})= 7.59$ (s, 4H), 7.21 (s, 16H), 2.64 (m, 16H, $\text{H}_{\text{CH}_2-\alpha}$), 1.66 (m, 8H, $\text{H}_{\text{CH}_2-\beta}$), 1.29 (br.s, 72H, H_{CH_2}), 1.09 (br.s, 24H, H_{CH_3}), 0.89 (m, 16H, H_{CH_2}), 0.80 (m, 16H, H_{CH_2}), 0.67 (s, 18H, $\text{H}_{t\text{-but}}$)

$^{13}\text{C-NMR}$ (250 MHz, THF- d_8 , 298 K): $\delta(\text{ppm})= 144.61, 141.49, 141.35, 139.92, 138.70, 131.23, 129.87, 128.88, 127.87, 125.20, 125.08, 35.96, 34.66, 32.18, 31.89, 31.42, 31.18, 29.97, 29.91, 29.62, 22.94, 22.67, 14.11, 14.02$

7.2.13 3,4,10,11-Tetra-hexyl-7,14-di-*t*-butyl-tetra-dodecyltetra benzo[*a,g,e,r*]ovalene (**2-27**)

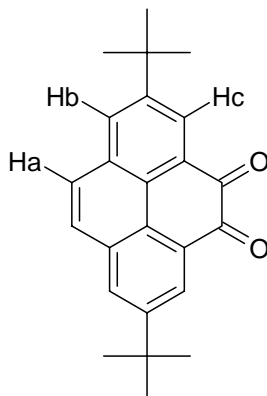


In a 50 ml 2-neck flask a solution of 2,7-di-*tert*-butyl-4,5:9,10-bis(3,4-dihexyl-2,5-di-*p*-dodecylphenyl)dibenzo[*e,l*]pyrene (**2-26**) (0.010 g, 0.006 mmol) in 6 mL of dry dichloromethane was degassed for 15 min, afterwards FeCl_3 (0.011 g, 0.070 mmol) in 0.11 ml nitromethane was quickly added. The reaction mixture was vigorously stirred at room temperature, while continuously argon was bubbling. After 1 h the reaction was quenched with methanol and the precipitate was filtered and washed with methanol. The crude product was dissolved in hot toluene and filtered over a short silica column.

Yield: 0.008 g (80%)

MS(MALDI-TOF), m/z [$\text{u}e^{-1}$]: 1721 (M^+) (cal. for $\text{C}_{128}\text{H}_{182}$ 1720.88)

UV/vis: λ / nm ($\epsilon / \text{m}^2 \cdot \text{mol}^{-1}$) = 524 (525), 451 (3 168), 383 (6 125)

7.2.14 2,7-Di-*tert*-butylpyrene-4,5-dione (**3-7**)

To a solution of 2,7-di-*tert*-butyl-pyrene (**2-5**) (10.00 g, 0.03 mol) in DCM (1L) and CH₃CN (1L) were added NaIO₄ (31.80 g, 0.15 mol), H₂O (1L) and RuCl₃·xH₂O (0.64 g, 3.07 mmol).¹ The dark brown suspension was stirred at room temperature overnight. The reaction mixture was poured into water and extracted with DCM (3 times). The organic phase was collected and solvent was removed under reduced pressure to afford a dark orange solid. Column chromatography (DCM) gave pure product as bright orange crystals.

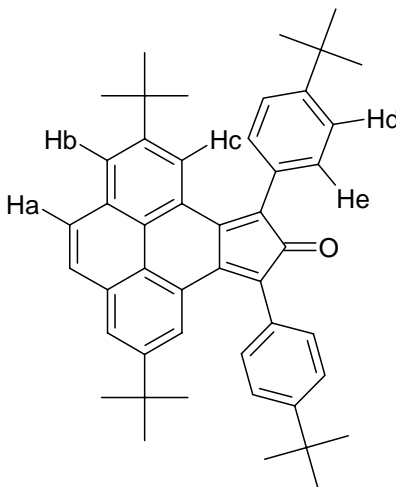
Yield: 4.00 g (36%)

FD-MS (8KV), m/z[ue⁻¹]: 344 (M⁺) (cal. for C₂₄H₂₄O₂ 344.46)

¹H NMR (250 MHz, CD₂Cl₂, 298 K): δ (ppm) = 8.51(d, ⁴J(H,H)=2 Hz, 2H, H_c), 8.17 (d, ⁴J(H,H)=2 Hz, 2H, H_b), 7.83 (s, 2H, H_a), 1.49 (s, 18H, H_{*t*-but})

¹³C-NMR (250 MHz, CD₂Cl₂, 298 K): δ(ppm)= 181.7, 151.9, 132.8, 132.6, 130.6, 128.7, 128.1, 127.2, 35.9, 31.7

Elemental Analysis: 84.51% C, 7.07% H (cal. 83.69% C, 7.02% H, 9.29% O)

7.2.15 2,7-Di-*tert*-butyl-4,5-bis-(4-*tetr*-butyl-phenyl)-cyclopenta[*e*]pyren-5-one (**3-9**)

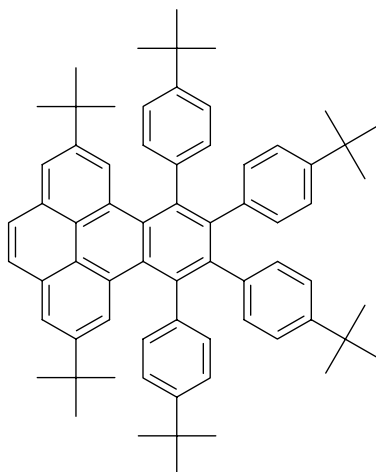
3.90 g (0.01 mol) 2,7-di-*tert*-butylpyrene-4,5-dione (**3-7**) and 3.32 g (11.00 mmol) 1,3-bis-(4-*tert*-butyl-phenyl)propan-2-one (**3-8**) were suspended in 0.17 L of ethanol under inert atmosphere.² A solution prepared from 0.31 g KOH (5.60 mmol) in 10 ml methanol was added dropwise at room temperature. The mixture was heated to 80 °C for 15 minutes. The product was extracted with DCM, concentrated and the residue was purified by column chromatography (petroleum ether/DCM=3:1) to yield product as dark brown solid.

Yield: 5.34g (77%)

FD-MS (8KV), m/z [ue^{-1}]: 630.8 (M^+) (cal. for $C_{47}H_{50}O$ 630.9)

1H NMR (250 MHz, CD_2Cl_2 , 298K): δ (ppm)= 7.80 (d, $^4J(H,H)=1.90$ Hz, 2H, H_b), 7.68 (d, $^4J(H,H)=1.90$ Hz, 2H, H_c), 7.61 (s, 2H, H_a), 7.58 (d, $^3J(H,H)=8.53$ Hz, 2H, H_f), 7.38 (d, $^3J(H,H)=8.53$ Hz, 2H, H_e), 1.39 (s, 18H, H_{*t*-but}), 1.10 (s, 18H, H_{*t*-but})

^{13}C -NMR (250 MHz, CD_2Cl_2 , 298 K): δ (ppm)= 201.63, 151.51, 150.06, 148.73, 132.34, 130.89, 129.89, 127.43, 127.36, 127.09, 126.90, 126.28, 125.03, 123.97, 35.01, 34.89, 31.41, 30.93

7.2.16 2,7-Di-*tert*-butyl-4,5,6,7-tetrakis-(4-*tert*-butyl-phenyl)-benzo[*e*]pyrene (**3-11**)

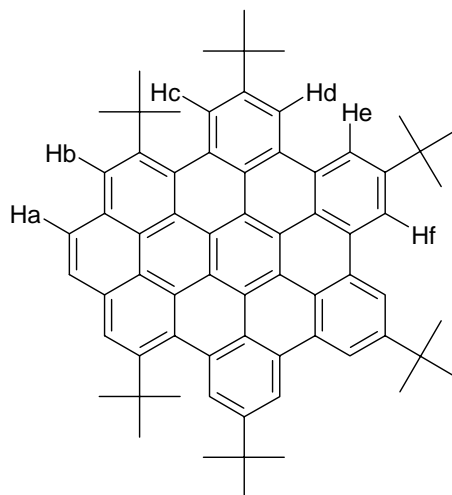
5.34 g (8.46 mmol) 2,7-di-*tert*-butyl-4,5-bis(4-*tert*-butyl-phenyl)-cyclopenta[*e*]pyren-5-one (**3-9**) and 2.45 g (8.46 mmol) di-*tert*-butyldiphenylacetylene (**3-10**) in 8 ml diphenylether were heated to 220 °C for 5 h.² Chromatography (petroleum ether/DCM=4:1) afford product as a yellow solid.

Yield: 5.47 g (72%)

FD-MS (8KV), m/z [ue⁻¹]: 893.7 (M⁺) (cal. for C₆₈H₇₈ 895.3)

¹H NMR (250 MHz, CD₂Cl₂, 298 K): δ(ppm)=8.29 (d, ⁴J(H,H)=1.75 Hz, 2H), 7.92 (d, ⁴J(H,H)=1.75 Hz, 4H), 7.09 (d, ³J(H,H)=8.53 Hz, 4H), 6.91 (m, 8H), 6.63 (d, ³J(H,H)=8.53 Hz, 4H), 1.22 (s, 18H, H_{*t*-but}), 1.18 (s, 18H, H_{*t*-but}), 1.08 (s, 18H, H_{*t*-but})

¹³C-NMR (62.5 MHz, CD₂Cl₂, 298 K): δ(ppm)= 143.66, 141.25, 140.97, 138.44, 132.36, 131.90, 131.67, 131.13, 130.20, 128.35, 128.26, 127.29, 126.87, 126.52, 125.71, 125.58, 125.56, 124.78

7.2.17 1,6-Di-*tert*-butyl-8,11,14,17-tetra(*t*-butyl)tetrabenzo[*bc,ef,hi,uv*]ovalene (**3-12**)

5.47 g (6.10 mmol) 2,7-di-*tert*-butyl-4,5,6,7-tetrakis-(4-*tert*-butyl-phenyl)-benzo[*e*]pyrene (**3-11**) was dissolved in 4.20 L DCM.² A constant stream of argon was bubbled into the solution through a glass capillary. A solution of 14.84 g (91.50 mmol) FeCl₃ in 80 ml CH₃NO₂ was then added dropwise via syringe. Throughout the whole reaction a constant stream of argon was bubbled through the mixture to remove HCl formed *in situ*. The reaction was stirred for 25 minutes and quenched by adding of methanol. The mixture was extracted with DCM, concentrated and the residue was purified by column chromatography (petroleum ether/DCM=5:1) to afford product as bright yellow powder.

Yield: 4.85 g (90%)

FD-MS (8KV), m/z [ue⁻¹]: 883.7 (M⁺) (cal. for C₆₈H₆₆: 882.5)

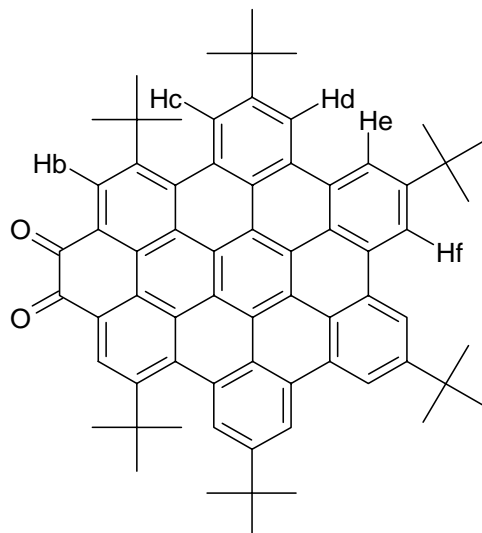
UV/vis: λ / nm (ε / m²·mol⁻¹) = 446 (1 900), 424 (1 800), 388 (5 800), 377 (5 415)

¹H NMR (250 MHz, CD₂Cl₂, 298K): δ(ppm)= 9.49 (s, 4H, H_{e+f}), 9.41 (s, 2H, H_d), 9.22 (s, 2H, H_c), 9.12 (s, 2H, H_b), 8.64 (s, 2H, H_a), 1.90 (s, 18H, H_{*t*-but}), 1.89 (s, 18H, H_{*t*-but}), 1.83 (s, 18H, H_{*t*-but})

¹³C-NMR (250 MHz, THF-d₈, 298 K): δ(ppm)= 150.45, 146.29, 132.04, 131.71, 131.15, 130.51, 130.36, 130.10, 129.43, 127.88, 127.72, 126.07, 124.79, 122.21, 121.18, 120.73, 120.35, 119.76, 119.65, 39.76, 36.62, 36.58, 35.31, 32.41, 32.36

Elemental Analysis: 92.31% C, 7.51% H (cal.: 92.47% C, 7.53% H)

7.2.18 1,6-Di-*tert*-butyl-8,11,14,17-tetra(*t*-butyl)tetrabenzo[*bc,ef,hi,uv*]ovalene-3,4-dione
(**3-13**)



To a solution of 1,6-di-*tert*-butyl-8,11,14,17-tetra(*t*-butyl)tetrabenzo[*bc,ef,hi,uv*]ovalene (**3-12**) (3.10 g, 3.50 mmol) in DCM (280 ml) and CH₃CN (280 ml) were added NaIO₄ (3.55 g, 16.40 mol), H₂O (280 ml) and RuCl₃·*x*H₂O (0.07 g, 0.34 mmol). The dark brown suspension was stirred at room temperature overnight. The reaction mixture was poured into water and extracted with DCM. The organic phase was collected and solvent was removed under reduced pressure to afford a dark solid. Column chromatography (DCM) gave pure product as dark brown solid.

Yield: 0.9 g (28%)

FD-MS (8KV), m/z [ue⁻¹]: 913.0 (M⁺) (cal. for C₆₈H₆₄O₂: 912.5)

UV/vis: λ / nm (ε / m²·mol⁻¹) = 588 (665), 460 (1 710), 433 (1 140), 397 (5 130), 368 (9 215)

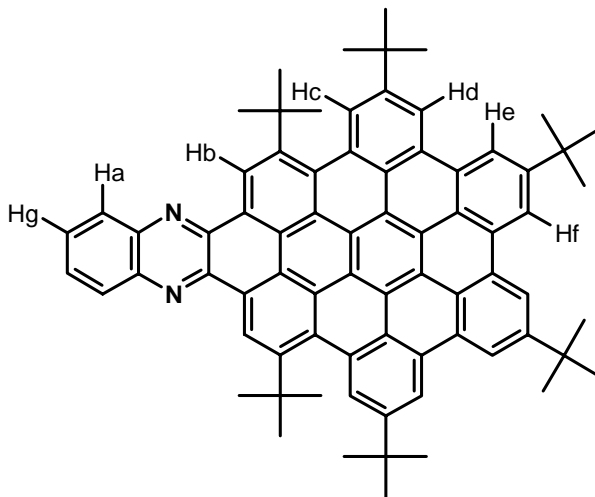
¹H NMR (250 MHz, CD₂Cl₂, 298 K): δ (ppm) = 9.47 (s, 2H, H_f), 9.41 (s, 2H, H_e), 9.34 (s, 2H, H_d), 9.14 (s, 2H, H_b), 8.76 (s, 2H, H_c), 1.86 (s, 18H, H_{*t*-but}), 1.77 (s, 18H, H_{*t*-but}), 1.75 (s, 18H, H_{*t*-but})

¹³C-NMR (250 MHz, THF-*d*₈, 298 K): δ(ppm) = 180.42, 150.80, 149.86, 147.52, 138.47, 131.42, 131.20, 131.10, 131.01, 130.87, 130.24, 128.49, 127.39, 126.11, 125.61, 123.95, 121.95, 121.45, 121.05, 120.25, 119.97, 39.49, 36.42, 34.27, 32.05, 31.91, 30.46

CV: E_{red}(V) = -0.66 (1e), -1.27 (1e)

Elemental Analysis: 89.44% C, 7.06% H (cal.: 89.43% C, 7.06% H)

7.2.19 1,6-Di-*tert*-butyl-8,11,14,17-tetra(*t*-butyl)tetrabenzo[*jk,mn,pq,st*]benzo[1,2-*a*]pyrazine[2,3-*d*]ovalene (**3-18**)



0.05g (0.05 mmol) of 1,6- di-*tert*-butyl-8,11,14,17-tetra- (*t*-butyl)tetrabenzo[*bc,ef,hi,uv*]ovalene-3,4-dione (**3-13**) and 0.01 g (0.05 mmol) of *o*-phenyldiamine dihydrochloride (**3-14**) were suspended in acetic acid (1 ml) under inert atmosphere. The mixture refluxed for 3 days. Column chromatography (DCM as eluent) gave pure product as an orange solid.

Yield: 0.04 g (76%)

MS(MALDI-TOF), m/z [ue^{-1}]: 985 (M^+) (cal. for $C_{74}H_{68}N_2$: 985.3)

UV/vis: λ / nm (ϵ / $m^2 \cdot mol^{-1}$) = 518 (855), 485 (950), 460 (1 330), 426 (2 090), 407 (4 465), 390 (5 795), 376 (8 360)

1H NMR (250 MHz, THF- d_8 , 298 K): δ (ppm) = 10.54 (s, 2H, H_b), 9.48 (s, 4H, H_{f+e}), 9.40 (s, 2H, H_d), 9.04 (s, 2H, H_c), 8.63 (m, 2H, H_g), 8.05 (m, 2H, H_a), 1.94 (s, 18H, H_{t-but}), 1.88 (s, 18H, H_{t-but}), 1.82 (s, 18H, H_{t-but})

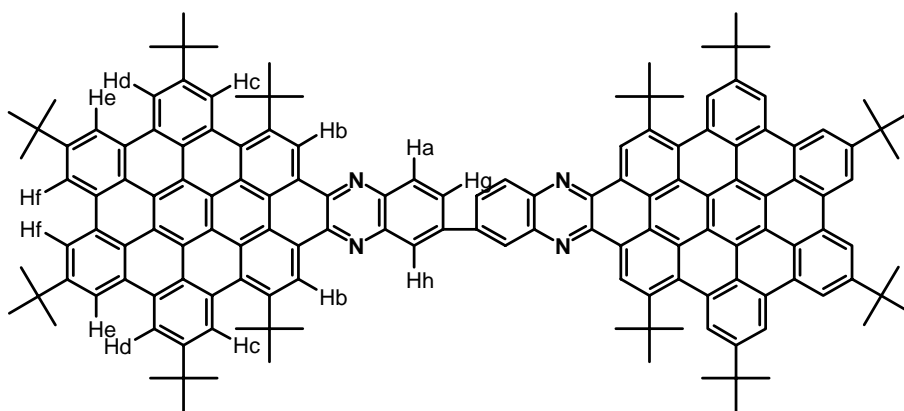
^{13}C NMR (500 MHz, $C_2D_2Cl_4$, 373 K): δ (ppm)= 150.16, 147.73, 146.48, 143.60, 142.92, 131.75, 131.12, 131.11, 130.70, 130.31, 130.07, 129.72, 129.53, 127.01, 126.86, 126.07,

124.76, 124.09, 123.21, 120.89, 120.35, 120.18, 119.78, 119.48, 119.21, 39.60, 36.05, 36.01, 35.13, 32.33, 32.22

CV: $E_{\text{red}}(\text{V}) = -0.87$ (1e), -1.38 (1e)

Elemental Analysis: 90.11% C, 6.95% H, 2.54% N (cal.: 90.20% C, 6.96% H, 2.84% N)

7.2.20 Bis(1,6-di-*tert*-butyl-8,11,14,17-tetra(*t*-butyl)tetrabenzo[*jk,mn,pq,st*]benzo[1,2-*a*]pyrazine[2,3-*d*]ovaleno)-[5,6:5',6'-*b,b'*]-5,5'-biphenyl (**3-19**)



0.05 g (0.05 mmol) of 1,6-di-*tert*-butyl-8,11,14,17-tetra-*t*-butyl)tetrabenzo[*bc,ef,hi,uv*]ovalene-3,4-dione (**3-13**) and 0.01 g (0.025 mmol) of 3,3'-diaminobenzidine tetrahydrochloride (**3-15**) were suspended in acetic acid (1 ml) under inert atmosphere. The mixture refluxed for 3 days. Column chromatography (DCM as eluent) gave pure product as a red solid.

Yield: 0.03 g (55%)

MS(MALDI-TOF), m/z [ue^{-1}]: 1968 (M^+) (cal. for $\text{C}_{148}\text{H}_{134}\text{N}_4$: 1968.7)

UV/vis: λ / nm (ϵ / $\text{m}^2 \cdot \text{mol}^{-1}$) = 541 (3 192), 498 (1 710), 471 (2 375), 428 (3 230), 409 (6 555), 376 (11 115)

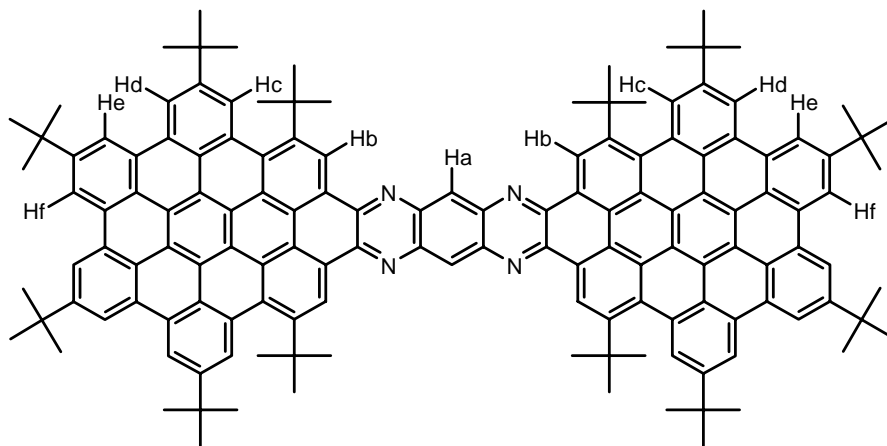
^1H NMR (500 MHz, $\text{C}_2\text{D}_2\text{Cl}_4$, 413 K): δ (ppm) = 10.52 (s, 2H, H_b), 10.47 (s, 2H, H_b), 9.32 (s, 8H, H_{f+e}), 9.23 (s, 4H, H_d), 9.17 (s, 2H, H_h), 8.96 (s, 4H, H_c), 8.79 (m, 2H, H_g), 8.60 (m, 2H, H_a), 1.94 (s, 18H, H_{*t*-but}), 1.86 (s, 18H, H_{*t*-but}), 1.82 (s, 18H, H_{*t*-but})

^{13}C NMR (500 MHz, $\text{C}_2\text{D}_2\text{Cl}_4$, 373 K): $\delta(\text{ppm}) = 150.44, 148.10, 146.78, 144.58, 144.51, 144.14, 143.41, 143.29, 142.96, 142.39, 141.72, 132.17, 131.41, 130.98, 130.54, 129.86, 128.53, 127.44, 127.39, 127.15, 126.41, 125.06, 124.37, 123.61, 121.18, 120.65, 120.47, 120.09, 119.72, 119.46, 39.91, 36.27, 35.43, 32.54, 32.46$

CV: $E_{\text{red}}(\text{V}) = -0.92 (2e), -1.32 (2e)$

Elemental Analysis: 90.15% C, 6.87% H, 2.61% N (cal.: 90.29% C, 6.86% H, 2.85% N)

7.2.21 Bis(1,6-di-*tert*-butyl-8,11,14,17-tetra(*t*-butyl)tetrabenzo[*bc,ef,hi,uv*]ovaleno)-[3,4:3',4'-*b,i*]-1,4,6,9-tetraazaanthracene (**3-20**)



0.05g (0.05 mmol) of 1,6-di-*tert*-butyl-8,11,14,17-tetra-*t*-butyl)tetrabenzo[*bc,ef,hi,uv*]ovalene-3,4-dione (**3-13**) and 0.01 g (0.025 mmol) of 1,2,4,5-tetraaminobenzene tetrahydrochloride (**3-16**) were suspended in acetic acid (1 ml) under inert atmosphere. The mixture refluxed 8 days. Column chromatography (DCM as eluent) gave pure product as green solid.

Yield: 0.03g (50%)

MS(MALDI-TOF), m/z [ue^{-1}]: 1892 (M^+) (cal. for $\text{C}_{142}\text{H}_{130}\text{N}_4$: 1892.6)

UV/vis: λ / nm ($\epsilon / \text{m}^2 \cdot \text{mol}^{-1}$) = 659 (3 990), 611 (2 660), 561 (1 140), 478 (3 610), 448 (2 660), 412 (11 210), 391 (12 065), 378 (12 255)

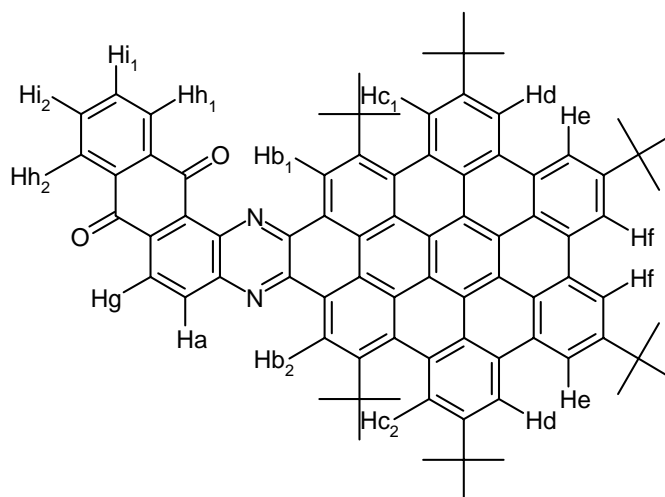
$^1\text{H-NMR}$ (250 MHz, CD_2Cl_2 , 298 K): δ (ppm) = 10.60 (s, 4H, H_b), 9.95 (s, 2H, H_a), 9.43 (s, 8H, H_{f+e}), 9.35 (s, 4H, H_d), 9.03 (s, 4H, H_c), 2.01 (s, 18H, $\text{H}_{t\text{-but}}$), 1.88 (s, 18H, $\text{H}_{t\text{-but}}$), 1.84 (s, 18H, $\text{H}_{t\text{-but}}$)

$^{13}\text{C-NMR}$ (700 MHz, $\text{C}_2\text{D}_2\text{Cl}_4$, 373 K): δ (ppm) = 150.27, 148.38, 146.71, 145.87, 141.88, 133.22, 131.18, 131.11, 130.80, 130.45, 129.64, 128.78, 128.22, 126.95, 126.44, 124.97, 124.08, 123.80, 121.02, 120.50, 120.15, 119.52, 119.30, 119.28, 39.71, 36.05, 35.14, 32.33, 32.24, 29.82

CV: $E_{\text{red}}(\text{V}) = -0.70$ (2e), -1.10 (2e)

Elemental Analysis: 90.12% C, 6.97% H, 2.82% N (cal.: 90.12% C, 6.92% H, 2.96% N)

7.2.22 1,6-Di-*tert*-butyl-8,11,14,17-tetra-
t-butyl)tetrabenzo[*jk,mn,pq,st*]anthraquinone[1,2-*a*]pyrazine[2,3-*d*]ovalene (**3-21**)



0.05 g (0.05 mmol) of 1,6-di-*tert*-butyl-8,11,14,17-tetra-
t-butyl)tetrabenzo[*bc,ef,hi,uv*]ovalene-3,4-dione (**3-13**) and 0.01 g (0.05 mmol) of 1,2-
diaminoanthroquinone (**3-17**) were suspended in acetic acid (2 ml) under inert
atmosphere. The mixture refluxed for 5 hours. Column chromatography (DCM as eluent)
gave pure product as a dark blue solid.

Yield: 0.03 g (57%)

MS(MALDI-TOF), m/z [ue^{-1}]: 1116 (M^+) (cal. for $C_{82}H_{70}N_2O_2$: 1115.4)

UV/vis: λ / nm (ϵ / $m^2 \cdot mol^{-1}$) = 602 (950), 481 (950), 451 (760), 432 (1 615), 413 (3 705), 388 (7 505), 380 (7 410)

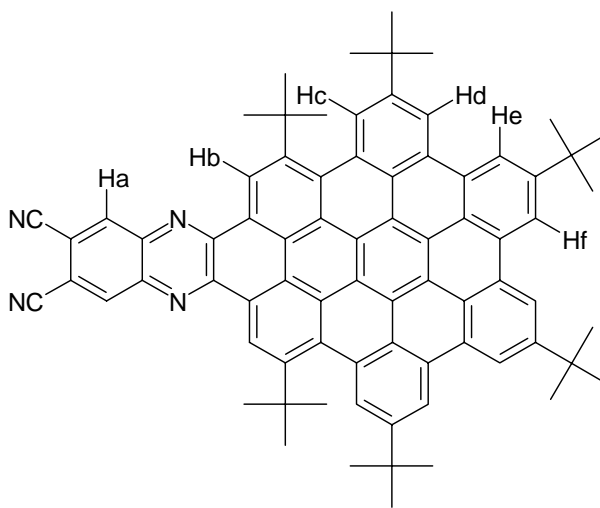
1H NMR (500 MHz, $C_2D_2Cl_4$, 373 K): δ (ppm) = 10.68 (s, 1H, H_{b1}), 10.38 (s, 1H, H_{b2}), 9.35 (s, 4H, H_{f+e}), 9.26 (s, 2H, H_d), 9.03 (s, 1H, H_{c1}), 8.98 (s, 1H, H_{c2}), 8.79 (d, 1H, $J=8.6$ Hz, H_g), 8.70 (d, 1H, $J=8.7$ Hz, H_a), 8.48 (d, 1H, $J=7.8$ Hz, H_{h1}), 8.25 (d, 1H, $J=7.8$ Hz, H_{h2}), 7.82 (m, 1H, H_{i1}), 7.72 (m, 1H, H_{i1}), 2.07 (s, 9H, H_{t-but}), 1.99 (s, 9H, H_{t-but}), 1.92 (s, 18H, H_{t-but}), 1.88 (s, 9H, H_{t-but}), 1.86 (s, 9H, H_{t-but})

^{13}C NMR (700 MHz, $C_2D_2Cl_4$, 373 K): δ (ppm)= 183.97, 182.84, 150.28, 148.41, 148.00, 146.64, 146.60, 146.16, 144.82, 144.16, 140.23, 135.93, 135.63, 135.48, 134.426, 133.27, 132.97, 132.70, 132.65, 131.15, 131.09, 130.72, 130.59, 130.50, 130.43, 129.99, 129.63, 127.48, 126.72, 126.63, 126.21, 126.05, 126.01, 125.95, 124.93, 124.87, 124.05, 123.56, 120.93, 120.49, 120.44, 120.20, 120.11, 120.07, 119.99, 119.52, 119.28, 36.05, 35.17, 35.12, 32.32, 32.25, 32.23

CV: $E_{red}(V)$ = -0.64 (1e), -1.25 (1e), -1.70 (2e)

Elemental Analysis: 87.98% C, 6.34% H, 2.32% N (cal.: 88.29% C, 6.33% H, 2.51% N)

7.2.23 1,6-Di-*tert*-butyl-8,11,14,17-tetra(*tert*-butyl)tetrabenzo[*jk,mn,pq,st*]-4,5-dicyanobenzo[1,2-*a*]pyrazine[2,3-*d*]ovalene (**4-9**)



0.20 g (0.20 mmol) of 1,6- di-*tert*-butyl-8,11,14,17-tetra-
(*t*-butyl)tetrabenzo[*bc,ef,hi,uv*]ovalene-3,4-dione (**3-13**) and 0.03 g (0.20 mmol) of 1,2-
diamino-4,5-dicyanobenzene (**4-8**) were suspended in acetic acid (2 ml) under inert
atmosphere. The mixture refluxed for 6 hours. Column chromatography (DCM as eluent)
gave pure product as a dark solid.

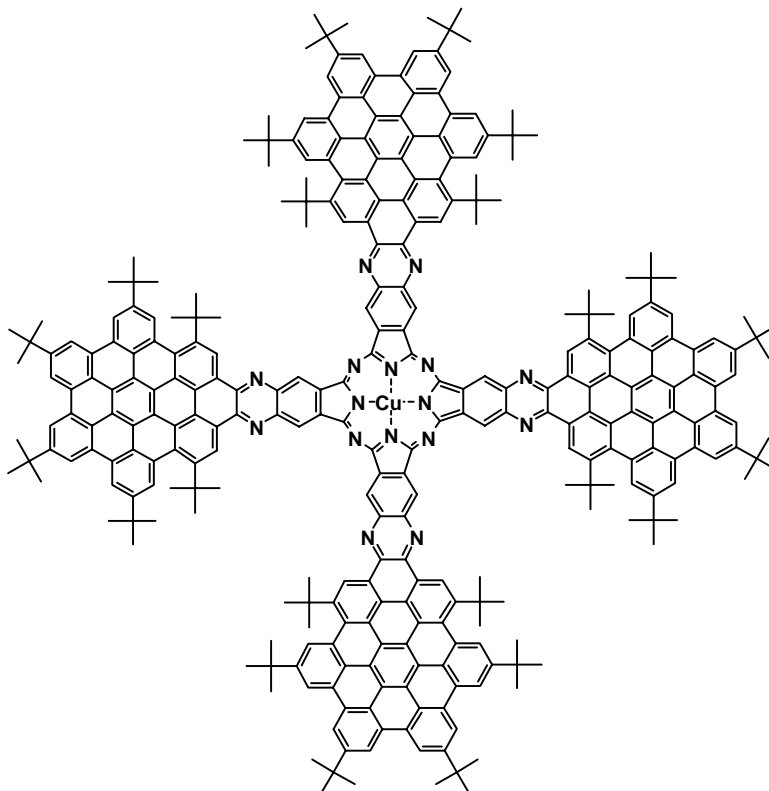
Yield: 0.16 g (77%)

MS(MALDI-TOF), m/z [ue^{-1}]: 1036 (M^+) (cal. for $C_{76}H_{66}N_4$: 1035.4)

1H -NMR (500 MHz, $C_2D_2Cl_4$, 373 K): δ (ppm) = 10.28 (s, 2H, H_b), 9.39 (s, 2H, H_f), 9.37
(s, 2H, H_e), 9.33 (s, 2H, H_d), 9.03 (s, 2H, H_c), 8.99 (s, 2H, H_a), 1.92 (s, 18H, H_{t-but}), 1.88
(s, 18H, H_{t-but}), 1.84 (s, 18H, H_{t-but})

^{13}C -NMR (500 MHz, $C_2D_2Cl_4$, 373 K): δ (ppm) = 150.33, 148.24, 146.61, 142.18,
137.21, 133.68, 130.95, 130.76, 130.28, 130.08, 129.45, 128.57, 127.58, 127.88, 125.91,
125.82, 125.02, 124.70, 123.84, 123.67, 120.68, 120.41, 119.40, 119.28, 115.47, 112.71,
39.48, 35.86, 35.84, 34.79, 32.08, 32.00, 29.60

Elemental Analysis: 87.88% C, 6.41% H, 5.02% N (cal.: 88.16% C, 6.43% H, 5.41% N)

7.2.24 1,6-Di-*tert*-butyl-8,11,14,17-tetra(*t*-butyl)tetrabenzo[*jk,mn,pq,st*]benzo[1,2-*a*]pyrazine[2,3-*d*]ovalenocyanine (**4-10**)

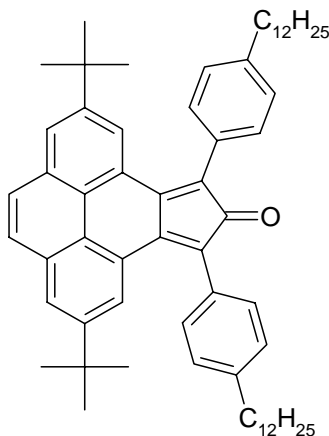
0.10 g (0.097 mmol) of 1,6-di-*tert*-butyl-8,11,14,17-tetra(*t*-butyl)tetrabenzo[*jk,mn,pq,st*]-4,5-dicyanobenzo[1,2-*a*]pyrazine[2,3-*d*]ovalene (**5-9**), 0.01 g (0.097 mmol) of CuCl₂ and 0.50 g of urea were suspended in 1-2 ml of quinoline under inert atmosphere. The mixture was heated at 220 °C for 16 hours. Column chromatography (DCM/THF=10/1 as eluent) gave product as a dark brown solid.

Yield: 0.03 g (7%)

MS(MALDI-TOF), m/z [ue⁻¹]: 4205 (M⁺) (calcd. for C₃₀₄H₂₆₄CuN₁₆: 4205.1)

UV/vis: λ / nm (ε / m²·mol⁻¹) = 865 (1 053), 785 (376), 563 (2 256), 474 (2 858), 379 (11 430)

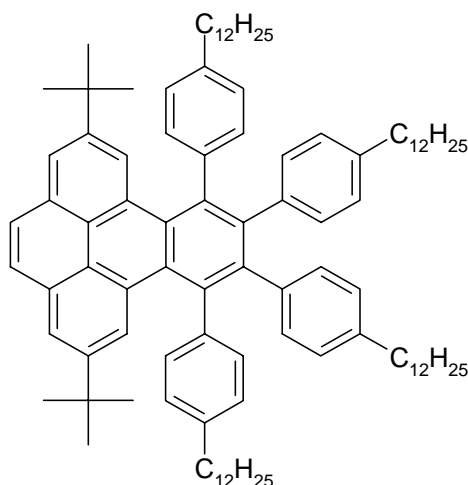
TGA, (°C): >450

7.2.25 2,7-Di-*tert*-butyl-4,5-bis-(4-dodecyl-phenyl)-cyclopenta[*e*]pyren-5-one (**4-12**)

3.00 g (8.70 mmol) 2,7-di-*tert*-butylpyrene-4,5-dione (**3-7**) and 5.23 g (9.58 mmol) 1,3-bis-(4-dodecyl-phenyl)propan-2-one (**2-6**) were suspended in 180 ml of ethanol under inert atmosphere. A solution prepared from 0.27 g KOH (4.79 mmol) in 12 ml methanol was added dropwise at room temperature. The mixture was heated to 80 °C for 1 hour. The product was extracted with DCM, concentrated and the residue was purified by column chromatography (petroleum ether/DCM=3:1) to yield product as dark brown solid, which is unstable and was thus used without complete characterization.

Yield: 4.55g (57%)

FD-MS (8KV), m/z [ue^{-1}]: 855.3 (M^+) (cal. for $C_{63}H_{82}O$ 855.3)

7.2.26 2,7-Di-*tert*-butyl-4,5,6,7-tetrakis-(4-dodecyl-phenyl)-benzo[*e*]pyrene (**4-14**)

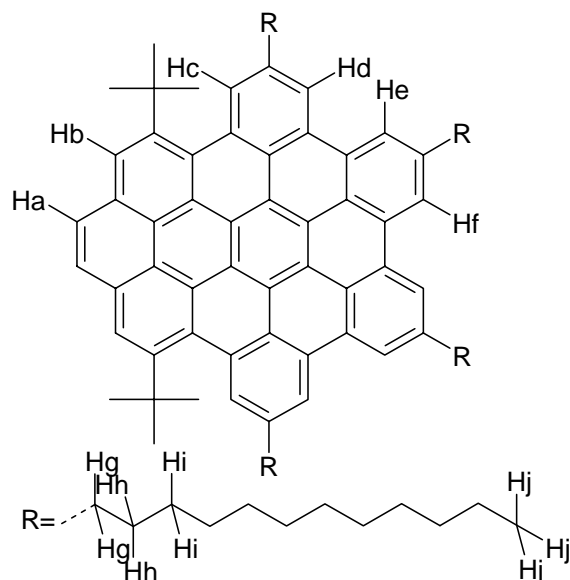
4.22 g (4.90 mmol) 2,7-di-*tert*-butyl-4,5-bis-(4-dodecylphenyl)-cyclopenta[*e*]pyren-5-one (**4-12**) and 2.00 g (4.00 mmol) bisdodecyldiphenylacetylene (**4-13**) in 5 ml of diphenylether were heated to 200°C for 5 h. Chromatography (PE) afford product as an yellow oil.

Yield: 1.38 g (21%)

FD-MS (8KV), m/z [ue⁻¹]: 1341.9 (M⁺) (cal. for C₁₀₀H₁₄₀ 1342.2)

¹H NMR (250 MHz, CD₂Cl₂, 278K): δ(ppm)= 8.14 (s, 2H), 7.85 (s, 4H), 6.89 (m, 8H), 6.68 (d, J(H,H)=7.97 Hz, 4H), 6.59 (d, J(H,H)=8.00 Hz, 4H), 2.49 (m, 8H), 1.53 (m, 8H), 1.27 (br.s, 72H), 1.09(s, 18H), 0.88 (m, 12H)

¹³C NMR (250 MHz, C₂D₂Cl₄, 278K): δ(ppm)= 146.94, 141.33, 140.99, 140.33, 139.04, 138.00, 131.77, 131.42, 131.23, 130.04, 129.58, 128.26, 127.03, 126.86, 126.82, 126.56, 123.46, 121.71, 35.69, 35.48, 34.82, 31.50, 29.89, 29.53, 28.84, 22.87, 14.38

7.2.27 1,6-Di-*tert*-butyl-8,11,14,17-tetra-*n*-dodecyl-tetrabenzo[*bc,ef,hi,uv*]ovalene (**4-15**)

1.35 g (1.00 mmol) 2,7-di-*tert*-butyl-4,5,6,7-tetrakis-(4-dodecyl-phenyl)-benzo[*e*]pyrene (**4-14**) was dissolved in 1 L DCM. A constant stream of argon was bubbled into the solution through a glass capillary. A solution of 4.05 g (25.00 mmol) FeCl₃ in 45 ml CH₃NO₂ was then added dropwise via syringe. Throughout the whole reaction a constant stream of argon was bubbled through the mixture to remove HCl formed *in situ*. The reaction was stirred for 25 minutes and quenched by adding methanol. The mixture was extracted with DCM, concentrated and the residue was purified by column chromatography (petroleum ether/DCM=5:1) to afford product as bright orange solid.

Yield: 1.26 g (94%)

FD-MS (8KV), m/z [ue⁻¹]: 1331.8 (M⁺) (cal. for C₁₀₀H₁₃₀ 1332.1)

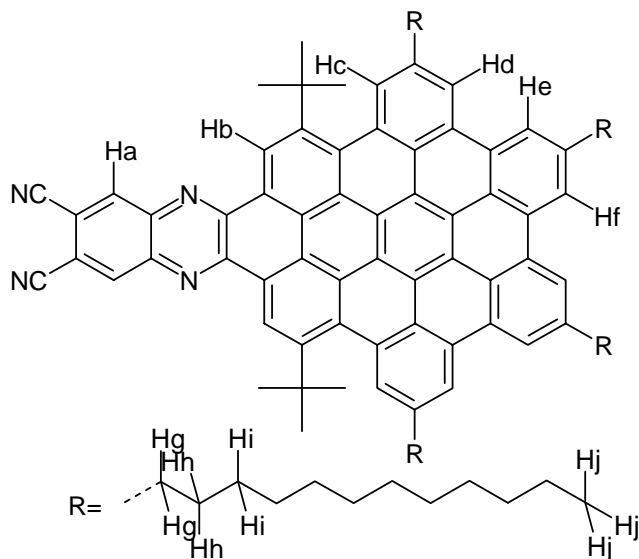
¹H NMR (500 MHz, C₂D₂Cl₄, 373 K): δ(ppm)= 9.06 (s, 2H, H_b), 8.86 (s, 2H, H_e), 8.82 (s, 2H, H_d), 8.79 (s, 2H, H_c), 8.70 (s, 2H, H_f), 8.53 (s, 2H, H_a), 3.04 (m, 4H, H_g), 3.00 (m, 4H, H_g), 2.00 (m, 4H, H_h), 1.96 (m, 4H, H_h), 1.79 (s, 18H, H_{*t*-but}), 1.49 (m, 4H, H_i), 1.43 (m, 4H, H_i), 1.21 (br.s., 56H, H_{CH₂-rest}), 0.87 (s, 12H, H_j)

¹³C NMR (250 MHz, C₂D₂Cl₄, 278 K): δ(ppm)= 145.36, 141.21, 137.32, 131.85, 130.32, 130.11, 129.71, 128.62, 128.16, 126.88, 126.46, 124.73, 123.44, 123.36, 121.58, 120.92, 119.90, 119.70, 119.42, 38.67, 37.06, 36.84, 35.00, 32.30, 31.84, 29.68, 29.31, 22.64, 14.13

124.74, 123.79, 122.75, 121.23, 121.00, 119.31, 39.28, 37.63, 37.08, 34.74, 32.21, 31.61, 30.01, 29.60, 22.92, 14.27

Elemental Analysis: 87.65% C, 9.45% H (cal.: 88.18% C, 9.47% H)

7.2.29 1,6-Di-*tert*-butyl-8,11,14,17-tetra-*n*-dodecyl-tetrabenzo[*jk,mn,pq,st*]-4,5-dicyanobenzo[1,2-*a*]pyrazine[2,3-*d*]ovalene (**4-17**)



0.20 g (0.15 mmol) of 1,6-di-*tert*-butyl-8,11,14,17-tetra-*n*-dodecyl-tetrabenzo[*bc,ef,hi,uv*]ovalene-3,4-dione (**4-16**) and 0.02 g (0.15 mmol) of 1,2-diamino-4,5-dicyanobenzene (**4-8**) were suspended in acetic acid (3 ml) under inert atmosphere. The mixture was heated at 130 °C for 7.5 hours. Column chromatography (DCM as eluent) gave pure product as a dark solid.

Yield: 0.11 g (52%)

FD-MS (8KV), m/z [ue^{-1}]: 1483.6 (M^{+}) (cal. for $C_{108}H_{130}N_4$ 1484.3)

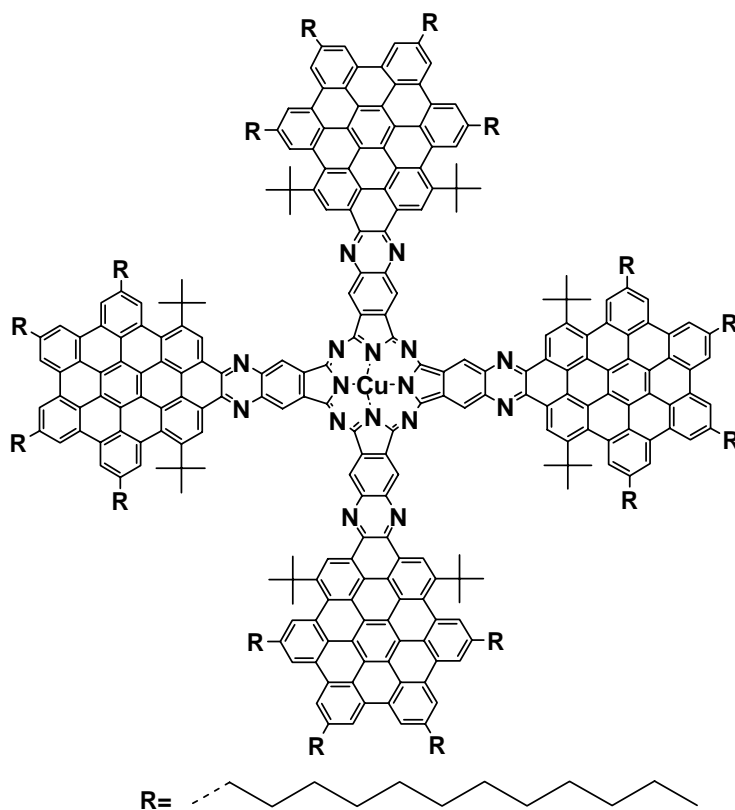
1H -NMR (700 MHz, $C_2D_2Cl_4$, 373K): δ (ppm) = 9.32 (s, 2H, H_b), 9.18 (br.s, 6H, H_{d, e+f}), 8.61 (s, 2H, H_c), 8.57 (s, 2H, H_a), 3.40 (m, 4H, H_g), 3.37 (m, 4H, H_g), 2.23 (m, 4H, H_h), 2.17 (m, 4H, H_h), 1.73 (s, 18H, H_{*t*-but}), 1.56 (m, 4H, H_i), 1.44 (m, 4H, H_i), 1.32 (br.s, 56H, H_{CH₂-rest}), 0.89 (m, 12H, H_j)

^{13}C NMR (500 MHz, $C_2D_2Cl_4$, 373K): δ (ppm)= 147.64, 145.76, 142.64, 141.49, 138.75, 136.55, 133.44, 133.05, 130.87, 130.97, 130.02, 129.53, 127.57, 125.42, 124.72, 124.76,

123.69, 123.66, 123.52, 122.77, 122.74, 120.53, 120.32, 119.46, 115.50, 112.10, 39.48, 37.57, 37.39, 35.16, 32.16, 32.07, 31.90, 29.94, 30.15, 30.08, 29.91, 29.83, 29.47, 22.77, 14.13

Elemental Analysis: 87.32% C, 8.85% H, 3.10% N (cal.: 87.40% C, 8.83% H, 3.77% N)

7.2.30 1,6-Di-*tert*-butyl-8,11,14,17-tetra-*n*-dodecyl-tetrabenzo[*jk,mn,pq,st*]benzo[1,2-*a*]pyrazine[2,3-*d*]ovalenocyanine (**4-18**)



0.10 g (0.07 mmol) of 1,6-di-*tert*-butyl-8,11,14,17-tetra-*n*-dodecyl-tetrabenzo[*jk,mn,pq,st*]-4,5-dicyanobenzo[1,2-*a*]pyrazine[2,3-*d*]ovalene (**4-17**), 0.01 g (0.07 mmol) of CuCl₂ and 0.50 g of urea were suspended in 1-2 ml of quinoline under inert atmosphere. The mixture was heated at 210 °C for 7 hours. Column chromatography (DCM:THF=10:1 as eluent) gave product as a dark brown solid.

Yield: 0.03 g (7%)

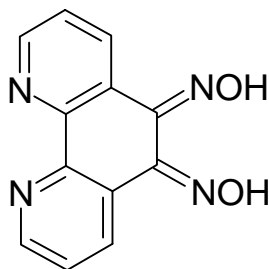
MS(MALDI-TOF), m/z [ue⁻¹]: 6003 (M⁺) (cal. for C₄₃₂H₅₂₀CuN₁₆ 6000.6)

UV/vis: λ / nm ($\epsilon / \text{m}^2 \cdot \text{mol}^{-1}$) = 869 (1 655), 785 (752), 577 (1 955), 480 (2 105), 379 (11 430)

TGA, (°C): >450

DSC (°C): no transition

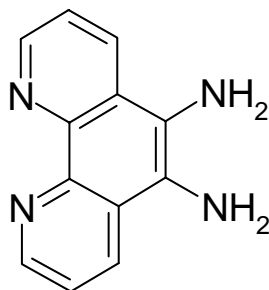
7.2.31 Phendioxime **5-15**



A mixture 3.00 g (0.01 mol) of phendione **5-14**, 3.45g (0.05 mol) of $\text{NH}_2\text{OH} \cdot \text{HCl}$, and 4.20 g (0.02 mol) of BaCO_3 in 225 ml of ethanol were stirred and refluxed overnight.³ After removal of solvent, the residue was treated with 300 ml of 0.2 M HCl, stirred for 30 min and filtered. The light yellow solid was washed with water, ethanol and ether, and dried.

Yield: 1.1 g (32%)

7.2.32 5,6-Diamino-1,10-phenanthroline (**5-16**)



Slurry 1.10 g (0.005 mol) of phendioxime **5-15** and 1.10 g of Pd/C (10%) in 262 ml of dry ethanol were purged with argon and heated to reflux.³ To this mixture, a solution of

9.10 ml of $\text{N}_2\text{H}_4 \cdot \text{H}_2\text{O}$ and 39 ml of ethanol was added during a period of an hour and the resulting mixture refluxed overnight. The mixture was filtered hot through a bed of Celite and the pad was washed a few times with boiling ethanol. The filtrate was taken to dryness and the residue was poured into water and left at 4 °C overnight. The tan solid that separated was filtered and washed with cold water and dried.

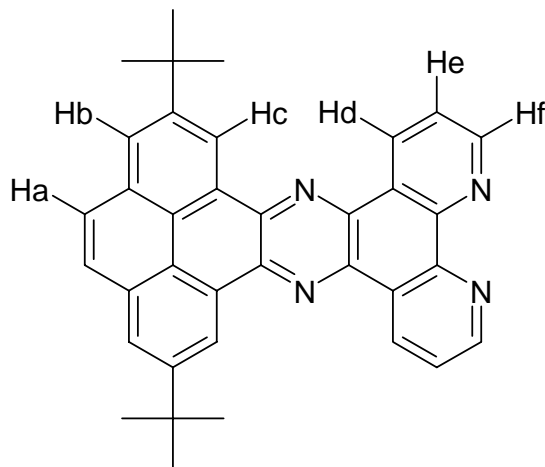
Yield: 0.69 g (72%), brown powder

^1H NMR (250 MHz, Dimethylformamid- d_7 , 298 K): δ (ppm) = 8.86 (d, $J(\text{H,H})=1.42$ Hz, 1H), 8.84 (d, $J(\text{H,H})=1.47$ Hz, 1H), 8.66 (d, $J(\text{H,H})=1.46$ Hz, 1H), 8.62 (d, $J(\text{H,H})=1.45$ Hz, 1H), 7.66-7.61 (m, 2H), 5.35 (s, 4H, H_{NH_2})

^{13}C NMR (250 MHz, Dimethylformamid- d_7 , 298 K): δ (ppm)= 150.32 (CH), 146.95 (C), 133.55 (CH), 128.49 (C), 127.82 (C), 127.28 (CH)

Elemental Analysis: 68.45% C, 4.79% H, 26.18% N (cal.: 68.66% C, 4.79% H, 26.65% N)

7.2.33 2,7-Di-*tert*-butyl-1,10-phenanthro[5,6-*e*]pyrazine[2,3-*e*]pyrene (**5-17**)



0.20 g (0.58 mmol) of 2,7-di-*tert*-butylpyrene-4,5-dione (**3-7**) and 0.12 g (0.58 mmol) of 5,6-diamino-1,10-phenanthroline (**5-16**) were suspended in dry pyridine (3 ml) under inert atmosphere. The mixture was refluxed overnight. After cooling down yellow solid was filtrated, washed with pyridine and dried.

Yield: 0.02 g (66%)

FD-MS (8KV), m/z [ue^{-1}]: 518.4 (M^+) (cal. for $\text{C}_{36}\text{H}_{40}\text{N}_4$ 518.7)

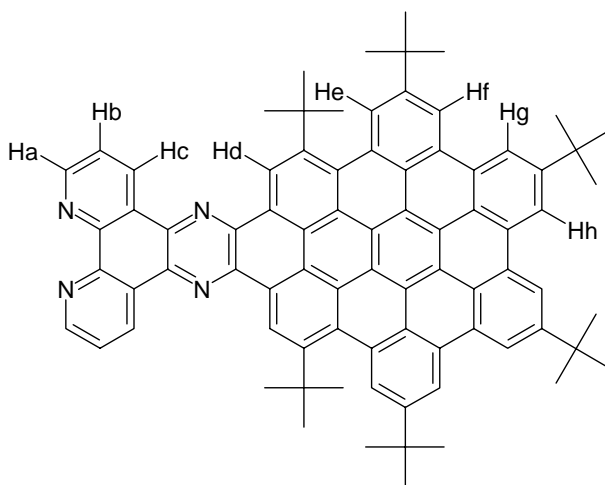
UV/vis: λ / nm (ϵ / $\text{m}^2 \cdot \text{mol}^{-1}$) = 450 (1 636), 427 (1 334), 364 (1 880), 348 (2 820), 336 (2 444), 295 (7 332), 284 (4 324), 252 (8 272), 244 (7 332)

^1H NMR (250 MHz, $\text{C}_2\text{D}_2\text{Cl}_4$, 373K): δ (ppm) = 9.80 (s, 4H, $\text{H}_{\text{d+c}}$), 9.41 (s, 2H, H_{f}), 8.43 (s, 2H, H_{b}), 8.02 (s, 2H, H_{a}), 7.86 (s, 2H, H_{e}), 1.89 (s, 18H, $\text{H}_{\text{t-but}}$)

^{13}C NMR (500 MHz, $\text{C}_2\text{D}_2\text{Cl}_4$, 373K): δ (ppm)= 152.96, 152.34, 150.47, 150.30, 148.79, 148.59, 147.47, 143.33, 140.64, 139.62, 136.15, 133.72, 133.63, 131.77, 129.16, 128.20, 127.88, 127.62, 126.27, 124.66, 124.44, 124.34, 124.04, 122.95, 121.45, 35.92, 32.38

Elemental Analysis: 83.45% C, 5.79% H, 9.88% N (cal.: 83.37% C, 5.83% H, 10.80% N)

7.2.34 1,6-Di-*tert*-butyl-8,11,14,17-tetra(*t*-butyl)tetrabenzo[*jk,mn,pq,st*]-1,10-phenanthro[5,6-*e*]pyrazine[2,3-*d*]ovalene (**5-18**)



0.05g (0.06 mmol) of 1,6- di-*tert*-butyl-8,11,14,17-tetra- (*t*-butyl)tetrabenzo[*bc,ef,hi,uv*]ovalene-3,4-dione (**3-13**) and 0.01 g (0.06 mmol) of 5,6-diamino-1,10-phenanthroline (**5-16**) were suspended in dry pyridine (2 ml) under inert atmosphere. The mixture was refluxed overnight. After cooling down the bright red solid was filtrated, washed with pyridine and dried.

Yield: 0.04 g (57%)

MS(MALDI-TOF), m/z [ue^{-1}]: 1087 (M^+) (cal. for $\text{C}_{80}\text{H}_{70}\text{N}_4$ 1087.4)

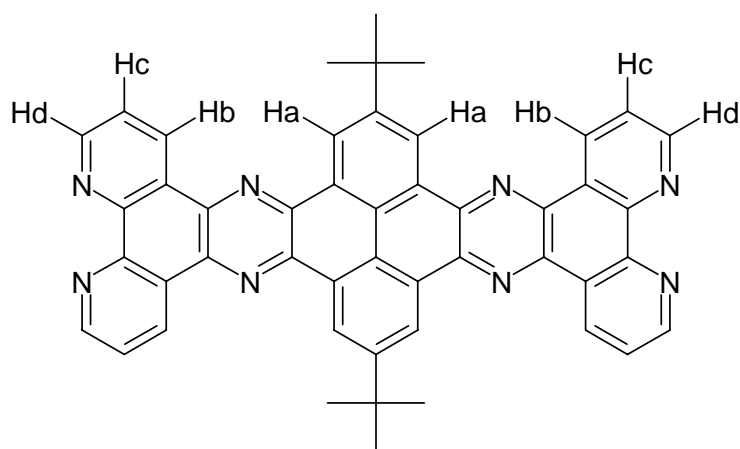
UV/vis: λ / nm (ϵ / $\text{m}^2 \cdot \text{mol}^{-1}$) = 518 (1 776), 490 (2 065), 474 (2 436), 436 (3 634), 415 (5 782), 401 (7 764), 383 (11 399), 366 (7 888), 300 (5 039), 269 (6 525)

^1H NMR (500 MHz, $\text{C}_2\text{D}_2\text{Cl}_4$, 373K): δ (ppm) = 10.43 (s, 2H, H_d), 9.63 (s, 2H, H_a), 9.41 (s, 2H, H_h), 9.38 (s, 2H, H_g), 9.34 (s, 2H, H_f), 9.28 (s, 2H, H_c), 9.15 (s, 2H, H_e), 7.89 (s, 2H, H_b), 1.88 (s, 18H, $\text{H}_{t\text{-but}}$), 1.82 (s, 18H, $\text{H}_{t\text{-but}}$), 1.80 (s, 18H, $\text{H}_{t\text{-but}}$)

^{13}C NMR (500 MHz, $\text{C}_2\text{D}_2\text{Cl}_4$, 373K): δ (ppm)= 151.85, 150.26, 147.62, 146.49, 142.25, 139.38, 137.82, 133.82, 133.57, 131.60, 131.10, 131.05, 130.57, 130.25, 129.64, 128.13, 126.41, 126.27, 125.98, 124.71, 124.28, 123.96, 123.18, 120.82, 120.37, 120.05, 119.51, 119.34, 39.69, 36.11, 36.08, 35.28, 32.35, 32.32

Elemental Analysis: 88.26% C, 6.48% H, 4.98% N (cal.: 88.36% C, 6.49% H, 5.15% N)

7.2.35 2,7-Di-*tert*-butyl-bis(1,10-phenanthro[5,6-*e*]pyrazine[2,3]-*e,l*]pyrene (**5-19**)



0.20 g (0.53 mmol) of 2,7-di-*tert*-butylpyrene-4,5,9,10-tetraone (**1-32**) and 0.22 g (1.00 mmol) of 5,6-diamino-1,10-phenanthroline (**5-16**) were suspended in dry pyridine (3 ml) under inert atmosphere. The mixture was refluxed for 16 h. After cooling down red solid was filtrated, washed with pyridine and dried.

Yield: 0.29 g (56%)

MS(MALDI-TOF), m/z [ue^{-1}]: 723 (M^+); 746 ($\text{M}^+ + \text{Na}^+$) (cal. for $\text{C}_{48}\text{H}_{34}\text{N}_8$ 722.9)

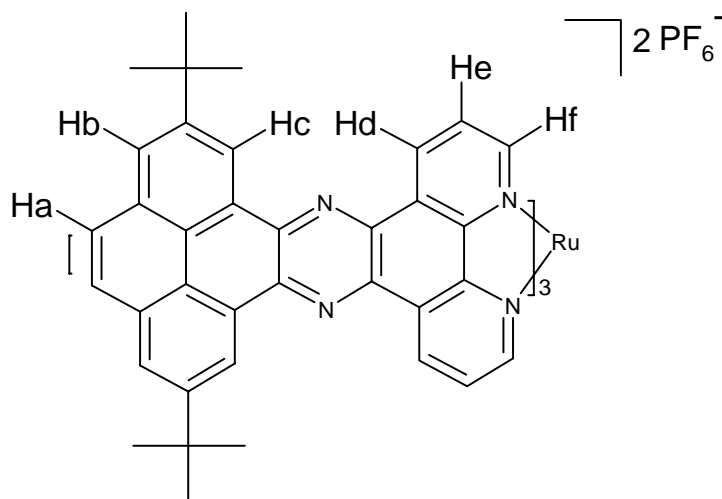
UV/vis: λ / nm (ϵ / $\text{m}^2 \cdot \text{mol}^{-1}$) = 427, 402, 392, 381, 343, 320, 309, 280

^1H NMR (500 MHz, Trifluoroacetic acid- d_2 , 348K): δ (ppm) = 10.75 (m, 4H, H_b), 10.50 (s, 3H, H_a), 9.86 (s, 4H, H_d), 9.29 (s, 1H, H_a), 9.01 (m, 3H, H_c), 8.95 (m, 1H, H_c), 2.55 (s, 12H, $\text{H}_{t\text{-but}}$), 2.27 (s, 6H, $\text{H}_{t\text{-but}}$)

^{13}C NMR (500 MHz, Trifluoroacetic acid- d_1 , 348K): $\delta(\text{ppm})= 157.76, 155.93, 150.66, 150.34, 146.99, 145.54, 142.55, 142.42, 141.61, 141.12, 140.65, 140.15, 135.51, 134.57, 133.18, 132.92, 132.32, 131.10, 130.02, 129.30, 33.30, 32.45$

Elemental Analysis: 78.12% C, 4.44% H, 15.05% N (cal.: 79.76% C, 4.74% H, 15.50% N)

7.2.36 Ruthenium (II) complex **5-20**



A suspension of $\text{RuCl}_3 \cdot x\text{H}_2\text{O}$ (0.003 g, 0.016 mmol) and the 2,7-di-*tert*-butyl-1,10-phenanthro[5,6-*e*]pyrazine[2,3-*e*]pyrene (**5-17**) (0.025 g, 0.048 mmol) in 1 ml of deoxygenated DMF was stirred for 14 days at 150 °C under an argon atmosphere. The color of the reaction mixture changed from yellow to red. The red complex was precipitated by addition a saturated aqueous solution of KPF_6 to the reaction mixture. The complex was purified by repeated precipitation (4 times) with *n*-pentan.

Yield: 0.03 g (40%)

MS(MALDI-TOF), m/z [ue^{-1}]: 1137 ($\text{M}^+ - 1$ ligand); 1654 (M^+); 1801 ($\text{M}^+ + \text{PF}_6^-$) (cal. for $\text{C}_{108}\text{H}_{96}\text{N}_{12}\text{Ru}$ 1663.12)

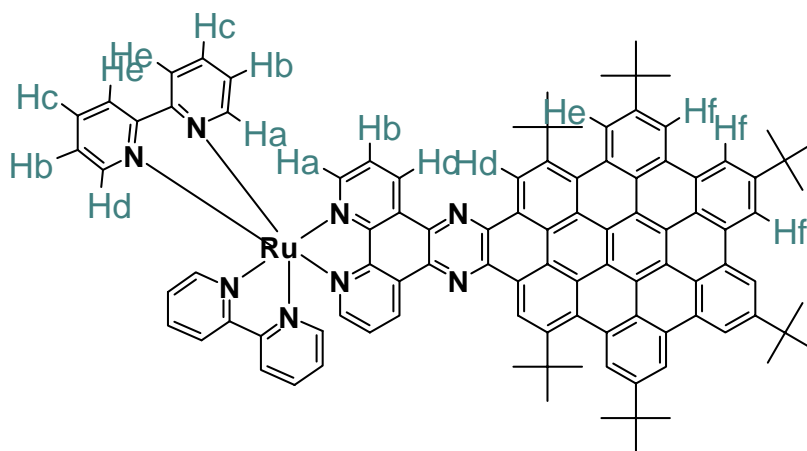
UV/vis: λ / nm ($\epsilon / \text{m}^2 \cdot \text{mol}^{-1}$) = 474 (3 196), 445 (3 196), 418 (2 444), 360 (4 700), 346 (4 324), 294 (9 964), 24 (15 980)

^1H NMR (500 MHz, $\text{C}_2\text{D}_2\text{Cl}_4$, 373K): δ (ppm) = 9.87 (s, 6H, H_c), 9.75 (s, 6H, H_f), 8.50 (s, 6H, H_a), 8.30 (d, 6H, $^3\text{J}=18.2$ Hz, H_e), 8.05 (s, 6H, H_b), 7.98 (s, 6H, H_d), 1.64 (br.s, 48H, $\text{H}_{t\text{-but}}$)

^{13}C NMR (700 MHz, $\text{C}_2\text{D}_2\text{Cl}_4$, 373K): $\delta(\text{ppm})= 150.51, 150.06, 149.24, 144.63, 137.76, 131.39, 131.29, 130.55, 128.48, 127.88, 127.46, 127.37, 126.91, 126.73, 126.00, 124.56, 124.23, 123.00, 121.71, 121.10, 121.05, 31.78, 31.73$

Elemental Analysis: 75.47% C, 4.82% H, 7.87% N (cal.: 78.00% C, 5.82% H, 10.11% N, Ru 6.08%)

7.2.37 Ruthenium (II) complex **5-22**



A suspension of $\text{Ru}(\text{bpy})_2\text{Cl}_2$ (0.0027 g, 0.0055 mmol) and 1,6-di-*tert*-butyl-8,11,14,17-tetra(*t*-butyl)tetrabenz[*jk,mn,pq,st*]-1,10-phenanthro[5,6-*e*]pyrazine[2,3-*d*]ovalene (**5-18**) (0.0030 g, 0.0027 mmol) in 1 ml of ethanol was stirred for 3 days at 110 °C under an argon atmosphere. The dark red complex was precipitated by addition of a saturated aqueous solution of KPF_6 to the reaction mixture.

Yield: 0.003 g (75%)

MS(MALDI-TOF), m/z [ue^{-1}]: 1505 (M^+); 1650 ($\text{M}^+ + \text{PF}_6^-$) (cal. for $\text{C}_{100}\text{H}_{92}\text{N}_8\text{Ru}$ 1506.97)

UV/vis: λ / nm ($\epsilon / \text{m}^2 \cdot \text{mol}^{-1}$) = 530 (1 239), 486 (1 817), 436 (1 982), 414 (2 478), 399 (3 056), 378 (4 295), 361 (3 593), 291 (8 177)

^1H NMR δ (500 MHz, CD_3CN , 348K): $\delta(\text{ppm})= 9.99$ (br.s, 4H, Ha), 9.85 (br.s, 4H, Hd), 8.51 (br.s, 6H, He), 8.42 (br.s, 6H, Hc), 8.12 (br.s, 6H, Hf), 7.94 (br.s, 6H, Hb), 1.89 (m, 54H, Ht-but);

^{13}C NMR (700 MHz, $\text{C}_2\text{D}_2\text{Cl}_4$, 373K): $\delta(\text{ppm})=$ no peaks were found

Elemental Analysis: 76.72% C, 4.87% H, 5.44% N (cal.: 79.70% C, 6.15% H, 7.44% N, Ru 6.71%)

7.3 References

1. Hu, J.; Zhang, D.; Harris, F. W., *J. Org. Chem.* **2005**, 70, (2), 707-708.
2. Wang, Z. H.; Tomovic, E.; Kastler, M.; Pretsch, R.; Negri, F.; Enkelmann, V.; Müllen, K., *J. Am. Chem. Soc.* **2004**, 126, (25), 7794-7795.
3. Bodige, S.; MacDonnell, F. M., *Tetrahedron Lett.* **1997**, 38, (47), 8159-8160.

